Learning To Move: Exploring the Neural Dynamics of Motor Learning

L. Marreel

A thesis submitted for the degree of Doctor of Philosophy

School of Computer Science and Electronic Engineering

University of Essex

April 2024

Thesis Abstract

This thesis reflects an interdisciplinary research project aimed, in part, to address the question: "How can Brain-Computer Interface (BCI)-based motor rehabilitation be optimized?" It also sought to expand the scientific understanding of the neural processes associated with motor learning. Specifically, we investigated three neural correlates of motor control – Event-Related Desynchronization (ERD), Motor Related Cortical Potential (MRCP), and the temporal evolution of Corticospinal Excitability (CSE) – with the goal of characterizing their interactive relationships and identifying any dynamic changes associated with motor learning. Despite the increasing use of these neural markers in contexts such as BCI-based post-stroke motor rehabilitation, the functional connectivity, and dynamics of these markers during the process of motor learning remain poorly understood. Especially in relation to improving performance in motor skill-based tasks. This research aims to clarify these dynamics to optimize BCI setups and advance motor rehabilitation.

Though this thesis is framed around improving motor rehabilitation, its exploratory nature necessitated working exclusively with healthy participants, serving as a foundational step toward future clinical applications. The first study covers our analysis of data by Daly et al. (2018), to further explore their suggested time dependent relationship between ERD and CSE. The second and third studies focus on two renditions of a new motor learning experiment, one to behaviorally validate the design and the other to collect EEG and TMS response data to replicate and expand on our findings in the data by Daly et al. (2018).

Taken together, our results indicate the temporal evolution of CSE, as measured by MEP amplitude in the 2 seconds leading up to Movement Onset, follows an S-like wave (third-degree polynomial). Where an initial increase in amplitude is followed by a decline after which it once again changes direction to strongly move upward. While ERD measures showed potential for predicting this changing CSE timeline, the cubic relationship between CSE and time did not extend to describe the relationship between CSE and ERD. Instead, preliminary insights suggest that the CSE-ERD relationship is unstable, implying that their connection is more likely correlational—based on a shared temporal progression relative to MOn—rather than functionally dependent. Furthermore, both CSE and ERD significantly changed with motor learning, with ERD power decreasing further and CSE amplitude reducing following early-stage learning but further unchanged. Despite our inability to quantify a stable relationship between ERD and CSE, our findings clearly demonstrate that learning affects the reliability of deriving CSE from ERD, as their relationship remains unstable over time.

These findings highlight that ERD dynamics vary between individuals and frequency bands, discouraging the use of fixed percentage thresholds to derive optimal excitability. Additionally, because learning alters ERD power, it must be accounted for when using ERD to infer CSE dynamics.

Future research should focus on refining methodologies to better understand these dynamic interactions and their implications for motor control and BCI applications. This newfound understanding of how motor learning occurs in the brain is of interest to further our understanding of how BCI-based rehabilitation works and will help to optimize the development of BCI-driven motor recovery paradigms.

Preface and Covid-19 statement

"We pass through the present with our eyes blindfolded. We are permitted merely to sense and guess at what we are actually experiencing. Only later when the cloth is untied can we glance at the past and find out what we have experienced and what meaning it has."

— Milan Kundera, Laughable Loves

We predict and anticipate the future, using our experiences and what we have learned from the past. This notion is a premise of the theoretical framework of this thesis, and a good description of my PhD journey. Coming straight from my MSc in Theoretical and Experimental Psychology, I went into my PhD with ideology, passion, and a sense of security. I knew this adventure, this new chapter in my life, would be bigger than anything I had navigated before. I knew it would not be easy. Yet, how different could it truly be? I try to not be too hard on the naiveté of my past self. Nothing could have prepared me for the series of unfortunate events that would stack up and plague this project, my PhD experience. I save you my tale of woe. No Tl;Dr (*) needed. Yes, the Corona Panini is a big part of the tragedy. However, it mainly functioned as an amplifier for delays and issues that came before. The result was a scramble to change course while staying on track to our original destination. Chapter 2 was unplanned but ultimately fit our story nicely. In hindsight, it was a very good idea. Yet, the whole experience came at a cost. The philosophical approach is to embrace the experience, learn from the mistakes and go forth to do better. I did. Look at Chapter 4. We regained lab access, and I dug deep for my second wind. Chapter 2 took a back seat as we returned to our original course, now at double time. Returning to the theme of learning from past mistakes. A nice lesson in consequences of one's actions. I should not have ignored Chapter 2. Nothing grates more than having to write up every single mistake when you know better. I tried. However, motivation is like toothpaste. At the end of the tube, you must squeeze harder. Yet, no matter how hard you try to squeeze, when you have run out – and the stores are closed – there is nothing left.

The thesis presented to you, readers, and my examiners, does not reflect the PhD project I had envisioned. However, is the collection of research that circumstances allowed. I look forward to the time when my present is my past. To glance back at this moment and find the silver lining.

(*) too long, didn't read.

Acknowledgments

The research presented in this thesis (especially the good parts) has benefited extensively from the comments and guidance provided by my supervisors, Dr. Ian Daly and Dr. Gethin Hughes. I would not have survived the trials and tribulations associated with a PhD, let alone one during a pandemic, without their support. Thank you both for your knowledge, patience, and compassion. There are many horror stories about PhD supervisors, and you lived up to none of them. I would like to express my deepest appreciation to my examiners, Dr. Nicholas Cooper and Prof. Dr. Tom Carlson, for reading this thesis and I look forward to an insightful discussion at my Viva. Additionally, this endeavor would not have been possible without the support from my family and my partner, Dr. István László Gyimes, who both made it possible for me to set aside my 'adult' responsibilities and focus solely on my work. I want to express my gratitude to the riot that is my group of friends. Many of whom will never read this thesis or even half understand (or care about) what I did, but who all believed in me when I no longer could. A special shout-out to Cheyoban De Winter and Peculiar Tattoos for letting me become part of the furniture (or perhaps the decorations) for a little while in their tattoo studio—a workspace as unconventional as it was stimulating—which gave me the push I needed to complete my corrections. Finally, I'd like to mention the BCI-NE lab and all its members, who are eager to laugh and inspire. It was a joy working alongside them.

Table of Contents

Glossary

ACC – Accuracy

ADM – Abductor Digiti Minimi

BCI – Brain-Computer Interface

BP – Bereitschaftspotential

CMS – Common Mode Sensor

CNS – Central Nervous System

CNV – Contingent Negative Variation

CSE – Corticospinal Excitability

DRL – Driven Right Leg

EEG – Electroencephalography

EMG – Electromyography

ERD – Event-Related Desynchronization

ERP – Event-Related Potentials

FDI – First Dorsal Interosseous

IC – Independent component

ICA – Independent Component Analysis

LRP – Lateralized Readiness Potential

MEP – Motor Evoked Potential

MI – Motor Imagery

MOn – Movement Onset

MRCP – Motor Related Cortical Potential

NS – Negative slope

PAS – Paired Associative Stimulation

RP – Readiness Potential

SCI – Spinal Cord Injury

SPN – Stimulus Preceding Negativity

STDP – Spike Timing Dependency Plasticity

tDCS – transcranial direct current stimulation

TMS – Transcranial Magnetic Stimulation

Chapter 1: Literature Review and Introduction

Shortly before our muscles contract to execute an action, neuroscientist can observe patterns in neural activity that are assumed to reflect the cognitive processes through which our brain ensures the smooth coordination of our movements. The studies in this thesis examined how such movement related neural patterns and processes occur together and how these neural patterns and their inter-pattern dynamics change during motor learning.

The studies contribute to the broader project goal of improving our understanding of how motor-related activity changes as we learn to move, and how we can help people re-learn to move. Insights into how the brain controls movement and learns are already being applied in new motor rehabilitation technologies. Technological advancements such as Brain-Computer Interfaces (BCIs) hold great potential to aid rehabilitation, particularly in cases where loss of motor function results from brain damage, such as caused by a stroke. However, BCIs are still in early development, with progress limited by an incomplete understanding of how to facilitate motor learning. We believe BCI setups can be improved by advancing our understanding of the neural activity involved in movement control. Such novel insights could provide new access points through which BCIs can help the brain support its own recovery.

1.1 Neural Activity of Motor Control

One of the most important functions of the brain is to allow us to move around. Look at the animal world, where the sea squirt even goes as far as to ingest its own brain once it has found a place to live and no longer needs to move (Bussler, 2020; Monniot et al., 1991; Zack, 2006). While the notion of “most important function” can be debated, we do have to acknowledge that moving around is the most common task the brain must juggle among all the others. The average able-bodied individual will not have to put much thought toward maneuvering through a doorway or around another person. However, despite the lack of conscious effort, our brain is constantly processing a myriad of input-output signals, enabling us to be responsive to the changes and demands of a given situation. As such, the brain can generally be thought to function as a ‘feedforward – feedback’ (i.e., act and react) system (Wolpert & Miall, 1996). In terms of movement, we speak of a feed forward command to act and getting (sensory) feedback on the executed actions (Remsik et al., 2017; Wolpert et al., 2001). The "act" phase of this ‘feedforward – feedback’ loop (which we shall refer to as the FoFe-loop) starts in the brain. Where the intention to initiate a specific movement arises from higher-level cognitive processes, such as decision-making and goal setting (Bagozzi & Dholakia, 2014, pp. 23–25; Butterfill & Sinigaglia, 2014). The desired movement is then planned and prepared by anticipating the set of muscle contractions required. A prediction-based feedforward command is generated and sent to the

relevant muscles through the motor neurons of the spinal cord, leading to the initiation and execution of the movement (Butterfill & Sinigaglia, 2014). The “react” phase involves the continuous monitoring of our environment and the state of our body. The brain obtains sensory feedback (through various sensory systems, not just tactile), which is then compared with the intended outcome. Any discrepancies result in refinement, correction, or change of the original commands; this update involves adjusting the internal motor representations—such as the kinematic and dynamic features of actions (e.g., joint displacement, muscle contractions), sensory features (e.g., visual, and tactile perceptions), and action outcomes (e.g., grasping or throwing) (Butterfill & Sinigaglia, 2014)—and initiating a new start of the “act” phase (Bagozzi & Dholakia, 2014, pp. 21–38; Jeannerod, 1995).

Motor control refers to the collection of cognitive processes that encompass the entire FoFe-loop, governing both the execution and refinement of movement. This thesis focuses specifically on the pre-movement phase of the FoFe-loop, including intention, anticipation, planning, and preparation. For clarity, the term movement preparation will be used to collectively describe these pre-movement stages, even though "preparation" also refers to a distinct cognitive process within this phase.

Conceptually, the FoFe-loop is made up of individual and sequential steps, with a start (act) and end point (react) to be repeated in order. This notion aligns with behavioral observations of actions being aborted, altered mid-execution, or stopped shortly after initiation. In reality, however, motor control is more complex and interactive (Klein-Flügge & Bestmann, 2012). The cognitive processes and underlying physiological mechanisms work together and are active simultaneously (Wolpert et al., 2001). This synchronized nature is further supported by observations of the temporal dynamics of brain activity. Although the exact roles and mechanisms of neural activity in motor cortex areas controlling muscle activity are not yet fully understood, research has consistently identified specific patterns in brain activity that precede voluntary movement. These patterns, observed through electroencephalography (EEG), involve changes both over time and in the frequency of brain activity. Such recurring changes, associated with an external stimulus or mental task, are referred to as ‘neural correlates’ or ‘neural markers,’ terms that will be used interchangeably throughout this thesis.

Schultze-Kraft et al. (2016) utilized one such neural correlate and illustrated a fundamental aspect of the synchronized nature of motor control: its 'constantly updating' quality. Providing support that the “react” phase can overlap with or even begin before the completion of the “act” phase (Klein-Flügge & Bestmann, 2012). In their study, Schultze-Kraft et al. (2016) instructed participants to press a button at their own pace (averaging about 2 seconds) after receiving a ‘go’ signal. Occasionally, a ‘stop’ signal (i.e., “do not press the button”) was presented, targeting various time points of a real-time neural measure of the participants’ movement preparation. Results showed participants being able to abort an action after the initiation of the preparatory processes of movement, up to 200ms prior to

movement onset (MOn). This suggests that incoming information can interrupt and update the FoFe-loop at any step, including prior to movement initiation but only up until a certain point. Any stop signals provided past this 'point of no return' could not cancel the triggered chain of events and prevent movement initiation (Schultze-Kraft et al., 2016). The neural correlate used by Schultze-Kraft et al. (2016) is the Movement Related Cortical Potential (MRCP) (Figure 1A). A negative shift in the EEG signal potential over the motor cortex, reflecting an increased level of brain activity, starting around 2s before MOn (Shakeel et al., 2015; Wright et al., 2011). Most commonly, the MRCP is defined with two pre-movement components, which occur in a stereotypical pattern across different experimental conditions: 1) Readiness Potential (RP), sometimes also referred to as the Bereitschaftspotential (BP; German for 'readiness potential'), and 2) Negative Slope (NS). Both components are described as "gradually arising" during their respective periods, with RP rising more slowly and NS exhibiting a much steeper ascent (Shakeel et al., 2015; Wright et al., 2011). The RP is more diffuse and centrally located over the scalp, while the NS is lateralized to the contralateral side of the moved limb, thought to reflect activation in the supplementary motor area and primary motor cortex, respectively (Fairhall et al., 2006). There is some disagreement about the name of this neural correlate in the literature. Some authors refer to the entirety of the MRCP as the 'BP' or 'RP' (see example in Figure 1A) (Fairhall et al., 2006; Leuthold et al., 2004; Schurger et al., 2012; Singh & Natsume, 2022; Travers et al., 2020), while others differentiate based on whether the movement is self-paced (i.e., move whenever you want), cue based (referred to as Contingent Negative Variation, CNV) or predicted (Stimulus Preceding Negativity, SPN) (Brunia et al., 2012; Jankelowitz & Colebatch, 2002; Mrachacz-Kersting et al., 2012; Neuper & Pfurtscheller, 2001; Shakeel et al., 2015). Some claim the late CNV component is equivalent to the (M)R(C)P (Leuthold et al., 2004; Rohrbaugh & Gaillard, 1983), a view that aligns with the observation that, while the CNV is typically measured in a 'two-warning cue' paradigm using central electrodes (e.g., FCz, Cz, etc.), rather than those over the motor cortices (e.g., C3 or C4), and is stimulus-locked (Leuthold et al., 2004). The CNV analysis is often accompanied by a 'Lateralized Readiness Potential' (LRP) (Figure 1B), calculated using the double subtraction method and focusing on electrodes over the motor cortex, which is a response-locked measure. Taken together these observations suggest that the CNV holds the information present in the RP component, while the LRP extracts the NS component of the MRCP, showing the same steep decline 400-200 ms before MOn (Leuthold et al., 2004; Leuthold & Jentzsch, 2002). However, others still argue that the late CNV is not exactly like the (M)R(C)P, as the CNV component reflects more than just motor preparation (Hamano et al., 1997). Nevertheless, there is a consensus that there is a display of a gradual buildup of electrical potential that occurs over the motor areas, reflecting processes of anticipation, planning and preparation preceding voluntary movements (Brunia et al., 2012).

Pre-movement Event-Related Desynchronization (ERD) (Figure 1C) is another neural correlate of movement and movement preparation (Fairhall et al., 2006). Where MRCP is a motor event induced potential shift in the time domain, ERD is a motor event induced shift in the frequency domain, specifically in ongoing sensorimotor rhythm power (8 - 20 Hz, i.e., alpha, and low beta band power) starting 2 seconds before MOn (Neuper & Pfurtscheller, 2001; Pfurtscheller & Lopes Da Silva, 1999; van Wijk et al., 2012). Unlike the MRCP, ERDs manifest contralaterally and become bilateral at the point of MOn. Initially, during the pre-movement stages, alpha activity is more spatially focused, while beta activity is more widespread (Toro et al., 1994). However, this pattern reverses shortly before and during motor execution, with alpha activity becoming more diffuse before refocusing at a later stage when the movement is sustained. In contrast, beta activity remains relatively more focused but returns to baseline more quickly than alpha, to the point that beta ERD is sometimes absent during motor execution (Crone et al., 1998).

Figure 1

Neural Correlates of Motor Control as Reported in the Literature

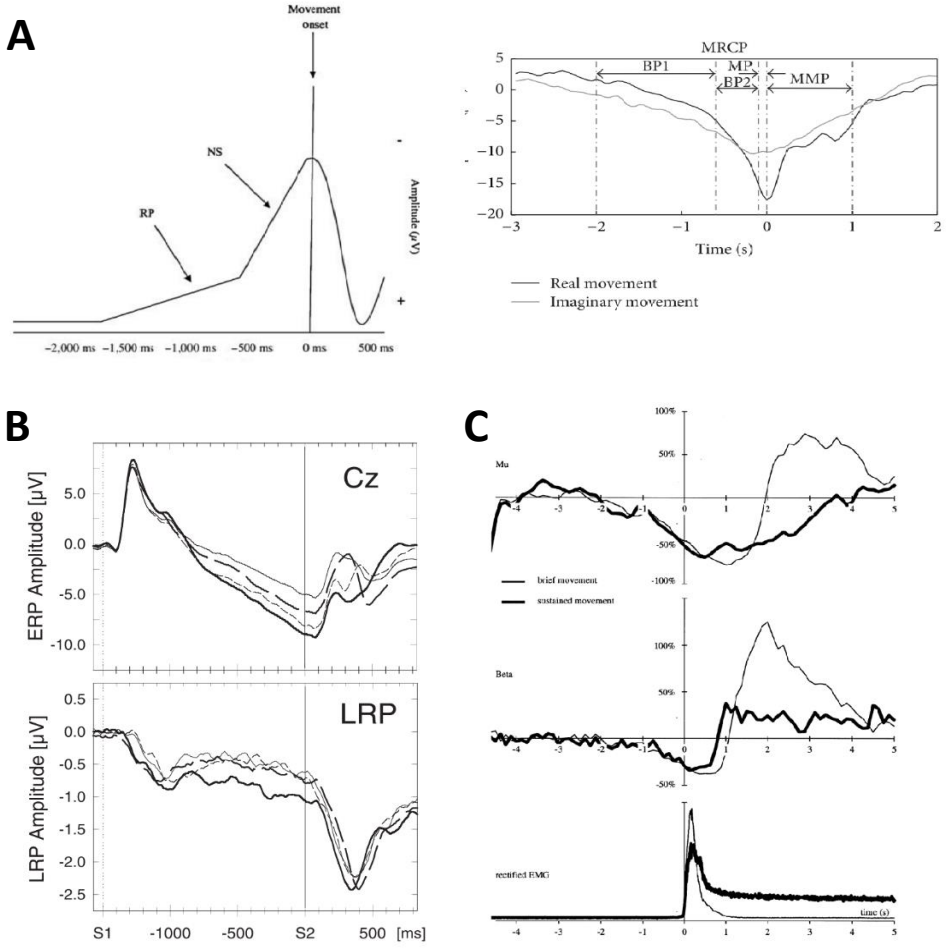

Note: The top of the figure (A) shows the MRCP from Wright et al. (2011) (left) and (A) Shakeel et al. (2015) (right). The bottom left (B) displays the CNV (top) and LRP (bottom) from Leuthold et al. (2004), while the bottom right (C) illustrates the average progression for alpha and beta band ERD around MOn from Cassim et al. (2000).

ERD and MRCP share several similarities. Both are observed during the same voluntary movement motor tasks and are generated by both action execution as well as Motor Imagery (MI), where a person imagines executing an action, activating the motor areas without acting upon this intention (Jankelowitz & Colebatch, 2002; Pfurtscheller & Neuper, 1997). The neural correlates further exhibit spatial overlap in cortical areas. Specifically, the regions showing the greatest MRCP amplitude correspond to those with the largest ERD response. This is mainly in the alpha band, while beta frequencies, being more diffused prior to movement, show less defined spatial similarities. This overlap implies the presumed origins of the ERD and MRCP could potentially reside in the same cortical structures (Leocani et al., 1997; Toro et al., 1994). However, research also identified differences between the neural markers, such as the mirrored lateralization of their topographical patterns and their inverted evolution over time leading up to MOn (Shibasaki & Hallett, 2006; Stancák & Pfurtscheller, 1996; Toro et al., 1994). Additional findings include the lack of correlation between ERD magnitude (in either frequency band) and MRCP amplitude—whether for the NS or peak MRCP (100ms after MOn; Toro et al., 1994)—and the preservation of beta frequency ERDs despite neural deterioration that leads to reduced MRCP amplitude (Bai et al., 2006; Toro et al., 1994). Preservation of one frequency band and not the other, combined with their distinct activity patterns across the scalp, further suggests that the two rhythms may also be somewhat independent, each serving a unique functional role (van Wijk et al., 2012). Meaning, despite MRCPs and both ERDs origins in seemingly the same cortical structures, the physiological mechanisms governing these events may be very different.

Having different generators suggests that the neural correlates provide distinct information, leading to the possibility that ERD and MRCP are independent indices of movement preparation (Schultze-Kraft et al., 2016). However, as noted by Toro et al. (1994) and discussed earlier, certain consistencies emerge in what might initially appear as differences in their topographical patterns, particularly in their mirrored and inverted temporal evolution (i.e., the opposing trajectories of ERD and MRCP). In the final 500ms before MOn, the bilateral spread of alpha ERD across the scalp coincides with the lateralization of the MRCP's NS/LRP component. Similarly, beta ERD starts more diffusely, aligning with the central spread of RP over the scalp, and later becomes more localized over the motor cortices (Fairhall et al., 2006), mirroring the lateralization of the NS/LRP component. These findings suggest that beta rhythms are more closely associated with motor preparation and execution processes, aligning with the presumed role of the NS/LPR component of MRCP (Lattari et al., 2014; Singh & Natsume, 2022). In contrast, alpha desynchronization is observed not only in motor areas but also in regions related to attention and sensorimotor integration (Crone et al., 1998; Fogassi et al., 2005). The progression of alpha ERD, which spreads contralaterally in tandem with increasing RP amplitude and

bilaterally with NS/LRP lateralization, suggests that alpha activity may play a broader role in coordinating the cognitive networks both before (planning and anticipation) and after (refinement) movement execution, likely through sensorimotor processing (Crone et al., 1998; Fogassi et al., 2005; Neuper & Pfurtscheller, 2001). Therefore, ERD in both frequencies and MRCP are likely to all be related to similar events in motor cortex activation, rather than completely individual and independent processes (Toro et al., 1994).

Despite the apparent similarities in how ERDs and MRCP relate to motor preparation and execution, the literature reveals notable inconsistencies in how different studies associate these neural correlates with specific cognitive processes. The precise nature of the distinct information these neural markers provide on the various stages of movement preparation remains an open debate. Traditionally, MRCP is considered to reflect planning and preparation, with its components—RP and NS—corresponding to these stages respectively (Shibasaki & Hallett, 2006; Wright et al., 2011). ERD, on the other hand, is often said to reflect a more general state of movement intention (Daly et al., 2018; Sakamaki et al., 2018; van Wijk et al., 2012). However, the MRCP (BP/RP) has also been stated to reflect movement intention (Shakeel et al., 2015; Singh & Natsume, 2022) and, conversely, the ERD described as an indicator of planning and preparation (Lakany & Conway, 2007). Some researchers argue that the classical view of planning and preparation, as captured by the MRCP, oversimplifies the pre-movement process. Rather than adhere to the two fixed stages, researchers suggest movement preparation processes emerge through a consistent reduction of neural variability prior to movement—a process akin to *making a decision to act* (Khalighinejad et al., 2018; Schurger et al., 2012). Ultimately, the literature disputes the precise mechanisms and cognitive functions (planning, preparation, intention, or decision-making) represented by these neural markers. This ongoing debate underscores the complexity of pinpointing the exact processes driving changes in neural activity. Perhaps the answer lies in a *both/and* perspective rather than an *either/or* interpretation. As previously discussed, these motor preparation and execution processes are inherently interwoven. Neural dynamics further illustrate this synchronous operating nature of motor control, with ERD and MRCP appearing to reflect overlapping contributions among the stages of movement preparation. Nonetheless, both ERD and MRCP are robust precursors of movement (Travers et al., 2020; van Wijk et al., 2012), appear over similar timelines to MOn (from approximately 2 seconds prior to movement), and are integral to the planning, preparation, and execution of movement. Observing either marker enables the detection of a person's intention to move and can therefore be described and used as such, underscoring their utility in movement-related studies and applications (Lakany & Conway, 2007; Shakeel et al., 2015).

Corticospinal excitability (CSE) is another widely explored component of the motor control neural substrate. Unlike ERD and MRCP, which reflect changes in brain activity measured via EEG, CSE

represents the activity of the corticospinal pathway and is assessed through Motor Evoked Potentials (MEPs). MEPs are changes in muscle activity induced by Transcranial Magnetic Stimulation (TMS) and recorded using electromyography (EMG) (Duque et al., 2017). Pre-movement changes in CSE are thought to correspond to the preparation of neural populations for movement initiation (Leocani et al., 2000, 2001), enabling the generation and transmission of coherent signals necessary for this process. As such CSE is often described as a marker of neural readiness for signal transmission, reflecting the state of excitability within the corticospinal pathway. Where the changes in neural populations prime the corticospinal tract for efficient signal propagation, facilitating rapid and accurate motor execution (Ibáñez et al., 2020).

Higher CSE levels, indicated by increased MEP amplitudes, suggest that the neurons in the pathway are optimally prepared for signal transmission, whether to process sensory feedback (Gandolla et al., 2021) or forward motor commands (Daly et al., 2018; Ibáñez et al., 2020). Interestingly, a notable aspect of the temporal evolution of CSE is its reduction shortly before voluntary movement execution. It has been suggested that the synchronous nature of the movement preparation processes, particularly their interaction with decision-making, gives rise to competition as different action representations contend for selection (Duque et al., 2017; Klein-Flügge & Bestmann, 2012). This pre-movement inhibition is then thought to result from resolving the competition between potential movements. However, the pre-movement CSE inhibition has been well-studied in the context of (warned/cued) Reaction Time (RT) tasks, which emphasize the execution speed of an already selected response (Ibáñez et al., 2020). In these tasks, inhibition is less likely to arise from competition resolution. Any competition is more likely to occur during the early stages of movement preparation and may contribute to pre-movement inhibition in CSE when the selected movement is not predetermined. Instead, this inhibition is proposed to primarily function as a necessary safety mechanism to prevent premature movement initiation (Duque et al., 2017). Recent studies by Hannah et al. (2018) and Ibáñez et al. (2020) challenge both these interpretations, noting that the temporal profile of CSE and its associated inhibition are similar for different types of movement, including speeded reactions, predictably timed movements, and self-paced actions (Ibáñez et al., 2020). Consequently, it is more likely that the pre-movement CSE reduction serves as an essential and more general component of movement preparation and initiation, regardless of how the movement is triggered (Ibáñez et al., 2020). Specifically, Ibáñez et al. (2020) propose that the CSE inhibition reflects a transition in neural populations toward more stable conditions (i.e., a state of reduced variability in their activity), shifting from a state of maintaining constant output to one that initiates movement. While the exact purpose of the inhibition remains debated, the various theories proposed in the

literature are not mutually exclusive. It is possible reduced CSE has different generators and performs distinct functions depending on the movement type, context, and goal (Duque et al., 2017).

In conclusion, it may seem intuitive or logical that the decision and intention to move must precede the planning and preparation of movement, and the act and react phases occur sequentially. However, the associated neural activity suggests otherwise. These processes likely occur in tandem. Some research even indicates that these neural correlates of movement preparation, along with the underlying processes, precede the conscious awareness of the decision to act (Fairhall et al., 2006; Haggard & Eimer, 1999; Lavazza, 2016; Libet et al., 1983; Soon et al., 2008). Regardless, these processes—reflected by the discussed neural correlates—function as prerequisites for the conscious intention to act (Khalighinejad et al., 2018; Travers et al., 2020). Ultimately, the temporal dynamics of movement preparation highlight the complexity and simultaneous nature of these processes, which are integral to both intentional and habitual action experiences.

1.2 Motor Learning

As mentioned at the beginning of this chapter, the average able-bodied individual moves with little conscious effort. This lack of effort, however, just reflects our efficiency and extensive practice in coordinating these movements. Optimal movement execution relies on the continuous monitoring of both our environment and the state of our body, with internal motor representations being constantly consulted and updated (Butterfill & Sinigaglia, 2014). This ongoing process of movement refinement is inherent to motor control, as demonstrated by the dynamic interactions within the FoFe-loop. Consequently, learning to move in new ways and gradually reducing the conscious effort required is integral to motor production and control.

Motor learning can thus be defined as the adaptive process of refining feedforward commands to act, based on (sensory) feedback obtained through the repetition of a movement or skill (Kitago & Krakauer, 2013; Wolpert et al., 2001; Yang et al., 2017). Initially, this process of motor learning begins with predictions formed from limited experience and knowledge, giving rise to early-stage motor representations. These representations are then used to generate imprecise or inaccurate feedforward commands. As the movement is repeated, these predictions are refined and updated in response to sensory feedback, resulting in more accurate and efficient execution over time through a process of error correction and adaptation (Butterfill & Sinigaglia, 2014; Wolpert et al., 2001). During automatic or well-learned actions, these motor representations are accessed unconsciously. However, they can also be accessed consciously, such as when imagining a movement (i.e., motor imagery (Butterfill & Sinigaglia, 2014; Jeannerod, 1995) or actively using knowledge to replicate an observed action. This

dual mode of access reflects the two ends of the motor learning spectrum: implicit and explicit learning.

Implicit learning underscores the automatic aspects of motor control. It primarily relies on repetition and sensory feedback to shape motor representations over time, often without the learner being fully aware of the process. For instance, an infant learning to walk relies on early-stage motor representations, which are initially formed through observing others—a process thought to be supported by the mirror neuron system. Observing others not only aids the formation of these representations but is also believed to enable their unconscious access (Cannon et al., 2014; McGregor et al., 2017), thought to facilitate mimicry, and enabling the infant to perform actions subconsciously (Bardi et al., 2015; Brass & Heyes, 2005; Cannon et al., 2014). Through repeated practice, the infant improves without being fully aware or employing intentional strategies aimed at walking better. In this way, a new skill is acquired without gaining increasing knowledge of the performance itself (Hashemirad et al., 2016; Jongbloed-Pereboom et al., 2015). Explicit learning, in contrast, involves conscious effort, knowledge, and goal-directed strategies aimed at improvement (Hashemirad et al., 2016). For example, when learning to play the piano, individuals follow explicit instructions on finger placement, rhythm, and key pressure, consciously monitoring their hand coordination to avoid mistakes. In this case, the learner knows the desired outcome, how and what is needed to execute the actions, and consciously adjusts aspects of their execution to refine the performance (Hashemirad et al., 2016).

Notably, these modes of learning are not mutually exclusive, nor are they processes with fixed sequential orders; they often coexist and interact dynamically, with their relative contributions shifting throughout the learning process (Maresch et al., 2021). A beginner might implicitly acquire a skill through repetition but later refine their performance by applying explicit strategies. The process of learning to walk, for example, is largely implicit during infancy. Infants repeat movements, improving without employing, or even being fully aware of, intentional strategies to enhance walking. Over time, this practice leads to competence. Later in life, however, a person may explicitly apply techniques to improve their gait and posture to reduce knee strain or address other biomechanical concerns. Conversely, learning to type on a keyboard initially requires conscious attention to key locations and finger movements. As the skill becomes well-learned, however, improvement occurs largely through repetition, without intentional focus on specific aspects of performance. These processes can also cycle back and forth. For instance, in learning a single action, one might start by applying explicit strategies to learn a specific component, then improve through sheer repetition, before advancing to the next component of the action. On a broader scale, someone adept at walking and running might find their coordination does not immediately transfer to riding a bike. Learning to cycle demands more

conscious effort initially, as one must master balance and propulsion. Once basic competence is achieved, cycling improves through repetition. If further refinement is desired—such as learning to ride without holding the handlebars—conscious effort and explicit strategies are again required. Further emphasizing the complementary nature of both learning types, research suggests there is little difference in the quality of skill performance once a certain level of proficiency is reached. Showing both implicit and explicit learning can result in similar levels of movement automaticity—that is, the extent to which a movement can be executed without directing attention to its details (Kal et al., 2018). Although both implicit and explicit learning contribute to skill acquisition, certain learning types may better suit specific tasks, particularly in terms of the speed of improvement. For instance, while it is not improbable to learn to play the piano by repeatedly pressing keys and developing a 'sense' for melody and rhythm without fully understanding the mechanics, such implicit approaches are often less efficient for mastering a complex task. In this specific scenario, and other tasks requiring intricate coordination or higher levels of precision, explicit learning, with its structured strategies and conscious refinement, is likely to yield faster improvements.

As discussed thus far, motor control, as conceptualized through the FoFe-loop, encompasses the processes central to both acquiring and refining new skills. However, the mechanisms of motor learning are not only essential for skill acquisition but also for regaining lost motor functions (Winstein et al., 2003). In many cases of motor impairment, the ability to move may be compromised, but the underlying principles of motor control often remain intact. This is particularly relevant in cases following stroke or injury to the neural motor pathways, where the loss of motor function results from impairments in the transmission of feedforward signals or the integration of feedback due to disruptions in these pathways, rather than irreversible damage to muscles or absent tissue[1] (Winstein et al., 2003). A stroke is a neurological event where brain cells die due to a (sudden) cut off blood supply or bleeding into the brain (Bonita, 1992; Hossmann, 2006). Given the high prevalence of stroke, millions of individuals worldwide live with its consequences, including cognitive and motor dysfunctions that significantly impact their quality of life (Hatem et al., 2016; Nys, 2005). While stroke symptoms vary depending on lesion location and severity (Barker-Collo et al., 2010; Nys, 2005), motor function deficits—particularly of the contralateral upper limbs—are among the most common (Hatem et al., 2016). Rehabilitation for stroke-based motor impairments is a key consideration within this thesis's theoretical framework. Stroke is used as the primary example due to its prevalence and well-documented impact on motor function, but the motor rehabilitation principles discussed extend to

[1] Damaged or absent tissues can sometimes be replaced with assistive technologies, such as (robotic) prosthetics. In such cases, individuals must relearn to move using the replacement limb, applying motor learning principles much as they would when relearning to move with their natural arm.

other conditions involving focal central nervous system (CNS) damage, such as spinal cord injury (SCI) and brain trauma (Dobkin, 2009). However, the core focus remains on understanding the neural mechanisms of motor learning, with the aim of leveraging these insights for motor recovery. To this end, this thesis emphasizes the parallels between motor learning and relearning. These principles, however, do not apply in the same way to progressive neurodegenerative disorders (conditions like multiple sclerosis and Parkinson's disease), where motor impairments arise from ongoing neuronal deterioration rather than a single injury event. Even though both involve damage to CNS, they differ in terms of pathology and rehabilitation approach. Any further mention of stroke and rehabilitation will refer specifically to motor impairments resulting from stroke-related neural damage, while recognizing that similar mechanisms may apply to other focal CNS-related motor deficits.

When part of the motor control system remains functional—assessable, for instance, through MI and EEG showing relevant activity patterns over the motor cortex—motor learning principles can be applied as a core part of motor rehabilitation. Through proper assistance and repetitive, task-oriented activities—alongside interventions such as increasing muscle strength and sensory processing (Bolognini et al., 2016; Chen & Shaw, 2014)—the rehabilitation process mirrors that of initial skill acquisition (Maier et al., 2019; Van Peppen et al., 2004).

For example, stroke patients recovering hand function might perform repetitive grasp-and-release tasks using objects of varying sizes to improve (fine) motor control. Therapists may initially guide the patient's hand to correct compensatory movement patterns and ensure proper muscle activation. This approach provides real-time feedback through visual and tactile cues from the movement of the affected limb, complemented by verbal input from the therapist to reinforce correct performance. As the patient's performance improves, assistance is gradually reduced to encourage independent attempts and foster self-regulation. To add challenge and target specific movement struggles, tools such as resistance bands or weights may be introduced. These tools can increase the difficulty of repetitive movements or enable focused training on distinct components of a movement sequence. For instance, repetitive arm extensions or lifting tasks can be practiced in isolation to strengthen specific muscles and improve coordination. By breaking down movements into manageable parts, therapists help patients refine their control over individual components, ultimately enhancing the execution of the complete movement (Franz et al., 2017; Maier et al., 2019).

As part of motor rehabilitation, these key principles of motor learning—repetition, feedback, and error correction—aim to engage the motor control system and adapt motor representations to overcome the disruptions in the system's feedforward and/or feedback pathways, with the goal of restoring motor function and supporting recovery (Kitago & Krakauer, 2013).

Motor learning is a process that relies heavily on neuroplasticity; the brain's innate ability to form new connections, strengthen existing ones, and prune unnecessary ones, allowing for neural adaptability (Dayan & Cohen, 2011; Murphy & Corbett, 2009). Motor relearning, in turn, leverages this capacity to overcome disruptions in neural pathways. This capacity for adaptation is intrinsic to the primary motor cortex, underscoring the inherent connection between motor control and learning. In particular, changes in synaptic strength are thought to represent the neural mechanisms by which motor skills are encoded within the nervous system (Kleim, 2009). This same mechanism, by extension, allows motor skills to be 're-coded' when necessary, such as during rehabilitation.

The parallels between the behavioral observations of motor learning and neuroplasticity are interesting, with the learning-dependent reorganization of movement representations corresponding closely to changes at the cortical level. Kleim (2009) even draws a direct comparison: conceptual motor representations align with the topography of neural connections in the motor cortex, referred to as 'motor maps.' The refining of motor representations—shaped by feedback and error correction—in turn mirrors the changes in synaptic strength within the motor cortical circuits responsible for specific movements (Kleim, 2009; Wolpert et al., 2001). This similarity becomes even more pronounced when considering the mechanisms of learning, whether acquiring a new skill, such as playing an instrument, or recovering from injury. Specifically, the repetitive aspect of learning and refining motor skills behaviorally mirrors the iterative adjustments occurring in neural networks (Lisman & Spruston, 2005). Just as repeated engagement with the FoFe-loop refines motor control behaviorally, the repeated activation of neural pathways strengthens synaptic connections, facilitating the reorganization of motor circuits. This iterative activation of specific neural pathways is essential for promoting neuroplasticity, driving synaptic strengthening and cortical reorganization of motor circuits (Lisman & Spruston, 2005). Ultimately, this improves motor control and enhances interactions with the environment (O'Malley et al., 2006; Ward, 2015). By applying motor learning principles, these processes can be harnessed to facilitate functional recovery and rehabilitation, supporting the restoration of motor skills through cortical reorganization. To continue our earlier example of recovering hand function following stroke, damage to the motor cortex often disrupts the pathways leading feedforward motor commands to muscle activation. Patients often show some degree of spontaneous recovery, as neuroplasticity allows the brain to reestablish connections to a limited extent (Murphy & Corbett, 2009). This recovery rate can then be further enhanced through rehabilitation therapy, where interventions help optimize the neuroplasticity process, guiding the brain to reorganize and strengthen motor pathways that were disrupted. In many cases, some motor commands may still pass through, allowing for traditional assistive physical therapy. Such rehabilitation protocols focus on reinforcing whatever motor function remains post-stroke, helping the patient regain movement

through repetition and error correction. While the original pathways cannot be fully reinstated, new neural connections can be forged, allowing the brain to reroute motor commands to the targeted muscles. However, in cases where no command can be transmitted at all, rehabilitation protocols can still apply motor learning principles to engage the motor system indirectly. For example, techniques like motor imagery, where patients respectively imagine performing movements, and action observation, where they watch others perform the movements, allow to activate the same neural pathways involved in motor control when no movement execution is possible yet (Cannon et al., 2014; Maier et al., 2019; McGregor et al., 2017). These methods are often seen as supplementary to physical therapy (Woldag & Hummelsheim, 2002), but when physical movement is not possible, these approaches can bypass the need for direct execution to still stimulate the motor circuits and help to facilitate cortical reorganization despite physical limitations.

So far, we have established neuroplasticity in a more general sense as the neural mechanism underlying learning, drawing parallels to the behavioral observations of motor learning. We noted that neuroplasticity is an inherent capacity of the brain, involving changes in the synaptic strength of connections between neurons and relying on repeated activation of specific neural pathways to drive and consolidate these changes.

Several theoretical frameworks have been proposed to further explain the principles of neuroplasticity and the biological processes that enable it. One of the most well-known is the Hebbian principle, which provides a broader functional framework for understanding synaptic strengthening. This theory outlines the core principles of what changes in the brain, focusing on the associative relationship among neural activity. According to Hebbian learning, the strength of a synaptic connection depends on whether the activity of a presynaptic neuron consistently contributes to the firing of a postsynaptic neuron. The theory highlights the importance of coordinated activation—either simultaneous or rapid sequential—in strengthening synaptic connections and shaping neural circuits. This idea is encapsulated in the now iconic phrase: *Neurons that fire together, wire together* (Feldman, 2012; Hebb, 1949).

Other theories have sought to delve deeper into the biophysical mechanisms underlying neuroplasticity at the cellular level. One such theory is Spike Timing-Dependent Plasticity (STDP), which mechanistically extends Hebbian principles by focusing on how precisely timed neural activity drives synaptic changes. STDP highlights the critical role of millisecond-level timing between pre- and post-synaptic activity. Not only to address the strengthening of synaptic connections but also incorporating the weakening of ineffective synapses. In short, STDP states that, when a presynaptic neuron fires just before a postsynaptic neuron, synaptic strength increases, a phenomenon known as long-term potentiation (LTP). Conversely, when the postsynaptic neuron fires first, synaptic strength decreases,

referred to as long-term depression (LTD). This model underscores a causality that is inherent in neural activity patterns and emphasizes that synaptic plasticity depends on the precise temporal coordination of neural signals (Feldman, 2012; Stefan, 2000).

However, critics argue that the processes and principles underlying neuroplastic adaptation, particularly synaptic plasticity, are far more complex than those classically defined by STDP (Carson & Kennedy, 2013; Lisman & Spruston, 2005). These critics propose an alternative perspective, which suggests that neuroplasticity, particularly potentiation, is influenced by the general activity state of the neural network (Carson & Kennedy, 2013; Ganguly & Poo, 2013). This activity-dependent plasticity framework emphasizes a mechanism where changes in neural circuits extend beyond synapses and involve broader biological processes. These changes are proposed to occur over, and are guided, by various levels of neural activity (e.g., calcium signaling, gene expression, and protein synthesis) (Berridge, 1998), with the magnitude and duration of neuronal activity driving both synaptic and structural changes. For instance, this framework describes how neurons subjected to sustained activity, through repetitive use or stimuli, undergo alterations in synaptic strength, dendritic growth, or pruning (Ganguly & Poo, 2013).

While incredibly interesting, an in-depth exploration of the biophysical working principles of neuroplasticity is beyond the scope of this thesis. For readers seeking further details, we recommend the works of Lisman & Spruston (2005), Feldman (2012), Carson & Kennedy (2013) and Ganguly & Poo (2013), who provide extensive discussions on the evidence supporting these theories as well as critiques and nuances necessary for a more comprehensive understanding.

How exactly the brain reorganizes (i.e., the precise mechanisms of neuroplasticity) remains a subject of ongoing debate, particularly regarding which theoretical framework best explains its workings and the driving biological mechanisms. Nevertheless, there is consensus across these theories on certain central principles of neuroplasticity. Broadly speaking, the brain is recognized as a self-organizing, plastic system that adapts through repeated, sequential activation of neural pathways. While the general Hebbian principle holds true across theories, the relationship between neural activity is now understood to be more nuanced. It is not simply that cell A must consistently activate before cell B; rather, if cell A and cell B fire simultaneously—or if B fires shortly after A—this temporal relationship is more likely to be interpreted as causal, thereby increasing the contingency between the two neurons. It is then crucial to repeat and sustain activation across this pathway to reinforce lasting neural changes.

While the specific mechanisms of neuroplasticity continue to be debated, it is well-established that learning is accompanied by the reorganization of synaptic connections—that is, the brain changes. As such, when motor learning occurs, it is reasonable to expect that these synaptic and structural changes will also manifest as changes in the neural correlates of motor control (Dayan & Cohen, 2011). Existing research supports this notion. For example, studies have demonstrated that the amplitude of the MRCP increases (i.e., neural marker becomes more negative) during the learning process. However, once performance stabilizes and no further improvement is observed, MRCP amplitude often returns to baseline or decreases even further. This aligns with findings comparing experts and novices in skilled tasks, where experts exhibit smaller MRCP amplitudes and later onset times (Wright et al., 2011). Siemionow et al. (1998) further suggest that MRCP amplitude reflects the number of neurons recruited for movement execution. Early in learning, when predictions of feedforward commands are inaccurate, greater neural resources are engaged, possibly reflecting competing motor commands. As learning progresses, movement execution becomes more efficient, requiring fewer resources—following the principle of minimal effort, where the most direct and efficient neural pathways are favored. Similarly, motor learning is associated with a reduction in oscillatory power, particularly an increase in ERD strength over the course of training. Both implicit and explicit learning are accompanied by a decline in alpha-band power, particularly at electrode C3 over the motor cortex (Yang et al., 2017; Zhuang et al., 1997). However, findings on CSE are more inconsistent. While some studies indicate that skill training increases CSE, as reflected in larger MEPs post-training (Kleim, 2009; Leung et al., 2017; McGregor et al., 2017), other studies report no significant changes in CSE during skill acquisition (Berghuis et al., 2016). The association between CSE and learning has led to the interpretation that MEPs may serve as an indirect marker of neuroplasticity (Kleim, 2009). However, CSE changes are more accurately understood as evidence that plasticity *has occurred*—suggesting that learning has already taken place rather than being actively in progress (Christiansen et al., 2018).

Overall, a reduction in neural activity following learning is often assumed to reflect stronger synaptic connections and more efficient cortical processing. This forms the foundation for examining how learning shapes specific patterns of brain activity, a key focus of this thesis.

What does this mean for studying the effects of learning? When examining neural changes due to skill acquisition, we must avoid the fallacy of reasoning in absolutes—i.e., assuming distinct, fixed levels of neural activity for a *highly learned skill* versus a skill that one has *just started acquire*. Much of the literature on neural correlates, particularly the studies reviewed in 1.1 Neural Activity of Motor Control, primarily reflects the average neural activity associated with well-practiced, nearly automatic movements. This is especially true for studies using simple movements performed by the dominant right hand—actions repeated daily across various contexts, environments, and goals, effectively

representing a kind of “final level of learning.” This raises a critical question: how does one establish a true equivalent of a “non-trained” state? This issue is particularly important when comparing neural activity across different movement conditions, as “final form” patterns in neural activity vary depending on factors such as limb type, force exertion, movement abruptness, and execution speed (Stancák & Pfurtscheller, 1996). A logical answer would be to compare “dominant hand with none-dominant.” However, when neural activity across limbs differ handedness further complicates comparisons, as left-handed individuals, due to living in a predominantly right-handed world, often exhibit ambidextrous tendencies not seen in right-handed individuals (Stancák & Pfurtscheller, 1996; Tarkka & Hallett, 1991).

Therefore, when discussing learning effects, it is more meaningful to focus on the *direction* of change rather than assume rigid start and end points. Instead of searching for an absolute baseline, learning can be examined through measurable improvements in motor skill and the corresponding shifts in neural activity. One way to approach this is by slightly increasing the complexity of previously studied well-practiced right-hand movements, thereby introducing a relative challenge while maintaining comparability to existing research (Wright et al., 2011).

1.3 Brain-Computer Interfaces

While the learning element inherent to the motor control/FoFe-loop system facilitates improvement and refinement through repetition, simply increasing repetition is not always sufficient to restore weakened or interrupted connections. Chen et al. (2020) found that even when progressive resistance training was increased to 10,000 repetitions over eight weeks (200 per day), there was no significant improvement in muscle strength following SCI. While progressive resistance training has been effective in enhancing voluntary strength in muscles, its benefits appear limited for muscles weakened due to SCI, regardless of the number of repetitions. This issue—where repetition alone is not enough—is also evident in robot-assisted therapy. Robots can deliver a higher volume of exercises compared to physiotherapists, effectively increasing the amount of therapy provided within the same time span. However, clinical results remain inconclusive regarding whether robot-assisted therapy offers significant advantages over conventional therapy (Lo et al., 2010; Wagner et al., 2011; Zorowitz & Brainin, 2011). One possible explanation is that robot-assisted therapy primarily increases repetition without fundamentally altering the underlying rehabilitation model. If mere repetition were enough, we would expect clearer benefits. Furthermore, while the quality of an acquired skill is often comparable across different learning methods in the context of learning a new skill (i.e., regular motor learning), research indicates that implicit learning is often hindered for limbs contralateral to the affected side of the brain following stroke (Kal et al., 2016). This aligns with our earlier discussion on how different actions and contexts may favor one type of learning over another. In the case of

relearning after neurological damage, implicit learning may be less effective, reinforcing the idea that mere repetition is insufficient. Instead, relearning may favor explicit learning, where conscious engagement plays a critical role in driving recovery. This distinction is important, as reports of post-stroke rehabilitation where repetitive practice leads to strength improvements typically involve goal-directed repetition (e.g., task-specific training, constraint-induced movement therapy, assistive technology, cycling, etc.) (de Sousa et al., 2018). As such, these studies show that performing a task repeatedly strengthens muscles through increased use—an expected outcome. In other words, recovery is not driven by repetition alone, but the repeated engagement of the full FoFe-loop. This does not contradict the necessity of repetition in relearning to move, but highlights that repetition alone is insufficient (de Sousa et al., 2018).

Altogether, these findings restate our central theme: to induce meaningful neural changes and enhance recovery—whether through behavioral exercises, MI and repeated mental practice, or electrical stimulation (Mrachacz-Kersting et al., 2012, 2016; Stefan, 2000; Stefan et al., 2002)—rehabilitative interventions must be timed to align with the FoFe-loop parameters of the brain (O'Malley et al., 2006; Wolpert et al., 2001). That is, we must work with and according to the principles of motor learning. In the context of relearning and rehabilitation, this means engaging in a structured, conscious process: generating an outcome, evaluating it against the intended goal, and iterating accordingly. The feedforward command is continuously compared to incoming feedback, motor representations are updated, and a revised forward command is generated. As sensory feedback is processed, neural pathways contributing to successful outcomes are repeatedly activated, reinforcing individual neural connections. These small-scale changes collectively restructure and strengthen the larger neural circuits responsible for executing movement successfully.

When motor function is at least partially retained, traditional assisted therapy (as detailed in Section 1.2) naturally facilitates engagement in the FoFe-loop. In this rehabilitation context, movement attempts are observed, execution is assisted, and proper form is guided to approximate a full run-through of the FoFe-loop. As such, the rehabilitation interventions help complete and reinforce the FoFe-loop by ensuring that actions generate sensory feedback. When a motor command is issued, resulting in an action, and sensory feedback informs the quality of the movement, enabling more informed repeated attempts.

However, what happens when no observable movement execution remains? How can we ensure that interventions are applied in a way that meaningfully supports recovery? How do we know if our assistive interventions align with any aspect of the FoFe-loop beyond simply moving limbs and hoping for the best? As noted earlier, MI and movement observation can help strengthen the preparatory aspects of movement execution (Maier et al., 2019). During MI, therapists may still assist by moving

the patient's limb, providing sensory feedback that simulates aspects of motor execution. In theory, this feedback can engage the FoFe-loop processes, facilitating adaptation. However, whether this engagement is sufficient to drive functional recovery remains uncertain. MI is typically considered complementary to more action-focused rehabilitation approaches (Maier et al., 2019; Woldag & Hummelsheim, 2002), with its precise contribution remaining unclear. Most rehabilitation gains are likely achieved through a complex combination of spontaneous and learning-dependent processes (Hatem et al., 2016), where recovery rates are enhanced by structured therapy. This raises the possibility that any observed benefits of MI and repeated mental practice may, at least in part, be due to an interaction with spontaneous recovery processes. Yet, the question remains: Is this enough? How crucial is the timing of feedback and these interventions for successful rehabilitation? How important is it to engage with the FoFe-loop versus meaningfully engaging with it? As we have argued, it is possible to engage with parts of the loop (e.g., generating motor commands without execution, as in MI, or receiving feedback without active motor engagement, as in robot assisted activity), but mere repetition of such partial interactions is insufficient. For functional recovery, the full cycle must be engaged within a way that drives adaptation.

The natural course of spontaneous recovery follows a logarithmic, nonlinear pattern, with most improvements reportedly occurring within the first three months following injury (Hatem et al., 2016). Since spontaneous recovery follows its own trajectory, this complicates efforts to isolate the effects of intervention (Hatem et al., 2016). Murphy & Corbett (2009) go further, suggesting that the optimal time window to engage and direct neuroplasticity to have a positive effect on motor recovery may span only a few weeks post-stroke. Beyond this period, the rate of recovery slows, and functional improvements become more difficult to attain (Nepveu et al., 2017). However, while challenging, recovery is not strictly confined to this early window. Research consistently shows functional progress remains possible through adaptive learning strategies alone (Carey et al., 1993; Kübler et al., 2017; Yekutiel & Guttman, 1993). Nevertheless, interventions that either promote neuroplasticity early after stroke or extend this initial window have the greatest potential to improve motor recovery (Nepveu et al., 2017; Pino et al., 2014).

Technological advancements and an increasing understanding of the human brain have provided new prospects to enhance the quality of life for people with disabilities that affect function and mobility (Winstein & Requejo, 2015). One such avenue is Brain-Computer Interface (BCI) therapy. By measuring brain activity and engaging specific neural signals, BCIs can translate brain activity into commands for various external devices, allowing users to interact with computers, robotic devices, or other assistive technologies (Guerrero & Spinelli, 2018; Pfurtscheller et al., 2003; Piña-Ramírez et al., 2018; Scherer et al., 2017). Traditional rehabilitation methods typically rely on independent movement execution,

often beginning with assisted movements. However, when movement execution is not possible, interventions are limited to passive limb movement (performed by a therapist or robot) or MI and repeated mental practice. Building on earlier discussions, MI can engage motor networks, yet its effectiveness is limited in rehabilitation due to the absence of the sensory feedback necessary for refining motor commands within the FoFe-loop (Maier et al., 2019). BCI technology offers a potential solution to bridge this gap by integrating motor intent detection with external reinforcement.

Unlike conventional rehabilitation techniques, BCIs use brain activity as a starting point, allowing for real-time estimation and tracking of FoFe-loop parameters and progression. This enables BCIs to integrate feedback with motor commands, facilitating neuroplastic changes more directly than traditional rehabilitation approaches. Noninvasive EEG-based BCIs, in particular, have shown promise in supporting motor recovery, helping patients re-learn movement, improve motor strength, and refine motor control (Guger et al., 2018). Their potential is especially notable for cases where movement execution is not yet possible, but where an individual can still access motor representations and cognitively plan movement at a cognitive level despite signal disruption between the brain and muscles. These BCIs leverage pre-movement neural signals, such as the ERD and MRCP, which are detectable even when overt movement is absent (Jackson & Zimmermann, 2012; Jankelowitz & Colebatch, 2002; Pfurtscheller & Neuper, 1997; Scherer & Vidaurre, 2018). These signals remain detectable even when the motor cortex is damaged, as seen in stroke patients (Remsik et al., 2017), allowing EEG-based BCIs to bridge the gap between movement intention and actual motor execution (Pichiorri et al., 2013, 2015).

This ability to decode movement intention allows BCIs to reinforce the FoFe-loop by providing real-time sensory feedback, mimicking the role of a therapist when voluntary movement is present. In traditional rehabilitation, therapists offer guidance by physically assisting movement, ensuring that sensory feedback aligns with the motor command. However, when no movement occurs, therapists lack direct indicators of the patient's movement plan or intent, making it difficult to provide well-timed reinforcement. BCIs circumvent this limitation by detecting neural activity linked to movement preparation and using this information to trigger sensory feedback in synchrony with detected neural markers of movement intent. To this end, the ERD and MRCP – two of the most widely explored neural correlates of motor control in EEG – have been recognized as valuable markers in the context of neural plasticity and the advancement of clinical rehabilitation protocols.

When BCI rehabilitation setups transform movement intention into real-time reinforcement feedback, this feedback can take various forms (Guger et al., 2018; Hurtier et al., 2016; Remsik et al., 2017), including:

(a) rewarding images or sounds,

(b) the movement of a virtual avatar performing the intended action (which doubles as visual feedback, potentially engaging the mirror system),

(c) actual movement via a motorized orthosis, providing both visual and proprioceptive feedback,

(d) functional electrical stimulation (e.g., TMS, tDCS), or

(e) combinations of these approaches

By providing feedback in response to movement-related brain activity, BCIs re-establish a closed FoFe-loop—where a feedforward command to act is met with sensory feedback on the executed action. This cycle is a fundamental feature of motor learning and is replicated in BCI-based therapy to support neural circuit reorganization (Ward, 2015). Ward (2015) emphasizes that motor learning depends on repeated sensorimotor integration and that a complete FoFe cycle is necessary for effective neural restructuring. This is where BCIs offer a key advantage over conventional physiotherapy: they allow reinforcement of the FoFe-loop even when the individual is unable to generate movement independently. By ensuring that sensory feedback is delivered in alignment with detected motor intention, BCIs provide a mechanism to sustain neuroplasticity-driven recovery.

The general belief is that the closer the feedback aligns with movement intent, the greater the potential for reinforcing adaptive neuroplastic changes (Hurtier et al., 2016; Remsik et al., 2017). Therefore, optimizing feedback timing within the FoFe-loop is thought to be a key factor in maximizing rehabilitation outcomes. With BCIs creating opportunities to augment recovery rates both in the critical early months post-injury and beyond (Kübler et al., 2017; Remsik et al., 2017). Rather than replacing traditional rehabilitation techniques, BCIs offer a complementary tool—enhancing recovery by providing precisely timed engagement with brain activity to promote neuroplasticity (Guger et al., 2018). Meaning, even in cases where some movement is preserved, BCIs can potentially provide more precise and timely engagement with the FoFe-loop than standard therapy alone. For example, BCIs have the potential to optimize robot-assisted rehabilitation, which has been explored as a means to increase therapy volume. While robotic devices can deliver more exercise repetitions than a human therapist, clinical outcomes have been inconclusive (Lo et al., 2010; Wagner et al., 2011), possibly because repetition alone is insufficient without appropriately timed feedback. BCIs could enhance robotic therapy by ensuring that robotic assistance is delivered in synchrony with detected neural markers of movement intent, rather than simply providing passive movement.

Other protocols besides BCI have demonstrated effectiveness in aiding individuals with motor impairments by leveraging neuroplasticity through the principles of closing the FoFe-loop. While BCI technology has proven effective in facilitating recovery by detecting motor intent and providing feedback to reinforce processes related to movement execution, another widely studied method—

Paired Associative Stimulation (PAS)—has been used to modulate neuroplasticity through a different mechanism and theoretical underpinning.

PAS protocols, like BCIs, aim to modulate neural circuits by timing sensory stimulation with cortical activity. Specifically, PAS involves the precise pairing of peripheral sensory stimulation (e.g., electrical stimulation of afferent pathways) with motor cortex activation, either through direct cortical stimulation (e.g., TMS) (Stefan, 2000) or through self-initiated cognitive processes, such as motor imagery (Mrachacz-Kersting et al., 2012, 2016). This repeated pairing over an extended period is thought to enhance the excitability of corticospinal projections from the primary motor cortex, making the neural connections more open/sensitive to input, which will reinforce the neural circuits responsible for motor function and thus also lead to changes (Stefan, 2000; Stefan et al., 2002). Unlike BCI, PAS relies on highly specific time windows to precisely pair cortical stimulation with afferent sensory input. PAS protocols require highly specific, millisecond-scale synchronization windows as small as 25 ms for the hands and 50 ms for the legs to maximize plasticity effects (Mrachacz-Kersting et al., 2012, 2016; Stefan, 2000). The underlying hypothesis is that optimal PAS effects occur when sensory input arrives at the motor cortex concurrently with motor-related cortical activation—a principle comparable to the need for synchronized feedforward and feedback interactions in the FoFe-loop. PAS has been widely used to investigate neuroplasticity mechanisms, and early successes were considered direct evidence supporting STDP-based plasticity models, suggesting that strict timing was essential for neuroplasticity-based rehabilitation (Feldman, 2012; Lisman & Spruston, 2005; Stefan et al., 2002). However, recent critiques challenge the assumption that such rigid time windows are necessary for plasticity induction (Carson & Kennedy, 2013). BCI-driven rehabilitation has demonstrated the ability to induce similar functional improvements despite not adhering to these strict intervals. Studies show that similar enhancements in MEPs have been observed following PAS and BCI-based interventions (Mrachacz-Kersting et al., 2012, 2016), suggesting that both approaches interact with neuroplastic mechanisms in comparable ways.

PAS aligns closely to the STDP framework, which emphasizes that a precise temporal relationship between sensory input and motor activity dictates whether synaptic connections strengthen or weaken. In contrast, BCIs provide real-time feedback in response to motor-related cortical activity (e.g., a virtual hand avatar moving in sync with ERD progression; Guger et al., 2018), without requiring pre-defined, externally imposed stimulation windows. Both PAS and BCI approaches have demonstrated efficacy in promoting neuroplasticity, yet BCIs' ability to dynamically adjust feedback based on ongoing brain activity gives them the potential to be a more adaptable and clinically viable approach for rehabilitation. This raises an important question: if both approaches can successfully leverage neuroplasticity, what is the most effective timing strategy for intervention? PAS suggests that

millisecond-precision windows are necessary, yet BCI-based approaches have shown improvements without adhering to such strict constraints. Given their conceptual similarities, PAS research—particularly on the relationship between sensory feedback and cortical activation—may offer valuable insights for optimizing feedback timing in BCI protocols (Mrachacz-Kersting et al., 2016).
However, understanding the optimal time window for interaction with the FoFe-loop remains an open challenge, highlighting the need for further exploration into which neural correlates should be targeted and when feedback should be delivered for maximum impact.

While BCIs have demonstrated potential in motor rehabilitation (Ang et al., 2011; Guger et al., 2018; Remsik et al., 2017; Winstein & Requejo, 2015), the technology remains in early development and faces numerous challenges. A key limitation is our incomplete understanding of how BCI-driven rehabilitation facilitates recovery and how to optimize its effectiveness—for example in refining the type and timing of feedback. We argue that both challenges stem from a broader issue: the lack of a well-informed framework linking BCI interventions to the fundamental mechanisms of motor learning and the neural circuits of motor control.

1.4 Problem Statement

As we have emphasized, effective rehabilitation depends on engaging the FoFe-loop in a way that promotes neuroplasticity (Ward, 2015). While traditional physiotherapy likely achieves this, its specific operative components remain unidentified (Maier et al., 2019; Woldag & Hummelsheim, 2002). Similarly, BCIs offer a unique opportunity to interface directly with motor learning mechanisms, but their full potential can only be realized by understanding *when* and *how* to engage with neural mechanisms underlying motor learning. Yet, the optimal parameters for leveraging BCIs to induce neuroplasticity most efficiently and effectively remain to be explored (Lisman & Spruston, 2005; O'Malley et al., 2006; Stefan, 2000). On one level, this includes identifying the neural correlates of motor control most relevant for recovery; on another, it involves determining the conditions under which the correlates are optimally engaged. Addressing these gaps is essential for advancing BCI rehabilitation beyond proof-of-concept studies and toward practical clinical application.
This thesis puts forward two interpretations through which the challenge of optimizing BCI can be approached. First, the role of timing in optimizing neuroplasticity-driven recovery is not well understood. Effective rehabilitation hinges on closing the FoFe-loop, yet it remains unclear which neural correlates are best targeted and what is the optimal point within motor-related brain activity for feedback engagement to maximize impact. Second, BCI protocols rely on static assumptions about neural markers of movement production, despite established evidence that these markers undergo changes as learning progresses. Motor-related brain activity is not fixed; rather, it adapts with

experience and skill acquisition, meaning that feedback timing and intervention strategies may also need to evolve dynamically.

1.4.1 Timing in Neuroplasticity & Rehabilitation

Rehabilitation relies heavily on neuroplasticity—functional recovery through neural reorganization. While the precise biological mechanisms underlying neuroplasticity remain debated, there is broad consensus on the importance of converging neural activity to (re)shape and reinforce motor pathways (Feldman, 2012; Ganguly & Poo, 2013; Hebb, 1949). The existence of a "critical (though heavily debated) time interval" for this convergence is left open to interpretation. Different theories propose varying constraints on the timing and order of neural activation—ranging from precise millisecond-scale intervals to broader activity-dependent frameworks (Carson & Kennedy, 2013; Feldman, 2012). However, regardless of the specific biophysical mechanisms, closing the loop remains the only widely accepted timing requirement for neuroplasticity to drive meaningful motor recovery. Yet, while closing the loop is a necessary condition, the optimal parameters—such as which neural correlates to target and when to provide feedback—remain largely unknown.

Most BCI rehabilitation protocols pair feedback with pre-movement motor-related neural activity using ERD or MRCP, as these are the most widely explored neural correlates of motor control in EEG and are considered valuable in the context of neuroplasticity and clinical rehabilitation (Remsik et al., 2017). However, while effective for detecting movement intent, their precise relationship to specific motor processes remains unclear (Khalighinejad et al., 2019; Lakany & Conway, 2007; Shakeel et al., 2015; Wright et al., 2011). These markers correlate with the progression of the preparatory phase of the FoFe-loop, yet may reflect different or only partial aspects along the motor execution timeline. Without a more precise understanding of the biophysical mechanisms underlying neuroplasticity, it is uncertain whether current BCI timing strategies optimally align feedback with the most effective neural states for inducing plasticity. This raises a critical challenge: how to determine the most suitable neural correlate for feedback timing, and how best to interact with it—whether by representing its continuous progression or, alternatively, by adopting an approach similar to PAS, timing feedback to a specific phase within the neural marker's activation window.

Where BCIs using ERD and MRCP have optimized rehabilitation by considering neural indicators of movement, it has been suggested that CSE may serve as a better neural correlate of motor control for timing feedback delivery (Daly et al., 2018). Unlike ERD and MRCP, which primarily indicate movement intent, CSE reflects the dynamic interplay between motor preparation and execution, providing a functional link to exploit for more precisely aligning feedback with the transition from intention to action.

1.4.1.1 Corticospinal Excitability as a More Suitable Neural Marker

It has been argued that learning benefits from, and relearning relies on, increased levels of cortical excitability (Clarkson & Carmichael, 2009; Lissek et al., 2013). As discussed in section 1.1 Neural Activity of Motor Control, CSE is considered a state of "neural readiness" that changes in response to the cortical activity before, during, and after movement (Leocani et al., 2000, 2001). Higher excitability increases the likelihood that neurons respond to incoming signals and synaptic connections will be strengthened. This heightened state of responsiveness is thought to represent an optimal condition for integrating sensory feedback, comparing predicted and actual movement outcomes, and refining motor commands; i.e., motor learning (Gandolla et al., 2021). Consequently, cortical excitability has been proposed as a neural marker for motor learning and use-dependent plasticity—the process by which repeated voluntary movements reshape neural connections within the primary motor cortex (M1) (Ackerley et al., 2011; Lissek et al., 2013).

CSE is particularly relevant within this framework, involved in both transmitting outgoing motor commands (Ibáñez et al., 2020) and relaying incoming sensory feedback (Gandolla et al., 2021), as both travel via the corticospinal tract. This directly ties CSE to the closure of the FoFe-loop, where learning depends on continuously comparing expected and actual sensory consequences of movement. The relationship between CSE and motor learning is further supported by its observed role in functional motor recovery. Studies show that increased CSE levels correlate with better motor performance and learning outcomes (Kleim, 2009; Leung et al., 2017), while impairments in sensory feedback transmission—such as proprioceptive deficits (reduced awareness of body in space)—have been associated with poor motor learning due to disrupted error correction and adaptation mechanisms (Gandolla et al., 2021). Similarly, stroke recovery has been associated with CSE changes, with initially low levels increasing as motor function is regained (Clarkson & Carmichael, 2009). Because plasticity is inferred from functional changes rather than directly measured, TMS-evoked MEPs are often used as an indicator of corticospinal plasticity (Kleim, 2009). Since MEPs are considered a measure of CSE, their modulation following rehabilitation suggests that successful motor recovery engages neuroplasticity mechanisms. However, it is important to note that while increases in MEP amplitude are generally interpreted as evidence of synaptic strengthening, they do not directly measure plasticity in real time or reveal its precise mechanisms. Instead, they provide an indirect indication that plasticity may have occurred (Kleim, 2009).

Thus, there is a clear link between CSE, motor learning processes, and the execution and improvement of motor skills, with research repeatedly showing that better motor performance and skill acquisition are associated with increased CSE levels. Furthermore, studies indicate that modulating CSE directly can further influence motor learning and functional improvement. One example is metronome-

synchronized training, which has been shown to enhance both motor performance and CSE. When motor actions are synchronized with a metronome, CSE levels increase, likely reflecting the strengthening of synaptic connections involved in the executed movement (Leung et al., 2017). Notably, repeated execution of the same movement without metronome guidance did not produce the same increase in CSE levels. Leung et al. (2017) proposed that this temporal coordination of action leads to increased activation of the motor cortex and supporting areas. More specifically, this effect is thought to result from stimulus-driven phase-locking of neural oscillations in these cortical regions, which modulate neuronal excitability and generate periods of maximal sensitivity to input (Crasta et al., 2018). This suggests that metronome-guided training fosters repeated activation of specific cortical areas, creating a more favorable neural state for integrating sensory information, inducing plastic changes, and ultimately reinforcing use-dependent plasticity (Leung et al., 2017; Van Der Cruijsen et al., 2021). The auditory and motor systems share rich interconnectivity across cortical, subcortical, and spinal levels (Schaefer et al., 2014; Thaut & Abiru, 2010), suggesting metronome pacing may influence broader motor control networks rather than directly modulating CSE. This idea—that rhythmic auditory stimulation potentially creates a more favorable state for motor learning—is further supported by studies showing that stimuli such as music or paced beats can alter alpha and beta power in the motor cortex during movement preparation, (Abbasi & Gross, 2020; Ivaldi et al., 2017; Ross et al., 2022). Specifically, it is suggested that the pre-activating or priming of the sensorimotor areas results into a beneficial increased state of excitability (Neuper & Pfurtscheller, 2001).

In a similar manner, neurostimulation techniques have also demonstrated the ability to enhance CSE and facilitate motor recovery. Repetitive TMS (rTMS) and transcranial direct current stimulation (tDCS) are widely studied as tools for modulating neural plasticity and supporting functional recovery in stroke rehabilitation (O'Malley et al., 2006). For instance, applying rTMS at 10Hz for 15 minutes has been shown to increase CSE up to 4 minutes post-stimulation. Given that CSE is a key mediator of motor (re-)learning, increasing excitability through neurostimulation may provide additional therapeutic benefits for individuals recovering from motor impairments. However, a major challenge is determining when crucial neural events occur, making it difficult to precisely time TMS or other forms of stimulation. This underscores the potential of CSE fluctuations as both a potential neural indicator of motor learning and a key variable for optimizing neuroplasticity-driven interventions. Aligning feedback delivery with periods of heightened excitability may provide a more effective window for enhancing plasticity-driven recovery. However, whether these excitability changes originate primarily at the cortical or spinal level remains difficult to determine and may be secondary in importance. Notably, single pulse TMS-evoked MEPs alone cannot distinguish whether observed changes reflect excitability in the motor cortex, descending axons, spinal motor neurons, or a combination of these (Weavil & Amann, 2018). Given

that motor learning and functional recovery depend on the coordination of multiple neural processes across hierarchical levels, the precise source of excitability shifts may be less relevant than their functional connectivity within the broader motor control system. Regardless of whether these changes originate at the cortical or spinal level, changes in excitability measures are linked to plasticity. Meaning, changing CSE levels provide a dynamic marker of motor learning and may serve as a key variable for identifying optimal states for engaging neuroplasticity-driven interventions.

1.4.1.2 Functional Connectivity & Neural Interactions

While CSE presents a promising neural correlate for optimizing feedback timing, a major challenge in utilizing it for real-time BCI applications is that it cannot be continuously measured like EEG-based signals. Unlike ERD or MRCP, which are recorded non-invasively from the scalp in real time, CSE is typically inferred through TMS-evoked MEPs. While MEPs serve as widely accepted indicators of changes in cortical activity (Kleim, 2009; Leocani et al., 2000, 2001), they provide only intermittent snapshots of excitability rather than a continuous signal that can be tracked during movement execution. This limitation can be circumvented by examining how motor-related neural signals interact over time. Since motor execution involves the coordinated activity of multiple neural circuits, investigating how these signals synchronize could refine our understanding of how excitability evolves in real time. By mapping these interactions and exploring the functional relationships between neural markers, we can develop indirect but reliable measures of CSE and improve feedback timing strategies in BCI rehabilitation. This approach also contributes to broader efforts to further our understanding of the neural substrate of motor activity and could help clarify relationships between neural circuits involved in motor control dynamics in the brain, offering insights that may challenge or refine existing frameworks of motor control.

Given the challenge of directly measuring CSE in real time, studies suggest that ERD—mu rhythm desynchronization, specifically in the alpha and beta bands over the motor cortex—may serve as such a proxy for real-time changes in CSE. Providing a functional index for CSE in both healthy individuals and stroke patients (Aono et al., 2013; Daly et al., 2018). If ERD progression reliably reflects shifts in CSE, then ERD could offer an indirect but practical solution for estimating optimal feedback timing in BCI-driven rehabilitation. The link between ERD and CSE follows logically from evidence showing that MI-based ERD-driven BCI paradigms are associated with improved functional recovery from stroke (Daly et al., 2018; Pichiorri et al., 2015). Moreover, how the same MI techniques that consistently produce ERD for BCI have been shown to engage the motor system and enhance motor cortical excitability, further supporting a functional link between ERD and CSE (Cicinelli et al., 2006; Stinear et al., 2006). Individual variability in MI ability has also been linked to differences in ERD strength (Müller-Putz et al., 2014; Williams et al., 2012), reinforcing the idea that ERD-based interventions play an active

role in modulating excitability rather than merely reflecting motor preparation. i.e., tapping into the FoFe-loop via ERD comes with increased CSE. Complementary findings indicate that CSE increases following tDCS interventions coincide with ERD enhancements, further suggesting a broader functional link between these neural markers (Aono et al., 2013). Together, these studies indicate that ERD-based BCI feedback is capable of modulating CSE as they aim to do (Daly et al., 2018), supporting the idea that CSE, rather than ERD, might be the neural marker we ultimately want to target.

Several studies have investigated the relationship between ERD and CSE more directly, with findings suggesting that stronger ERD correlates with increased MEP amplitudes—a direct measure of CSE. Early studies reported that this relationship only becomes apparent within the final 100ms before MOn (Chen et al., 1998; Leocani et al., 2000, 2001; van Wijk et al., 2012). Similarly, Neuper & Pfurtscheller (2001) noted that ERD strength correlates with increased excitability during MI, while subsequent event-related synchronization (ERS) is associated with decreased CSE. Lepage et al. (2008) further demonstrated that MI training-induced changes in the motor cortex are associated with MEP modulation. More specifically, modulation in the low to mid-range beta band (12-18 Hz) correlated with MEP size during both rest and movement execution, whereas no clear relation was found with alpha activity. This suggests that specific ERD frequency bands may be more closely associated with CSE than others. While Chen et al. (1998) suggests that the early onset of ERD, or MRCP for that matter (Leocani et al., 2001), is unlikely to be associated with CSE, more recent findings indicate a broader temporal relationship between ERD-CSE. Aono et al. (2013) found that CSE increases in tandem with ERD strength following a relative reduction in power from 10% to 30%. Notably, the 10% (as well as the 30%) decrease in power for the average ERD occurs prior to the earlier mentioned 100 ms window (Cassim et al., 2000). This pattern has been observed in both healthy individuals and stroke patients (though with substantial individual variability in the latter) (Aono et al., 2013), suggesting the gradual increases in ERD corresponding to heightened excitability levels to be a robust association between the two neural markers.

While these findings support the idea that ERD can serve as an indirect measure of CSE, critical questions remain. How precisely does ERD progression align with CSE fluctuations over time, what do those temporal dynamics of CSE exactly look like? Can ERD not only reflect CSE but also predict the optimal moment for delivering sensory feedback?

1.4.1.3 Identifying the Optimal Timepoint for Feedback Engagement

In considering when to interact with the FoFe-loop, PAS research provides valuable insights. PAS protocols have long emphasized that the precise timing between afferent sensory signals and efferent motor commands plays a crucial role in shaping synaptic connectivity. While the strict time constraints of PAS protocols remain debated, their core principle—that neural activity follows distinct temporal

windows for optimal information integration—offers a useful perspective (Daly et al., 2018). Following this logic, if CSE reflects a neural state most conducive to motor learning, rehabilitation protocols should aim to engage with CSE at its optimal point to enhance recovery. This raises two key questions: When is CSE optimally increased for facilitating plasticity? And how does this point relate to the progression of ERD to determine the ideal moment for sensory feedback delivery?

The concept of "optimal excitability," however, remains underdefined. The reasonable interpretation suggests that sensory stimulation should be delivered when excitability is maximized, as this may provide the most favorable conditions for reinforcing new motor patterns. However, identifying when this peak occurs and whether it represents the best moment for feedback engagement remains an open question.

Daly et al. (2018) investigated the broader nature of the temporal relationship between CSE and ERD strength. Whereas earlier studies examined only limited ERD thresholds (e.g., 10% and 30% power reduction; Aono et al., 2013), Daly et al. (2018) analyzed CSE changes across a more continuous range of ERD progression (10%, 20%, 30%, and 40%). Their findings revealed an approximately nonlinear relationship between ERD strength and CSE, with CSE peaking at 20–30% ERD strength before declining at 40%. This suggests that maximal excitability does not coincide with the strongest ERD signal but rather occurs at an intermediate point. The implication is that sensory feedback, whether in the form of artificial stimulation (e.g., tDCS) or natural cues (e.g., visual feedback), may be most effective when delivered during this 20–30% ERD phase. This window could represent an optimal period for engaging neuroplastic mechanisms, allowing sensory feedback to be integrated most effectively into motor learning processes. Beyond assessing ERD-CSE dynamics, Daly et al. (2018) also examined whether visual feedback itself directly modulated CSE levels. While prior studies have linked ERD-based visual feedback to functional recovery and increased CSE, Daly et al. (2018) found no direct effect of visual feedback on CSE changes. This finding was unexpected given prior evidence suggesting that ERD-driven visual feedback contributes to neuroplastic adaptations. However, Daly et al. (2018) their results could not confirm a direct causal link between visual feedback and CSE enhancement. This raises an important question: How, if at all, does ERD based feedback interact with excitability? Further research could investigate different types of feedback interactions to explain this (absence of) finding. One possibility is that the relationship between CSE and feedback is mediated by learning rather than direct stimulation effects. If so, investigations should focus on contexts where feedback leads to recovery or learning rather than assessing feedback in isolation. Nonetheless, Daly et al. (2018) provide further support for the idea that CSE evolves dynamically throughout ERD progression rather than being limited to the final 100 ms before movement onset. Daly et al. (2018) ultimately put forward the same core argument we make in this thesis: optimizing BCI rehabilitation may require aligning sensory

feedback delivery with periods of optimal excitability. Their findings propose that “optimal excitability” equates to maximal excitability, which can be inferred from a 30% reduction in ERD power. However, whether maximal excitability is truly the most effective point for feedback engagement remains an open question—one that requires further investigation into how ERD and CSE evolve dynamically over time.

To begin with, while Daly et al. (2018) provide a valuable starting point, their assumption that maximal excitability falls around 20–30% ERD strength fails to align with other findings on the temporal evolution of CSE**.** Most studies on CSE timing have focused on pre-movement inhibition, reporting a suppression of CSE between 500 to 200 ms pre-MOn, with a flat baseline before this point, and a rapid increase in excitability post-suppression (starting approximately 100 ms pre-MOn) (Ibáñez et al., 2020; Leocani et al., 2000, 2001; van Wijk et al., 2012). Additionally, correlations between ERD-CSE were primarily observed in the final 100 ms before MOn (Chen et al., 1998; van Wijk et al., 2012). If maximal CSE truly represents the ideal window for feedback engagement, then—based on PAS research—stimulating closer to MOn may be more effective, or in case of MI-based paradigms, closer to when movement execution would have occurred. This does not fully align with the reported findings of Daly et al. (2018), who claim that CSE peaks at 30% ERD strength, as this window precedes the CSE suppression phase in the final 200 ms leading up MOn (Cassim et al., 2000). This discrepancy suggests that the increase observed by Daly et al. (2018) may instead reflect a preparatory increase in CSE prior to its inhibition phase, rather than a true “peak of excitability”. As such we still do not know where maximal excitability truly lies, not in the least caused by CSE having been primarily studied in the context of inhibition, rather than its full progression relative to movement onset.

This represents a major gap in the current research. If ERD and CSE are truly linked, then earlier changes in ERD should correspond to earlier shifts in CSE. Yet, while studies have attempted to establish this relationship (Aono et al., 2013; Daly et al., 2018), currently known research lacks a clear depiction and understanding of CSE’s temporal evolution and its relationship to neuroplasticity. As such, before we can optimize intervention timing in relation to “optimal excitability,” we must first establish how CSE unfolds over time relative to MOn.

Furthermore, to optimize intervention timing in relation to “optimal excitability,” it is also possible that maximal excitability is not the ideal state for feedback engagement. Much of the existing CSE research focuses on its suppression as part of pre-movement inhibition, which plays a crucial role in motor planning. However, physiological inhibition does not necessarily equate to functional inhibition. The spotlight hypothesis proposes that this suppression promotes rapid action preparation and execution, by selectively reducing competing activity and facilitating motor output (Duque et al., 2017). Alternatively, Ibáñez et al. (2020) and Hannah et al. (2018) argue that CSE suppression does not

function to *select* movement *per se* but rather indicates a transition in cortical activity toward an "optimal" state for movement initiation—characterized by reduced signal variance. Regardless of the mechanism underlying the CSE inhibition, Ibáñez et al. (2020) further demonstrated that stimulation coinciding with this inhibitory dip in MEP amplitudes accelerated movement execution, though only for RT and self-paced movements, not predictive movements. These findings imply that the ideal excitability state for feedback delivery may depend on both the type of movement and the type of feedback applied—whether visual feedback (as studied by Daly et al. (2018)) or neurostimulation (e.g., TMS, as commonly used in PAS protocols; Stefan et al., 2002). Moreover, CSE inhibition lines up time wise to the "point of no return" in movement intention, as indicated by MRCP (Schultze-Kraft et al., 2016). Given this, a larger inhibitory dip may facilitate faster, more efficient movement execution, meaning that providing sensory feedback at the point of inhibition has just as much theoretical justification to enhance neuroplastic effects as interacting with “maximal excitability” just prior to or after inhibition. CSE suppression may also be a key functional marker for intervention as peak excitability.

1.4.1.4 Current Insights & Next Steps in Optimizing Feedback Timing

Thus far, the literature provides a compelling rationale for exploring CSE as a target for optimizing feedback timing, with ERD serving as a potential online indicator of CSE dynamics. However, the precise temporal evolution of CSE remains poorly understood, and current assumptions regarding the "optimal" feedback timing window may be incomplete or misaligned. This highlights a critical gap in the literature—if BCI rehabilitation aims to optimize feedback timing, then accurately mapping the full temporal dynamics of CSE is essential. Additionally, a better understanding of functional connectivity among motor-related neural markers is necessary to determine how CSE, ERD, and MRCP interact within the FoFe-loop.

While arguments exist for inferring CSE through other, more easily measurable neural markers, we find it striking that despite the vast research on CSE, ERD, and MRCP as independent markers, their interactions remain poorly studied. ERD and MRCP originate from overlapping cortical regions, follow a similar preparatory timeline (both beginning approximately 2 seconds before MOn) and are discussed in relation to each other (Bai et al., 2006; Schultze-Kraft et al., 2016). Moreover, both have been individually linked to CSE (Daly et al., 2018; Leocani et al., 2001). Yet, research that investigates all simultaneously, especially in relation to CSE, is exceedingly scarce (Toro et al., 1994). This lack of integration leaves fundamental questions unanswered—could MRCP function just as well as ERD in predicting CSE? (Mrachacz-Kersting et al., 2016). How do these markers collectively contribute to motor preparation, execution, and feedback? How are they similar or different in their contribution?

Beyond these functional interactions, we lack a clear picture of the CSE timeline itself. Research investigating the temporal dynamics of CSE has been largely limited to brief windows close to MOn, primarily focusing on pre-movement inhibition. Early studies (Chen et al., 1998; Leocani et al., 2000, 2001) suggested that early onset ERD and MRCP were unlikely to be associated with CSE, yet no direct investigations were conducted. More recent studies, which inadvertently included early onset ERD measures (e.g., 10% and 20% ERD threshold associated with timepoints as early as 1.5s before MOn; Cassim et al., 2000; Neuper & Pfurtscheller, 2001), hint that a broader temporal relationship may exist. However, even these studies fail to provide a comprehensive temporal model. Most research looking at ERD-CSE focused on the 100 ms before MOn, or the relation between post movement inhibition and ERS (van Wijk et al., 2012), while ignoring potential fluctuations occurring much earlier. Whereas the current idea of premovement CSE indicates a temporal profile of up to -1sec before MOn (Ibáñez et al., 2020; Klein-Flügge & Bestmann, 2012) where the preparatory increase at 30% ERD also seems to fall more around -500 ms (Cassim et al., 2000; Neuper & Pfurtscheller, 2001), raising the possibility that previous studies simply overlooked earlier CSE dynamics.

Without a full understanding of how CSE evolves over time, any attempt to correlate it with ERD—or to determine optimal excitability for intervention—is premature. The first step should be to establish the full temporal profile of CSE relative to movement onset, exploring its fluctuations beyond the well-studied suppression phase. Does CSE ramp up earlier than previously assumed? How does it fluctuate across different movement types? Answering these questions will lay the foundation for future work aimed at defining optimal excitability states for feedback timing in neurorehabilitation. Once we establish a more comprehensive CSE timeline, we can further refine its functional relationships with ERD and MRCP—determining whether these markers provide reliable, predictive indicators of CSE fluctuations. Investigating these dynamics in parallel will allow us to assess how well ERD and MRCP reflect CSE activity at different points in time, ultimately helping to refine BCI-based rehabilitation strategies.

1.4.2 Accounting for the Changing Neural Landscape during BCI

A second challenge in the development of BCI-based rehabilitation stems from its failure to account for how neural activity changes as individuals learn and regain motor function. While BCI protocols are designed to promote neuroplasticity, they largely rely on static assumptions about neural markers of movement production, even though learning inherently drives changes in the brain.

As highlighted by Maier et al. (2019), a major limitation in rehabilitation science is how current approaches often lack exact operationalization of insights gained from research on skill learning into practical applications. Their review specifically points to the absence of a bridge between motor

learning theory and clinical work, arguing that this disconnect hinders the ability to guide and optimize interventions. While Maier et al. (2019) focused on traditional rehabilitation techniques, the same issue holds true for BCI-based rehabilitation, which depends on our ability to measure and interpret changes in brain activity related to motor learning.

BCI rehabilitation is explicitly designed to reshape neural activity, promoting synaptic changes that support motor recovery. There is clear evidence that neural correlates of movement change as a result of learning (see 1.2 Motor Learning). However, to the best of our knowledge, BCI protocols designed for motor recovery do not account for these changes. The neural markers used in BCI protocols—such as ERD and CSE—are typically treated as stable, unchanging features, rather than recognizing them as dynamic signals that evolve with learning. This is paradoxical, as the goal of rehabilitation is to drive neuroplasticity—i.e., to change the brain itself.

BCI-based feedback paradigms have already been shown to increase functional recovery following stroke (Ang & Guan, 2013; Guger et al., 2018; Hurtier et al., 2016; Pichiorri et al., 2013, 2015; Remsik et al., 2017). If CSE is a key neural marker for optimizing BCI feedback timing, and if ERD is used as a proxy for real-time CSE fluctuations, the success of these protocols does not mean that the relationship between ERD, CSE, and motor recovery remains constant over time. Lepage et al. (2008) noted that while the ERD-CSE relationship has been investigated in a limited capacity, it has not yet been explored in a longitudinal context—i.e., how these markers change over the course of learning. The work of Daly et al. (2018) represents an important step in understanding this relationship, but their findings still reflect a static and incomplete view of CSE-ERD dynamics. Their study does not examine whether CSE and ERD evolve at the same rate during learning, nor does it account for potential nonlinear changes that may emerge as neural circuits reorganize.

This raises a fundamental question: how does neural activity change as motor function improves, and how should BCI protocols adapt accordingly? If BCI rehabilitation is designed to promote change, then BCI models must incorporate how these neural signals themselves evolve during learning. Otherwise, protocols risk being misaligned with the very plasticity they are trying to induce. Addressing these issues requires answering several key questions regarding the relationship between ERD and CSE over time. For instance: How does CSE change over time relative to ERD? Do ERD and CSE develop in parallel, or does one change more rapidly than the other? If ERD shifts at a different pace than CSE, does this create a moving target for feedback timing that BCI protocols must continuously adjust to? If timing strategies are based on an inferred relationship between ERD and CSE, we must determine whether this relationship remains stable over time, or if changes in one marker leads to a misalignment in feedback delivery as learning progresses.

If BCI feedback timing is based on an inferred relationship between ERD and CSE, then it is critical to understand whether this relationship remains stable over time. If the link between ERD and CSE shifts with learning, then timing strategies based on early measurements may become misaligned as recovery progresses. It remains unclear whether these changes impact rehabilitation outcomes, but their potential influence must be investigated to ensure that BCI protocols are not working against the very neural adaptations they seek to facilitate. As such, BCI protocols must either (1) rule out that changes in neural signals affect the efficacy of existing and new feedback strategies, or (2) develop methods to adjust for these changes dynamically. This may involve real-time recalibration, feedback adjustments based on behavioral milestones, or staged interventions that adapt at key points in neural recovery.

1.4.3 Bridging the Gaps: Summary of Challenges

While we may not yet fully understand the exact mechanisms of plasticity, various protocols have proven effective in assisting individuals with motor impairments. We have identified two significant limitations that hinder the advancement and optimization of BCI-driven rehabilitation:
(1) the absence of a clearly defined neural target and timing strategy for feedback delivery.
(2) the static assumptions underlying current BCI protocols, despite clear evidence that neuroplasticity leads to changes in motor-related brain activity.
Addressing these issues is essential for improving the precision and adaptability of rehabilitation paradigms.

On refining the neural target and timing strategy, our review supports CSE as a more suitable neural marker for feedback engagement compared to ERD or MRCP. However, two key challenges remain. First, CSE cannot be measured in real time, requiring indirect estimation through other neural markers. Second, the temporal evolution of CSE remains poorly understood, making it difficult to determine the true optimal state of excitability for feedback delivery. While studies suggest that peak excitability occurs at 30% ERD strength, conflicting findings on CSE suppression and inhibition raise questions about whether maximal excitability is indeed the ideal point of interaction. Before feedback timing can be reliably optimized, a more comprehensive understanding of CSE's full temporal profile is needed.

Concerning the static nature of BCI, BCI protocols currently operate under the assumption that the neural markers they target remain functionally consistent throughout rehabilitation, yet neuroplasticity inherently involves dynamic changes. Evidence from motor learning research suggests that as synaptic connections reorganize, neural activation patterns shift in ways that may meaningfully affect feedback timing strategies over time. This is particularly relevant in the context of CSE and ERD, as both are subject to change during learning, yet their interaction remains poorly understood. If

neural markers of movement intent and execution change as rehabilitation progresses, BCI feedback parameters should adapt accordingly. However, current BCI models do not account for these evolving neural states, potentially limiting their long-term effectiveness.

Moving forward, this thesis aims to investigate these questions by:

1. **Mapping the temporal evolution of CSE relative to movement onset**—establishing a clearer timeline of its fluctuations before movement execution.
2. **Determining whether ERD and MRCP can serve as real-time predictors of CSE changes—** assessing their reliability in estimating excitability fluctuations.
3. **Investigating how the neural markers change in relation to one another over the course of motor learning**—assessing whether their relationship remains stable or requires continuous recalibration.

By addressing these fundamental gaps, we seek to refine the theoretical framework underlying BCI-based motor rehabilitation and contribute to the broader goal of designing more precise, adaptive, and effective interventions for individuals recovering from motor impairments. While this thesis is framed within the context of improving motor rehabilitation, the studies conducted exclusively involved healthy participants. This approach was taken as a necessary first step in laying the groundwork for future clinical applications, allowing for a controlled investigation of the neural mechanisms underlying motor learning and feedback timing before extending these findings to patient populations.

Chapter 2: Preliminary Insights from Existing Data

2.1 Introduction

Throughout Chapter 1, we extensively argued that to realize the full potential of motor rehabilitation BCIs, we need to better understand when and how to engage with the neural mechanisms underlying motor learning. While review of the literature indicates that CSE is a valuable neural target and that points of optimal excitability could be inferred from associated, more easily measurable neural markers such as the ERD or MRCP. To explore the concept of optimal excitability and estimate its occurrence in real time through other, but correlated, neural measures, we first need to develop a better understanding of how these neural markers evolve over time. By establishing and exploring the temporal evolution of these markers, as well as their progression relative to each other, we will lay the groundwork for future studies to investigate the efficacy of different points of excitability, as well as mediators to the neural window considered 'optimal' for intervention.

To this end, this first study primarily focused on characterizing the temporal dynamics of CSE, as it remains mostly unknown in the literature. Daly et al. (2018), building on the work of Aono et al. (2013), provided one of the most complete timelines of CSE changes available, particularly by including measures at earlier time points. However, their CSE measures were gathered and analyzed relative to ERD power percentages, meaning their insights into CSE dynamics are inherently tied to changes in ERD rather than presenting an independent assessment of changes in CSE. This dependency makes it difficult to integrate their findings on changes in early onset CSE with existing literature, as most prior research on CSE is discussed in time relative to MOn. A further complication of discussing CSE relative to ERD is the assumption that ERD power decreases in a consistent trajectory across individuals. In actuality, there is considerable inter-individual variability in how a given frequency band exhibits ERD, particularly in terms of its power decline profile as presented in percentages (Cassim et al., 2000; Neuper & Pfurtscheller, 2001; Pfurtscheller & Lopes Da Silva, 1999). Daly et al. (2018) reported that CSE peaks around 20-30% of a person's ERD strength. When literature describes that the average ERD power decrease of 20–30% would fall between -1s and -0.5s relative to MOn (Cassim et al., 2000; Neuper & Pfurtscheller, 2001), these values are meaningful when discussing theoretical underlying processes. However, for practical applications—such as inferring CSE state in real time—relying on a single fixed percentage-based metric that varies between individuals and across trials is problematic. At the very least, BCI set ups should account for this variance. For example, a 30% ERD power reduction may occur closer to MOn in one individual, but earlier in another. Without fully understanding how CSE behaves relative to ERD power percentages, we do not yet know whether to define an 'ideal CSE

points' based on ERD's relative reductions in power or adjust the to target ERD strength within individuals to target a specific CSE time point.

By re-analyzing the Daly et al. (2018) dataset using a novel methodological approach, guided by a slightly different research goal, we aim to better understand Daly et al. (2018) and their findings by replicating and expanding on their results. A key methodological distinction is that we approached the data from a more conventional 'offline' analysis perspective. Rather than relying on the experimental conditions under which the data were originally collected – as part of an online BCI setup, i.e., relative ERD decrease in power was calculated in real time with TMS applied to specific ERD thresholds – we recalculated the data points relative to MOn. This should produce the same general findings as reported by Daly et al. (2018) while filling in the gaps stemming from the lack of a direct 2 second timeline-based definition of CSE progression.

While we noted our concerns regarding the reported peaking of CSE around 20-30% ERD not necessarily holding on a trial-by-trial or interindividual basis. We do recognize that trial-averaged results offer a valuable starting point. Accordingly, our analysis first assessed average neural marker dynamics across trials, allowing for direct comparisons with previous studies on which we based our hypotheses. However, recognizing the practical need to translate findings to a trial-by-trial basis, we followed up our initial analysis with trial-by-trial assessments. Specifically, we used a predictive model of ERD relative to MOn, allowing for a descriptive assessment of how well within-subject ERD dynamics can predict concurrent changes in CSE, given the variability that exists on an individual trial level.

Beyond ERD, we also explored MRCP as a potential predictor of changes in CSE as suggested by Daly et al. (2018). MRCP has previously been associated with CSE changes in protocols similar, but not identical, to BCI-based interventions for neuroplasticity induction (Leocani et al., 2001; Mrachacz-Kersting et al., 2012, 2016). Expanding the investigation to include MRCP allows us to examine whether its temporal progression provides additional insight into CSE dynamics, potentially enhancing our ability to estimate optimal intervention timing or at least contributing to our understanding of functional connectivity within the motor neural circuit.

Most importantly, we argue for exploring CSE and ERD over time (i.e., in milliseconds) relative to MOn, rather than anchoring CSE fluctuations to ERD strength thresholds. Specifically, we aimed to provide an initial characterization and visualization of the pattern underlying the evolution of CSE over time. Additionally, we sought to explore how changes in CSE relate to the ERD and MRCP when assessed on the same timescale—from 2 seconds leading up to movement execution. While our initial analyses are largely descriptive, our goal is to provide a foundational characterization of CSE's temporal evolution. In the longer term, we hope these insights can serve as the basis for developing predictive models that function as a tool to estimate CSE state based on either ERD or MRCP progression.

As such, in this first study, we will gain preliminary insights from existing data to address the first two of our research questions. To this end, we propose the following hypotheses (see also Figure 2):

Regarding *What do the temporal dynamics of CSE look like on a timeline relative to movement onset?* **Hypothesis 1**: With the aim of establishing a clearer timeline of the fluctuations in CSE before movement execution. We expect changes in CSE activity, as indicated by MEP, to follow an S-like wave in the 1.5 to 2 seconds leading up to movement execution (i.e., MOn), which can be described by a third-degree polynomial function. This trajectory is expected to include:

- An initial increase in MEP amplitude, beginning around -2 to -1.5 seconds before movement onset, peaking intermediately at approximately -800 to -500 ms
- A subsequent decline in amplitude, bottoming out between -200 ms and -100 ms
- A final steep increase immediately preceding MOn

These exact timepoints are derived from existing literature on CSE alone, as well as recent insights on CSE behavior based on its relation to progression of ERD strength. Most research on CSE focuses on late pre-movement phases starting about 500 ms before MOn. Ibáñez et al. (2020) explored the temporal evolution of CSE, in view of its inhibitory characteristic, for three types of voluntary movements (a reactor (RT; as fast as possible to unannounced presentation of a cue), predictor (PT; react to cue that is being count down) and self-paced (SP)). Found a similar degree of premovement inhibition for all three types of voluntary movement; reducing around 200 ms prior to “GO” cue for both RT and PT and 140 ms (between 180 ms and 100 ms) prior of SP movements. Important to note, this dip is short lived. Inhibited CSE activity seemingly declines slowly (around 800 ms from base to dip at 200 ms), it rises again (relatively fast) at 60 ms and even steeper at the 30 ms stimulation points (RT and PT) with similar findings for self-paced actions showing an increase for CSE -80 ms to 0 ms prior to movement onset.

Unfortunately, not much is known about CSE before this point. However, we can piece a prediction together by comparing the different puzzle pieces in the literature on the neural circuit of motor control. We know ERD and MRCP on average start between 2 and 1.5 seconds prior to MOn as measured by EMG (Toro et al., 1994). CSE is described as part of the same neural network, thus we took 2 seconds before MOn as our starting point to explore any consistent tendencies in the activity. Furthermore, Daly et al. (2018) described an CSE peaking around 30% ERD strength. From the literature we know that ERD rise is slow-paced, with 30% typically occurring between the 1s and 0.5s before MOn; though this heavily depends on the individual and the frequency band. Specifically, alpha frequency band (8-12 Hz) seems to reach an average ERD strength of around 50% at MOn, peaking at approximately 60-70% 1 second post-MOn. Beta (13 -35 Hz), on the other hand, reaches around 30-

45% at MOn and peaks in that same interval approximately 500 ms post-MOn (Cassim et al., 2000; Neuper & Pfurtscheller, 2001).

Regarding *What are the relationships and dynamics between the three neural markers of motor control: ERD, MRCP and CSE? Can we replicate the findings and claims from studies on the individual neural markers all in one dataset? How can we quantify these relationships?*

Hypothesis 2: With the aim of assessing ERD and MRCP their reliability in estimating excitability fluctuations, whether they can serve as real-time predictors of CSE. We expect to replicate previous findings on the temporal evolution of each individual neural marker when calculated from the same dataset. Including

- ERD, where alpha frequency band (8-13Hz) will on average increase in ERD strength by around 50% at MOn, peaking at approximately 60-70% 1 second post-MOn. Lower beta (14 - 20 Hz), on the other hand, reaches around 30-45% at MOn and peaks in that same strength interval approximately 500 ms post-MOn. Expecting both frequencies to reach about half of their 'at MOn strength' at the 500 ms to MOn point.
- MRCP to slowly progress until about 500 ms before MOn (RP), followed by a steeper incline until about 200 ms before MOn (NS) followed by a peak negativity shortly after MOn (Schultze-Kraft et al., 2016; Wright et al., 2011)

We specifically expect to replicate the findings of Daly et al. (2018) showing an initial preparatory increase in MEP amplitude at around 30% reduction in power for ERD. Both to occur around 500 ms prior to MOn. Furthermore, Daly et al. (2018) suggested MRCP peak may also line up with their proposed "CSE peak" at 20-30% ERD strength. However, MRCP is noted to peak within 100 ms post-MOn, and ERD supposedly peaks at 45-75% strength 500-750 ms after MRCP (depending on the frequency). As such, considering all ERD strength measures are pre-MOn, going with the time point of 500 ms before MOn for 30% ERD strength, and considering the confusion in the literature on the terminology of MRCP and its individual components, we presume this 'peak MRCP' moment to mean the point where RP switches for NS.

We expect to quantify the correlative nature of the ERD and the temporal evolution of CSE leading up to movement initiation, including the MRCP in a descriptive way through predictive modeling.

Our rationale for approaching the ERD-CSE relationship differently is to establish a framework for real-time BCI applications, where CSE state can be inferred from ERD progression in a subject-specific manner. Defining their relationship on a uniform time scale (relative to movement onset) rather than through static ERD power percentages, which are highly variable across individuals and trials. Not only

will this function better to have an overview of all the neural markers and dynamics in the same framework from the start. There is also the practical aspect of people having different progressions of ERD strength. For example, the average ERD strength reaches 50% right after MOn, this will not be the case for everyone. As such, working with a fixed point of 30% ERD will result in landing on variable timepoints compared to MOn depending on the individual. Instead with BCI use in mind, establish a 'to target point of CSE' in time relative to MOn (e.g., 500 ms before MOn). Then establish what level of ERD strength a particular individual has at 500 ms to MOn. likely different per person. The use of a fixed ERD percentage across individuals only applies if, for example, the CSE inhibition always occurs at an ERD strength of 40% in the alpha frequency band. However, before we can decide one over the other, we need to further explore their relation.

Figure 2

Schematic Representation of Hypotheses 1 and 2

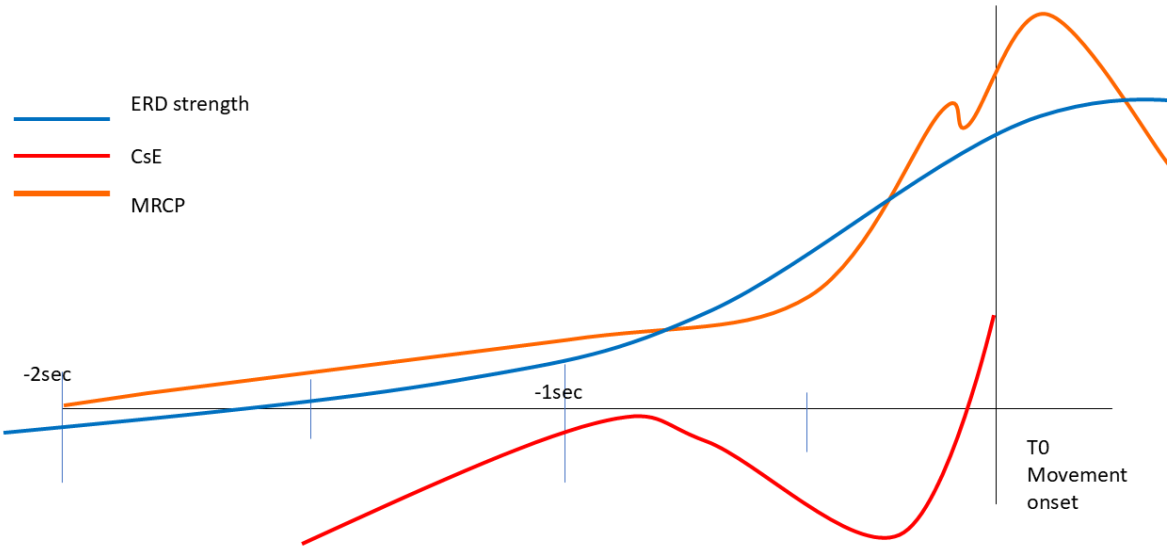

Note. This schematic visually represents the described expected inter-dynamics of the neural markers ERD, MRCP, and CSE. The red line specifically illustrates the expected temporal evolution of CSE in the 2 seconds preceding MOn. Orange and blue lines depict the more generalized expected trajectories of MRCP and ERD, respectively, in relation to CSE and each other. The y-axis is intentionally undefined, as each neural markers measure on a different scale. For ERD and MRCP, assume an inverted y-axis (negative values at the top).

2.2 Method

2.2.1 Data description

In this study we made use of data originally collected by Daly et al. (2018), consisting of EEG and EMG data recorded from 12 healthy individuals (seven female, eight right-handed) between the ages of 21 and 36 years old (as reported by Daly et al. (2018)). EEG data was recorded during movement execution alongside TMS in order to explore changes in CSE. Throughout the experiment participants were instructed to keep their right arm and hand resting with open palm facing up. Presentation of a cue told participants to either stay relaxed and still ('rest' cue) or to flex and extend their right-hand fingers ('move' cue). Participants were instructed to repeat the movement for the five seconds the 'move' cue was on the screen (noted as the trial 'action phase'), at a speed that was comfortable to them. For all movement trials a single-pulse TMS (either sham or real) was delivered (during the action phase) over the participants motor cortex. The different time points and corresponding 5 trial types of TMS delivery were determined by the ERD's time course, specifically aiming for a relative decrease in power of 10%, 20%, 30% or 40%, as well as at a fixed time point of 33ms after cue presentation. All 12 participants completed 4 runs of 50 trials each, 10% being rest trials, amounting to a total 2400 trials.

Delivering TMS in direct relation to the ERD time course allows us to evaluate the relationship between ERD strength and cortical excitability (measured through MEP, a TMS induced change in EMG data), making it a suitable dataset for our analysis.

The setup for the acquisition of the experimental EEG data used 32 channels, recording at a 500 Hz sample rate and impedances kept below 10 kΩ, with the electrodes arrangement focused over the left motor cortex, using FCz as reference. EMG was recorded with a sample rate of 4000Hz, via electrodes placed on the right forearm over the flexor digitorum superficialis muscle and with the ground electrode placed over the ulnar styloid process near the wrist. TMS was delivered using a figure 8 coil (10 mm diameter) at 120% of the participants resting motor threshold. The present analysis focused on the offline measures of EEG neural markers, opposed to the online measures obtained through the BCI set up in the original data collection experiment, and is independent of the specific data processing, research questions and results previously published (Daly et al., 2018).

2.2.2 Data Evaluation and Preprocessing

2.2.2.1 Trial Removal

In the initial analysis, reported by Daly et al. (2018), 4 runs were excluded (across participants) from the dataset. In addition to these 4 runs, we also excluded the remaining 3 runs from participant 6 due to large TMS artifacts within our epoch and channel of interest (C3, see section 2.2.3 Neural Marker Characterization). Specifically, within these runs we observed amplitude shifts greater than 100μV in the EEG channel baseline activity, taking up to a second or longer to return to equilibrium (i.e., slow

decay artifacts; Varone et al., 2021) (Figure 3A). Similar artifacts were present in other channels, for multiple participants. However, only participant 6 exhibited the artifact in channel C3.

Figure 3

EEG and EMG Signal Variations Induced by TMS

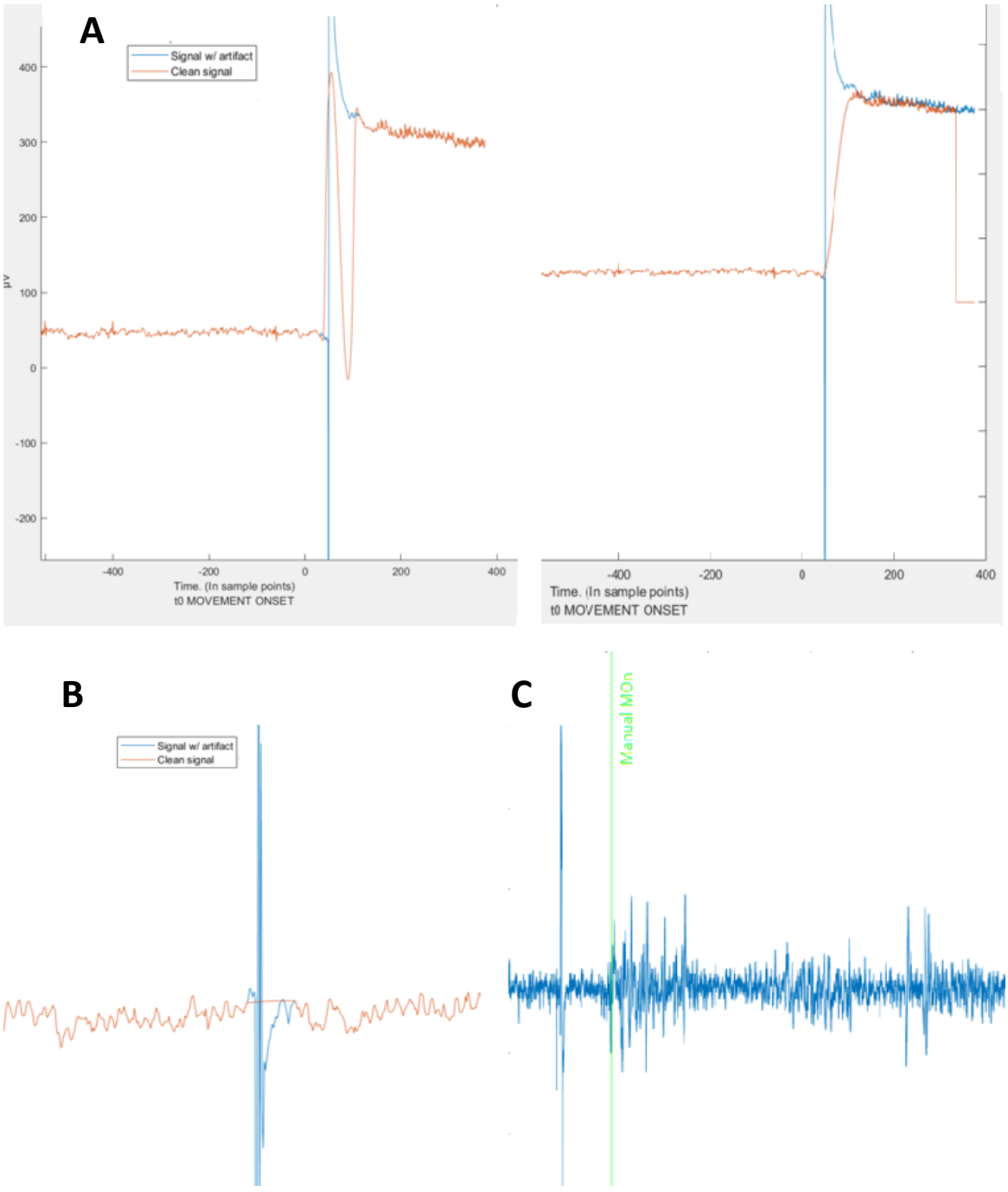

Note. This figure illustrates different EEG and EMG responses to TMS. (A) shows examples of TMS induced baseline shifts in EEG, highlighting how extreme artifacts affected interpolation attempts: spinal interpolation (left) and cubic interpolation (right). (B) presents a typical TMS pulse artifact in EEG with successful cubic interpolation. (C) displays a standard EMG signal containing a TMS pulse artifact, and EMG bursts indicating muscle contraction. The green line marks the onset of the first muscle contraction after TMS, indicating MOn. Sample rate 500Hz.

We further removed trials from our analysis if any of the following conditions were met.

(i) The trial was a Rest trial.

(ii) Found no event code indicating TMS delivery within the EMG signal set.

(iii) Found no event code indicating TMS delivery within the EEG signal set.

(iv) Presence of artefacts within the fixation cross or action phase. Specifically, trials were excluded if EMG and/or movement artefacts were identified on one or more EEG channels (identified by visual checking as reported in Daly et al., (2018).

(v) Trials are not relevant to our analysis, as indicated by no movement registered during the trial, or movement onset occurring prior to stimulation (see section 2.2.2.2 Determining Movement Onset).

Removing these trials from the dataset before further analysis ensures the results are based on trials where: 1) the participant-initiated movement, 2) delivery of TMS happened prior to movement, and 3) there is no artefact contamination.

2.2.2.2 Determining Movement Onset

The data were not gathered with the intention to establish a measure relative to MOn. Leaving us with the task to identify the exact moment of participant-initiated movement. A common approach to identify MOn is to include a mechanical indicator as part of the experimental design such as pressing a button (e.g., Demandt et al., 2012; Maslovat et al., 2018; Travers et al., 2020) and/or to manually determine the exact point of MOn from EMG data (e.g., Cassim et al., 2000; Jankelowitz & Colebatch, 2002).

It has been argued the only way to be truly sure MOn is correctly determined in an EMG signal is by manually inspecting every trial (Kamen & Gabriel, 2010). However, the process of visual inspection is tedious, time-consuming and the level of accuracy relies on the investigator's subjective judgment and experience. This has led increasing numbers of researchers to develop and rely on automated detection methods to increase processing speed, objectivity, and data reliability (Micera et al., 2001). As a result of the growing interest, a variety of options are available. Some algorithms share similarities in their process to detect MOn through a common precursor (Avila & Chang, 2014; Hodges & Bui, 1996), others are entirely new creations (Trigili et al., 2019). Looking at more recently developed algorithms we see an increased focus to detect MOn in EMG signals for movement prediction in real time, intended for robotic assistive devices (Avila & Chang, 2014; Gandolla et al., 2017; Tabie & Kirchner, 2013; Trigili et al., 2019). The issue with online oriented methods is the need to adapt for offline processing, and may require similar data collection set up (e.g., the number of EMG electrodes used; Gandolla et al., 2017) that needs to be considered in advance. Overall, the different approaches are similar in performance of MOn detection, but caution is needed when applying them in relation to

the type of movement recorded, data quality, and intended analysis; all of which can affect the detection accuracy (Hodges & Bui, 1996; Van Boxtel et al., 1993). It is furthermore suggested to not use any automated detection algorithm on their own, but include a 'catch method' on the side to avoid big misses in detection, for example by cross referencing with reaction times (Van Boxtel et al., 1993).

Our data does not include markers to tell when participants start moving, or provide information for a catch method, and in the absence of a 'general standard' among detection algorithms (Hodges & Bui, 1996; Tabie & Kirchner, 2013; Van Boxtel et al., 1993) we looked for our own reliable and appropriate method to detect MOn in the EMG data (taking inspiration from common approaches). The successful method would 1) accurately identify trials with no movement or where movement started early (before TMS) and 2) reliably determine the MOn timepoint.

Our method starts by defining a 5.25 second epoch, from the final 250 ms of the fixation cross presentation up until the end of the 5-second-long action phase. We then zeroed the signal mean and converted the signal into absolute values. A 70 ms window (-10 to +60 ms relative to the TMS pulse) is cut out of the signal epoch to split the epoch into pre- and post-TMS windows, and to remove both the TMS artefact and any MEP related activity as they will affect the movement detection method. Part of the fixation cross is included in the pre-TMS window to identify trials where the participant had initiated movement prior to the 'Go' cue (i.e., the start of the action phase). The majority (94%) of the trials had TMS applied in the first 2 seconds of the action phase with movement following shortly after. As such, movement during the fixation cross would qualify as 'movement before TMS'.
For the movement detection process (see also Figure 4), we took the 99^{th} percentile value of the amplitude of the pre-TMS epoch as a baseline value. We then, first, ascertained whether the trial had early or no movement by searching in the post-TMS epoch for a value higher than 2.4 times the base value (or 240% of the base value). Not finding a value would indicate there was no movement, or (early) movement present in baseline, causing the 240% threshold to overshoot all post-TMS values. Next, continuing with those trials identified as having valid movement activity, we identified the MOn timepoint. Using the same baseline value, but now looking for the first value bigger than 1.8 times the base value (or 180%).

These thresholds (i.e., 99^{th} percentile, 240% and 180%) were determined by manually comparing the performance of different baseline measures (Max value, 90^{th} ,95^{th} ,99^{th} percentile) and deviation (1 to 3 SD, 100% to 320%) from these baseline values. Using a sub-set of the dataset of 51 trials (of which 32 trials were considered valid movement trials, 37.5% with a clear movement burst and low noise, 62.5% with high noise or less clear movement bursts. In all these trials MOn was manually identified via visual inspection, see Figure 3C for an example. The remaining 19 trials in this set had early or no

movement. We then chose the threshold set with the highest accuracy (94.12%) to differentiate trials (240% of the 99th percentile was chosen over alternative options with competitive accuracy, as the less conservative option. It allows us to reliably identify all movement trials but occasionally let an early movement trial pass as being a valid movement trial) and had the smallest median distance to the manual defined MOn (180% of the 99th percentile had the overall smallest Median < 10 ms, and 68.8% of the movement trials a deviation of < 20 ms).

Figure 4

Flowchart on Process for Movement Onset Detection.

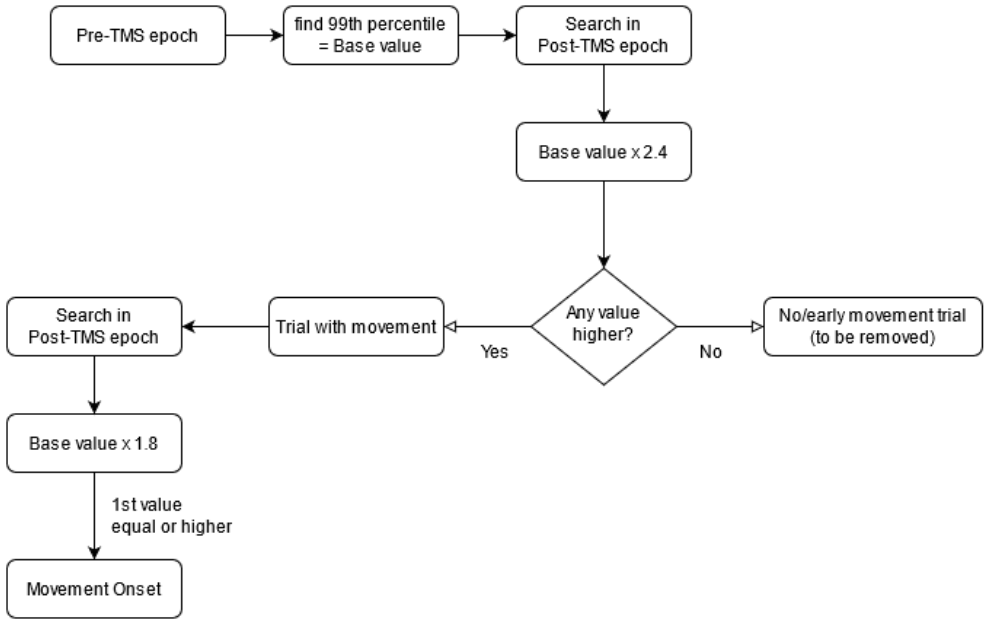

2.2.2.3 TMS Artefact Removal

All our trials of interest contain a large amplitude TMS artefact. To avoid contamination of our neural marker measures we removed this artefact by first cutting the EEG data centered around the TMS artefact (-0.02 to +0.1s) from each trial and then using the preceding and proceeding EEG data to reconstruct the cut-out data.

Specifically, to remove the artefact, we first defined a 0.15s search window around the point of TMS delivery (-0.05 to +0.1s) (defined as the start position of the TTL trigger that indicated TMS stimulation). We then defined a window of length 0.12s around the maximum absolute value of the EEG (-0.02s to +0.1s). New datapoints were constructed via interpolation, using the Piecewise Cubic Hermitian Interpolation Polynomial (PCHIP) approach (Fritsch & Butland, 1984; Fritsch & Carlson, 1980). Prior to this interpolation, we filtered the data using a low pass IIR Butterworth 2nd order filter at 30 Hz; to ensure the interpolated data reflected our frequency bands of interest (Alpha, 8-13 Hz,

and low beta, 14-20 Hz). The difference in frequency range, however, would result in the interpolated datapoints having sharp connections with the remaining EEG data, affecting the neural marker calculations. To further ensure a smooth connection between interpolated and real data we low pass filtered the interpolated datapoints (with an additional 0.02s on each tail end) again using an IIR 2nd order low-pass Butterworth filter at 45 Hz. It is important *not* to confuse the signal filtering described in 2.2.2.3 TMS Artefact Removal with the filtering applied in 2.2.2.4 ICA and Filtering. The filtering in 2.2.2.3 TMS Artefact Removal was used exclusively during the interpolation process and applies *only* to the interpolated data points. In contrast, the filtering in 2.2.2.4 ICA and Filtering pertains to the final state of the signal as used in further analysis. Figure 3B illustrates this distinction—after successful interpolation, only the interval surrounding the TMS pulse was modified, while the rest of the signal remained identical to the original raw data.

2.2.2.4 ICA and Filtering

We then used Independent Component Analysis (ICA) to subtract blink artefacts from the, now cleaned of TMS artifacts, EEG data. First, we filtered the EEG data using a 1 Hz high-pass filter (IIR Butterworth, 3rd order) to remove slow drifts in lower frequencies, as per recommended practice (Makoto's Preprocessing Pipeline. (n.d.).; Winkler et al., 2015), and (though not required for ICA) further filter the data using a 50 Hz notch-filter (6th order) to remove line noise, and applied a low-pass filter at 40 Hz (6th order) to further remove line noise and ensure ICA decomposition focuses on our frequency range of interest. Then we excluded bad channels, flagged by based on joint probability (using EEGLAB, version 2019.0, pop_rejchan function, with trimmed normalization and threshold set at 5 SD; (Delorme & Makeig, 2004), and further confirmed via visual inspection, before running the ICA. Independent components (ICs) that contain blinks (identified by visual inspection) are then removed from the EEG data. However, the data from which ICs were removed held a different (lower) high-pass filter than the data on which the ICA was ran. A 1 Hz high-pass filter has been reported to diminish the low frequency components of event related potentials (ERP) (Rousselet, 2012). The MRCP has been reported to only occur in frequencies around 0-5 Hz (Wright et al., 2011), having led previous researchers to apply either no high-pass filter at all (Bai et al., 2006; Khalighinejad et al., 2018) or use one below 1 Hz (Mrachacz-Kersting et al., 2016) to preserve changes in the lower frequencies. As such we adjusted our filters in-kind. Keeping a 50 Hz notch and 40 Hz low-pass (both 6ths order) but high-pass was now 0.01 Hz (3rd order) instead of the 1 Hz used to run the ICA (Makoto's preprocessing pipeline (n.d.)). As a final step we interpolated the bad channels removed prior to running the ICA.

2.2.3 Neural Marker Characterization

For every trial the Epoch of Interest (EoI) was defined as a time window of 3 seconds relative to the MOn. Specifically, our window started 2.25 seconds before and ended 0.75 seconds after MOn. The

EoI covers 2.5 seconds (2s before and 0.5s after MOn). With an additional 250 ms added onto both ends of the interval to account for edge effects. The start of the epoch is based on the premise both ERD and MRCP start, on average, 2 seconds before MOn (Park et al., 2013; Shibasaki & Hallett, 2006).

As we are using the EEG signal to look at (right-hand) movement preparation, we extract the relevant information from the contralateral motor regions. When recording the ERD and MRCP, researchers often select the electrodes for which the largest ERD response and/or MRCP amplitude was observed, noting the main recording locations (according to the international 10/20 system) to be C3, C3' (positioned 1cm in front of C3), Cz and FCz (Bai et al., 2006; Cannon et al., 2014; Cassim et al., 2000; Jankelowitz & Colebatch, 2002; Khalighinejad et al., 2018; Neuper & Pfurtscheller, 2001; N. J. Seo et al., 2019; Wright et al., 2011). Unfortunately, our dataset was recorded using FCz as a reference electrode, making it unavailable to us and Cz is most likely compromised because it is directly adjacent to the reference site.

We also do not have an option to re-reference the data as the asymmetric electrode set up prevents average referencing, nor are mastoid or related electrodes recorded. Furthermore, the electrodes that could work for re-referencing (i.e., the ones that were symmetrically present, e.g., T7-T8, P7-P8) held baseline shift artefacts in some participants. As such we focus on recordings from C3 for both MRCP and ERD measures.

2.2.3.1 ERD pre-processing

The ERD is expressed as the power decrease in the EoI, in relation to a baseline interval, here defined as the 500 ms before the start of the EoI.

Working with time series data (such as EEG recordings) means information is presented over, or in function of, time (Buzsáki, 2011). Meaning, for some aspects of the time series, it is not possible to take a single measure to represent a single time point. However, we can try to estimate the measure of a single timepoint as close as possible. Such is the case for frequency band power. The issue with frequency is that frequency is defined over time, it is a cycle over time, where power is the squared amplitude of the defined cycle (e.g., a frequency of 1 Hz means one cycle covers 1 second, 8 Hz means one cycle covers 1/8th of a second (0.125s), or alternatively understood as a rhythm of eight cycles per 1 second) (Buzsáki, 2011). By moving a window over the time series in certain defined steps we can calculate frequency power within the boundaries of this sliding window. The power measure will then in turn correspond to the timepoints covered by the window. Take for example a time series of 3 seconds, using a window the size of 1 second and moving over the time series in steps of 1 second (i.e., window size is equal to stepping size, there is no overlap between the windows). We now have 3 measures of frequency power in the time series. We could say these 3 measures represent frequency power at the 1st second, 2nd second and 3rd second marker of the time series. Meaning, to discuss

changes in power over time, we say "1 second into the recorded time the signal band power measured X, which was different (or not) to the measured band power Y, at 2 seconds, and a band power measure of Z at the 3rd second". However, we need to practice caution with such interpretation of (time series) information gathered within a (moving) window of time. The measure reported at the 2nd second marker does not reflect just band power at that specific point. It reflects power of the entire time interval covered by the (in this case 2nd) window, spanning everything between the 1st and 2nd second marker. We merely chose to present the calculated band power at the most right edged point of the window. We could have also chosen 0.5s, 1.5s and 2.5s as timepoints instead, indicating the middle of the window.

It shows that our estimated values of a single time point depend on how we go about calculating frequency power (window size and stepping size) as well as how we interpreted the calculated output (i.e., start, middle or end of the window). A bigger window will cover more cycles of the frequency of interest, which comes with a higher frequency resolution, however, at the cost of a smaller temporal resolution (and vice versa) (Cohen, 2019). To increase our temporal resolution (estimate closer to a specific timepoint), without having to sacrifice our spectral resolution, we can move the window (same size) with smaller steps (i.e., the window moves with overlap). As a result, we have more values at different timepoints, giving us a better idea of how the time series changes in respect to a specific characteristic (e.g., band power). Take the same 3 second time series and a window size of 1 second from our last example, however, now we move the window in steps of 0.1s. We now have 21 different frequency measures. If we again choose to present the window values at their most right edge, 1st value would correspond to 1st second, 2nd value would be 1.1s, 3rd value would be 1.2s … 12th value to 2.1s and so on. Note that, because our window size was unchanged 1st, 11th and 21st measure will (in respective order) hold the same values as the 3 points of the previous example. Besides providing more measures to reflect changes over time, moving the window with overlap also results in more balanced estimates. The window only moves 100 ms at a time, meaning the difference between 2 timepoint estimates is only due to the information in those new 100 ms. The other 900 ms of data were present in both windows. Here lies the argument to report the band power measures at the timepoint on the window's right edge. If the window moves from left to right, the difference lies in those 100 ms on the right side of the moving window. On the other hand, reporting to the window's right edge side means there are no band power measures described before the 1st second of the time series. Take the first 5 values from our earlier example, reported as band power values in 100 ms intervals between 1s and 1.4s. However, the window over which the band power of these first 5 values was calculated largely consisted of the first second in our 3 second time series, yet, will not represent any of it. If we choose to report the calculated band power at the middle of the time window, there

will be a more even spread of the time series as whole. Take the 3 second time series example, reporting estimated time values to the middle of the window would give us the 1st value at 0.5s, 2nd value at 0.6s, 3rd at 0.7s, 4th at 0.8s … 12th at 1.6s… and the final 21th value at 2.5 seconds of the time series. Choosing to present window calculations at the midpoint further addresses another point in need of caution when calculating band power. Namely edge effects: the occurrence or introduction of a distortion or artifact at the boundaries of a time series when applying a certain analysis technique. For band power calculation, specifically, the datapoints towards both ends of the time series boundaries will contribute to fewer windows (and thus band power estimates for timepoints) than in the middle of the time series. Potentially skewing the interpretation of the true differences in changing band power over time. E.g. the datapoints between 0 to 0.1s will only be included in the first window of our earlier example. Data from the 0.1s to 0.2s time interval will only be included in the first two steps of the window. Whereas the datapoints between the 1st and 2nd second timepoint will all equally contribute the maximum amount a data point can be included in a window (10 times for a 1-second-wide window moving in steps of 100 ms). Similar case for the values at the end of the time series. Edge effects are another reason for why a moving window cannot cover the entire time series equally, regardless of whether you choose to report the calculated output left, middle or right to the window. If you report to the right edge, you are short on calculations at the start of the series, if you report left edge, you are equally short at the end of the series. Even when you report to the middle of the window you will miss some timepoints on both ends. See our example, reporting to the middle turns our 3 second time series in values between 0.5 and 2.5s. The issue here is, to get those earlier values (e.g., 0.2s) the window would only be partially filled with datapoints. What holds no data is interpreted as "no power" which will result in faulty output. A meaningful output will only come from having a meaningful data point for the entire window. A solution to both edge effect issues is to make the actual time series bigger than the points you are interested in. A bigger time series and reporting to the middle of the window ensures a more balanced representation of the timepoints contributing to the band power calculations, e.g., the difference in band power over the first 1.5 seconds is presented between 0.5s and 1s rather than between 1s and 1.5s. As well as an equal number of data points contributing to the window calculations.

As such, in our interest to investigate the changes of power over time the EoI relative to the baseline, for both time intervals band power was calculated in the alpha (8-13 Hz) and lower beta (14-20 Hz) frequency bands (BioSig toolbox *bandpower* function; Vidaurre et al., 2011) using a sliding window of 626 ms, to cover 5 cycle lengths of the lowest frequency of interest to avoid aliasing and retain a high-resolution spectral precision (Cohen, 2019). The window then moved over the epoch in steps of 1 sample point for maximal overlap and to compensate for the temporal resolution we lost by choosing

a wide sliding window. Resulting in a single band power value for each sample point. The timescale was adjusted to reflect the midpoint of the sliding window. Generally, ERD can then be quantified for every trial by subtracting the average baseline band power from each sample point band power value. Subsequent averaging over trials and sample points would then be used to get individual participant ERD values. Followed by averaging over participants to estimate the grand average ERD.

However, further analysis steps required a more generalizable description of the event related decrease in power. To obtain a more generalizable interpretation of the event related decrease in power, we calculated the decrease as a percentage relative to baseline (also referred to as baseline normalization of the time series; Khalighinejad et al., 2018). As a decrease of 40% translates easier to other datasets than a decrease of '0.2' on the log10() scale of the power (as calculated by the BioSig toolbox *bandpower* function using; Vidaurre et al., 2011).

Before we calculate the ERD strength, we need to consider the effect of removing the TMS artefacts. With cubic interpolation we ensured the new datapoints reflect the signal's (average) amplitude and no false data was introduced (as would have been the case with, for instance, spline interpolation; (Fritsch & Carlson, 1980). By covering a period of 120 ms (i.e., at least 1 cycle length for all frequencies of interest), however, the interpolated data forms a flat line; i.e., the signal holds no variance for this period. For band power calculation, where the measure relies on the divergence of the signal from its equilibrium within the sliding window, no variance is perceived as 'no power.' This results in up to 750 ms of datapoints with band power calculations corrupted by the 'no variance' window due to the size of the sliding window. To safeguard against this lack of variance introducing errors into subsequent analysis steps, all 750 ms of affected datapoints were replaced by NaN (Not a Number; representing missing data points in a dataset) values before averaging. Specifically, the no variance window resulted in such low power values that the log10() transformation (as part of the bandpower function used) returned negative power values. These negative power values in turn skewed the percentage calculations. Replacing the affected sample points with NaN values, which in turn would be ignored when averaging sample points, circumvented this issue.

Baseline normalization was then calculated as described by Graimann & Pfurtscheller (2006), by first averaging the band power per sample point (first within subject, then across), then subtracting the average baseline power (R) from every sample point (individually) band power (P) (i.e., how we calculated ERD on a trial level) and then by dividing by the average baseline power (P-R/R). With negative values indicating the frequency power at a specific time point was lower than the average power of that same frequency during the baseline interval. i.e., a decrease in power reflecting an increase in regional desynchronization.

2.2.3.2 MRCP pre-processing

For the MRCP we, once again, have our EoI and a baseline interval defined as the 500 ms before the start of the EoI. We baseline correct every trial by subtracting the mean baseline amplitude from every sample point in the EoI; after which all EoIs are averaged within participant. Note that, for the MRCP, we work directly with the signal amplitude. Unlike the ERD, the interpolated sections of the EEG signal do not cause significant issues for ERP interpretation as individual sample points still hold a value reflecting a close approximation of the signal amplitude.

2.2.3.3 Corticospinal Excitability

Motor evoked potentials (MEPs), as a measure for corticospinal excitability, were measured in terms of their peak-to-peak difference (max – min value) in amplitudes in the time interval of 0.015–0.040 seconds relative to delivery of the TMS (either real or sham). MEP values were then standardized (z-scored) within participants, to account for inter-individual differences in the amplitude measures, so all datapoints are comparable on the same scale.

Signal to Noise Ratios (SNRs) were calculated to ensure the values included were actual MEPs. 89.12% of the SHAM trials were seen to have a SNR value lower than or equal to 1 (meaning the signal has a similar or a lower value than the noise), compared to 16.99% of the TMS trials. As our control condition SHAM trials are assumed to have no MEPS, only noise. Therefore, we took the 90th percentile (SNR =1.1) of the SHAM SNR distribution to identify trials with no MEP.

2.2.4 Data Preparation and Quantification for Analysis

The trial rejection process resulted in 35.76***%*** of all included trials (2050) being rejected, of which 37.93% were rejected due to early or no movement and 27.83% were rejected because they were rest trials. This left a total of 1317 trials (675 SHAM and 642 TMS) in the dataset over all participants.

Table 1

Number of Trials Remaining, per Original Experiment Condition, After Initial Trial Removal.

	ERD 10%	**ERD 20%**	**ERD 30%**	**ERD 40%**	**Fixed 33ms**	**total**
TMS	135	127	118	108	154	642
SHAM	136	113	135	125	166	675
Total	271	240	253	233	320	1317

Note. Trials are presented per experimental condition to show we retain a relatively even spread of MEP values per theoretical time point/ key moments (i.e., points relative decrease in % relative to which TMS was applied as defined by Daly et al. (2018)). The experimental conditions used in the original data acquisition are not considered in our further analysis.

For the CSE, we further excluded all trials with an SNR equal to or lower than 1.1, reducing the TMS trials to 532. Looking at the distribution of retained MEP datapoints (see Figure 5), however, shows how most of the datapoints fall in the second half of our EoI. Note how, while our general EoI covers the 2 seconds leading up to Mon, our hypotheses describe (see 2.1 Introduction as well as Figure 2) an activity window of interest (in terms of the CSE peak and inhibition points in relation to ERD strength (as percentage)) from around -1s to 0s relative to MOn. As such we will focus all further analysis where most of the data is located, and the CSE data that fell outside of this smaller activity of interest time window (i.e., MEP values occurring more than 1 second before Mon; 9.39% of 532) were further cut. Bringing us to a total of 481 remaining TMS trials to be included for the analysis of the CSE.

To assess each neural marker their changes over time, we converted the -1s to 0s time interval with 500 sample points into a discrete variable with 10 levels by working with 100 ms intervals, calculating the mean value for each interval. Using linear models with categorical predictors, we encoded the factors using sigma parameter restrictions (i.e., effect coding, where the sum of the regression coefficients equal zero). Furthermore, we applied SAS type III to construct the sums of squares in the rmANOVA table (opposed to type I or II). Where Mauchly's Test of Sphericity indicated sphericity assumptions were violated, Greenhouse-Geisser corrections are applied to degrees of freedoms and p-values. Significant effects for time intervals are followed up with trend analysis using polynomial contrasts to see if the differences in neural activity follow the expected progressive trends (linear for the ERD and MRCP, cubic for CSE).

2.3 Results

2.3.1 Statistical Assessment of the Neural Markers

The focus of the analysis was to compare the ERD strength, MRCP and CSE timeline and assess the relationship dynamic between these neural markers in terms of timing relative to MOn. A visual comparison of the 3 neural markers is displayed in Figure 5.

We first assessed the neural markers' changes across time to ensure our measures are meaningful and reliable measures of motor control. We would expect to see a statistically significant difference (specifically a decrease for the EEG measures) in amplitude or power, relative to the baseline (average amplitude or power calculated over the 500 ms before start EoI) and progressively overtime. Lack of significant changes relative to baseline and over time would mean a marker is not really a movement potential, and thus despite what we see in Figure 5 cannot continue with it in analysis.

Figure 5

Changes in Neural Markers over Time Leading up to MOn

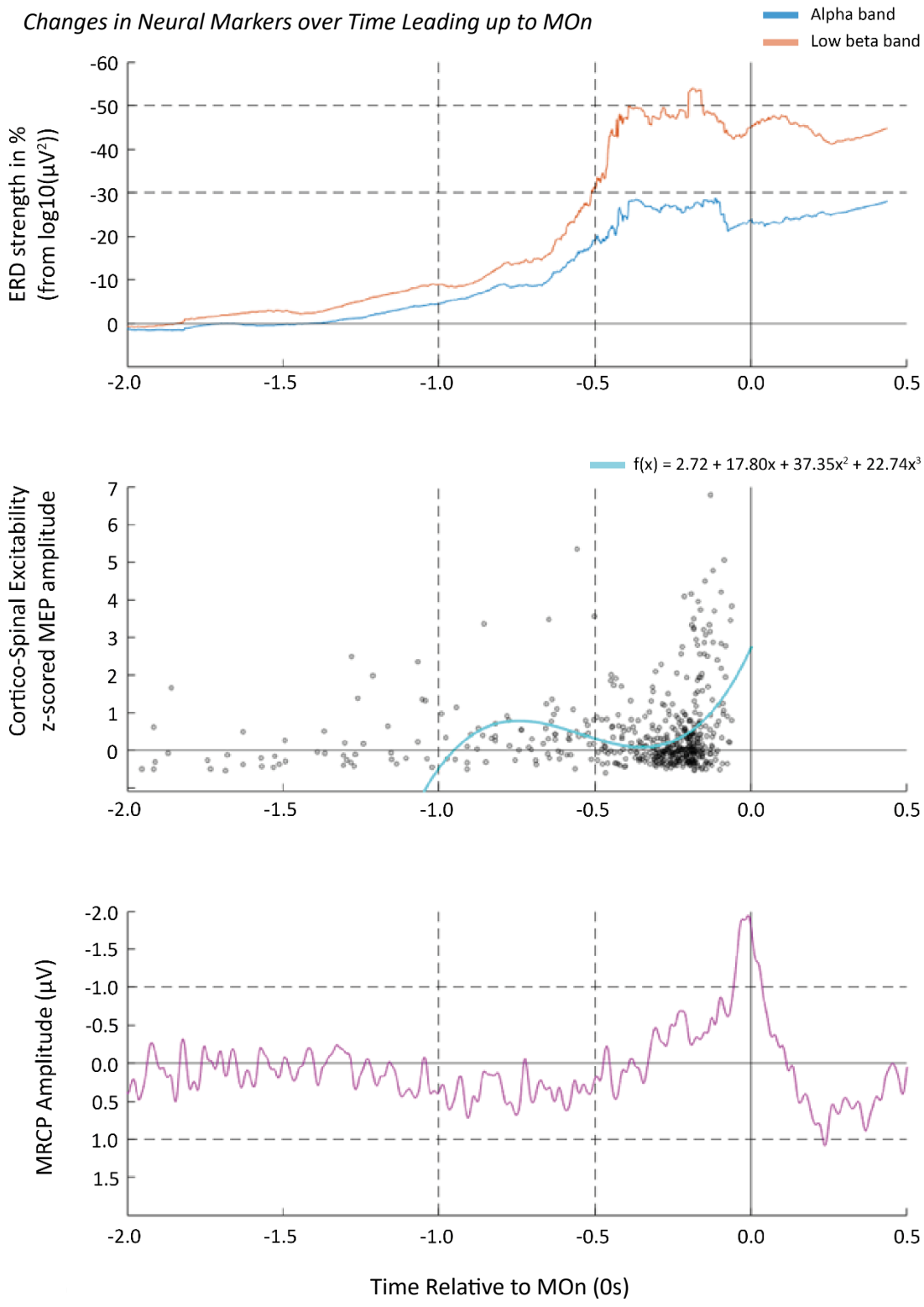

Note. Measures are plotted with precise alignment to EMG burst onset, with the x-axis representing time in seconds relative to t_0 = movement onset. ERD and MRCP represent grand averages across participants. The top panel shows the relative decrease in ERD strength (%), where each time point reflects band power at the midpoint of the sliding window. The middle panel displays z-scored MEP values, with a cubic regression model fitted to all data points to describe the temporal evolution of CSE over time (see 2.3.2.1 CSE dynamics over Time). The bottom panel depicts MRCP, with a reversed y-axis for both MRCP and ERD.

2.3.1.1 ERD

For both alpha and beta ERD, the transition from a smooth to jagged line between -500 ms and MOn in Figure 5 indicates where TMS was removed, and consequentially a reduced number of trials contributing to the calculation of the ERD averages. Time points of MEP values (see dots Figure 5, middle) visualize (consider a 15-40 ms latency period of MEP following TMS) the time points of TMS stimulation, with 86.28% falling between -500 ms to -50 ms before MOn. The concentration of MEP values reflects the degree of noise introduction in ERD, where at -500 ms to MOn only 20% trials were left, with the lowest number of trials contributing to the ERD at any point being 18% of the total number of trials at -445 ms. Despite the significant replacement of data values with NaN for EEG recording, only one participant had one time interval that ended up having no values.

A one-way repeated measures ANOVA (ran twice, once for each frequency) with time intervals as factor with 10 levels showed significant differences, over time, in power decrease relative to base line (quantified as percentage) for both alpha [$F(2.31, 20.79) = 9.38$, $p < .001$, $\eta^2 = .143$] and beta [$F(1.95, 17.56) = 6.25$, $p = .009$, $\eta^2 = .07$]. Follow up tests with linear contrasts (with separate error terms) indicated a statistically significant decrease of strength in power over time, for both alpha [$t(9) = -4.9$, $p < .001$] and beta [$t(17) = 6.22$, $p < .001$]. Together these tests indicate that, despite being noisy and affected by cutting in trials, ERD strength significantly increased over time for both alpha and beta.

2.3.1.2 MRCP

The same one-way rmANOVA with time intervals as factor showed no significant differences in amplitude (relative to baseline) over time for the MRCP [$F(1.71, 17.13) = 2.04$, $p = 0.16$, $\eta^2 = .029$]. Ten additional one-sample t-tests showed how none of the 10 intervals covering the 1 second timeline to MOn could be considered significantly different from 0 (i.e., baseline; [$t(10) = -1.16$ to 0.55, all $ps > .05$]). Indicating there was no statistically significant decrease in amplitude relative to baseline. As such the MRCP, as measured in our data, is an overall not meaningful or reliable measure ad indicator of movement preparation and will be discontinued from further analysis.

2.3.1.3 CSE

Ideally, we would also assess the changes in CSE over time using a rmANOVA. However, due to low numbers of retained trials per participants in EMG recordings, many participants had missing values for parts of the time leading up to MOn. When presented with imbalanced responses, rmANOVAs drop participants from the test in their entirety. As such, we used one sample t-tests as an alternative to assess each interval individually. The middle panel in Figure 5 shows CSE changes overtime. What we need to know is whether the change in an interval is on average significantly different from 0. Values

not being different from zero would imply there is no difference to the individuals' average MEP response (considering amplitudes were z-scored within participants).

One sample t-test for the CSE showed the only 2 out of 10 time-intervals (the 5th covering -0.6s to -0.5s [M = 0.52, SD = 0.354; t(5)= 3.561 p = .016] and 10th for -0.1s to 0s to MOn [M = 1.46, SD = 1.75; t(8)= 2.513 p = .036]) to be significantly different from 0. Being positive z-scores means for those intervals the participants MEP values were significantly higher than their average MEP amplitude.

Figure 5 (middle) further shows the MEPs of the 481 remaining TMS trials plotted on a timeline in terms of their z-scored amplitude and position relative to Movement onset. There is a visually apparent functional relationship between CSE and time, following the pattern of a third-degree polynomial as described in our hypotheses. The time intervals that showed to be significantly different from zero are in accordance to where increased amplitude was expected (see hypotheses Figure 2). As such, based on the statistical output our, CSE measure can be considered a meaningful measure of motor control, and further supports the predicted third-degree polynomial trend observed in our initial plotting (Figure 5).

2.3.2 Predictive Modeling

Continuing with the two neural markers considered meaningful in this analysis we aimed to further quantify and test the hypothesized trends (i.e., CSE over time) and relationships (i.e., dynamics of CSE in relation to the decrease of event related band power (ERD %) over the motor cortex).

2.3.2.1 CSE dynamics over Time

There is a visually apparent, functional relationship between CSE and time. We wanted to discover (a) what this relationship is and (b) how robust the relationship is over participants. Visually the relationship seems to follow the pattern of a third-degree polynomial, the same pattern as theorized and described in our hypothesis for temporal dynamics of CSE. Using a third-degree polynomial, we aimed to establish a model to mathematically describe the hypothesized underlying pattern of the changes in CSE (as measured by MEP) over time, relative to the Movement Onset.

Fitting our CSE model to all the data (481 MEP values; see middle panel Figure 5, Polynomial graph illustrates model fit $f(x) = 2.72 + 17.80x + 37.35x^2 + 22.74x^3$) showed time relative to Movement Onset explains approximately 10.6% (R^2= 0.106) of the variability in MEP amplitude.

We would test the fit of a cubic trend to describe CSE over time using polynomial contrast. However, the low number of retained trials, and 86% of the measures falling between -500 ms and MOn leading to an imbalance in responses, makes contrast testing not an option. Instead, to determine whether our model is truly the best fit to describe the CSE pre-movement onset timeline, we compared our

model with other candidate models in terms of their ability to describe and predict our data. The candidate models are: Zero slope (*f(x) = a*), linear regression (*f(x) = a + bx*), and an exponential model ($f(x) = a * e^{bx}$). These classic models are chosen to compare our model to the potential scenarios of 1) there not being a relation at all, what we find is a coincidence (zero-slope), 2) expressing the simplest relation between two variables (linear) and 3) the alternative relation we can observe in the visual presentation of CSE in time (exponential, Figure 5). R^2 is used as our main differentiating measure and tells us how well a model explains the variation in the response variable, going from 0 to 1. With a 0-value indicating the model does not explain any of the variance in our data. 95th percentile confidence intervals (CI) were calculated as a precision estimate, by generating a sample distribution through jack-knife resampling (Efron, 1982) (i.e., 11 resamples, leaving one participant and their datapoints out at each iteration), for each of the 4 models around their observed sample statistics (R^2 when fit the function to all the retained MEP values).

Jackknife resampling (see also Figure 6) indicated the third-degree polynomial model explained between 8.5 to 12.85% of the variability, with a point estimate of 10.6% (R^2 95% CI: [0.085, 0.129]), the zero-slope model explained 0% (R^2 95% CI: [0, 0]), the linear model explained 1.15% (R^2 95% CI: [0.005, 0.025]) and the exponential model explained 7.65% (R^2 95% CI: [0.044, 0.108]). Out of the 4 models to describe CSE based on time relative to movement onset, all but the zero-slope model explained a significant portion of the variance in the MEP amplitude (i.e., the 95% CI did not include 0; Du Prel et al., 2009). Furthermore, while the third-degree polynomial models' 95% CI overlapped with the exponential model their 95% CI, there was no overlap with either linear or zero-slope model. Meaning, the third-degree polynomial model is a statistical significantly better fit than the linear and zero-slope model in terms of explained variability (Tan & Tan, 2010). Following the third-degree polynomial and exponential overlap, a pairwise sample test was done on the point estimates of each iteration, to further determine statistical difference. Results showed the cubic model explained, on average, significantly more of the variance in the data than the exponential model [$t(10) = 13.4$, $p < .001$].

Figure 6

R^2 values and 95CI for 4 Candidate Models to Describe the Temporal Evolution of CSE

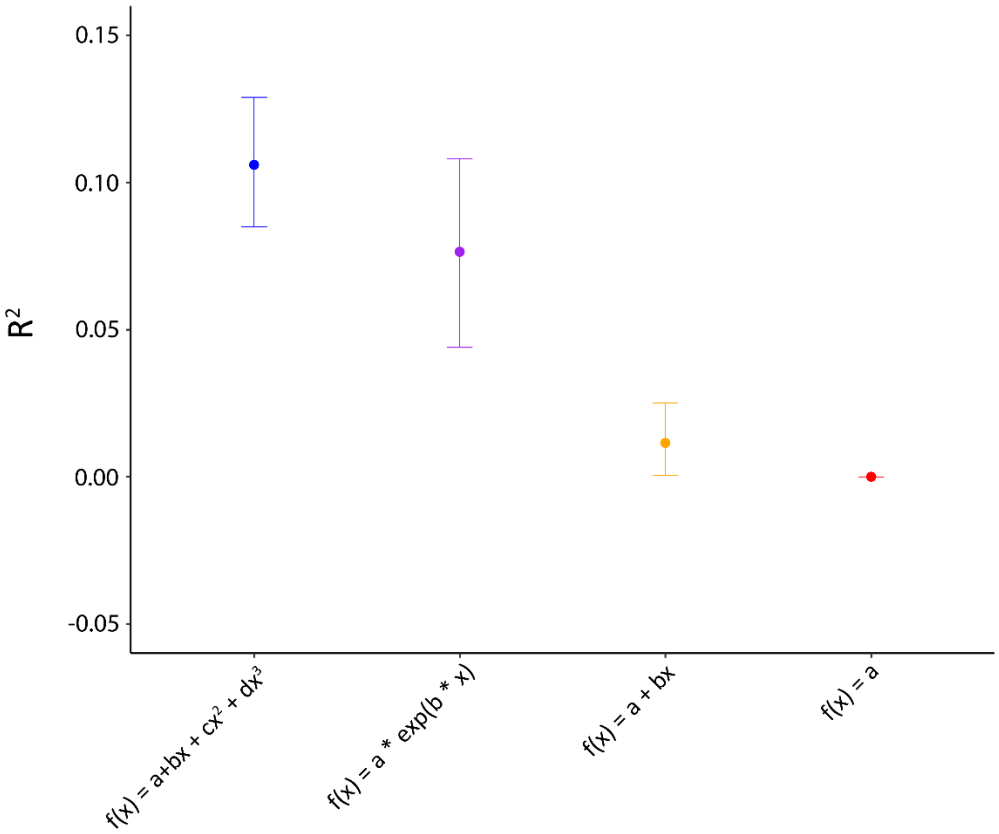

We used cross validation to further test and compare the goodness of fit of the models to the data; focusing on the models' predictive power as measured by the Mean Absolute Error value (MAE; Li, 2016, 2017) (indicating how far of the mark, on average, the predicted CSE values were from the observed values, measured as the test set's average absolute distance between estimated and observed MEP amplitudes). i.e., how well did the models predict the observed values in function of time.

Most classic cross validation methods describe the resampling of individual datapoints. Where the chosen type of cross validation (e.g., leave p out, k fold, etc.) determines how datapoints are handled and how many assigned are to training compared to test set). Consistent across cross validation methods is that the difference in data size between training and test set remains constant throughout the process (i.e., for every resampling). However, our data was obtained through a within-subject design. Meaning, the datapoints are not independent from each other and cannot be handled as such. Nor did we retain enough datapoints to execute a cross-fold validation model training and testing process on an individual participant basis (see Table 2 for number retained trials per participant; median = 45, min - max = [18 - 67]). Therefore, resampling of the data into training and test sets will need to happen with respect to the independent structure of the data. Meaning, rather than focus on

the individual datapoints to organize the data in training and test sets, we resampled participants and handled their respective retained trials as fixed subsets. Another issue is the unequal distribution of retained trials and MEP measures across participants. As we resample datapoints via participant, training and test sets will constantly change in size. Thus, we decided to approach the cross validation using a leave-5 out cross-fold validation scheme. Having only 11 participants we are limited to the number of data point combinations we have. The number of participants in the held-out set (5) was chosen to optimize the ratio of training and testing set sizes and to use the maximum number of combinations possible (i.e., 462 unique combinations). Having an odd number of participants, the 6-to-5 split will further lead to the training set to (on average) be bigger than the test set. Furthermore, will a 50-50 split in participant allocation help to approximate a consistent size of training and test set over the different resampling iterations as the participants with a lower number of trials will be prevented to have too much weight. Specifically, at 240.5 is exactly half of our 481 retained trials. Leaving p = 5 out training and test sets swing on average between [220, 260] trials (see Appendix A1 for more details).

Table 2

Number of MEP Values Included per Participant

Participant	1	2	3	4	5	6	7	8	9	10	11
Number of trials	24	45	52	43	36	67	27	18	55	55	59

Note. Number of trials reflects number of MEP values retained after all exclusion criteria applied.

Taken together, this means we assessed the fit of a third-degree polynomial model compared to an exponential model, using the training-based coefficient estimates to predict the Y (MEP values) values for every X (time relative to MOn) value in the test dataset, consisting of the combination of the 5 remaining participants. We focused exclusively on the exponential model who, despite explaining statistically significantly less variance, remains the second-best contender in describing the temporal dynamics of CSE.

Cross-fold validation outcome shows how, on average, predictions by the third-degree polynomial (mean ± SD = 0.71 ± 0.053, 95CI: [0.61,0.82]) were, according to a pair wise t-test, not significantly different [$t(461) = 1.81$, $p = .065$] in error rate from the predictions made by the exponential model (mean ± SD = 0.71 ± 0.044 , 95CI: [0.62, 0.8]). Indicating that, while the third-degree polynomial model explains more variance in the MEP values, it does not perform differently from an exponential model in terms of predicting MEP amplitude based on time relative to Movement Onset.

2.3.2.1 CSE dynamics in Relation to ERD

Our analysis aim was to further explore the suggested relation between the ERDs relative increased strength (quantified as percentage) and CSE. We are interested in the general ability to predict CSE based on ERD strength (i.e., how consistent would a 30% decrease in band power predict the raised MEP amplitudes between -1 and 0.5s to MOn?). Also, whether the changes in relative ERD strength proportional to MOn would be better able to predict CSE values, compared to a model purely on time relative to MOn. Earlier results showed the ERD strength to change linearly over time leading up to MOn and the changes for CSE on the same timeline to be best described with a third-degree polynomial (Figure 5). As such we expected the relation of CSE and ERD to resemble the cubic relation of CSE and time; i.e., MEP values will increase and decrease in function of decreasing ERD power following the pattern of a third-degree polynomial. To determine how well a third-degree model can describe the CSE-ERD relationship, we applied the same cross validation methodology as described in section 2.3.2.1 CSE dynamics over Time. However, focusing on the third-degree polynomial model and assessing its ability to predict CSE in function of ERD power percentages, with lower error rates indicating a third-degree polynomial appropriately described the synchronized progression over the same timeline. Comparing the predictions for alpha to those of beta.

The analysis beyond this point is exploratory, because we have reached the extent of what we can get out of this data. The following describes our best effort to investigate the CSE and ERD relationship considering limited and noisy data. We struggled particularly with mapping the ERD measures directly to the corresponding CSE measures. As described in section 2.3.1.1 ERD, the highest number of CSE values are where the lowest concentration of ERD data is. Leaving time points without any data or high noise. As an alternative we attempted to capture a delayed effect using reliable data points in the time window of -1s to -0.4s before MOn for ERD strength and -0.4s to 0s before MOn for CSE (for CSE this means a reduction in data points of 21.8%; from 481 to 376). Y(CSE at time t) = X(ERD% at time t-n) where n = -400 ms so that CSE at t = -100 ms (i.e., 100 ms before MOn) gets predicted by the last "clean point" (i.e., not TMS contaminated) of ERD at -0.5s.

Cross-fold validation outcome shows how, on average, predictions for CSE values using the third-degree polynomial were significantly more accurate [$t(461) = -10.5$, $p < .001$] when made based on the changing power leading up towards MOn in the alpha frequency band (mean ± SD = 10339.04 ± 10995.04, 95CI: [-11151.3, 31949.3]) than the beta frequency band (mean ± SD = 82766.21 ± 150116.14, 95CI: [-211461.8, 376994.2]).

2.4 Discussion

It has been argued that learning benefits from, and relearning relies on, increased cortical excitability (Clarkson & Carmichael, 2009; Lissek et al., 2013). CSE is considered to reflect a state of "neural readiness" that changes in response to the cortical activity (Leocani et al., 2000, 2001). As a result, cortical excitability has been proposed as a neural marker for motor learning and use-dependent plasticity. Previous work suggests a link between CSE and ERD strength, indicating that changes in CSE may be deduced from its association with ERD, a neural marker that is easier to measure (Daly et al., 2018). However, the exact nature of this relationship—including how it is shaped and how stable it is over time and contexts—is still unclear. Since the temporal dynamics of CSE play an important role in shaping its relationship with ERD, it is essential to establish a clearer timeline of CSE fluctuations before movement execution. This would allow to assess the reliability of the CSE and ERD association, both in general and as a means of inferring excitability fluctuations.

2.4.1 Temporal Dynamics of CSE

Our preliminary insights into the broader CSE timeline tentatively support our first hypothesis—that the temporal dynamics of CSE leading up to MOn are best described as an S-like wave. Our results indicate that a third-degree polynomial explains significantly more variance in MEP amplitudes as a function of time compared to other theoretically plausible descriptive models. However, to further evaluate the dependability of this model—i.e., how well the progression of CSE over time can consistently be described by an S-like wave or a third-degree polynomial (cubic) relationship with time—we assessed how accurately it estimated MEP values based on time. Despite the third-degree polynomial having the strongest descriptive fit, it did not outperform the exponential model in this predictive test. Furthermore, while both models were at times less far off from observed values, neither was ever truly accurate, as indicated by the fact that neither model's CI included or was close to 0, which would signify no difference from the observed values. This suggests that the cubic model's ability to characterize CSE dynamics may not be as stable or generalizable as initially expected. At the same time, these results do not disprove the cubic model's suitability to characterize CSE dynamics. Especially as this lack of difference in performance could potentially be explained by the severe imbalance of data distribution over time. As shown in Figure 5, 86% of retained data points fell between -500 ms and MOn—exactly where we both hypothesized and observed the CSE to decrease before a steep increase. As a result, in the most data-heavy window, we have a pattern that closely resembles an exponential trajectory, artificially advantaging the exponential model simply because most of the data fell within the portion of the timeline where amplitude naturally increased sharply. This data imbalance likely may have skewed the models' outcomes, causing the cubic model to perform worse while the exponential model did better than it otherwise would. The issue would then have

been further amplified by the already small dataset, which was then split for either training or testing, effectively limiting both model's ability to capture the full trajectory of CSE dynamics.

It is entirely possible that the third-degree polynomial's ability to explain higher variance is due to overfitting rather than capturing meaningful structure in the data. However, if overfitting was an issue here, we would expect overall higher R^2 values. Furthermore, if our model was overfitted to capture the specific variance in this dataset we would also expect the overfitted model to outperform less well fitted models when testing predictability. Instead, our R^2 are rather low and the cubic model did not do great predicting MEP amplitudes, let alone do better than less fitted models.

While generally low R^2 values indicate that the cubic model does not explain a large proportion of variance, it did explain more variance than other, simpler models that also had valid theoretical justification for describing the observed trend in the data. Furthermore, it was never the goal or expectation of this study to identify the exact trajectory of the data on our first attempt. Our intent was to provide a first attempt at describing and quantifying the temporal evolution and dynamics of CSE over a broader timeline, and test our hypothesis that these dynamics appear to follow a cubic trend. To this end, while an S-like wave represented by a cubic function may not be the best fit or fully explain all the nuances underlying the CSE structural nature, our results indicate there is some merit to this hypothesis, enough to explore further as stronger evidence is needed for both disproving or supporting our claim.

2.4.2 Inter-Dynamics of the Neural Markers

We expected to replicate previous findings on the temporal evolution of individual neural markers when calculated from the same dataset and anticipated that these markers will align with descriptions found in the literature.

A visual evaluation of the *MRCP* in Figure 5 (bottom panel) aligns with the test results, showing that the negative potential shift never diverges significantly from zero. Indicating that the signal amplitude in the two seconds leading up to MOn never significantly differed from baseline. While we do observe the classical MRCP shape, its amplitude ranges from 0 to -2 µV, which is substantially lower than the -5 to -30 µV range typically reported in the literature (Schultze-Kraft et al., 2016; Shakeel et al., 2015; Wright et al., 2011). Specifically, we seem to observe the late lateralization of the NS component between -500 ms and MOn. However, the characteristic slow decrease in amplitude of the RP between -2s and -1s is absent. A likely explanation lies in how the data was recorded. The FCz electrode (frontal-central scalp location) was used as the reference during recording (Daly et al., 2018). Since the RP arises as a diffuse, central distributed signal across the scalp (Fairhall et al., 2006), it was likely largely removed due to volume conduction (Holsheimer & Feenstra, 1977). In contrast, the NS, as a lateralized and more spatially focused component, was less affected. Unfortunately, the asymmetrical electrode

set up (see Figure 3 in Daly et al., (2018)), absence of mastoid electrodes, and the inconsistent presence of artifacts in several channels left no reasonable options to re-reference the data to recover the lost RP. Consequently, MRCP measures could not contribute further to this study's analysis. However, in the absence of the RP, a graphical review still provided valuable insights, allowing for comparisons between the MRCP, CNV, and LRP (as briefly discussed in 1.1 Neural Activity of Motor Control). Notably, there are clear similarities between our (presumably) retained NS component and the LRP. Both occur over a 500 ms window and while the NS—when following an RP buildup—will normally reach higher amplitudes, our observed -2 µV aligns well with the average LRP amplitude (around -2.5 µV) (Leuthold et al., 2004; Leuthold & Jentzsch, 2002). In contrast, the amplitude range we did not reach due to an absent RP closely resembles the range typically observed for CNV. This is particularly noteworthy because these similarities emerge in a context of self-paced voluntary actions, rather than the "two-warning cue' paradigm typically used to assess the CNV, and by some used as a reason to differentiate form MRPC.

While these insights, based on visual assessment, do not directly contribute to the answering of the study's hypotheses, they provide interesting observations in the broader framework of understanding neural circuit of motor control.

Looking at Figure 5 (top panel), we observe, supported by test result, that the grand average ERD strength significantly increased across participants relative to baseline. By 500 ms before MOn, ERD strength reached around 20% (alpha) and 30% (beta), followed by a 50% strength increase at MOn (beta, compared to approximate 29% for alpha).

Overall, the observed ERD strength pattern is consistent with our expected 20-30% range around -500 ms to MOn and 50% at MOn. However, we note some interesting differences between the ERD measures of the alpha and low-beta frequency bands. Specifically, most studies report higher relative ERD strength in alpha compared to beta (Cassim et al., 2000; Neuper & Pfurtscheller, 2001), we observed the inverse of this expected differences in ERD magnitude between alpha and beta. While alpha ERD follows its expected trajectory, reaching an average 25% increase in strength shortly after the predicted -500 ms to MOn mark, it then unexpectedly peaks at 30% shortly thereafter and remains constant until MOn. In contrast, the low-beta frequencies unexpectedly also reached the 30% threshold at -500 ms, even more unexpected is that beta then went on to peak at 50% and did so ahead of the predicted point of MOn. The most likely explanation for this pre-mature peaking is the "flattening" of the ERD strength trajectory curve, as observed in Figure 5 (top panel). This effect is likely due to the high density of TMS pulses within the -500 ms to MOn window, which required extensive signal-cleaning measures to prevent contamination, as detailed in section 2.2.3.1 ERD pre-processing. Although our inverted strength trajectories appear to contradict previous literature, rigorous

verification of our methodology confirmed that this discrepancy was not due to procedural or analytical errors.

Regarding the correlative nature of the ERD and the temporal evolution of CSE leading up to movement initiation, as well as our attempts to quantify it, a qualitative and comparative assessment of the individual CSE and ERD trajectories suggest that we did replicate Daly et al. (2018) their original findings to some degree through our alternative, time-based approach.

As discussed in section 2.4.1 Temporal Dynamics of CSE, we cannot make definite claims that an S-like wave is the best representation of CSE evolution, nor can we conclude that time relative to MOn alone is sufficient to reliably estimate CSE. However, our results do indicate a cubic model explains a significant portion of the variance and performs better than alternative models in that regard. This suggests that the hypothesis of an S-like wave as a descriptor of CSE dynamics remains the most promising avenue for further exploration. This interpretation is further supported by our findings that for CSE, significant differences from zero average amplitude were observed in the intervals -0.6s to -0.5s and -0.1s to 0s relative to MOn. The positive z-scores in these time windows indicate that participants' MEP values were significantly higher than their individual average MEP amplitude, aligning with expectations based on Daly et al. (2018) their “peak CSE”. This, combined with the increase in CSE between -100 ms and MOn—which is in line with prior literature—supports the idea that the increase in CSE around -500 ms reflects a preparatory phase increase preceding pre-movement inhibition. Together, these two findings suggest that we successfully replicated the two main characteristics of CSE—drawn from different parts of the literature—which informed our conceptualization of an S-like wave for CSE dynamics when analyzed over a broader timeline within a single dataset. Furthermore, we found that both alpha and beta ERD reached a 20-30% strength increase around the -500 ms time point. While the observation of alpha and beta their inversed strength trajectories contradicts the existing literature, and one leans to 20% the other 30%, these ERD magnitudes remain in line with Daly et al. (2018) their findings. it is important to note that Daly et al. (2018) did analyze separate frequency bands but instead calculate a single ERD measure over the wider 8-20 Hz range, capturing the full sensorimotor rhythm. Since this combined frequency range (spanning both alpha and low beta) contains the majority of ERD during motor execution tasks (Daly et al., 2018; van Wijk et al., 2012), this likely explains the observed consistency between our results and theirs.

When it comes to quantifying the relationship between ERD and CSE and evaluating how well ERD functions as a real-time predictor to CSE, our results are rather inconclusive. Specifically, we were unable to determine how well a cubic model works to describe their relationship. We attempted to quantify this through predictive modeling, but results were difficult to interpret. Our findings do not

provide strong evidence or clear insight into whether a cubic model is the best representation of this relationship.

Given the high error rates (MAE), it is challenging to assess how well a cubic model consistently and reliably describes CSE activity based on ERD progression. The high MAE values suggest that the model struggles to account for the high variance in the data and is likely overfitting to noise rather than capturing an underlying trend. The most likely causes of overfitting in our case are: 1) having noisy data. A solution would be to use a more and cleaner data, but this was not applicable in our study as the data was as clean as possible while maximizing retention. 2) Additional variance caused by training and testing on between-subject data. We know there is high inter individual differences for neuroimaging data. We know that neuroimaging data exhibits high inter-individual variability. While we addressed this issue for CSE by standardizing MEP amplitudes, no comparable solution was available for ERD power values.

Despite the significant linear increase in both alpha and beta ERD (as shown in Figure 5) and the higher magnitude of beta ERD, predictive modelling performed better for alpha than for beta. Although both models had extremely high error rates, alpha ERD exhibited a significantly lower error rate, suggesting that the relationship between ERD and CSE is more stable when using alpha. This difference is likely rooted in the higher inter-individual variance in beta power, which is consistent with prior literature. Alpha power tends to peak consistently around C3, whereas beta power is more spatially distributed across the scalp (Crone et al., 1998; Fogassi et al., 2005; Neuper & Pfurtscheller, 2001; Toro et al., 1994). This greater spatial and individual variability in beta ERD may explain why predictive modeling performed worse in this frequency band.

Overall, we have pushed the limits of what can be extracted from this dataset. The high noise levels and limited statistical power due to low level of retained trials constrain the strength of our conclusions. Nevertheless, our findings indicate a probable relationship between ERD and CSE. At the very least, there appears to be a correlation driven by a shared factor—both progress and change over the same timeline leading up to MOn.

2.4.3 Bridging Research and Application in BCI

Preliminary considerations on using ERD measures to anticipate changes in CSE via a cubic model as representation of this relationship, particularly in terms of predictive capabilities.

Our findings indicate that alpha ERD performs better than beta ERD in predicting CSE, but given the high error rates, it is reasonable to question whether either measure is truly useful in this context. One likely explanation for the observed difference between alpha and beta is the higher variance in beta power. A more practically informed approach—such as determining which electrode sites to focus

on—could improve predictive performance. This ties back into the need to better understand how ERD behaves across different frequency bands and their spatial distribution over the cortex. Currently, there is no clear consensus on whether to focus on a single frequency band or a combination of bands. For example, should low-beta be ignored in favor of alpha, or should we work with combined frequency bands (like the cross-frequency approach used by Daly et al. (2018), where a single ERD was calculated across alpha and low-beta and the strongest response was selected). Regardless of the chosen method, further research is needed to establish a clearer understanding of ERD dynamics independently and to establish its relationship with CSE.

Taken at face value, our findings suggest that estimating CSE from ERD strength via a cubic model is not useful in a practical application. However, this interpretation must be considered within the context of our specific study design and analytical approach. For starters, our primary aim was to describe and quantify the relationship between ERD and CSE, rather than to optimize a real-time predictive model. We sought to determine whether CSE changes could be described as a third-degree polynomial over the linear progression of time, and we hypothesized that this S-like pattern might also describe CSE changes as a function of the linear progression ERD strength over time. Predictive modeling was then used as a quantification tool, as a means of testing whether a cubic model could effectively capture this pattern. Furthermore, our specific cross-validation approach (across participants) and the MAE metric may not necessarily be the most appropriate way to establish, capture, or describe this relationship. However, given the high noise levels and limitations of our dataset, it is difficult to determine whether these methodological choices truly affected the results or whether the data itself was simply insufficient.

While we agree that there is potential value in using one measure to inform changes in the other over time (e.g., using ERD to anticipate CSE), our current model is not yet viable for practical application, regardless of the frequency band used.

Furthermore, what remains unclear is whether the observed changes in CSE hold a functional relationship or merely a correlational one to ERD. Either scenario would allow ERD to be used as a predictor of CSE, enabling more precise timing of feedback relative to (planned) movement initiation. However, the previously discussed differences in alpha and beta ERD behavior should be carefully considered. Alternatively, it may be beneficial to adopt a more standardized approach by measuring ERD over the broader range of sensorimotor rhythms (8–20 Hz) (Daly et al., 2018)—particularly in BCI applications.

BCI setups tend to differ from each other and conventional ERD research in two key ways:
Referencing Methods: Many BCI systems process EEG signals differently in real-time (i.e., online), such as bipolar referencing (e.g., Daly et al. (2018)) versus single-electrode referencing with mastoids or earlobes (e.g., Mrachacz-Kersting et al. (2016)). This contrasts with most published ERD research, which typically involves offline processing. Feature Selection: Many BCIs select the strongest power response for each participant, prioritizing consistency over meaning.
This is reasonable for general BCI applications, where neural signals do not need to encode complex meanings beyond consistent event-related responses. For instance, using MI of the right hand to move a video game character (Scherer et al., 2017). However, when the goal is to predict the behavior of one neural marker based on another, greater attention must be given to the sources of variance in ERD power responses. These include differences between frequency bands, electrode placements, and individual participants.

Based on both our findings and prior literature, the temporal evolution of CSE remains largely theoretical—let alone the precise point of "optimal" excitability. Furthermore, do MEP amplitudes exhibit high variability both across and within individuals, influenced by several factors such as: Coil positioning shifts if a participant moves, stimulation timing within an oscillatory cycle, Hormonal fluctuations (e.g., menstrual cycle effects in females) (Rivas-Grajales et al., 2023). However, despite this variability, both previous research and our preliminary findings suggest that CSE follows a general, consistent trend leading up to MOn. This trend appears to be stable across different movement types (Ibáñez et al., 2020). If there is a functional dependence between CSE and ERD, a fixed point of relative ERD strength (such as the 30% increased strength suggested by Daly et al. (2018)) may serve as a reliable indicator of CSE changes. Further research is needed to define the conditions necessary for consistency. Conversely, if CSE and ERD are only correlational, meaning they occur on a similar timeline (approximately 2 seconds before MOn) but as independent contributors to a larger movement preparation mechanism, their temporal alignment may be more variable. Under this scenario, a 30% increase in ERD strength would not consistently map to the same phase of CSE evolution across participants, frequency bands, or electrodes. Instead, the timing of this increase relative to MOn would shift depending on these factors.
The existence of this variability and the tentative evidence supporting a correlational relationship between ERD and CSE are further reinforced by an exploratory visual analysis (see Figure 7). In this analysis, we plotted MEPs relative to MOn based on the relative ERD power decrease used by Daly et al. (2018) to differentiate experimental conditions. We expected power to decrease linearly relative to MOn, with MEP values obtained at 10% occurring before a 30%. However, Figure 7 contradicts this

expectation, showing that MEPs measures at 10% ERD strength occurred at the same distance from On as MEPs from 30% ERD.

Granted, further investigation is necessary to understand the underlying causes of this inconsistency.

Figure 7

Changes in MEP Amplitude over Time Relative to MOn by to ERD % Condition

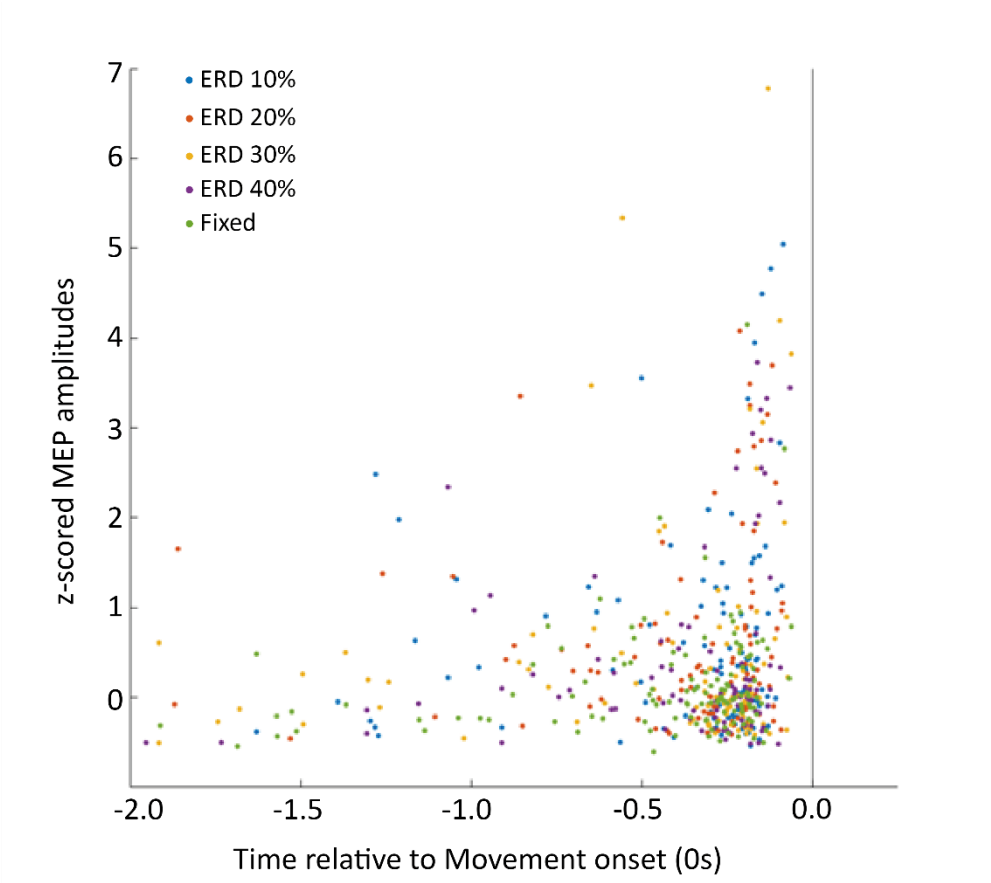

Note. MEP values are plotted relative to MOn (0s) and categorized based on the relative ERD strength at the time of stimulation, as measured by Daly et al. (2018). "Fixed" condition refers to stimulation 33 ms after 'go' cue, regardless of time of movement initiation. The figure illustrates how the reported MEPs do not follow the linear progression relative to MOn we would expect to see based on the ERD strength categories (i.e., clustered together and 10% on the left side of the graph with 40% more on the right, with fixed spread throughout).

One possible approach would be to recalculate the ERD percentage for these trials and compare it to values obtained by Daly et al. (2018). Additionally, we could assess whether these findings remain consistent at C3, which we used in this study, as well as explore the alternative bi-polar reference approach used by Daly et al., and select the electrode with the strongest response.

Another important avenue for exploration is to examine the changes in ERD across both frequency bands and their spatial distribution over the scalp, particularly in relation to the temporal evolution of

CSE. A potential solution for more accurate CSE prediction could involve a BCI setup that monitors ERD changes across multiple electrodes rather than relying on a single fixed location.

Ultimately, we believe there is significant promise in leveraging ERD to infer changes in CSE over time. However, this depends on both measures being well characterized and understood. In the context of this study, the still under-researched and poorly understood temporal trajectory of CSE remains a major limitation to the development of a reliable predictive model. Until CSE dynamics are better characterized, actively advancing such a model remains premature.

2.4.4 Future Directions and Next Steps

This study has laid the foundation for future research to further explore the timelines of these neural markers and their correlational relationship. Additionally, it provides a basis for investigating whether the specific dynamics and quantifiable measures of these markers could offer deeper insight into their relationship—whether it remains purely correlational or whether systematic changes in one marker induce measurable effects in the other, indicating a potential causal link.

As we mentioned earlier, we exhausted all available information from the dataset by Daly et al. (2018). Despite probably being the most suitable existing dataset for our research intent, we must recognize it does not suffice to appropriately challenge our hypotheses. As such, a follow up study is needed with an experimental design that allows us to fully control the collected data. With the highest priority being an even distribution of CSE measures across the two second timeline leading up to MOn.

One avenue for future research lies in the practical application of the relationship between CSE and ERD to optimize BCI and rehabilitation protocols. Where a key focus should be determining the precise point within the CSE timeline that is optimal for pairing stimulation or feedback with movement execution. Understanding when to intervene in relation to CSE fluctuations could enhance motor rehabilitation strategies and improve BCI efficiency. Another crucial direction is the investigation of factors that mediate CSE activity and, by extension, this "optimal point".

Among these, learning is particularly relevant mediating factor for both BCI based rehabilitation and the CSE timeline with its ERD association. Learning comes with changes in the brain, and it is a primary mediator of CSE fluctuations (Kleim, 2009; Kleim et al., 2007), alongside variations in movement type. If learning modifies CSE activity, it may also shift the optimal point for stimulation or feedback. Thus, before directly exploring "optimal excitability", future research should aim to refine our understanding of the CSE timeline and how it behaves in the intended application context (i.e., BCI use for rehabilitation and motor learning).

In the following chapters (3 and 4), we aim to broaden the foundation of knowledge on CSE using our own experimental design and collected data. Doing so we hope to further explore our preliminary findings as well as ensuring that future research exploring the optimal point in a learning-based rehabilitation context can account for CSE changes induced by learning. Specifically, by looking at the neural markers' dynamics in a motor learning task we investigate whether quantifiable measures of neural markers, their timelines, and their correlational relationship provide additional insight into their interaction. However, establishing causality will be challenging, as learning itself could act as a third variable influencing both CSE and ERD simultaneously. Instead, our focus will be on assessing the consistency and reliability of their relationship. If CSE and ERD exhibit strong parallels in how they are affected by learning, this would suggest a stable, reliable relationship, strengthening the case for predictive applications. If their changes are less synchronized, it would indicate a weaker dependency, suggesting that their correlation may arise from shared involvement in motor system processes rather than direct dependency or interaction. Nonetheless, even in the absence of direct causality, a well-characterized correlation between CSE and ERD could still be leveraged for practical applications, provided their interaction is systematically mapped and understood.

Chapter 3: Behavioral Experiment

3.1 Introduction

Ultimately, the theoretical background of this project is framed around optimizing BCI setups for motor rehabilitation, primarily for—but not limited to—stroke-related impairments. The research in this thesis addresses this by exploring the concept of an "optimal point" for providing feedback, specifically to enhance interactions with preserved elements of the FoFe-loop in motor control. CSE is considered central to identifying this optimal point. To this end, Chapter 2 provides preliminary insights into the viability of using ERD strength to infer CSE dynamics and CSE's potential role in determining the timing of feedback. Another key aspect this thesis explores is how learning-related neural changes could affect BCI setups that work with static assumptions of neural markers. Specifically, this involves examining learning as a mediator of CSE and improving our understanding of ERD and MRCP dynamics—two of the most commonly used neural markers of motor control in BCI—independent of their relationship to CSE. As argued in 1.4.2 Accounting for the Changing Neural Landscape during BCI, BCI rehabilitation setups that focus solely on relative changes in ERD strength—such as simple hand-opening/closing paradigms or their motor imagery equivalents—should still be aware of and account for learning-driven shifts in ERD progression rather than blindly updating their models. This raises a further concern: if ERD or MRCP is used to guide CSE inference, how stable is this relationship over time? If one or both neural markers change, does the inferred link to CSE remain valid?

As noted in the discussion of Chapter 2, our research questions and hypotheses are highly specific. We utilized the Daly et al. (2018) dataset to its fullest extent, but we are not aware of any other existing dataset suitable for further exploration of our research questions or hypothesis testing. Therefore, we must collect the data ourselves. Beyond simply gathering more and better-quality data to investigate neural marker relationships, the primary application of this research—its relevance in a learning context—necessitates examining learning effects directly. Consequently, we must design an experiment that enables this investigation.

Motor skill learning has been investigated using a range of experimental tasks and paradigms, such as juggling, continuous tracking, visuomotor tracking, and isometric force-production tasks (Christiansen et al., 2018; Dayan & Cohen, 2011; Yang et al., 2017).

When designing our experiment and selecting a task, we need to ensure movement measurements are comparable to previous research. This ensures that our neuroimaging data and measure align with existing findings, allowing for meaningful comparisons. To achieve this, our experiment task must: (1) involve right-hand-dominant participants, (2) be reasonably paced, (3) remain simple, and (4) allow the hand to be fully at rest between trials to obtain pre-movement CSE measures via MEPs. The

challenge lies in designing an experiment that meets these criteria while maintaining compatibility with prior studies.

Some of the simplest real-life examples of hand motor learning involve tapping-based skills, such as typing or playing musical instruments, and even knitting—activities that require practicing sequential movements. Motor sequence learning is fundamental to skill acquisition, many complex tasks in daily life emerge from such smaller, well-practiced sequences of actions (Hashemirad et al., 2016), and has been shown to lead to lasting improvements beyond baseline performance over time (Dayan & Cohen, 2011). This inherent ability to learn sequential actions plays a crucial role in human motor skill development, enabling us to perform everything from simple button presses to intricate musical performances (Hashemirad et al., 2016).

Commonly used sequential motor learning tasks include the Serial Reaction Time Task (SRTT). In this paradigm, participants respond to a visual cue appearing in one of four horizontal locations on a screen by pressing a corresponding key. Some trials follow a random order, while others present a recurring sequence, allowing participants to learn and anticipate responses, resulting in faster reaction times (Dayan & Cohen, 2011; Robertson, 2007). Although the stimuli follow a repeating sequence, only one stimulus appears at a time, making the learning process implicit (Vernet et al., 2011). A modified version of the SRTT by Zhuang et al. (1997) distinguished between implicit and explicit learning by asking participants to reproduce the 10-item sequence they had been exposed to. The rationale was that the knowledge required for consciously recalling task elements in the correct temporal order constituted explicit learning. Another task used to study sequential learning is the sequential visual isometric pinch force task (SVIPT), where participants (primarily through implicit learning) learn to control fingertip force in a specific sequence of target force levels. Performance is typically assessed through changes in movement speed, accuracy, and overall skill (a combination of both), serving as behavioral measures of improvement in motor sequence learning (Hashemirad et al., 2016). The Sequential Finger Tapping Task (SEQTAP) is another widely used paradigm for studying motor sequence learning. In this task, participants press buttons corresponding to a series of numbers (usually 1–4) displayed on a screen. While SEQTAP is often used to assess explicit learning but can also involve implicit learning. For example, Walker et al. (2002) used an implicit version in which participants were aware of the task but did not receive feedback on their performance.

Note how these sequential motor learning tasks can be categorized into two groups: explicit and implicit. In Chapter 1 (Section 1.2 Motor Learning), we introduced the learning spectrum, ranging from implicit to explicit learning. Explicit learning involves the use of conscious knowledge to execute actions and guide motor performance, whereas implicit learning occurs without a corresponding increase in awareness of skill execution (Jongbloed-Pereboom et al., 2015; Robertson, 2007).

To investigate learning-induced neural changes in healthy, able-bodied participants we designed an experiment with the aim to simulate a motor rehabilitation context. In stroke rehabilitation, patients engage in goal-directed (i.e., explicit) learning by repeatedly practicing specific movements to improve motor skills and restore voluntary function. Since our study examines motor learning within this framework, the experimental design must reflect rehabilitation principles—emphasizing repetitive, task-oriented activities that promote neuroplasticity and the re-establishment of functional motor patterns. Furthermore, is an explicit learning context is not only encouraged for its similarity to rehabilitation but also further reinforced by evidence against using implicit learning. Research shows that following a stroke, implicit learning mechanisms are disrupted on the affected side (pertaining to affected hemisphere and the contralateral body side). This further emphasizes the focus on consciously, goal-directed practicing of specific movements repeatedly to improve motor skills.

Another issue with many existing learning tasks, particularly implicit ones, is their reliance on response time reductions as a primary measure of motor skill learning. Typically, improvements are assessed through faster reaction times, fewer errors, and changes in movement synergy and kinematics (Dayan & Cohen, 2011) However, ERD—our main neural marker of interest—is highly sensitive to movement type. Increased movement speed has been shown to influence ERD strength (Cassim et al., 2000; Stancák & Pfurtscheller, 1996; Tarkka & Hallett, 1991), adding unnecessary variability. Given the natural interindividual differences in ERD strength, allowing participants to respond at different speeds would introduce further variance in our neural measures.

To mitigate this, our task should prioritize lower error rates and encourage consistently paced movements both within and across individuals. While improved response time may still be a factor in a button-press task, the goal is to integrate it as part of a structured skill—ensuring movements occur at a controlled, consistent pace rather than simply becoming faster.

For these reasons, we chose the SEQTAP task as it provides a simple, hand-based movement paradigm that meets key experimental criteria. (1) It is comparable in movement to existing (not necessarily learning focused) research, (2) it allows for reliable CSE and EEG measurements, and (3) it offers flexibility in task design. Unlike self-paced tasks, a reaction-time (RT) and preparatory (PT) setup ensures controlled timing without compromising CSE (Ibáñez et al., 2020) or ERD, CNV, and MRCP dynamics.

The biggest challenge in designing this experiment was ensuring the task was challenging enough to observe learning effects in the well-trained dominant right hand (Hund-Georgiadis & Von Cramon, 1999) while remaining simple enough to allow for comparisons with previous research.

We drew inspiration from Hund-Georgiadis & Von Cramon (1999) and Furuya et al. (2011), particularly their work and task design relating to hand kinematics in expert pianists. The study discussed in this chapter details our experimental design aimed to replicate the conscious motor learning task of playing the piano. Furuya et al. (2011) analyzed joint motions during piano playing, where participants played short excerpts (9–24 notes) from various classical pieces. Keystrokes were executed sequentially, with inter-keystroke intervals set by a metronome (125 ms). From a sequential tapping perspective, this task represents structured, multi-finger sequential tapping task, where pianists played fixed keypress sequences with each digit in a controlled, rhythmic manner. Their study analyzed five successive keypresses, focusing on motion coordination and independence. Seeing the sequence in full and receiving auditory feedback made the task goal directed—the objective was to play the melody accurately— ensuring explicit learning, as participants consciously used performance feedback to correct and refine their movements.

Building on these principles, our experiment was designed to replicate key aspects of conscious motor learning observed in piano playing while removing unnecessary complexities such as hand posture requirements or musical literacy. The task ensured explicit learning by providing auditory feedback, allowing participants to consciously monitor performance and refine motor execution. Instead of focusing on full piano playing, our task isolated finger sequencing and timing, using musical notes only as feedback to guide improvements of button order and timing. Specifically, participants learned and executed sequences of finger taps in different orders. We expected improvements in execution accuracy over repeated trials, reflecting increased motor control. Additionally, we anticipated a generalized learning effect, where participants would improve at executing sequences more efficiently overall—further reinforcing the explicit learning framework embedded in our design.

To conclude in the following study, we aimed to behaviorally validate our experimental paradigm by examining whether participants show improvements in motor skill within our adapted sequential tapping task. Specifically, we asked: *Does our task elicit measurable motor skill improvement?*

Hypotheses: We expect participants to improve in accuracy, which includes both reaction time and the precision of individual taps within a sequence. Improvement should be observed at two levels: (1) within a single sequence over repeated trials and (2) across blocks, reflecting a more generalized enhancement in sequential tapping performance

3.2 Materials and Method

3.2.1 Participants

In total 18 students (6 male, between 18 and 31 years of age; mean ± SD = 23.94 ± 3.98) at the University of Essex participated in our experiment after giving informed consent for the study. In return for their participation each student received 1 course credit. All participants were self-declared right-handed healthy adults, with normal or corrected-to-normal vision and no history of motor impairment. 67% reported to have some form of musical background and training (between 0.5 and 15 years of active practice; median = 2.5 and Inter Quartile Range (IQR) = 7.5), of which 75% was in some form of key-based instrument. Only 42% indicated they actively practiced (in any capacity) at the time of testing. Out of all participants, 44% reported some video game background (playing between 2 to 24h per week; median = 5 and IQR = 11). The study was conducted in accordance with ethical guidelines and was approved by the University of Essex Research Ethics Board (ETH2122-0179).

3.2.2 Experiment Design and Protocol

Upon arrival participants were asked to read a briefing, provide informed consent and fill out a short survey on their self-reported music proficiency and video game experience. The survey was included to assess if a background in music or gaming would affect the learning outcome due to pre-existing extensive training in hand muscle skills and contained the following open-ended questions (see Appendix A2 for the complete survey). For musical skills we enquired about: Any type of musical practice (e.g., Instruments, Singing, Dance, etc.), Self-taught or traditional music education, Number of years they have actively practiced to play music, period of active practice (e.g., from age 5-15), whether they were currently playing, and any other information the participant considered relevant or wanted to share. For the participants gaming background we asked: Do you play any games (video or physical) involving high amounts of dexterity, if yes please specify the type. If video-based gaming, please circle type of controls: hand-held controller/mouse and keyboard. How often do you game (specified in average amount of hours per week).

Participants sat in an electrically shielded test booth, on a TMS-Robot chair (Axilum Robotics, Strasbourg, France), at 3 meters from a screen (32inch, refresh rate 60 Hz) placed at eye level outside the booth. They were instructed to sit in a relaxed position with their right hand placed on a standard UK qwerty keyboard. The response keys, chosen to encourage a neutral and relaxed hand position, were: index finger - X key, middle finger - F, ring finger - G and the little finger on the N (or M, according to participant's preference; e.g., participants with very big hands may prefer the M key). The experimental paradigm was custom-made in MATLAB (MathWorks, MA, USA) using the Psychophysics Toolbox extensions (Psychtoolbox-3, version 3.0.18; Brainard, 1997; Kleiner et al., 2007;

Pelli, 1997); in addition to LoopMIDI (Version 1.0.16.27, Erichsen, 2019) and KONTAKT 6 PLAYER software (version 6.2.2 (R51), Library: Kontakt Factory Selection, Ragtime Piano – Grand Piano; Native Instruments GmbH, Berlin, Germany) for audio output (via Genlec speakers placed in the test booth).

Figure 8

Flowchart Detailing Behavioral Experiment Protocol

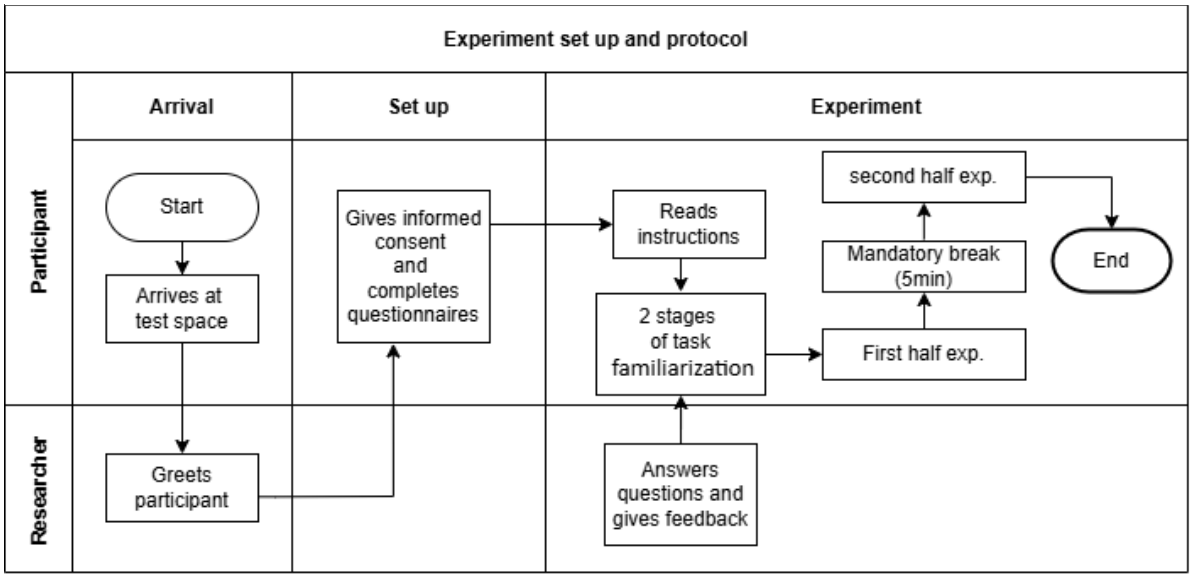

The experiment consisted of a 1h session and aimed to train participants' right hand finger motor control skills by simulating learning to play the piano. Taking inspiration from Furuya et al., (2011), we adapted a sequential finger tapping task to include both auditory and visuomotor elements. Auditory feedback was provided in an ecological manner, replicating the natural setting of playing piano and receiving sensory feedback to monitor performance, to measure goal directed (explicit) motor learning. The task was designed to be challenging enough to observe learning in the well-trained dominant right hand (Hund-Georgiadis & Von Cramon, 1999); yet a simple enough movement to compare with previous research.

Participants were presented with different numeric sequences made up of 4 numbers ('1', '2', '3' and '4'). Where each number was associated to a specific finger (1= index, 2 = middle, 3 = ring and 4 = little finger) and music note. Specifically, following the piano key format, the notes (C-D-E-G/F) were scaled to go up with the finger order. As such, the index finger (1) would always hold the lowest note (C) and the little finger (4) the highest note (G or F). To avoid participants starting to anticipate tones instead of focusing on motor planning, sequences were split-up over two sets of notes. The notes in the sets were identical, except for the octave and the highest note (C4 (4=G) or C5 (4=F)) (see Figure 9). As the sequence scrolled over the screen, participants had to tap their fingers, pressing buttons when doing so, in the right order, at the right time, and for the right duration; receiving the associated auditory

feedback of the buttons they had pressed. Pressing the correct button at the correct time made the sequence play out a melody.

Figure 9

Music Notes of the Melodic Phrases Underlying the Numeric Sequence Presented to Participants

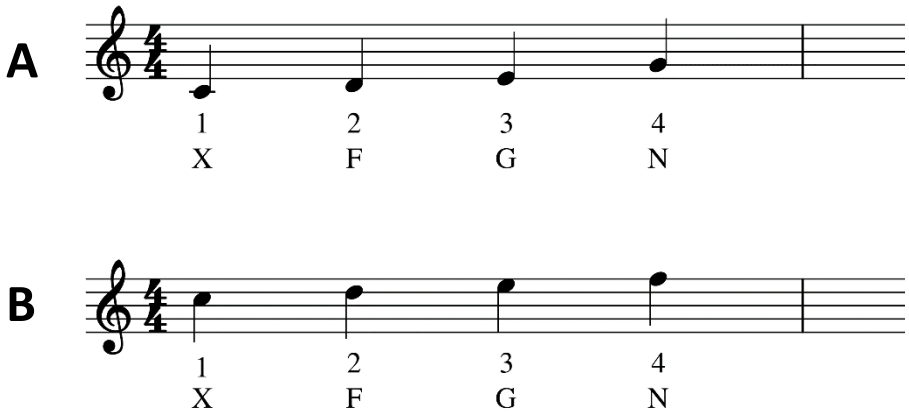

*Note. (*A) Notes C D E and G; starting at middle C (i.e., C4). (B) Notes C D E and F; starting an octave above middle C (i.e., C5). The number and letter below each note indicate that note their associated numeric stimuli and to be pressed down finger/response key. E.g., The number 1 requires the participant to press the X button with their index finger, which will then play the C note. However, the notes were associated directly with the response keys. Meaning if the number 1 was presented on the screen, but the participant wrongly pressed down their middle finger (and thus the F key). They would hear a D note instead of a C. The melody would sound 'off', reinforcing and informing the participant they made a mistake.

Before data collection, participants read through detailed task instructions and went through 2 stages of task familiarization. They pressed the F key (middle finger) to navigate forward. The *first* practice stage focused on finger/key and number association. A single white number was presented against a black background in the middle of the screen. Participants were asked to press the button (i.e., make a tapping motion with the associated finger) corresponding to the number on the screen. A pressed button resulted in feedback being given to the participants on their performance; by presenting the words 'CORRECT key' in green or 'INCORRECT' key in red. As well as auditory feedback through the number associated note (using only the C4 scale at this stage for simplicity). If no button was pressed after 2 seconds participants were shown the message ''too slow'' for 1 second. A total of 8 numbers were presented, each of the four number stimuli were presented twice in the following order: the first run order was Index-middle-ring-little finger (1-2-3-4) and a second run with the order randomized (e.g., 3-2-4-1). In the *second* stage, participants were given two practice trials that were identical to the test trial setup, to ensure everyone knew what to expect and understood the task. A trial (see Figure 10) would start with a countdown. A fixation cross, with 4 green circles at the end of each axis (Y+, X+, Y- , X-), was presented in the middle of the screen. Over a period of 2 seconds the green circles moved smoothly, in increments of 100 ms, towards the middle of the fixation cross, counting

participants in for their performance, as a conductor would. It was specified to participants that the fixation cross did not indicate rhythmic timing and merely functioned as a countdown. Next, the sequence was presented with the first number in the middle of the screen and the next 6 numbers lined up on the right. Initially, all numbers were presented in white, against a black background, with the first number turning blue after a 200 ms delay. A number remained blue for either 0.5s or 1s, after which all numbers would shift one position to the left with the next number in the sequence now blue and in the middle of the screen. As such the sequence would scroll over the screen from right to left, all numbers equally spaced, with the target number always in blue and in the middle of the screen. The format of sequence presentation was designed to minimize head and eye movements (the target number always appeared at the same spot, in the middle of the screen), and to allow explicit movement preparation without involving the cognitive strain of working memory (Walker et al., 2002). A trial would end with the presentation of the fixation cross with 4 green circles remaining stationary for 2 seconds. After which a new trial would start with the circles counting down.

Participants were asked to respond to the visual cue by pressing the corresponding button with the corresponding finger. A number turning blue indicated when and which key/finger needed to be pressed. The duration for which the number remained blue indicated how long they needed to keep their finger down. The practice session was limited to 2 trials to avoid too much learning during the familiarization stage. An additional difference between practice and test trials was that we used the recognizable tune of Jingle Bells for the practice sequence melody. A recognizable tune was used to further encourage understanding of the rhythmic nature of the task. First, numbers repeating in the sequence requires the finger to be lifted and pressed down again for each number (e.g., '3 3 3' required the ring finger to be pressed down three times). Another point was the need to keep the key pressed down for the duration that the number remained blue and in the middle of the screen and that the sequences should play out a melody. The test sequences, though also taken from existing music compositions, were mostly unfamiliar so as not to influence motor skill learning.

The familiarization session was concluded with an opportunity to ask any remaining questions and a general learning tip to, going forward in the experiment, "focus on the order of the button presses and timing with changes on the screen, before worrying about duration of a button press." Continuing to the test part of the task, participants ran through 10 test blocks of 24 trials each. There were 10 unique sequences to learn, which were presented in a random order over the blocks with 1 sequence per block. The sequences were 8 to 11 notes long (mean ± SD = 9.6 ± 0.96) melodies, made up of combinations of 3 or 4 of the available different notes. All notes were quarter or half notes at a 4/4 time signature and a tempo of 120 beats per minute; making the total duration of a sequence between 4.9s and 7.4s (mean ± SD = 6.35s ± 0.6s) .The melodies were excerpts from the following

compositions: “The Cookie Jar, Lemonade Stand and 3 Finger Parallel Movement Challenge” all by Yigal Kaminka, and “For The Beauty Of The Earth” by Folliott S. Pierpoint (arranged by Carolina Savchuk); some with slight adjustments (see Appendix A4 for specific sequences and melodies). MuseScore (version 3.4.2, MuseScore Ltd, Limassol, Cyprus) was used to ensure adjustments did not feel musically off. These compositions were chosen as they were inconspicuous melodies, beginner friendly and made up of the same 4 notes. Sequences were further set up so 40% of the trials started with the index finger and 40% the little finger. The remaining 20% of the trials would start with either the ring or middle finger. Every block started with a visual presentation of the full sequence for that block. Participants would then press the F key (middle finger) to start the first trial of the block, with a total of 24 tries to execute the melody as accurately as possible.

Figure 10

Visual Representation of a Single Trial

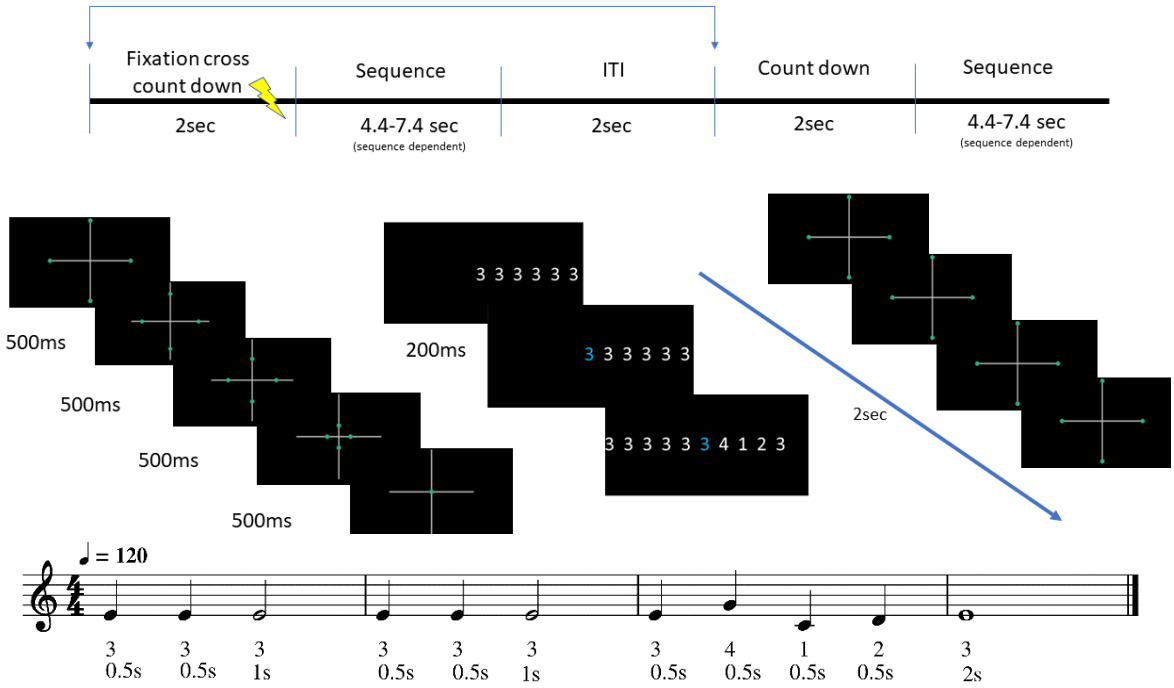

Note. The top part of the figure shows how trials were presented to the participants during the experiment. The lower part illustrates the conversion of a melodic phrase (here Jingle Bells, used for the practice trials) to a numeric sequence. Numbers illustrate how the sequence was presented to participants. The number of seconds below each number indicate note duration (i.e., the time participants need to press the button down for), converted according to 120 beats per minute and a 4/4 time signature.

Participants had the opportunity to take a small break of up to 5 minutes between blocks or, after 30 seconds, press the F key to continue to the next block. At the midway point, after block 5, participants took a compulsory 5-minute break, irrespective of any earlier breaks taken. The midway point break was in response to pilot findings and feedback relating to our future intentions to measure EEG and

TMS responses. The combination of sitting still and up, in a relatively uncomfortable chair, for the length of the experiment resulted in a strain and discomfort for the participant, leading to decline in attention and increased fidgeting. After the enforced 5-minute break, participants were reseated, their hands were repositioned, and they resumed with the second part of the task.

3.2.3 Data preparation and planned analysis

Improved motor control of sequential finger movements was measured by learning the responses to numerical sequences and the underlying melody. As such participants had to learn a) to press the correct buttons in the correct order, b) to press a button down at the correct time and c) keep the button pressed down for the correct duration. Performance accuracy was quantified for the whole sequence. The melodical aspects (i.e., b and c) were added to increase the degree of control required and add to the challenge rate of the sequential tapping task.

Button responses were recorded as a time series. However, because of the variable elements in the recording process throughout a trial, the sample rate (SR) (i.e., number of, and time difference (few milliseconds) between iterations) was inconsistent over trials. Based on pilot data, looking at the shortest sequence of 4 seconds, we know the minimal number of sample points were consistently over 8500. As such we took 8500 samples at 4 seconds to establish a constant behavioral SR of 2151 Hz, and sequences of larger magnitude will be down sampled to this SR. Meaning a key press of duration 0.5s would be represented as a key press of 1076 samples.

Overall accuracy of performance was defined as the percentage of a participant's response that was correct compared to "the perfect sequence." We compared participants response series time point per time point with a "perfect sequence" at SR of 2151. Matching timepoints were given a value of 1 and timepoints that did not match a value of 0. The values were added up and then averaged over the total number of time points in the respective sequence series, and multiplied by 100 to have performance as an accuracy percentage.

Data analysis was performed using Rstudio in R statistical software (R Core Team, 2023). With our experimental set up, a 24 (tries per sequence) x 10 (different sequences) factorial design, the analysis we apply here will cover repeated-measures analysis of variance (rmANOVA) and variations of it (rstatix package; Kassambara, 2023).

Accuracy (ACC) rates were submitted to rmANOVAs to assess the effects of learning a specific tapping sequence (scores for sequential trials within a block - improving over 24 attempts - will further be referred to as factor 'Trials'), general improved coordination and motor control of the right hand (scores for sequential blocks - general improvement over 10 different sequences - will further be referred to as factor 'Blocks'), and to investigate differential effects of participant's musical training on both these dimensions (groups of people having a musical background or not). Using linear models

with categorical predictors, we encoded the factors using sigma parameter restrictions (i.e., effect coding, where the sum of the regression coefficients equals zero). Furthermore, we applied SAS type III to construct the sums of squares in the rmANOVA table (opposed to type I or II). Where Mauchly's Test of Sphericity indicated sphericity assumptions were violated, Greenhouse-Geisser corrections are applied to degrees of freedoms and p-values. Significant effects for Trials and Blocks are followed up with trend analysis using polynomial contrasts to see if the differences in performance (ACC scores), i.e., the learning effect, follow the expected linear trend.

3.3 Results

As responses influenced by attention slips can confound the learning effects, we removed extreme values (outliers) in the ACC scores. As executing a sequence with 50% accuracy may be an uncommonly high score for one participant, but an average performance to another. Outliers were determined for every participant individually to account for the interindividual differences in performance scores. Using *Tukey's method* (Dhana, 2016; S. Seo, 2006) no trials were identified as needing to be removed as outliers. However, for one participant, 4 trials were removed from further analysis due to no recorded button press. In total 0.09% (4 out of 4320 trials) of the trials were removed.

A one-way rmANOVA indicated a significant difference [$F(9,153) = 4.66$, $p < .001$, $\eta^2 = .063$] when comparing average ACC scores between different sequences, irrespective of their sequential order (i.e., Trial and Block order not being considered). Specifically, pairwise post-hoc analyses with Bonferroni adjustment revealed ACC scores for sequence 3 (see Appendix A4, third bar) were statistically significantly lower than four of the other sequences [$p < .05$; see Table 3 and Figure 11], while no such notable differences existed among the other nine sequences [$p > .05$; see Table 3]. This means, considering the randomized (and thus semi balanced) presentation of the stimuli order, participants performed consistently worse on sequence 3; regardless of this sequence being presented as one of the first or later ones in the experiment. As such, we violated our theoretical assumption that our chosen sequences were of equivalent difficulty.

Table 3

P-values of Pairwise Post-Hoc tests for a One-Way rmANOVA on Equivalence of Sequence Difficulty

Sequences	Seq 1	Seq 2	Seq 3	Seq 4	Seq 5	Seq 6	Seq 7	Seq 8	Seq 9	Seq 10
Seq 1	1	1	.046*	1	1	1	1	1	1	1
Seq 2		1	.360	1	1	1	1	1	1	1
Seq 3			1	.002**	.205	.082	.268	.004**	.033*	1
Seq 4				1	.163	1	1	1	1	.200
Seq 5					1	1	1	1	1	1
Seq 6						1	1	1	1	1
Seq 7							1	1	1	1
Seq 8								1	1	1
Seq 9									1	.374
Seq 10										1

Note: Differs significantly from each other, * at $p < 0.05$ (Bonferroni adjusted). See appendix A3 for associated t test statistics.

Figure 11

Mean Performance Accuracy per Participant per Sequence, Irrespective of Presentation Order

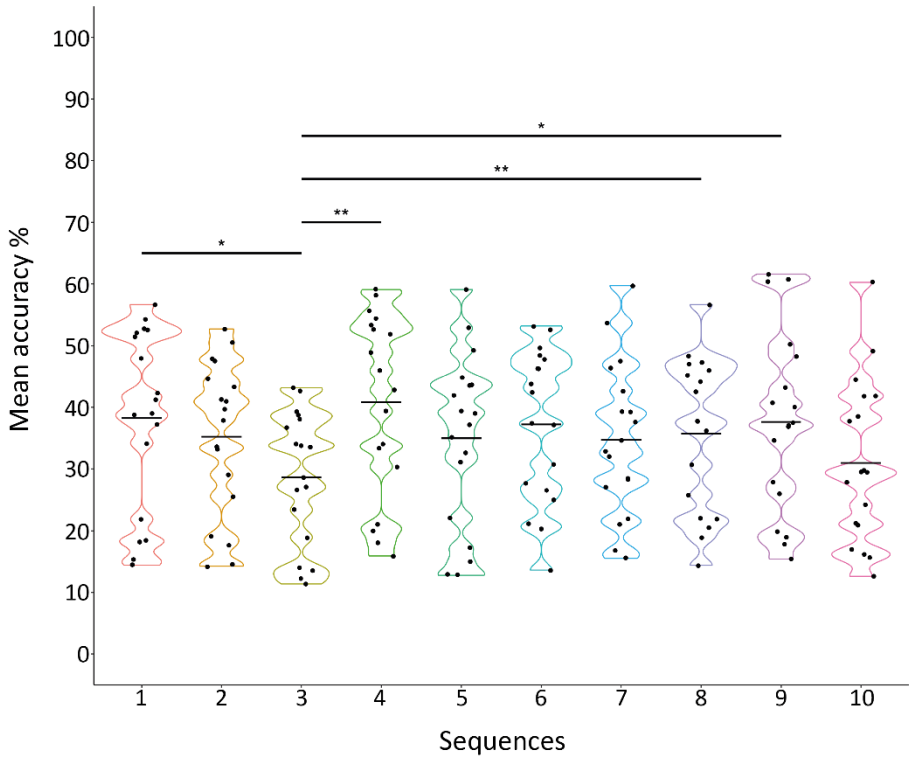

Note. Sequence order was randomized before presentation for every participant. Individual datapoints indicate average accuracy score per participant per sequence. Horizontal black line indicates the overall average performance accuracy per sequence across participants irrespective or presentation order. Significance of *p*-values as presented in Table 3.

The present paradigm was designed to test motor learning, while also containing a musical aspect. Therefore, we evaluated the impact of pre-existing advantages from trained musicality, and any resulting training in hand muscle skills, confound learning outcomes. A three-way mixed effect ANOVA, including musical background as a between subject factor with two levels (yes or no) alongside Trials and Blocks, showed no such confounding effects. There was no statistically significant difference between the overall performance scores for those with and without musical background [$F(1,15) = 1.04$, $p = .325$, $\eta^2 = .038$] (see Figure 12 and Appendix A7). Neither were there any interactions between musical background and Trials [$F(23,345) = 0.74$, $p = .800$, $\eta^2 = .002$] or Blocks [$F(4.78,71.75) = 0.65$, $p = .655$, $\eta^2 = .008$]. This indicates that people with musical training did not have an advantage in the task or had their performance at a rate any different than those with no musical background.

Figure 12

Mean Performance Accuracy for Different Blocks and Trials, Split over Musical Background.

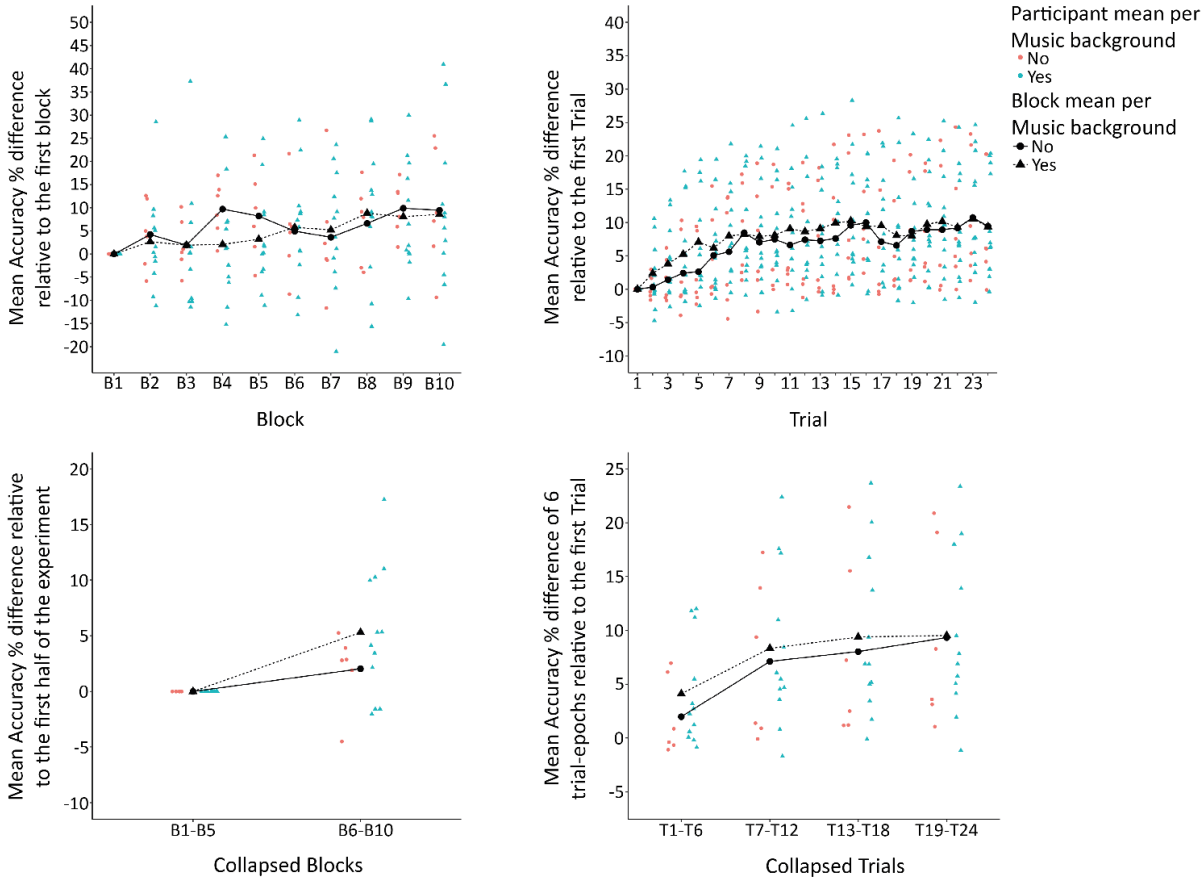

Note. Figures show the differences in average performance scores over blocks and trials between participants with and without a musical background. Showing a general difference in ACC score, where those without musical background score on average slightly lower than those with musical background.

As there was no effect, musical background was removed from the model to further assess learning effects. The two-way rmANOVA with Trials and Blocks showed a significant effect in difference of performance scores over Trials [$F(23,368) = 13.24$, $p < .001$, $\eta^2 = .026$] as well as over Blocks [$F(4.92,78.64) = 2.69$, $p = .028$, $\eta^2 = .028$], however no significant interaction was found between the two factors [$F(207,3312) = 1.1$, $p = .171$, $\eta^2 = .014$]. Follow-up tests with linear contrasts (with separate error terms) indicated performance ACC to increase linearly over both Trials [$t(17) = 6.22$, $p < .001$] and Blocks [$t(17) = 3.64$, $p = .002$]. Meaning participants performed, on average, significantly and consistently worse on their first try to tap out a sequence compared to the last try of that same sequence, with performance differences increasing linearly over the sequential order of the trials in between the first and the last trial. Participants then became significantly better at tapping out sequences in general, with the average performance scores increasing linearly between the first sequence (first block) and the last (sequence, i.e., block), without significantly affecting the learning trend for any individual and new sequence.

The 10x24 design (2x(10x24) if we count musical background) is intricate. The abundance of levels and potential interactions can make future analysis appear convoluted and chaotic. Especially when having the intent to employ the present paradigm as base for a neuroimaging study where additional factor variables will be introduced. Therefore, we simplified the analysis, and reran the previous tests with the redefined variables to check if we preserve the observed learning effects in condensed form. We collapsed the factor levels according to the main turning points of learning we can see in Figure 12. Blocks became a 2-level factor variable, to reflect the overall difference of the first compared to the second half of the experiment (i.e., split around the 5-minute mid experiment break); ~~s~~plit in half by averaging the 1st five blocks combined and again averaging over the last five blocks combined. Trial levels were combined to form a 4-level factor variable, averaging measures per 6 trials; reflecting how, seemingly (Figure 12), most learning happens over the first 12 trials and scores plateau in the later 12 trials. The simplified three-way mixed effect ANOVA, once again showed no difference in the overall performance scores [$F(1,16) = .74$, $p = .403$, $\eta^2 = .041$] or learning trends [over Blocks $F(1,16) = 1.57$, $p = .228$, $\eta^2 = .005$; or Trials $F(1.41,22.58) = .60$, $p = .501$, $\eta^2 < .001$] between those with and without musical background. Similarly, a simplified two-way rmANOVA retained the significant learning trends for both learning an individual sequence [$F(1.42,24.2) = 33.1$, $p < .001$, $\eta^2 = .040$], as well as learning over sequences in general [$F(1,17) = 11.11$, $p = .004$, $\eta^2 = .031$], without significantly affecting the learning trend for any individual and new sequence [$F(3,51) = 1.84$, $p = .152$, $\eta^2 < .001$].

To inform our future intentions to use the current paradigm to measure EEG and TMS responses relative to movement onset, we need to know the consistency and changes relating to the average timing of the first button press in a trial. Trial reaction times (RT) were measured as the difference in

time between the *first* button press and the first number turning blue**.** We then removed extreme values (outliers) in the RT responses, once again using *Tukey's method* (Dhana, 2016; S. Seo, 2006). Given that some people are naturally faster than others, we took interindividual RT differences into account by determining and removing outliers for every participant individually. In total 1.69% (73 out of 4320 trials; incl. the 4 'no response' trials), spread over 16 participants (between 1 and 13 trials per person; mean ± SD = 4.31 ± 2.84), of the observations were identified as outliers and removed. The remaining 4247 trials were used to look at the changes in RTs over the course of trials and blocks for every participant. Once again using the simplified analysis set up [2x(2x4)], a two-way rmANOVA showed participants became significantly faster in their response to the start of a trial as they became more practiced in the sequences and task. Specifically, participants consistently [$F(3,51) = 1.135$, $p = .344$, $\eta^2 < .001$] sped up over trials within a block [$F(3,51) = 41.09$, $p < .001$, $\eta^2 = .046$], even when they overall got faster over blocks [$F(1,17) = 18.38$, $p < .001$, $\eta^2 = .080$]. Specifically, participants generally decreased their response time over the course of the experiment, shown as a significant difference in the average RT in the first half of the experiment compared to the second half. Participants also responded consistently faster over the course of learning a specific sequence, as indicated by the linear trend of the differences over trials in a block [linear contrasts with separate error term showing a significant downwards trend, $t(17) = -7.86$, $p < .001$]. A three-way mixed effect ANOVA showed these findings did not change when including musical background. Meaning regardless of musical training participants sped up in equal measures over trials [$F(1.97,31.58) = .57$, $p = .571$, $\eta^2 < .001$, and over blocks $F(1,16) = 1.05$, $p = .322$, $\eta^2 = .005$]. While Figure 13 implies people with musical background on average respond faster and more consistently, this difference is not significant [$F(1,16) = 1.03$, $p = .325$, $\eta^2 = .054$].

Table 4

RT of First Button Press in Seconds Per Condition

	Median (IQR)					
	Trials 1-6	Trials 7-12	Trials 13-18	Trials 19-24	Total	Total min-max
1st half	0.379 (0.121)	0.346 (0.171)	0.295 (0.116)	0.314 (0.181)	0.337 (0.170)	0.097 – 0.690
2nd half	0.292 (0.197)	0.249 (0.196)	0.265 (0.174)	0.245 (0.196)	0.269 (0.190)	-0.019 – 0.551
Total	0.341 (0.163)	0.301 (0.199)	0.290 (0.161)	0.275 (0.197)		
Total min-max	0.113 - 0.690	-0.012 - 0.628	-0.019 - 0.635	0.001 - 0.583		

Note: 1st half experiment denotes scores averaged over Blocks 1 to 5, 2nd half experiment denotes scores averaged over Blocks 6 to 10. Values calculated over participant averages of each condition. E.g., The total for the 1st half of the experiment was calculated over 18*4 values.

Table 5

P-values of Pairwise Post-Hoc tests for RT over Trials

Trial Levels	Trial 1 – 6	Trial 7 – 12	Trial 13 –18	Trial 19 – 24
Trial 1 – 6	**1**	**<.001*** **	**<.001*** **	**<.001*** **
Trial 7 – 12		**1**	**.068**	**<.001*** **
Trial 13 –18			**1**	**.411**
Trial 19 – 24				**1**

Note: Differs significantly from each other, * at $p < 0.05$ (Bonferroni adjusted). See appendix A5 for associated t test statistics. T7-12 was significantly diff from T13-18 before corrections.

Figure 13

Mean RT for First Button, for Trials in the First and Second Half of the Experiment, Split over Musical Background.

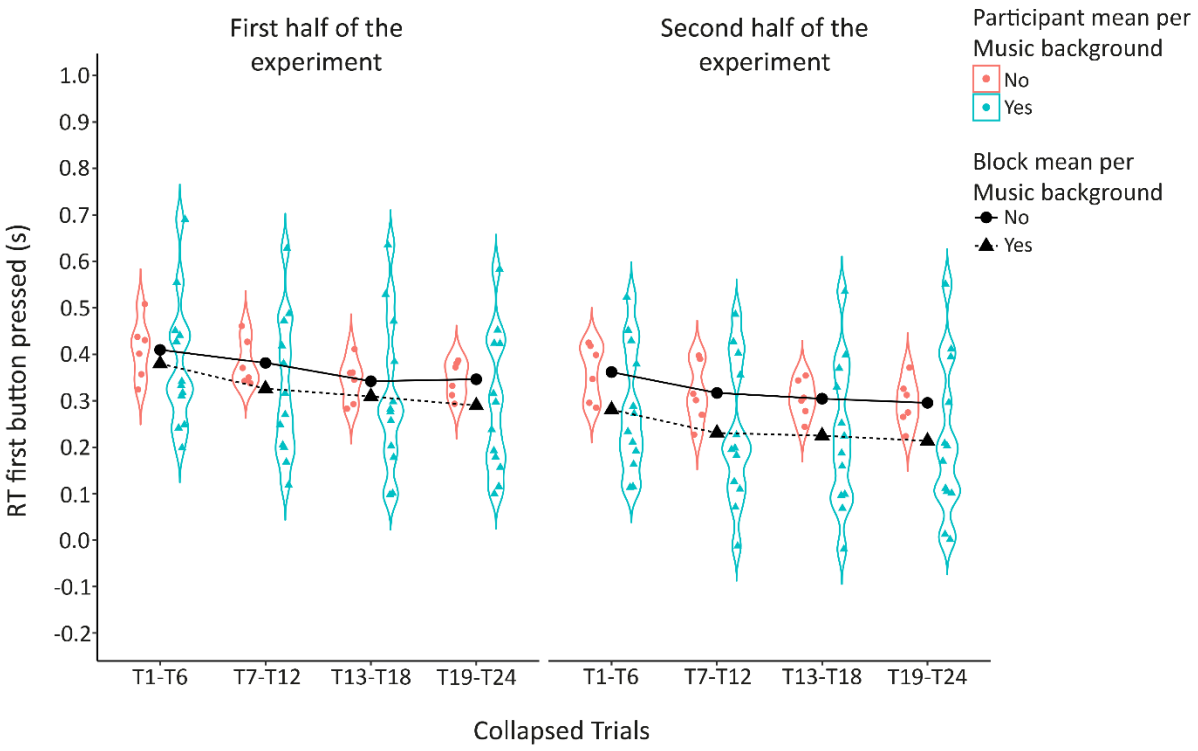

Note. Figure shows response time for the **first** button press only, measured from the "you can start" cue (i.e., first number turning blue). Assessment of a mechanical element of design with the sole purpose to explore people their consistency in starting the tapping sequence. ***Not*** to be confused with the average RT across all presses, which pertains to learning the rhythm and is part of sequence performance measure. Insight required for intended TMS use in Chapter 4, where stimulation is timed relative to a theoretically predicted button press. Greater consistency increases the likelihood that TMS pulses occur at their intended time.

3.4 Discussion

We set out to create an experimental paradigm to measure explicit motor learning in the dominant right hand. We expected participants to become better in executing sequences over the course of several trials, with increased performance accuracy used as an indicator for increased motor control. Our results showed participants did indeed learn. In line with our expectations, we observed participants consistently and significantly improved at performing a specific sequence (i.e., learning over trials within a block) and became better at executing sequences in general (i.e., learning over blocks) without affecting the learning rate of the individual sequences. These learning effects were further preserved when we simplify the analysis by collapsing trials and blocks. Based on these outcomes we can consider our task to be successful in tasking participants to learn to tap out sequences and use real-time feedback to improve their motor coordination, to tap out the sequence in accordance to the more high-level demands of timing (the release and pressing down of buttons), beyond just getting the order of the buttons right-and responding as fast as possible.

The present paradigm was designed to test motor learning. However, it contained a musical aspect consequential to our chosen methods of setting up the task to encourage explicit learning. While our data indicated participants with a musical background had higher overall performance scores, our test results showed that this difference was not statistically significant, nor was there a difference in the relative increase of performance accuracy. More importantly, participants having trained musicality (and any resulting advantages in musical or motor skills) did not confound the tasks' ability to train motor control and measure motor learning. Similarly, everyone speeds up when pressing the first button in response to the first number turning blue ("go cue"), both over trials and blocks, with participants with a musical background seemingly, though not statistically significantly, responding faster on average. This suggests that while musical experience may influence initial performance, it does not affect the ability to learn or improve in our task. As such, our present findings do not provide reason to exclude these participants from future data collections that use the same task.

While statistically a musical background seems to have no effect, we do have to note the reasonable, though small, effect sizes (at the very least they are of the same size as the effect sizes for trial and block). As well as our small sample size that underpowers our analysis (n=18 per condition instead of the advised n=30) (Billingham et al., 2012; Button et al., 2013) and the unbalanced split of 12 participants with some form of musical experience (though a wide spread of how much) compared to the 5 participants with no experience at all. However, even if there is a true effect of musical training, and as a thought experiment let us assume for a bit that there is (such as responding on average faster response to 1st cues and having on average higher performance scores; see Appendix A7), it does not seem to interfere with our behavioral measures of interest or the tasks' ability to pick up on them.

What we mean is, performance wise we are not interested in absolute performance scores; but in improvement of the scores, presumed to reflect improved motor control (i.e., motor learning). The task appears difficult enough that it is highly unlikely for someone to start with perfect scores or have a ceiling effect (i.e., maxing out before the end of the experiment is reached, resulting in us no longer being able to observe changes in motor learning). As such, participants of a certain group starting at a higher performance score does not impede the task in terms of our ability to train motor control and observe improved performance scores over trials and blocks (see Figure 11); as indicated by our results and main effects, even with a sample size as small as ours (though we will need more replications to rule out our findings as a case of serendipity). Potentially a full sample of participants with no musical background would display a steeper learning curve. However, this is outside of the scope of the present research study and interests, where we are looking for a measure of motor learning rather than investigating how different variables affect the rate of motor learning. Though in future research it would be interesting to see if such differences exist and whether a different learning curve goes together with a different rate of changes in brain activity.

On the part of having musical training leading to faster reaction times to the first cue; again, while there may be difference in the absolute RT values of the first button press for the two groups, we are more interested in, and concerned about, the progression of RT scores over the course of the experiment. The increase in speed, for some participants, resulting in them responding too early (before cue change), is a general issue (shared by and observed in both groups) for our future intent of wanting a consistent estimate of movement onset. As well as skewing the learning curve, affecting the interpretation of 'degree of improved performance reflects degree of skill improvement (i.e., true degree motor control improvement is lower than scores imply). While getting the tap timing right when switching from one finger to the next (i.e., RT to individual number cues in the sequences changing from white to blue) is part of learning the sequences, RT to the first cue is less a matter of planning and preparing a sequence of actions, and more a matter of timing action initiation. As such, future use of this task should implement a form of training to ensure participants respond to the first cue within a certain response range (Ibáñez et al., 2020). Useful both for our intent of having a (relatively) consistent-estimate of movement onset, as well as to have a more accurate measure of motor control learning.

Manipulation of sequence difficulty could be considered mostly successful as most of the sequence stimuli appeared to be of equivalent difficulty; based on similar average performance scores (assuming any order differences get canceled out due to randomized presentation. Meaning some participants had a sequence at the start, whereas others had that same sequence later). However, participants performed consistently worse on sequence 3, implying this one sequence was generally experienced

as more difficult than others. While this is not ideal, it did not affect the tasks' ability to measure learning. Any issues this 'more difficult' sequence could have brought were most likely canceled out because of stimuli randomization. Potentially, with more balanced stimuli (i.e., sequences) presentation, the task effects would be more profound. It is difficult to identify why some sequences were perceived as more challenging than others. This is unlikely to be due to the melodical aspects of the sequences, and instead has likely more to do with the kinematic aspect of the associated fingers. E.g., it is easier to tap fingers in the order of little finger to index, rather than index to little finger. While index to little finger movements were present in all sequence stimuli, only sequence 3 (also the 3rd sequence in Appendix A4) had the switch from index to ring finger and then focused for nearly half of its taps on switching between ring finger and little finger. However, due to (pandemic induced) time constraints we did not change this stimulus or look further into the aspects driving differences in sequence performance (nor was there any mention of knowing factors, or how to choose sequences, in literature on classical SEQTAB tasks regarding any standardized or conventional used sequences that we know of (Furuya et al., 2011; Hashemirad et al., 2016; Walker et al., 2002). Instead, we prioritized data collection and analysis.

There follow some notes to consider when implementing the present experiment in a neuro imaging context: It intuitively makes sense for a behavioral task to enforce breaks to retain attention, however, with further feedback from our pilot experiments, in a context of a TMS study, this would boil down to asking participants to just sit still for 30 seconds staring at a black screen. They would therefore not be able to gain any of the benefits participants normally would enjoy from having a break (e.g., changing posture, stretching, moving around).

We further found no evidence to support the exclusion of future participants based on their musical background. While our results showed that musicians start on average with higher ACC scores, they overall still improved in terms of motor skill. Original concern stemmed from studies showing how music familiarity and expertise affecting melody prediction (i.e., how the sequence might continue after a certain part) (Pesek et al., 2020). For similar reasons, during task design, gaming expertise was considered an important factor that could possibly confound learning outcomes. Original reasons to include the gaming expertise questions was to account for any unfair hand dexterity advantage. However, upon further consideration of gaming set ups and participant feedback, we realized: console gamers mainly use thumbs, right-handed PC gamers would use mouse and key combos would be executed with left hand. Similarly, why we should not be too surprised for no motor control advantages for right-handed musicians, of the most played instruments pianist and flutists would have sequence training with both hands, however string players would use their dominant hand for rhythm (bows on cello and violin, guitar, etc.) while the left hand is used for chords and different placement.

In conclusion, we are satisfied to move forward with the presented experiment in a neuroimaging context. Confident there is enough of a behavioral basis to explore the dynamics of neural markers when we learn in this experiment paradigm.

Chapter 4: Neuroimaging Experiment

4.1 Introduction

Effective rehabilitation depends on closing the FoFe-loop. If CSE represents a neural state most conducive to motor learning, rehabilitation protocols should aim to engage with CSE at its optimal point to enhance recovery. This optimal timing for feedback engagement—to maximize neuroplasticity-driven recovery—has been suggested to correspond with maximal excitability. Previous studies have attempted to identify this point using single time markers, such as when ERD reaches 30% (Daly et al., 2018). However, this approach assumes a static relationship between ERD and CSE, despite evidence that both evolve dynamically during learning (Berghuis et al., 2016; Dayan & Cohen, 2011; Yang et al., 2017).

Learning induces changes in the brain's functional connectivity (Dayan & Cohen, 2011; Ganguly & Poo, 2013). Consequently, motor learning is expected to produce synaptic and structural changes that manifest in the neural correlates of motor control. BCI rehabilitation is explicitly designed to reshape neural activity, promoting synaptic changes that support motor recovery. To effectively use neural information—such as recurring brain activity patterns—to facilitate learning, we must ensure that our approach accounts for potential learning-induced changes as they unfold. At the very least, verify and guarantee the efficacy of the protocol remains unaffected by such changes.

In Chapter 2, we focused on expanding our understanding of the temporal dynamics of CSE, as it has been proposed as a key marker for determining the optimal time to interact with motor control and production processes. Additionally, we explored its relationship with other neural measures that may help infer CSE dynamics and estimate this optimal point.

However, the data in Chapter 2 was suboptimal, leaving our findings rather inconclusive towards our first two research questions. Specifically, our preliminary insights were limited by high levels of noise and a substantial loss of trials due to data cleaning and exclusion criteria. As a result, the analysis in Chapter 2 was underpowered (Billingham et al., 2012; Button et al., 2013), owing to a dataset that was not designed to directly test our hypotheses. Despite these limitations, our preliminary findings provided some support for the hypothesis that CSE activity, as indicated by MEPs, follows an S-like wave in the 1.5 seconds leading up to movement onset. However, we were unable to determine the extent to which a cubic model accurately describes the relationship between ERD and CSE. Even less conclusive was whether one measure could be used to predict changes in the other over time (e.g., using ERD to anticipate CSE dynamics).

In this chapter, we aimed to replicate and extend our findings from Chapter 2, this time using data specifically collected to establish a more conclusive descriptive timeline of CSE relative to MOn over a broader range, while ensuring sufficient data points. Additionally, using the experiment detailed in Chapter 3, we sought to expand our understanding of how neural markers behave in a learning environment—particularly regarding the need to account for learning-induced changes when inferring CSE dynamics in practical applications. When discussing our findings in Chapter 2 we indicated that our current model, which uses the S-like pattern (descriptive for CSE changes over time) to predict MEP amplitudes based on of the linear progression of ERD strength over time, is not yet viable for practical application, regardless of the frequency band used. However, we propose that this model can still provide valuable insights into how learning-induced changes impact neural markers by comparing its performance when continuously updated versus left static.

Ultimately, the model should be designed to account for learning-based changes, rather than being blindly updated. However, we hypothesize that *any* form of updating will outperform a non-adaptive model. If a difference is observed, it would indicate that learning affects the stability of the CSE-ERD relationship, reinforcing the need to investigate comparative learning effects on neural markers before relying on CSE alone to target optimal excitability.

The present study utilized the experiment designed in Chapter 3, which was specifically developed to investigate how motor learning affects the three neural markers of motor control—ERD, MRCP, and CSE—as motor function improves. The primary goal was to assess whether the relationships between these markers remain stable or require continuous recalibration in a BCI context.

We expect these neural markers to change both individually and in relation to one another as motor skill performance improves. As discussed in 1.2 Motor Learning, neural activity is generally expected to decrease with learning, as reduced cortical activation is thought to reflect stronger neural connections and more efficient resource utilization (Siemionow et al., 1998; Wright et al., 2011). Specifically, for MRCP, we anticipate an initial increase in amplitude (i.e., greater negativity) over trials as participants learn a sequence. However, by the final trials and the end of the experiment, we expect MRCP amplitude to return to baseline or decrease even further (Wright et al., 2011). Similarly, we predict a continued reduction in relative power for both alpha and beta bands as performance improves (Yang et al., 2017; Zhuang et al., 1997).

Expectations for CSE are less clear, partly because, to our knowledge, no study has examined how learning affects the temporal dynamics of CSE—particularly over as broad a time scale as we intend to investigate. The literature generally suggests that skill training increases CSE when comparing MEPs before and after training (Kleim, 2009; Leung et al., 2017; McGregor et al., 2017). However, findings on CSE dynamics during skill acquisition remain inconsistent, with some studies reporting an increase

and others showing no change (Berghuis et al., 2016). Given these inconsistencies, we tentatively expect CSE to retain its characteristic shape while increasing in amplitude as participants' performance improves both within and across sequences. With our current level of knowledge, it is furthermore difficult to predict how learning-related changes will impact the relationship between neural markers or how these changes will manifest in the measures attempting to quantify the relationship.

In general, we expect to replicate our earlier findings while expanding the analysis to include MRCP. Specifically, we anticipate observing a preparatory CSE peak around -500 ms relative to MOn. At this same time point, we expect to see a 30% increase in ERD strength and the approximate transition point between the MRCP's RP and NS components. After this point, we expect ERD and MRCP to continue their linear trajectories, while CSE begins to decrease. Additionally, we hypothesize that the CSE pre-movement suppression will peak alongside the MRCP's NS component around 200–100 ms before MOn. However, it remains unclear whether these patterns will be evident from the start of the experiment or emerge only in later trials as learning progresses. Specifically, for CSE, it is uncertain whether learning will affect only MEP magnitude or if the hypothesized cubic trajectory of CSE will also be altered. Furthermore, it is unclear how individual learning-driven changes will impact the ability to predict CSE based on ERD. For instance, Daly et al. (2018) aligned the CSE (now considered preparatory and pre-inhibition) peak with 30% ERD strength in highly trained movements. Whether a similar preparatory peak will be present early in learning remains an open question.

4.2 Materials and Method

4.2.1 Participants

All 59 participants (33 female and 2 non-binary, between 18 and 41 years of age, mean ± SD = 23.22 ± 4.72) filled out a questionnaire screening for any contraindication for TMS, based on the recommended screening procedures outlined by Rossi et al. (2009, 2011) as well as Wassermann (1998). All were self-declared right-handed healthy adults, with normal or with corrected-to-normal (via contacts) vision and had no (history of) neurologic or psychiatric disorders, or any (history of) alcohol or substance abuse. All participants indicated they were free of any medicinal treatments, conditions, or history likely to modulate their cortical excitability. 75% reported to have some form of musical background and training (between 1 month and 17 years of active practice; median = 3 years, IQR is between 2 and 5), of which 36% included some form of key-based instrument (to 25% string based, 9% wind based instrument and 30% non-instrument-based music related experience, e.g., dancing, singing, etc.) Only 25% of the participants indicated they actively practiced music at the time of testing, of which nearly half (45%) specified they only practice occasionally for their own enjoyment.

One participant was excluded from both behavior and neural analysis due to excessive movement, and unusable data leading to early termination of the recording.

The study was conducted in accordance with ethical guidelines and was approved by the University of Essex Research Ethics Board and the Neuromodulation committee (ETH2122-0179).

4.2.2 Experiment design

4.2.2.1 Recordings

Participants sat in an electrically shielded test booth, on a TMS-Robot chair (Axilum Robotics, Strasbourg, France) (see Figure 14)**,** at 3 meters from a screen (32inch, refresh rate 60 Hz) placed at eye level outside the booth, with Genlec speakers placed in the test booth for audio output. They were instructed to sit in a relaxed position with their head resting against the headrest. Their right upper arm was vertically oriented along the body, with the elbow at an angle of about 90° and their forearm resting on a pillow for support. Supports (head, back, and arm) were adjusted for the participant to obtain a comfortable resting position. The right hand was placed on a standard UK qwerty keyboard. The response keys were chosen to encourage a neutral and relaxed hand position: index - X key, middle - F, ring - G and the little finger on the N (or M, according to participant preference, e.g., participants with very big hands may prefer the M key). Visual inspection of the participant's EMG signal was used to ensure a relaxed position. Specifically, we looked for the EMG signal to be comparable to the hand hanging completely at rest next to the body (i.e., to show no sign of muscle tension or contractions).

Hand and keyboard positions were adjusted until satisfactory signals were realized and participants could maintain the position without strain.

Figure 14

TMS-Robot Chair Setup in an Electrically Shielded Test Booth

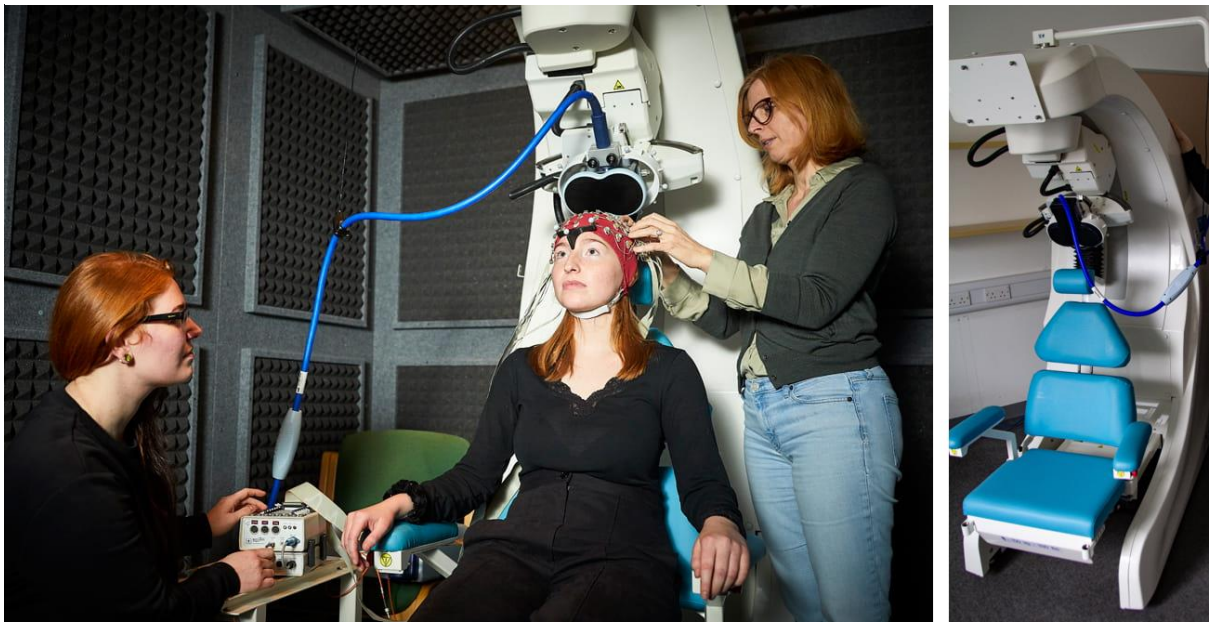

Note. The left image shows the general set up with a participant wearing EEG while seated in the TMS-Robot Chair inside a faraday cage. The right image shows the empty TMS-Robot Chair. The left image was obtained from the university of Essex website https://www.essex.ac.uk/departments/computer-science-and-electronic-engineering/research/brain-computer-interfaces-and-neural-engineering/facilities

EEG and EMG signals were recorded using an ActiveTwo Biosemi system (BioSemi, Amsterdam, The Netherlands), all electrodes were TMS compatible and applied according to the manufacturer's guidelines. Participants wore a 64-channel EEG cap (10/20 placement system) and reference electrodes were positioned on the mastoid bones behind the right and left ears. A trigger channel was used to mark experiment events on the signal. EMG signals were obtained from the right first dorsal interosseous (FDI; i.e., the index finger) and abductor digiti minimi (ADM; i.e., the little finger) muscle; using a bipolar set up of active flat surface electrodes. The recording electrodes were placed on the muscle bellies, with reference electrodes above (FDI) or below (ADM) the closest metacarpophalangeal joint. The diameter of each electrode was 0.3 cm and the distance between two electrodes within a pair was approximately 5 cm.

Both EEG and EMG signals were amplified and recorded at a 2048 Hz sampling rate without re-referencing or filtering applied. Specifically, Biosemi records signals against a feedback loop between a Common Mode Sensor (CMS) active electrode and a Driven Right Leg (DRL) passive electrode as

ground and no reference (for more information see Biosemi website). During the experiment, the CMS and DRL electrodes were placed in the cap as part of the standard EEG electrode set up, serving as ground for both EMG and EEG electrodes. However, while EEG electrodes were fully set up for the TMS hotspot hunting (detailed further below), they were not plugged in to the amplifier and an alternative CMS and DRL loop was set up (the CMS electrode was placed at the center of the dorsal side of the right hand and the DRL electrode was placed over the right wrist styloid) to serve as ground to the EMG electrodes. The cap placed CMS and DRL did not adversely affect the MEP signal quality (as verified in the offline recordings), they did, however, make the TMS artifact very wide (> 50-100 ms, called decay artifacts (Hernandez-Pavon et al., 2022; Varone et al., 2021)). Offline data analysis can work around TMS artifacts by, for example, fitting an exponential function to bring the pulse artefact back to its standard form (Ilmoniemi & Kičić, 2010; Litvak et al., 2007). The online display of the signal, which we used for TMS hotspot hunting in our experiments, did not have this option, with the wide artifact making it impossible to observe MEPs and their differences. As such the alternative set up was used for the TMS hotspot hunting procedure and removed afterwards in favor of the EEG cap CMS/DRL loop.

Once EEG and EMG were set up, each participant their TMS hotspot was located. TMS was delivered in single pulses via a MagStim D70² figure 8-coil (MagStim, Dyfed, UK), equipped with a force sensor, plugged into a Magstim 200² TMS stimulator (MagStim). The coil was controlled using a TMS-Robot (Axilum Robotics) and neuro-navigation software (Localite GmbH, Bonn, Germany). Providing a procedure with, compared to the traditional TMS set up with the coil stationary in a clamp or held by researcher, increased accuracy and control of the position, orientation, and contact pressure of the stimulation coil relative to the participants' head (Ginhoux et al., 2013). The coil was placed at a 45° angle to the sagittal plane with the handle pointing backwards; inducing a posterior to anterior current flow (Adank et al., 2018; Gomez-Tames et al., 2018). The hotspot was defined as the cortical target giving the largest Motor Evoked Potentials (MEPs) in the contralateral FDI and ADM for a given stimulus intensity. The favorable coordinate gave the highest response for both FDI and ADM, however for unclear ADM responses the position that produced the highest MEPs for the FDI was chosen.

For each participant the stimulation threshold and location were identified following procedural steps outlined in Rossini et al. (2015). First, the robot held stimulation coil was directed systematically through a 7x7 grid (7 mm apart, top edge placed parallel to the interhemispheric fissure; Giuffre et al., 2021; Raffin et al., 2020), placed over the left hemisphere and centered around a theoretical cortical target for the FDI (located using the anatomical landmark of the precentral gyrus hand knob; Yousry et al., 1997; referential coordinate in the standard Montreal Neurological Institute (MNI) dataset frame: -40, -13, 68). We began by stimulating at each of the four cardinal points around the center, while

visually inspecting the recorded EMG signals. Visual inspection of the MEP responses in the signal further informed the coil trajectory through the grid. Then, once the hotspot was found, the resting motor threshold (rMT) intensity was determined for every participant by adjusting the TMS intensity until the EMG signal displayed 5 out of 10 MEPs for which the peak-to-peak amplitude was at least 50 µV. The experimental threshold (eMT) was then set at rMT + 2% of the maximum TMS output (e.g., for an rMT of 65% the eMT is set to 67%), rather than the more conventional 120% of rMT. The 120% scaling is disproportional at higher intensities (e.g., 120% of 55 is 66) compared to lower intensities (e.g., 120% of 30 is 36). Without EEG electrodes placed on the participant's scalp, the rMT tends to be around 30-40% of the stimulators maximum power. We found, with EEG, the average stimulation power needed to be around 55-65% of the stimulators maximum power. The difference to the conventional range of stimulation power is most likely caused by an increased distance between coil and scalp due to the EEG electrodes, requiring a higher stimulation intensity to elicit equivalent MEP responses. Thus +2% functioned as an alternative to the conventional 120% of rMT intensity used as thresholds for experiments.
Participants wore ear plugs to reduce the influence of the loud sounds resulting from the TMS discharges.

Stimuli presentation and recording of neural activity happened on different computers. The experimental paradigm was custom-made in MATLAB (Version R2022b; MathWorks, MA, USA) using the Psychophysics Toolbox extensions (Psychtoolbox-3, version 3.0.18; Brainard, 1997; Pelli, 1997; Kleiner et al, 2007); in addition to LoopMIDI (Version 1.0.16.27, Erichsen, 2019) and KONTAKT 6 PLAYER software (version 6.2.2 (R51), Library: Kontakt Factory Selection, Ragtime Piano – Grand Piano; Native Instruments GmbH, Berlin, Germany) for audio output. Remote stimulation of the TMS pulses was realized using the MAGIC toolbox (Habibollahi Saatlou et al., 2018) and an inhouse made serial cable to control the Magstim 200² TMS stimulator (MagStim) from the stimuli presentation PC. Data analysis was carried out using custom-made MATLAB functions and R software.

4.2.2.2 Procedure

Participants were asked to read a briefing, provide informed consent, and fill in a short survey (see Appendix A3 for the complete updated survey) on their self-reported motor skill level and music proficiency upon arrival. The survey consisted of two 9-point Likert scales. First, *"How would you rate your right-hand dexterity / muscle control?"* (1 = Far worse than most, 3 = Worse than most, 5 = Average, 7 = Better than most, 9 = Far better than most). Followed by, *"What would you rate your general musical competence?"* (1 = Very poor, 5 = Average , 9 = Excellent). Likert scales were followed by open questions enquiring about any background relating to music. The questions were: Type of musical practice (e.g., Instruments, Singing, Dance, etc.), Total number of years actively practiced, Time

period of active practice (e.g., from age 5-15), Currently playing, and any other information the participant considered relevant or wanted to share (e.g., Self-taught, or traditional music education).

Figure 15

Flowchart Detailing Neuroimaging Experiment Protocol

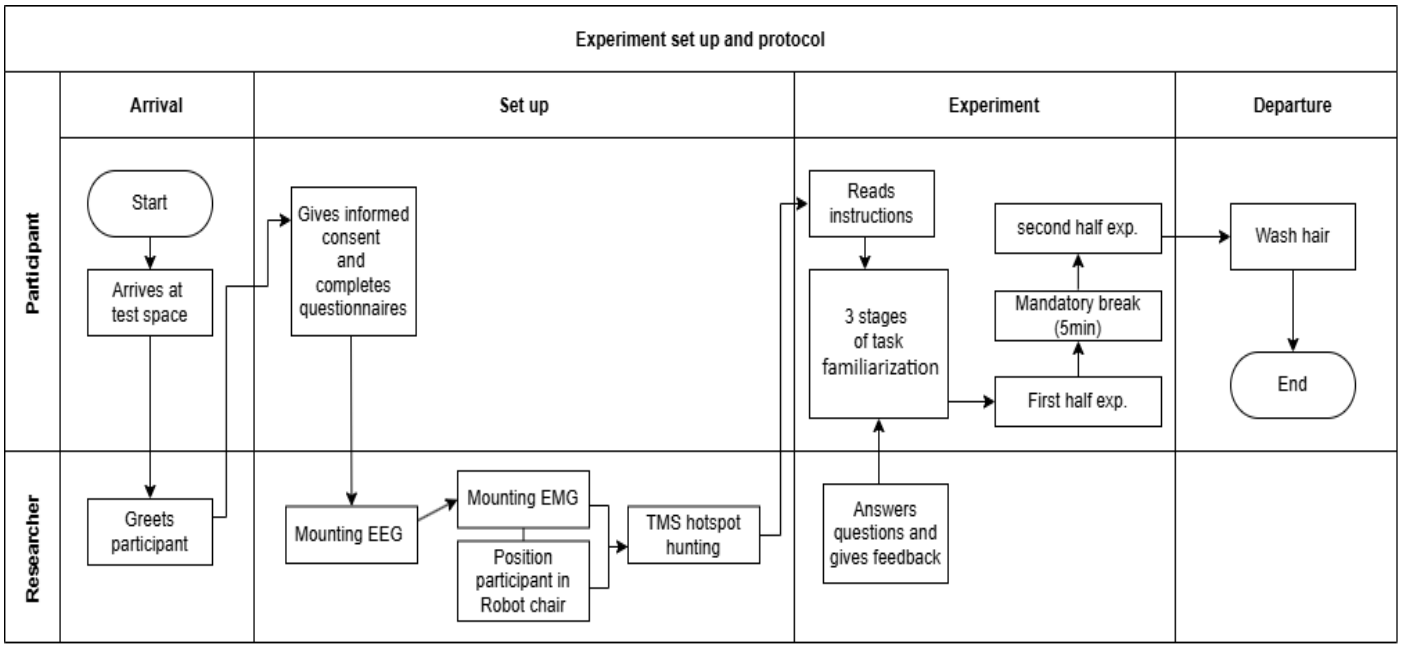

The experiment consisted of one 3h session (of which 2h were needed for set up) and aimed to train participants' right hand finger motor control skills using the piano learning task introduced in Chapter 3. During the experiment EEG and EMG were recorded and TMS was delivered at 6 predefined key time points, at -1.250s, -1s, -0.750s, -0.500s, -0.200s, -0.100s, relative to a fixed estimated time point at which movement onset (MOn; t0) was assumed to occur in the EMG signal. MOn was estimated based on the following parameters: 1) An electromechanical delay of around 90 ms between MOn and button press detection 2) the average response delay in a reaction time task is around 300 ms (Ibáñez et al., 2020). Consequently, the average MOn time was estimated to be 200 ms after the signal for the first button press (first target number turning blue, see the description of the learning task in 3.2.2 Experiment Design). These exact stimulation timepoints were chosen considering our timepoints of interest as described in the hypotheses: 1) wanting to have a better idea of the CSE timeline between -1.5s and -0.5s to MOn, 2) exploring the relation of EEG neural markers to the pre-movement dip in CSE occurring between -0.5s and -0.2s, as well as the observed increase between -0.1 to 0s to MOn and 3) to ensure a better and more equal spread of TMS across the 2 second timeline before MOn to improve the data quality of both EMG and EEG and address the issues outlined in Chapter 2. Presenting the stimulation timepoints at fixed times in the experiment combined with a variable MOn further encouraged more spaced-out measures of the evolution of the CSE timeline.

Before data collection, participants read through detailed task instructions and went through 3 stages of task familiarization. They pressed the F key (middle finger) to navigate forward in these instructions. The TMS coil was not aligned and no stimulation was applied during familiarization. The first and second stage were identical to the learning task described in Chapter 3. The third stage of the familiarization process focused on the timing of the first button press in the sequence; and was added to encourage reliable timing for our assumed MOn (Ibáñez et al., 2020), and minimize the learning curve for timing the initial button presses from influencing the measure of learning the sequence.

To train their response times, we ran participants through 4 blocks of 12 abbreviated trials (stopped short after the first number in the sequence turned blue, participants had up to 800 ms after the cue change to respond) and gave feedback immediately after each response. Reaction times (RTs) between 50 ms and 350 ms after the cue change from white to blue resulted in the words ''well timed!" being presented on screen. RTs before and up to 50 ms after the cue change resulted in a message informing the participants that they were ''too fast'', and any response later than 350 ms resulted in the words ''too slow'' presented to participants. Each block had a different sequence (once again different from the one used in the test part of the experiment) and started with a different finger so participants received timing training with all four fingers.

The familiarization was concluded with an opportunity to ask any remaining questions, a message to emphasize participants to keep their hand in the relaxed position obtained at the start of the experiment, and a general learning tip to, going forward in the experiment, "focus on the order of the button presses and timing with changes on the screen, before worrying about the duration of a button press."

Before starting the test part of the experiment, the TMS coil was aligned with the previously defined stimulation target. Once contact was established the participant was given the signal to proceed with the experiment.

For the task, participants ran through 10 test blocks, presented (in a random order) with 1 of the 10 unique sequences to learn per block. For each block they were given a total of 24 tries to execute the melody as accurately as possible (see the learning task described in 3.2.2 Experiment Design). Because we are interested in neural activity in the pre-movement period, sequences were further setup so that a recorded muscle related to the first number in 80% of the trials, split evenly between index and little fingers. The remaining 20% of the trials would start with either the ring or middle finger. Participants were shown, albeit of a smaller magnitude, muscle responses of their middle and ring finger in the EMG signals during set up. Giving the intentional impression that middle and ring finger would also be picked up with the electrodes placed over the index and little finger. Every block started with a visual

presentation of the full sequence for that block. Participants would then press the F key (middle finger) to start the first trial of the block.

During the test trials, a single TMS pulse was given at one of six predefined time points: 1.150s, 1.400s, 1.650s, 1.900s, 2.200s or 2.300 seconds relative to the start of the fixation cross. Which is equivalent to -1.250s, -1s, -0.750s, -0.500s, -0.200s and -0.100 seconds before the estimated observation of MOn in the EMG signal, which was expected to occur around 200 ms after cue change. Stimulation occurred a total of 4 times per time point per block, in a semi randomized order (to avoid order effects while ensuring an even spread of our measures, e.g., avoiding all stimulations at 500 ms relative to MOn to happen in the first 4 trials) per 12 trials. Meaning, all 6 stimulation points will be randomly allocated twice over the first 12 trials in a block, and again for the next 12 trials in the block.

Participants had the opportunity to take a small break of up to 5 minutes between blocks or to press the F key to continue to the next block. However, participants were informed to, even when taking a break, avoid moving as their head was still in contact with the TMS coil.

At the midway point, after block 5, participants took a compulsory 5-minute break, irrespective of any earlier breaks taken. At this point the researcher unaligned the TMS coil and allowed participants to stand up, have a drink of water and stretch their legs. The midway point break was in response to pilot findings and feedback. Previously, the combination of sitting still and up, in a relatively uncomfortable chair, for the length of the experiment resulted in strain and discomfort for the participant, leading to a decline in attention and an increase of fidgeting. After the enforced 5-minute break, participants were reseated, their hand was repositioned until satisfactory EMG signal was reobtained, the TMS coil was realigned and the participant resumed with the second part of the task.

Upon completing the task participants were freed of electrodes, got a chance to ask any remaining questions and to wash their hair.

4.2.3 Data preparation and planned analysis

4.2.3.1. Behavioral data

Improved motor control of sequential finger movements was measured by learning the responses to numerical sequences and the timing of each response based on an underlying melody. Button responses were measured as a time series, and performance accuracy was defined as the percentage of correspondence between a participant's response series and that of 'a perfect sequence'. Trial reaction times (RT) were measured as the difference in time between the first button press and the first number turning blue. Both accuracy (ACC) rates and RTs were submitted to rmANOVAs following our simplified design version; with Blocks as a 2-factor variable and Trials as a 4-factor variable.

For full details on data preparation and planned analysis of behavioral output see 3.2.3 Data preparation and planned analysis.

In total 10 trials, spread over 8 participants (between 1 and 3 trials per person; mean ± SD = 1.25 ± 0.71), were removed from further analysis due to no recorded button presses. Additional trials with outliers were removed, once again identified using *Tukey's method* (Dhana, 2016; S. Seo, 2006). A total of 0.15% (16 out of 13920 trials) of the trials were removed for ACC scores, and 3.30% (459 out of 13920 trials) were removed for analysis relating to RT (both totals include the 10 'no response' trials).

4.2.3.2. Neuro imaging data

Biosemi saves EEG and EMG recordings as one data file. As such, datasets were initially loaded in without reference. We re-referenced the 64 EEG electrodes to the average of both mastoids. EMG signals were bipolarly referenced to their respective reference electrodes.

Artefact removal. Large amplitude artefacts, such as those introduced by TMS, are known to negatively interact with (i.e., introduce additional artifacts surpassing the duration of the original artifact) steps of the data preparation process further down the line (e.g., ICA, filtering, etc.). All large amplitude artefacts were removed through the interpolation process described in 2.2.2.3 TMS Artefact Removal, with the difference that the smoothing of the edges now covered 5 ms on each side (compared to the 20 ms utilized in Chapter 2).

First, major TMS induced negative baseline amplitude shifts (difference > 5000 µV, see Figure 16) observed on some trials (having very sharp points of offset and return to baseline, unlike the slow decay return described in Chapter 2) were interpolated for both EEG and EMG over a window of 1s, starting 0.02s before the TMS event marker. Other oddities, observed through visual inspection, were removed at the same time via interpolation. With manually defined window sizes of minimal length required we removed the noted artefact.

Figure 16

EEG Signal With Both Regular and Irregular TMS Induced Artifacts

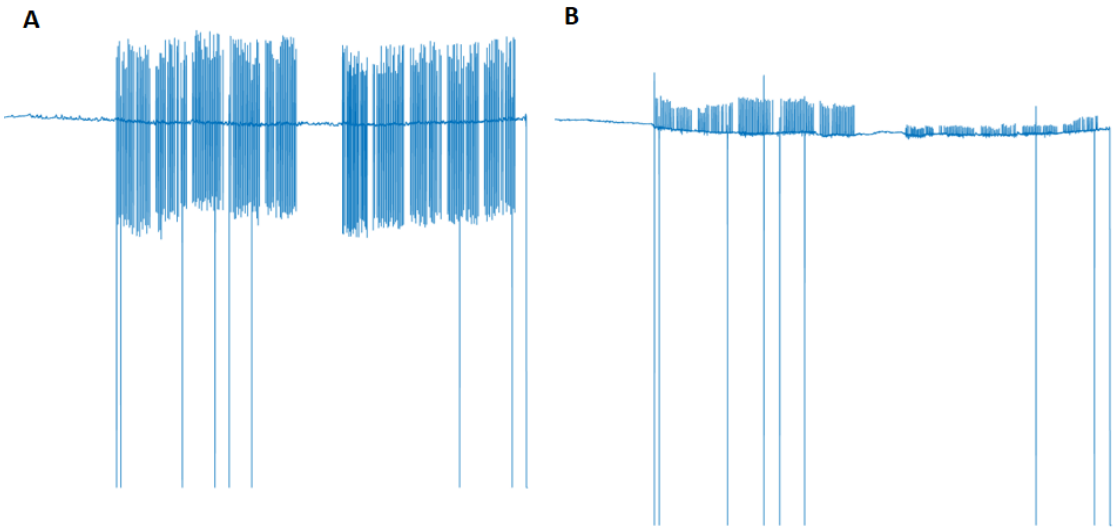

Note. Raw, unreferenced, EEG from a single electrode for two participants. TMS was applied to every trial, these expected TMS artifacts show consistent within individuals despite inter-individual differences (e.g., A vs. B). Unexpectedly, some trials show large artifact shifts beyond typical TMS-induced effects.

Second, we interpolated the TMS pulse artefact present in all our trials of interest (see Figure 17 for removal process). Once again, many trials and channels showed TMS pulses with a decay artefact (Hernandez-Pavon et al., 2022; Varone et al., 2021). However, spanning tens of milliseconds and thus looking more like wide TMS pulses (see also Figure 18B) rather than a shift in baseline as noted in Chapter 2. The slow dissipation of electrical charge, resulting in the observed decay, shows an exponential curve (Varone et al., 2021). To not interpolate (and thus lose) more data than necessary, we fitted an exponential function to bring the pulse artefact back to its standard form (Figure 17B) of spanning around 7 ms (Ilmoniemi & Kičić, 2010; Litvak et al., 2007). Specifically, we high-pass filtered both EEG and EMG (IIR Butterworth, 4th order; EEG at 0.01 Hz and EMG at 0.1 Hz). Filter frequencies were chosen to be high enough to center the waveform around the zero-amplitude line, and low enough not to introduce additional artifacts or violate theoretical filtering requirements (2.2.2.4 ICA and Filtering, EEG pre-processing for MRCP). This was followed by fitting and subtracting an exponential function for each channel and trial (both EEG and EMG). Finally, the TMS pulse was removed by interpolating a window of 12 ms around the maximum absolute value (-0.002s to +0.01s) for EEG and 17ms (-0.005s to +0.012s) for EMG (22 ms and 27 ms respectively when including the 5 ms edge smoothing on each side of the window). Window sizes were chosen to retain as much data as possible (i.e. as small as possible), while ensuring a consistent result across participants in an automated process.

Figure 17

Process of TMS Artifact Interpolation

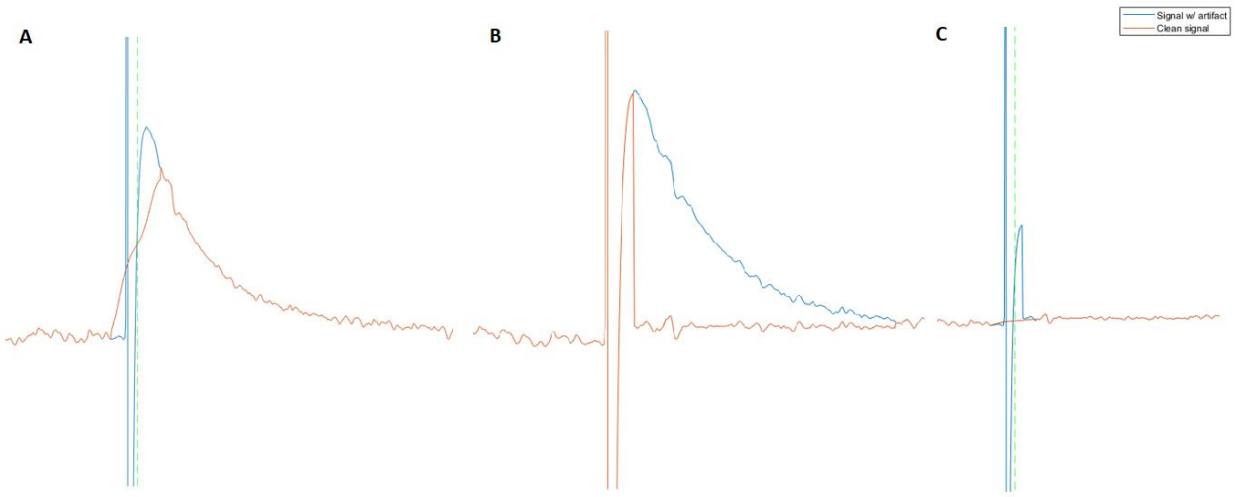

Note. The general TMS artifact interpolation process was identical for both EEG and EMG, shown here is an EMG signal with a very small MEP. (A) illustrates how the decay artifact compromises the interpolation attempt and completely obscures the presence of an MEP. (B) shows the signal before and after fitting and subtracting the exponential, with a now discernable MEP. (C) presents the successful interpolation of the TMS pulse artifact. Dotted green line shows the stimulation marker in EEG overlaps with the location of the TMS pulse artifact.

Figure 18

EMG Signal Showing TMS Artifacts, MEPs and Muscle Contraction Bursts

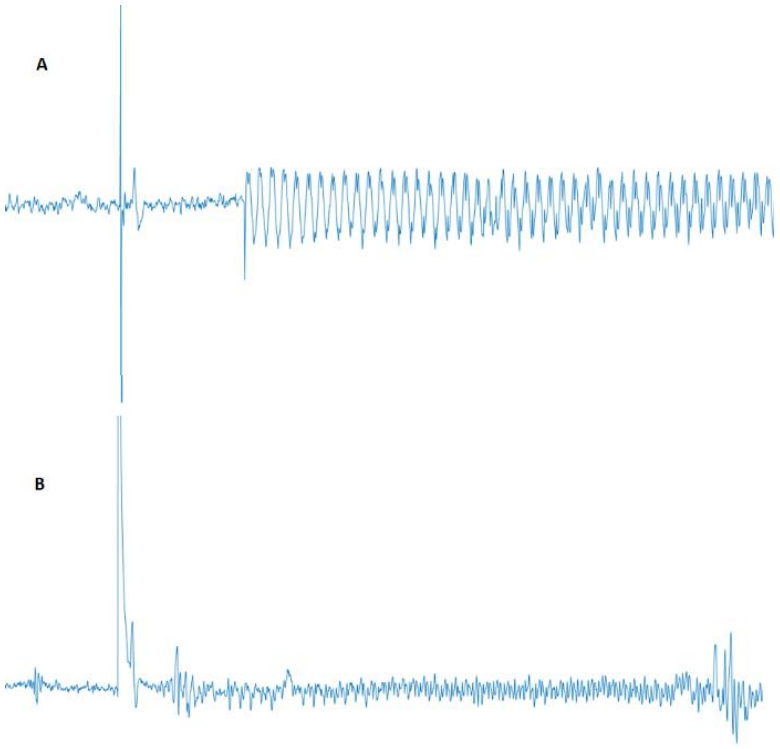

Note. Bipolar referenced FDI-EMG single for two participants.

(A) shows a typical TMS pulse followed by a clear MEP and unexpected post-stimulation noise that occurred at 200 ms post-pulse, identified as line noise burst over lapping in intervals of 50 Hz (50, 100, 150, etc.). However, for EMG this artifact fell outside of our window of interest.

(B) shows a TMS-pulse with an MEP appearing fused to the decay artifact, resembling a normal but wider pulse artifact. Shortly followed by an EMG muscle contraction burst. Further showing inter-individual differences in the post stimulation line noise. Here still present but smaller.

EMG data was then high-pass filtered at 20 Hz (FIR filter, 4020th order) (Nikolov et al., 2021)and both EEG and EMG were down sampled to 1024 Hz (Ives & Wigglesworth, 2003).

EEG was subjected to further cleaning. Using ICA to remove blink artefacts, as well as reoccurring robot induced artifacts (Figure 19), from the EEG data, now cleaned of TMS artifacts. As described in 2.2.2.4 ICA and Filtering, we first filtered the EEG data using a 1 Hz high-pass filter (IIR, 4th order), a 50 Hz notch-filter (IIR, 6th order), and a low-pass filter at 40 Hz (FIR filter, 4020th order). Bad channels, flagged based on joint probability (using EEGLAB, version 2023.1, pop_rejchan function, with trimmed normalization and threshold set at 5 SD; Delorme & Makeig, 2004), and further confirmed via visual inspection, were excluded before running the ICA. Independent Components (ICs) were then identified by visual inspection. Once again, the data from which ICs were removed held a different (lower) high-pass filter than the data on which the ICA was ran (0.01 Hz (IIR, 4th order) instead of the 1 Hz used to run the ICA) (Makoto's preprocessing pipeline, n.d.). To finalize data cleaning and preprocessing we interpolated the bad channels removed prior to running the ICA.

Figure 19

EEG Signal with Blink, Robot-Induced, and Post-TMS Line Noise Artifacts

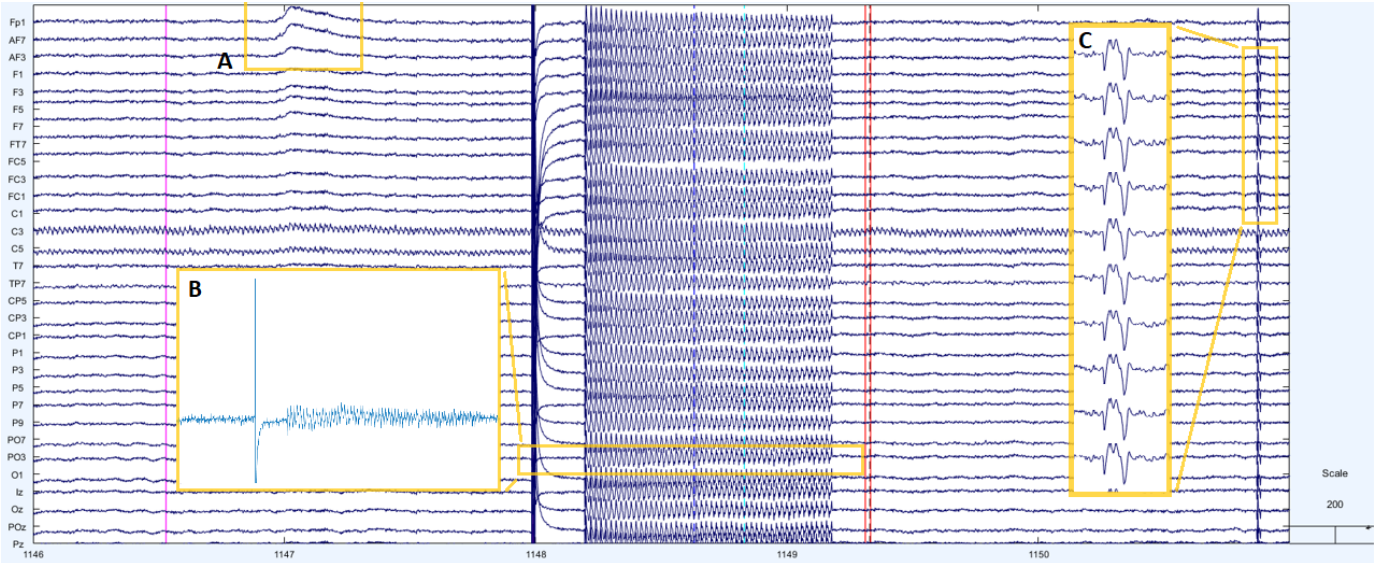

Note. Segment of EEG signal from multiple channels highlighting different artifacts. (A) shows a blink artifact. (B) displays unexpected post-stimulation noise at 200 ms, identified as line noise bursts at 50 Hz intervals, previously shown in EMG. In EEG, this artifact was effectively removed with low-pass filtering at 40 Hz. (C) highlights a repetitive yet irregular robot-induced artifact. Both A and C were successfully removed using ICA.

Unchanged from Chapter 2, the Epochs of Interest (EoI) were defined as a time window of 3 seconds relative to the MOn. Starting 2 seconds before and ended 0.5 seconds after MOn, with an additional 250 ms added onto both ends of the interval to account for edge effects. MOn was once again defined as onsets of increased EMG activity to indicate movement initiation. However, different to Chapter 2, the data was gathered with the intention to establish a measure relative to MOn. As such it contained a mechanical indicator as part of the experimental design (reflecting the exact time point a button was pressed) to obtain these EMG onset times in each trial. To properly estimate these EMG-based MOns, timepoints of a button press were shifted 90 ms earlier to account for the electromechanical delay between electrical muscle activation and production of force output (Demandt et al., 2012; Ibáñez et al., 2020; Klein-Flügge & Bestmann, 2012).

Trial Removal. 5 participants were excluded from further analysis as a whole, due to uncorrectable issues with the recording. An additional 7 participants were excluded for different parts of the analysis due to low quality of their data or retained less than 1/3 of their trials following the exclusion criteria listed below. Specifically, 4 were excluded for the EEG analysis and 3 for the EMG based analysis.

For the remaining participants (50 for EEG, 51 for EMG) we further removed individual trials in accordance of the following conditions:

(i) Absence of a response (i.e., no button presses within the presentation of the first two numbers of a sequence).

(ii) Incorrect first response.

(iii) Presence of major TMS induced baseline amplitude shifts (> 5000) in both EEG (μV) and EMG (mV), spanning a duration between 0.8s and 1s.

Exclusively for EEG measures, trials were further removed due to

(iv) Presence of artefacts between the start of the fixation cross and 1st button press. Specifically, trials were excluded if EMG and/or movement artefacts were identified on one or more EEG channels (identified by visual checking).

Exclusively for EMG (MEP) measures, trials were further removed due to

(v) Absence of TMS delivery.

(vi) Middle or Ring finger as a sequence start response.

(vii) Trials were not relevant to our analysis, as indicated by movement onset occurring prior to, during or more than 2 seconds removed from stimulation.

Removing these trials from the dataset before further analysis ensures the results are based on trials where: 1) the participant-initiated movement, 2) there is no artefact contamination and 3) for EMG (i.e., MEP measures) we have reliable measures of the relevant muscle with the delivery of TMS that happened prior to movement.

Differences in trial removal criteria for EEG to EMG measures is dictated by the different types of data presenting different challenges (both practical and theoretical) to what makes a trial measure informative. Consequentially, a higher number of trials were able to contribute to EEG measures than to EMG measures, as EEG measures are not dependent on the contraction of a specific muscle, nor require the presence of TMS. See 4.3.2 Neuroimaging result for exact numbers.

Neural marker Characterization. These were once again near identical to the characterization defined in Chapter 2 (2.2.3 Neural Marker Characterization). With the difference that, for ERD, the sliding window to calculate the frequency band power (which was 625 ms to cover 5 cycle lengths of the lowest frequency (i.e., 8 Hz) in Chapter 2) was adjusted to 250 ms. Still covering a minimum of 2 cycles, as calculated on the lowest frequency, to avoid aliasing (as per the Nyquist theorem; Por et al., 2019) but smaller for a more balanced time-frequency trade-off (a wider window yields a higher frequency resolution at the cost of a decreased temporal precision; Cohen, 2019) (i.e., reduce the unnecessary

high spatial resolution handled in Chapter 2). Final TMS interpolation for EEG once again covered 120 ms, as described in Chapter 2, as we were unable to consistently remove the TMS induced artifacts in an adequate and timely manner. However, combined with the adjusted sliding window for power calculation, only 370 ms (compared to the 750 ms in Chapter 2) of calculated band power is affected by the lack of variance in the interpolated window and needs to be replaced by NaN values before averaging.

The MEPs, as a measure for corticospinal excitability, were once again measured in terms of their peak-to-peak difference (max – min value) in amplitude, 0.015–0.045 seconds after TMS delivery. Signal to Noise Ratios (SNRs) were calculated to ensure the values included were actual MEPs. In absence of SHAM trials to function as a control measure, we retained the 90^{th} percentile (SNR =1.1) of the SHAM SNR distribution in Chapter 2, to differentiate between trials with and without MEPs.

Remaining MEP values were then log transformed (to the base e) to ensure normality of samples, and standardized (z-scored) per finger and per participant, to ensure comparability of amplitude across response type (i.e., finger) and individuals.

No changes were made in the calculation of MRCP.

The focus of the analysis was to compare the ERD strength, MRCP and CSE timeline. Specifically, to assess the evolution of CSE over time relative to MOn and its relationship to the EEG-based neural markers on this same timeline. We then wanted to know how learning affects the neural markers individually, as well as the relationship dynamic between all 3 of the neural markers in terms of timing relative to MOn.

To assess the effect of learning on each neural marker their evolution over time, the timeline relative to MOn was converted from a continues to a discreet variable. Focus was on 7 timepoints informed by, and best suited to test, our hypotheses: -1.25, -1, -0.75, -0.5, -0.25, -0.1, -0.05 seconds relative to MOn. We calculated the value of each neural marker for each timepoint per participant, by first averaging the neural measures over trials and then as an average of the surrounding timepoints according to the following time intervals (in order of the prior listed timepoints):]-1.375,-1.125],]-1.125,-0.625],]-0.625,-0.375],]-0.375,-0.150],]-0.150,-0.075],]-0.075,0]. Meaning, all participants ended up with 7x2 aggregated measure values for Blocks and 7x4 for Trials; per neural marker. Where for example, participant 20 their MRCP amplitude was at -1s to MOn in first half of the experiment, this resulted from first averaging all trials in the first half of the experiment, and then averaging all average amplitude values between 1.125 and 0.625s before MOn.

Each neural marker was then subjected to two two-way rmANOVAs; containing the discreet timeline as a 7-level factor (further referred to as “Timepoints”) and one of the two ‘learning conditions’ (Block as a 2-factor variable or Trial as a 4-factor variable). Two-way rmANOVAs were chosen over one three-

way rmANOVA as the learning interaction of blocks and trials held little relevant meaning as indicated by the behavioral data (see 4.3.1 Behavioral results).

The neural marker relationships (i.e., dynamics of CSE in relation to changes in neural activity over the motor cortex) were further quantified by exploring the neural markers in EEG their ability to describe and predict MEP amplitudes. However, without the delay effect described in 2.3.2.1 CSE dynamics in Relation to ERD. In Chapter 2, replacing part of the band power measure with NaN lead to severely reduced number of contributing trials (with only 18% trials remaining at its lowest), the current study provides a better spread of TMS over the 2 seconds leading up to MOn, with 73% of the total number being the lowest number of trials contributing to the ERD measure at -0.065 ms to MOn. The effect of learning is then assessed by comparing the model's ability to predict datapoints within and across the different stages of learning. Another difference in the predictive modeling approach from Chapter 2 to Chapter 4 is that the current study MEP amplitudes matched with the participant's unique average ERD % at that time. This is different from the predictive modeling in Chapter 2, where the relative decrease in band power needed to be calculated from sample point values averaged over all the subject averages. The reason for this difference lies in the low number of trials retained in Chapter 2 and the overlap of TMS timepoints, and thus overlap in windows removed by NaN. This led to several of the participant in Chapter 2 to have an average ERD measure that would still be plagued by having no value or a value determined by a single trial. Working with an across subject average to calculate the relative decrease in ED (i.e., percentage) was a work around for this issue. The better spread of TMS stimulation and higher number of retained trials in Chapter 4 means we do not need to have these extra measures and can work with the participant averages directly.

4.3 Results

4.3.1 Behavioral results

Having music-based training can improve an individuals' musical competence. Playing an instrument can, in addition, result in increased hand dexterity and/or muscle control. However, for both musical competence and hand muscle control, a higher-than-average capability can exist outside of musical (or any) training. In the current study the participant sample had a 44 to 15 (yes/no) ratio on the questions of having any musical background and training. On a 9-point Likert scale, those with music-based training rated their own musical competence as "average" (M ± SD = 5.36 ± 2.04), which was significantly higher [$t(57)$= -2.95, p = 0.005] than those with no music training who rated their musical competence as "below average" (M ± SD = 3.60 ± 1.88). No such difference was observed for self-reported muscle control of the right-hand [$t(57)$= -0.56, p = 0.578] where both those with a musical background (M ± SD = 6.64 ± 1.33) and those without (M ± SD = 6.4 ± 1.64) perceived their right-hand muscle control, on average, better than most. Based on these results we can confidently move forward

with the factor of 'having musical training or not' to further assess any confounding effects of musicality on our task performance and learning curves. We conclude that any differences in performance on the task between the groups is due to an advantage of musicality and not in (self-perceived) muscle dexterity. Additionally, if no such difference in performance is found, our task is well made and suitable to allow us to conclude that any observed learning effects are motor learning effects.

The three-way mixed effect ANOVA, including musical background as a between subject factor with two levels (yes or no) alongside Trials and Blocks, once again showed no confounding effects of pre-existing advantages from trained musicality. There was no significant difference between the general performance scores for those with and without musical background [$F(1,56) = 0.13$, $p = .721$, $\eta^2 = .002$]. Neither were there any interactions between musical background and Trials [$F(1.67,93.32) = 0.61$, $p = .515$, $\eta^2 < .001$] or Blocks [$F(1,56) = 2.26$, $p = .138$, $\eta^2 = .003$] indicating people with musical background did not have any general advantage in the task or improvements in performance scores at a rate any different than those with no musical background.

A two-way rmANOVA with Trials and Block showed the expected significant differences of performance scores over Trials [$F(1.68,95.57) = 113.68$, $p < .001$, $\eta^2 = .066$] as well as over Block [$F(1,57) = 13.19$, $p < .001$ $\eta^2 = .017$], as well as an unexpected interaction between the two [$F(2.27,129.54) = 21.515$, $p < .001$, $\eta^2 = .006$]. While the interaction term is statistically significant, the eta squared implies the effect is of a negligible size. Two separate (Bonferroni corrected) one-way rmANOVA follow-up tests showed our significant learning effect over trials is retained in both the first half [$F(1.7,96.7) = 112$, $p < .001$, $\eta^2 = .106$] and second half [$F(2.12,121) = 50.9$, $p < .001$, $\eta^2 = .035$] of the experiment. However, with notably different F and eta square values. These results are in line with the observations in Figure 20 showing a present, yet slightly less pronounced sequential increase in performance ACC over trials in the second half of the experiment. Four Bonferroni corrected pairwise comparisons were used to further explore the interaction and the difference between the first and second half of the experiment for the average performance accuracy of the first 6 trials [Trial 1-6; $t(57) = -6.66$, $p < .001$], the second 6 trials [Trial 7-12; $t(57) = -2.82$, $p = .007$], third set of 6 trials [Trial 13-18; $t(57) = -2.21$, $p = .031$] and the final 6 trials [Trial 19-24; $t(57) = -1.68$, $p = .098$]. All showed a significant difference between the first and second half of the experiment, except in the last 6 trials. Taken together, our results here show participants do learn, and performance significantly improved over trials (learning an individual sequence) and the experiment in general (learning over several sequences). The learning curve for an individual sequence, however, became less steep as participants became better.

Figure 20

Mean Performance Accuracy per 6 Trials Split over First and Second Half of the Experiment

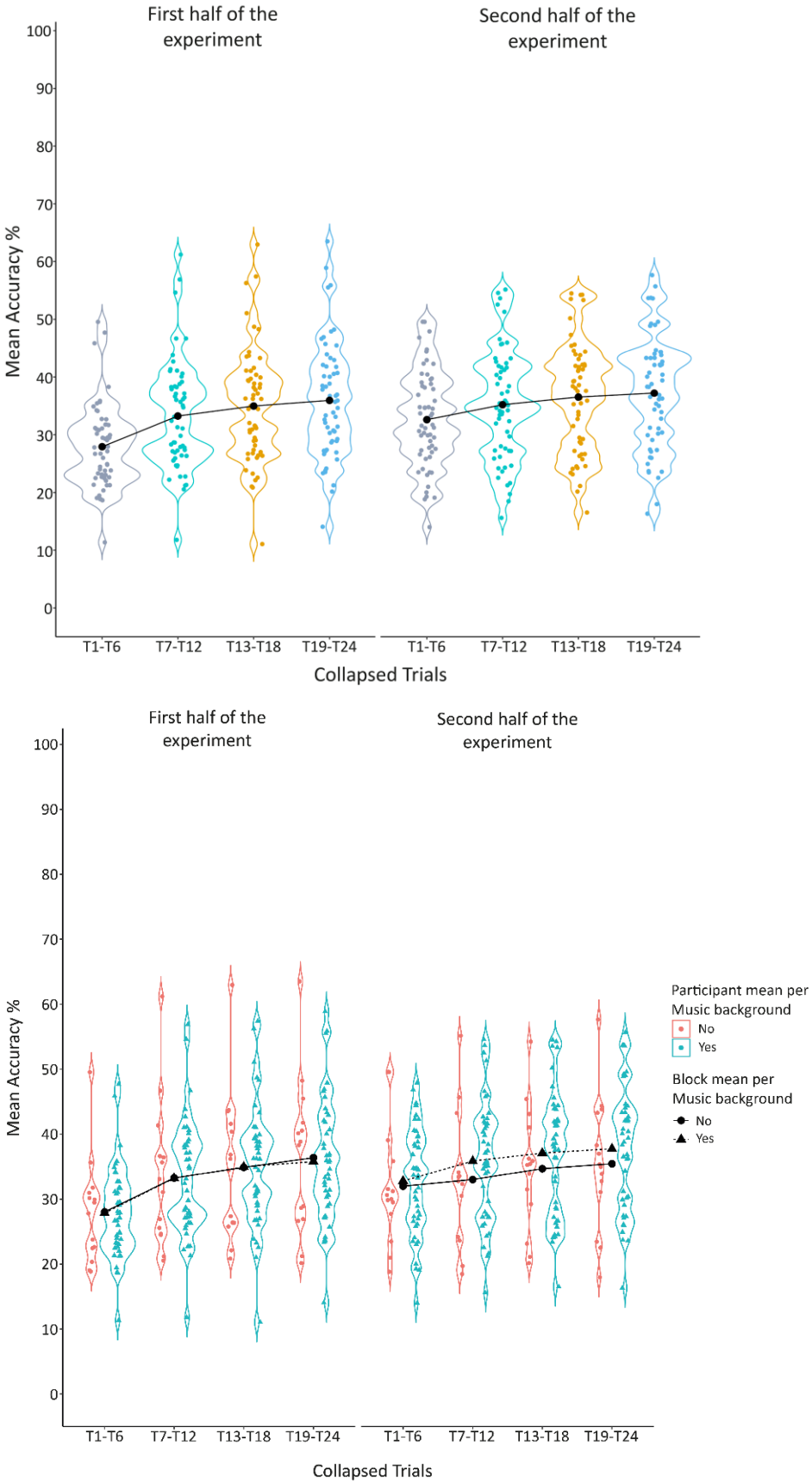

We once again tested the theoretical assumption of equivalence among sequence difficulty. The one-way rmANOVA indicated a significant difference [$F(6.4,364.66) = 27.39$, $p < .001$, $\eta^2 = .128$] when comparing average ACC scores between different sequences, irrespective of their sequential order (i.e., Trial and Block order not being considered). Specifically, pairwise post-hoc analyses with a Bonferroni adjustment revealed ACC scores of four sequences (3, 4, 7 and 10; see corresponding bars in Appendix A4) were statistically significantly different than nearly all the other sequences [$p < .05$; see Table 6], while no such notable differences existed among the six other sequences [$p > .05$; see Table 6]. Meaning, based on Figure 21 and the randomized (and thus semi balanced) presentation of the sequence order, participants performed significantly worse on the sequences 3, 7 and 10; regardless of these sequences being presented as one of the first or later ones in the experiment. While sequence 7 appeared to be significantly more challenging than other sequences, scores were still not as low as on sequence 3 and 10; as indicated by significant difference between sequence 7 and 3 [$t(57) = -3.62$, $p = .028$] and 10 [$t(57) = 3.57$, $p = .033$]. On the other hand, participants scored equally low on sequences 3 and 10 [$t(57) = -.63$, $p = 1$], implying these sequences were experienced, by participants as being of similar difficulty. Differences in scores with sequence 4 on the other hand resulted from participants scoring on average higher on sequence 4 compared to other sequences. The difference is seemingly driven by sequence 4 being experience as easier than the others.

Table 6

P-values of Pairwise Post-Hoc tests for a One-Way rmANOVA on Equivalence of Sequence Difficulty

Sequences	Seq 1	Seq 2	Seq 3	Seq 4	Seq 5	Seq 6	Seq 7	Seq 8	Seq 9	Seq 10
Seq 1	1	1	< .001 ***	.283	1	1	< .001 ***	.148	1	< .001 ***
Seq 2		1	< .001 ***	.028*	1	1	.003**	1	1	< .001 ***
Seq 3			1	< .001 ***	< .001 ***	< .001 ***	.028*	< .001 ***	< .001 ***	1
Seq 4				1	.001**	.023*	< .001 ***	< .001 ***	.023*	< .001 ***
Seq 5					1	1	.082	1	1	< .001 ***
Seq 6						1	.022*	1	1	< .001 ***
Seq 7							1	.419	.054	.033*
Seq 8								1	1	< .001 ***
Seq 9									1	< .001 ***
Seq 10										1

Note: Differs significantly from each other, * at $p < 0.05$ (Bonferroni adjusted). See appendix A3b for associated t test statistics.

Figure 21

Mean Performance Accuracy per Participant per Sequence, Irrespective of Presentation Order

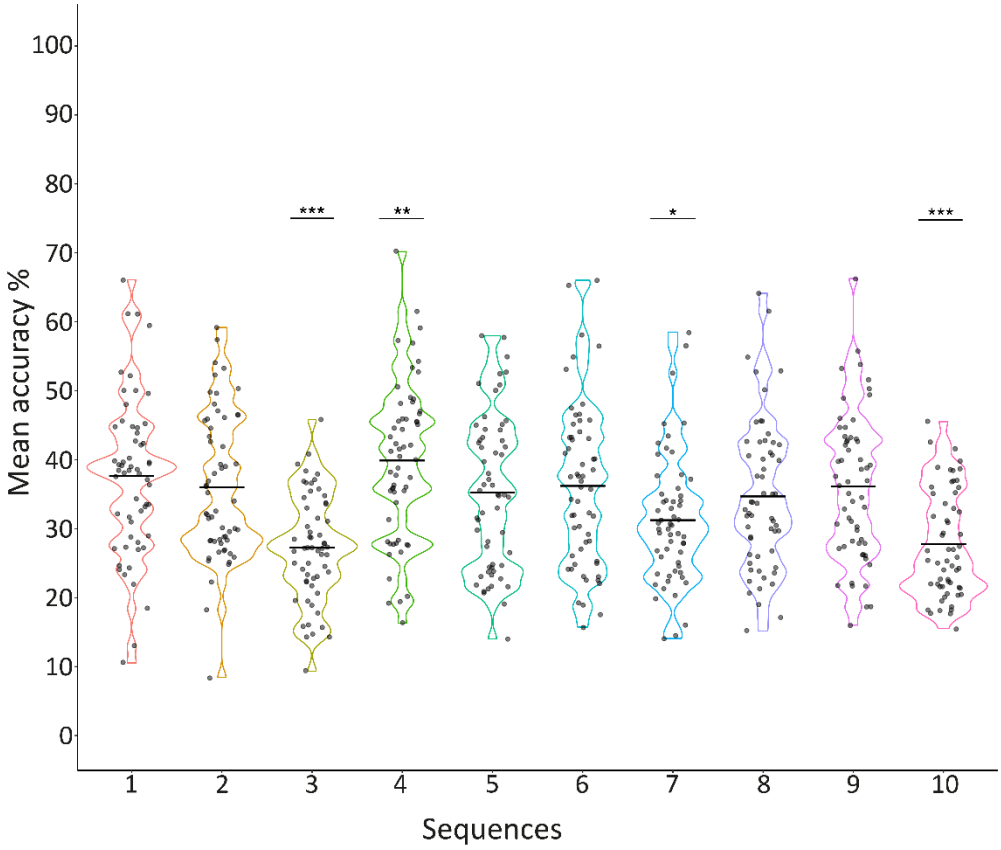

Note. Sequence order was randomized before presentation for every participant. Individual dots indicate average accuracy score per participant per sequence. Horizontal black line indicates the overall average performance accuracy per sequence across participants irrespective or presentation order. Significance of *p*-values indicate general difference between the specific sequence and others as presented in Table 6.

We had two issues regarding RTs of 1st button presses in Chapter 3. First, that participants sped up significantly over the course of the experiment. Second, the magnitude of the increase in speed. To assess the training effects from the 3rd familiarization stage, on the timing of the first button press in a trial, we first ran a three-way rmANOVA and ensured there was once again no significant difference in RT for those with trained musicality. We found no general main effect [$F(1,56) = 0.48$, $p = .493$, $\eta^2 = .007$], nor interaction on the level of Trial [$F(2.08,116.23) = 0.11$, $p = .907$, $\eta^2 < .001$] or Block [$F(1,56) = 0.15$, $p = .700$, $\eta^2 < .001$] (see Figure 22). Following up with a two-way rmANOVA showed us participants still became significantly faster in their response to the start of a trial as they become more practiced in the sequences and task. As seen in Figure 23, participants consistently sped up as they practiced individual sequences [$F(2.08,118.35) = 31.84$, $p < .001$, $\eta^2 = .024$], even when they got faster over the course of the experiment [$F(1,57) = 57$, $p < .001$, $\eta^2 = .046$]. Results also indicated the rate participants sped up over as they learned an individual sequence differed between the first and

second half of the experiment [$F(3,171) = 4.06$, $p = .008$, $\eta^2 = .002$]. Though, once again, while the interaction term is statistically significant, the eta squared value implies the effect is negligible. Two separate Bonferroni corrected one-way rmANOVAs showed a retained significant decrease in RT over trials in both the first half [$F(2.33,133) = 25.1$, $p < .001$, $\eta^2 = .038$] and second half [$F(2.57,147) = 18.9$, $p < .001$, $\eta^2 = .018$] of the experiment. However, with notably different F and eta square values. These results are in line with the observations in Figure 23 showing a present, yet slightly less pronounced sequential decrease in RT over trials in the second half of the experiment. Where for ACC scores the interaction was driven by an absence of differences in Trial level scores between first and second half of the experiment, Figure 23 shows how for RT the interaction term is driven by different trial levels not being different within each of the experiment halves. Specifically, in the first half of the experiment participants started out with consistent RTs and then sped up over the final 12 trials of learning a new sequence (i.e., they became faster the more times they try to get a sequence right). On the other hand, in the second half of the experiment participants sped up in their first 12 tries of a new sequence but found a consistent response time in the later 12 trials. Twelve Bonferroni corrected pairwise comparisons were used to further explore the interaction. Showing how, as seen Figure 23, all levels differed significantly from each other [$p < .001$, see Table 7] except for the first 6 and the 2nd 6 trials (i.e., combined the first 12 trials) [Trials 1-6 vs Trials 7-12; $t(57) = 2$, $p = .305$] and 2nd 6 from 3rd 6 [Trials 7-12 vs Trials 13-18; $t(57) = 2.36$, $p = .130$; *note: this was a significant difference at p = .022 before correction*], in the first half of the experiment. As well as the final 3 sets in the second half of the experiment [Trials 7-12 vs Trials 13-18; $t(57) = 1.84$, $p = .427$; Trials 13-18 vs Trials 19-24; $t(57) = 1.40$, $p = .167$; Trials 7-12 vs Trials 19-24; $t(57) = 2.73$, $p = .051$; *note: the last effect was significantly different at p = .009 before correction*].

Table 7

P-values of Pairwise Post-Hoc tests for RT over Trials

	1st half experiment				**2nd half experiment**			
Trial Levels	**Trial 1 – 6**	**Trial 7 – 12**	**Trial 13 –18**	**Trial 19 – 24**	**Trial 1 – 6**	**Trial 7 – 12**	**Trial 13 –18**	**Trial 19 – 24**
Trial 1 – 6	**1**	**.305**	**< .001*** **	**< .001*** **	**1**	**< .001*** **	**< .001*** **	**< .001*** **
Trial 7 – 12		**1**	**.130**	**< .001*** **		**1**	**.427**	**.051**
Trial 13 –18			**1**	**< .001*** **			**1**	**.167**
Trial 19 – 24				**1**				**1**

Note. Differs significantly from each other, * at $p < 0.05$ (Bonferroni adjusted). See appendix A for associated t test statistics.

Table 8

RT in seconds Per Condition

	Median (IQR)					
	Trials 1-6	Trials 7-12	Trials 13-18	Trials 19-24	Total	Total min-max
1st half	0.340 (0.107)	0.343 (0.107)	0.322 (0.090)	0.299 (0.091)	0.331 (0.103)	0.144 – 0.735
2nd half	0.309 (0.110)	0.289 (0.108)	0.274 (0.114)	0.273 (0.098)	0.284 (0.105)	0.079 – 0.781
Total	0.319 (0.109)	0.317 (0.131)	0.296 (0.105)	0.285 (0.089)		
Total min-max	0.148 - 0.702	0.098 - 0.705	0.079 - 0.782	0.095 - 0.733		

Note. 1st half experiment is scores averaged over Blocks 1 to 5; 2nd half experiment is scores averaged over Blocks6 to 10. Values calculated over participant averages of each condition. E.g., Total for 1st half experiment was calculated over 58*4 values.

Figure 22

Mean RT for First Button, for Trials in the First and Second Half of the Experiment, Split over Musical Backaround.

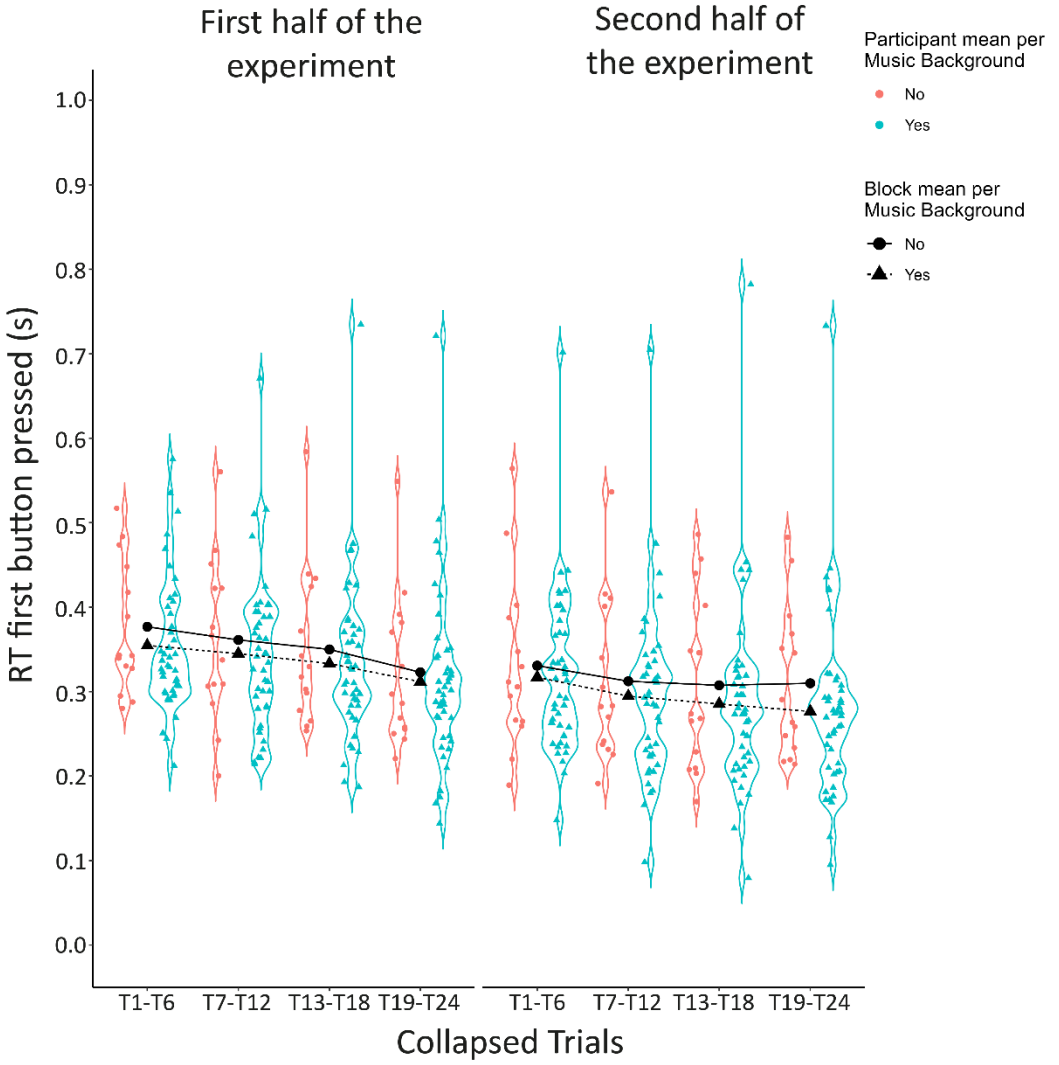

Note. Figure shows response time for the **first** button press only. Assessment of a mechanical element of design with the sole purpose to explore people their consistency in starting the tapping sequence. ***Not*** to be confused with the average RT across all presses, which pertains to learning the rhythm and is part of sequence performance measure.

As such training did not prevent RTs decreasing over the course of the experiment. When it comes to the magnitude of the decreased speed, however, it gets tricky. Table 4 and Table 8 show how median RT is around 0.3s, within our desired range (see 4.2.2.2 Procedure) for all conditions in both experiments. For the behavioral experiment the difference in median RT between first and second half of the experiment was 0.068s. Meaning in the behavioral experiment the average RT decreased by 68 ms. For the neuroimaging experiment this same difference came down to 0.047s. Similarly, the difference in median RTs over trials, when comparing the first set of 6 trials and last set of 6 trials, is 0.0.66s in the behavioral experiment and 0.034s for the neuroimaging experiment. These differences are in line with the RT rmANOVA results in both experiments, displaying once again how, regardless of training, participants sped up over the course of the experiment. Participants without training (i.e., those in the behavioral experiment of Chapter 3) did, however, on average speed up slightly more (0.068s-0.047s = 0.021s) over the course of the experiment compared to those with training. Or alternatively we could say after training participants were slightly more consistent in their responses, because difference in response times between the first and second half of experiment was on average 21 ms smaller for those with training (i.e., participants in Chapter 4). According to the Asymptotic Wilcoxon-Mann-Whitney Tests these differences of speeding up by 32 ms over trials [$Z=3.42$, $p < .001$] and 21 ms over the course of the whole experiment [$Z=2.16$, $p= 0.031$] were statistically significant. While statistically we can say training had a positive effect in the direction of our desired outcome. We can argue these differences are not of a magnitude relevant for our experiment. This is not surprising, considering the central tendency values in Table 4 and Table 8 are all around 300 ms. The differences in median RT over the course of both experiments imply training did not change much in terms of the magnitude by which participants sped up over the experiment.

A better indicator for any change in magnitude is when we compare both experiments in terms of their difference between the points where participants responded the slowest (the average of 1st 6 trials in the first half of the experiment) and where they responded the fastest (the average of last 6 trials in the second half of the experiment) (see also Figure 13 and Figure 23). Here we see a difference of, on average, 0.134s for the behavioral experiment (0.379-0.245) and 0.067s for the neuroimaging experiment (0.340-0.273). Meaning, on average, participants without training (in Chapter 3) sped up nearly twice as much between their slowest and fastest point, compared to participants who had training (in Chapter 4) [$Z=3.03$, $p = .002$].

Figure 23

Mean RT to Start of Trial per 6 Trials Split over First and Second Half of the Experiment

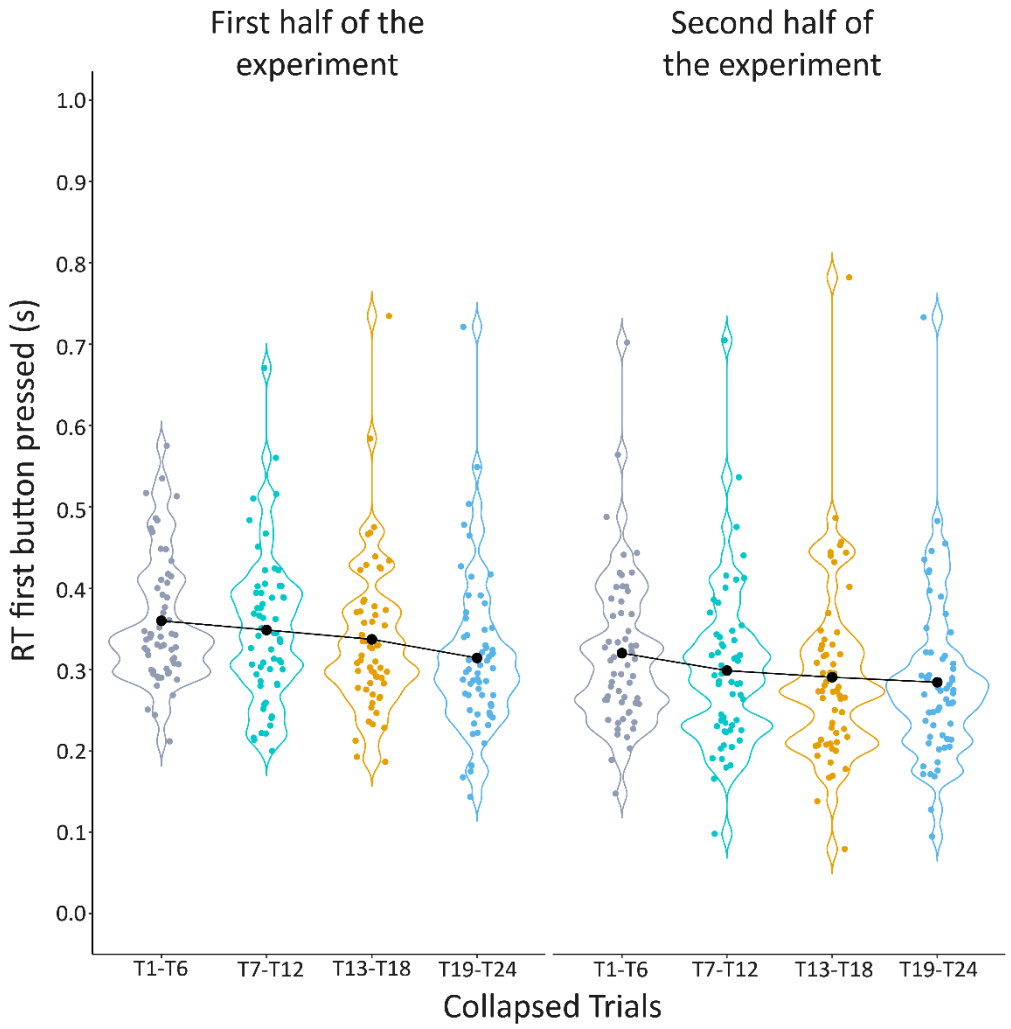

4.3.2 Neuroimaging result

For EEG, the trial rejection process removed 6.88% of all included trials (12000). For the EMG (CSE), an initial 20% of trials were removed because they started with middle or ring finger movements. A further 18% of trials were rejected due to TMS being absent or outside our window of interest relative to MOn. Of the remaining 7584 EMG trials we excluded all trials (16.32 %) with an SNR equal or lower than 1.1. This left us a total of 11175 EEG trials, and 5986 EMG trials to be submitted to further analysis. Specifically for EMG measures. Table 9 shows us the spread of TMS stimulation across the timeline leading up to MOn was successful. In that we hit our intended timepoints, as well as were successful in obtaining a natural spread across the timeline. Table 10 further indicates that even after trial removal, a relatively even spread of trials was retained to cover all timepoints of interest equally.

Table 9

Timepoint of stimulation (MEP) relative to MOn: intended time and average real time

	TMS -1,25s	TMS -1s	TMS -0,75s	TMS -0,5s	TMS -0,2	TMS -0,1s
Mean ± SD	-1.22s ± 0.16s	-0.98s ± 0.16s	-0.71s ± 0.16s	-0.48s ± 0.17s	-0.24s ± 0.16s	-0.24s ± 0.2s
Median	-1.20s	-0.97s	-0.70s	-0.47s	-0.21s	-0.16s

Note. the table shows the actual timepoint of applied TMS relative to MOn relative to the fixed 'assumed' and aimed for theoretical point. Measures of central tendency show our set out intent with the bonus of continues spread over the timeline was successful.

Table 10

Number of EMG trials remaining, per experiment condition, after trial removal.

	TMS -1,25s	TMS -1s	TMS -0,75s	TMS -0,5s	TMS -0,2	TMS -0,1s	total
EMG > 1,1SNR	1154	1013	1227	1036	917	639	5986
FDI	618	538	672	568	511	348	3255
ADM	536	475	555	468	406	291	2731

Note. Trials are presented per experimental condition to show we retain a relatively even spread of MEP values per theoretical time point (i.e., points relative to assumed MOn, based on time progression since start of fixation cross).

4.3.2.1 Individual neural markers

For ERD, two rmANOVAs (one for each frequency band) with Timepoints and Block showed the expected significant differences in power over time for both alpha [$F(2.22,108.76) = 16.32$, $p < .001$, $\eta^2 = .05$] and beta [$F(2.07,101.55) = 30.88$, $p < .001$, $\eta^2 = .09$]. However, only alpha showed an overall significant change (a more severe decrease) in power for the second half of the experiment compared to the first [$F(1,49) = 5.14$, $p = .028$, $\eta^2 = .018$]. Any observed difference for Beta showed not to be significant [$F(1,49) = 3.52$, $p = .067$, $\eta^2 = .01$]). With neither alpha [$F(3.2,156.94) = 0.27$, $p = .720$, $\eta^2 < .001$] or beta [$F(3.32,162.62) = 0.47$, $p = .828$, $\eta^2 < .001$] showing an interaction.

Similarly, the rmANOVAs with Timepoints and Trials showed once again a significant change in power over time for both alpha [$F(2.23,109.4) = 16.22$, $p < .001$, $\eta^2 = .043$] and beta [$F(2.55,110.49) = 31.25$, $p < .001$, $\eta^2 = .067$]. Yet, only for alpha [$F(3,147) = 4.19$, $p = .007$, $\eta^2 = .016$] were changes in decreased band power, related to learning over trials, considered statistically significant (beta [$F(3,147) = 1.92$, $p = .130$, $\eta^2 = .006$]). Neither alpha [$F(8.34,408.48) = 1.2$, $p = .290$, $\eta^2 = .004$] nor beta [$F(6.56,321.6) = 0.66$, $p = .700$, $\eta^2 = .003$] showed a significant interaction between the timepoints and stages of learning.

Taken together, both frequencies showed a notably linear decrease in power leading up to MOn. A trend persisting irrespective of any learning conditions or effects (linear contrasts, separate error

terms, alpha Trial [$t(49) = -5.4$, $p < .001$] and Block [$t(49) = -5.05$, $p < .001$]; Low beta Trial [$t(49) = -7.04$, $p < .001$] and Block [$t(49) = -6.84$, $p < .001$]). The power decrease was further found to be, on average, of a significantly larger magnitude in the second half of the experiment compared to the first, for all time points, though, only for alpha. Similarly, only alpha showed a significant decrease in power over the course of learning an individual sequence. Pairwise follow-up tests with a Bonferroni adjustment showed the individual sequence learning effect to be driven by the average differences between the first 12 trials and the latter 12 trials. Specifically, there was no significant difference in average power decrease among the first 12 trials [Trials 1-6 compared to Trials 7-12 $t(349) = 0.69$, $p = 1$] or latter 12 trials [Trials 13-18 compared to Trials 19-24 $t(349) = -1.29$, $p = 1$]. Whereas every other comparison was significantly different [$t(349) = 3.97$ to 5.6, and all $ps < .001$]. This means that we observed an increased event-related desynchronization as participants displayed improved motor skill. Both on the level of learning an individual sequence (Trial) and integrating the learned skill more generally (Block; learning over several sequences). However, the differences were found to only be statistically significant for alpha frequencies.

MRCP, too, showed the expected significant changes in amplitude over time for both the model with Block [$F(1.43,70.25) = 18.44$, $p < .001$, $\eta^2 = .029$] and Trials [$F(1.43,70.19) = 17.9$, $p < .001$, $\eta^2 = .019$]. Linear contrasts (with separate error terms) once again showed a linear trend leading up to MOn, over both Trials [$t(49) = -4.62$, $p < .001$] and Blocks [$t(49) = -4.69$, $p < .001$]. Meaning, amplitude decreased, on average, consistently and significantly in the time leading up to MOn. However, none of the observed amplitude changes related to improved motor performance showed to be of any statistically significance (Trials [$F(2.46,120.75) = 2.23$, $p = .1$, $\eta^2 = .02$] or Block [$F(1,49) = 0.002$, $p = .97$, $\eta^2 < .001$]). Nor was there a significant interaction between learning and the timepoints (Trials [$F(2.16,105.66) = 0.75$, $p = .480$, $\eta^2 = .001$] or Block [$F(1.37,67.03) = 0.57$, $p = .510$, $\eta^2 < .001$]).

Figure 24

Mean ERD % for Alpha and Beta frequencies per learning condition

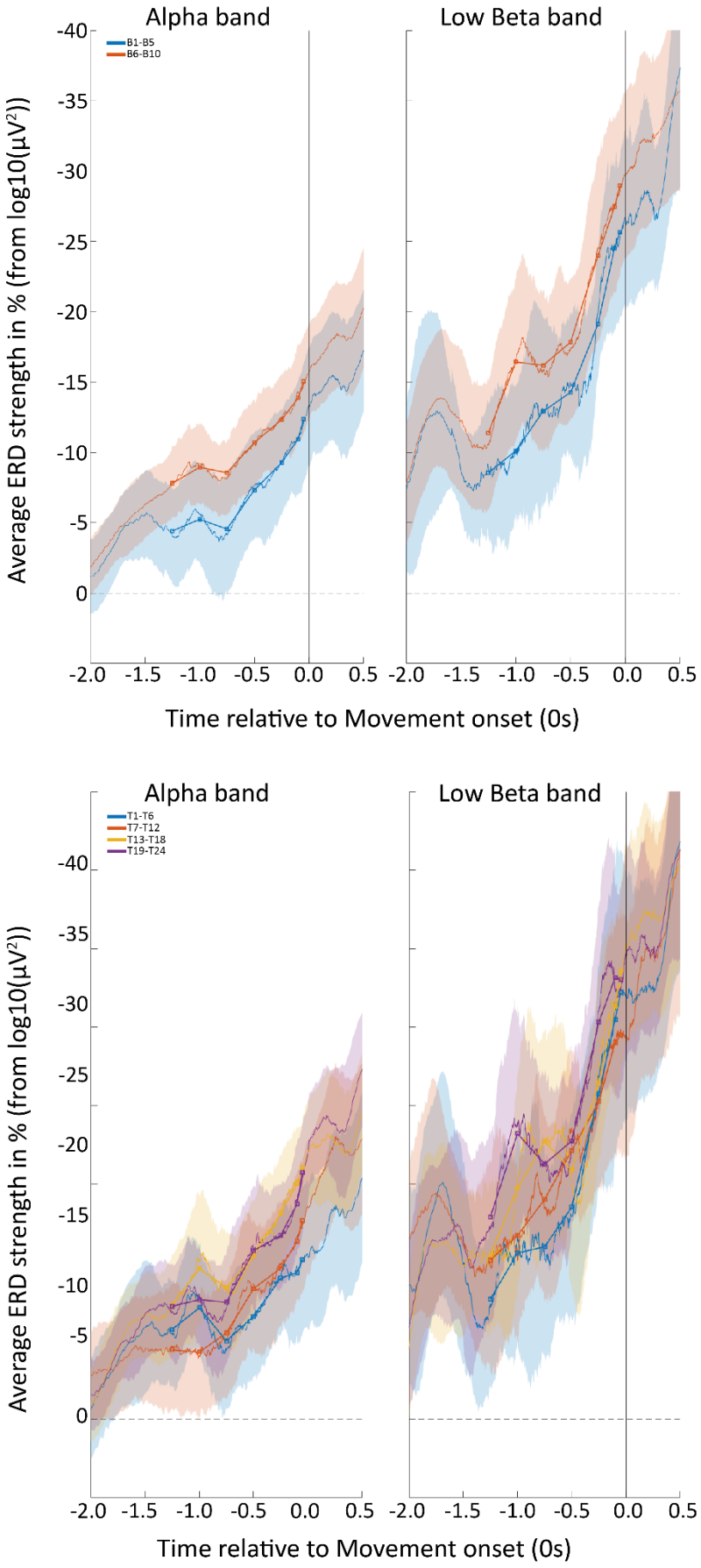

Figure 25

MRCP Amplitude per Learning Condition

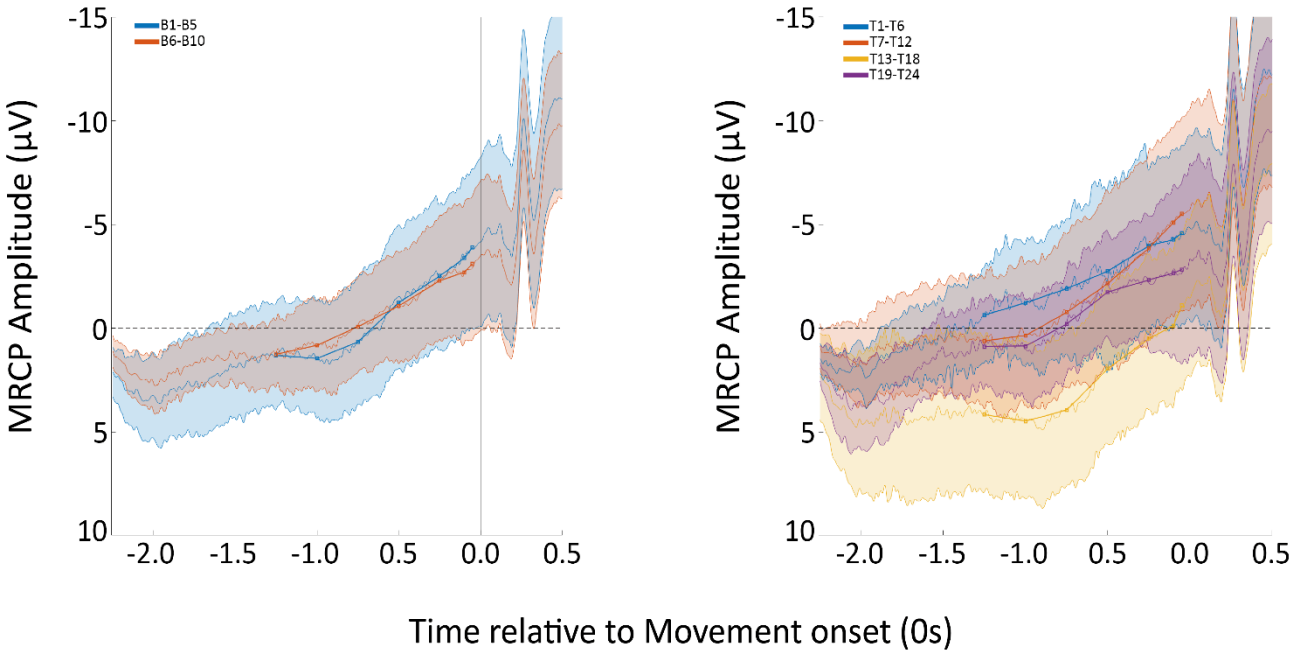

For CSE, we faced the challenge of missing values, as when presented with imbalanced responses, rmANOVAs drops participants from the test in their entirety. As such, the Timepoints variable was adjusted to have 6 levels instead of the original 7. In more detail, the lowest number of retained trials are those categorically closest to MOn (see Table 10). Meaning, for all participants, we were less likely to retain any MEP values for timepoints -0.1s and -0.05s. To have more participants contribute to the test output (i.e., not be dropped) we combined participant their values for the last two levels of Timepoint, resulting in 6 levels total, with the final one reflecting as *average amplitude around -0.075s*. As shown in Figure 26 this will not affect test output or interpretation given the constant increase over time for CSE in the final 3 timepoints. As indicated by the degrees of freedom in the tests that follow. While the combined level could not save all, the number of dropped participants went from 22 to 1 for Blocks and from 42 to 15 for Trials.

The two separate rmANOVAs for CSE, Timepoints having 6 levels, again showed significant changes in amplitude over time, in both the model with Block [$F(2.85,136.71) = 81.71$, $p < .001$, $\eta^2 = .468$] and Trials [$F(2.43,85) = 71.24$, $p < .001$, $\eta^2 = .388$], unaffected by any learning effects present (Trials [$F(8.78,307.44) = .47$, $p = .89$, $\eta^2 = .007$] or Block [$F(4.04,193.71) = 1.76$, $p = .140$, $\eta^2 = .010$]). With polynomial contrast follow up tests further showing the changes over time did follow the expected cubic trend (Block [$t(50) = 4.05$, $p < .001$]; Trial [$t(50) = 4.53$, $p < .001$]). Motor skill improvement had a significant effect on MEP amplitude when learning an individual sequence (Trials [$F(3,105) = 5.48$, $p =$

.002, η² = .017]). With no notable differences for the observed generalized learning; i.e., when comparing the average MEP amplitude in the first to the second half of the experiment (Block [$F(1,48) = 1.52$, $p = .220$, η² = .006]). Pairwise follow up tests with a Bonferroni adjustment showed the effect of learning a new tapping sequence on CSE, was driven by the average MEP amplitude in the first 6 trials to be significantly higher compared to all later trials [Trials 1-6 compared to Trials 7-12 $t(297) = 3.47$, $p < .001$; to Trials 13-18 $t(296) = 3.24$, $p = .001$ and to Trials 19-24 $t(299) = 4.85$, $p < .001$]. While Figure 26 shows a trend of steady decrease in amplitude as participants further improve in their sequential tapping, the changes are not big enough to be of notable statistical significance [Trials 7-12 compared to Trials 13-18 $t(294) = -0.7$, $p = 1$; Trials 7-12 compared to Trials 19-24 (298) = 1.19, $p = 1$ and Trials 13-18 to Trials 19-24 $t(296) = 1.88$, $p = .367$].

Figure 26

CSE Amplitude per Learning Condition

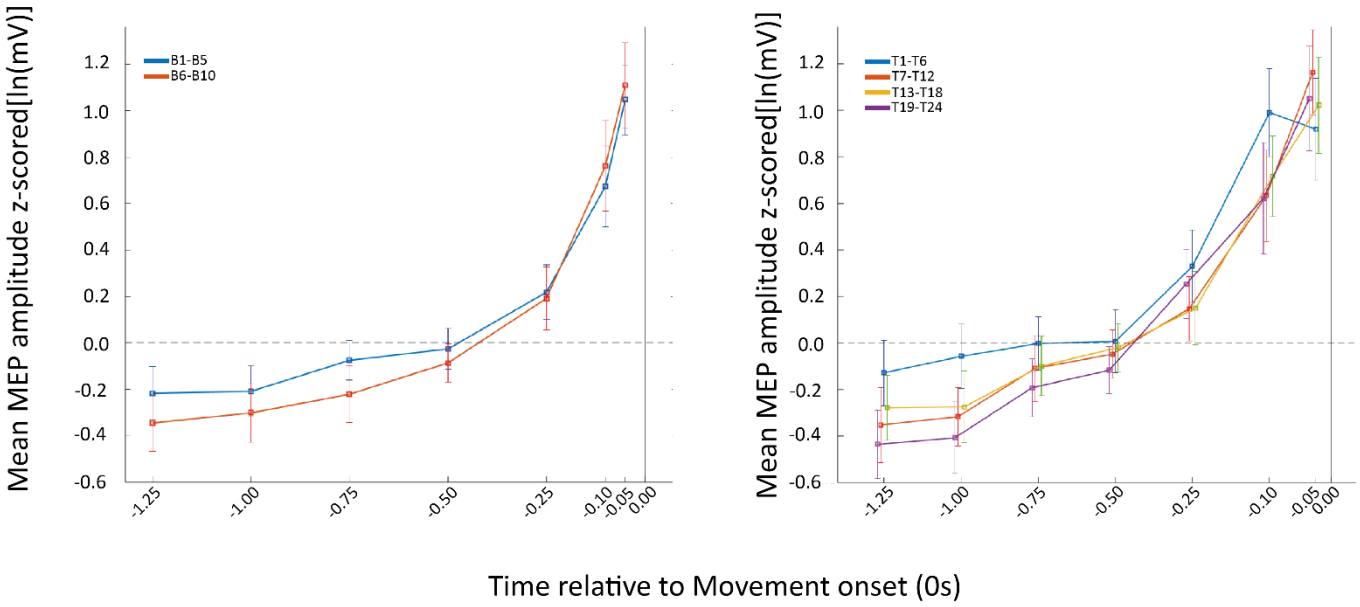

Note. Left shows changes in CSE as participants improved in general. Right shows changes in CSE as participants improved in their performance of a single sequence. Figure on the right was visually manipulated along the x-axis to increase visual differentiation amongst lines between -0.25s and 0. Figures show original 7 timepoints, for analysis timepoints between -0.1s and 0 were combined.

4.3.2.2 Predictive Modeling

Predictive modelling (PM) was used to assess the ERD's ability to predict MEP values (as a reflection of CSE) and to describe their relationship over the shared timeline in the 2 seconds leading up to MOn. More specifically, through PM we sought to test how consistent these predictions are when applied to a motor learning context, as would be the case with rehabilitation.

With a within-subject design, the datapoints are not independent from one another and cannot be handled as such. Ideally, model performance and the effects of learning would be assessed by training and testing on data from a single participant. However, as only learning over trials showed a consistently significant difference in neural activity (i.e., ERD alpha and CSE), further analysis required splitting the data over four learning stage (one stage per 6 trials). This means that, despite the current study retaining twice the number of EMG trials per participant, compared to Chapter 2, we still do not have enough remaining datapoints per participant per learning stage (median = 30, min - max = [21 - 40]) to execute a cross-fold validation model training and testing process on an individual participant basis. As such, rather than focusing on individual datapoints, we (as in 2.3.2 Predictive Modeling) performed cross validation across participants by treating their data as a single, non-split up, collection when allocating it into train and test sets. In other words, we used the data of one group of participants to predict the data of another group, specifically by using a leave-2 out cross-fold validation scheme. The test set size (2 participants) was chosen to optimize the ratio between training and testing set sizes while maintain a manageable number of combinations, which increases exponentially (i.e., 1081 unique combinations for p = 2 vs 16 215 unique combinations for p = 3). We then used the coefficient estimates from the training set to predict the Y (MEP values) for each X (ERD % at timepoint of MEP, relative to MOn) in the test dataset, consisting of the combined data of the 2 remaining participants. For each of the 1081 iterations, the same train and test dataset were used to produce a Mean Absolute Error (MAE) value for each of the four learning stages. Each iteration was then stored and analyzed as if it were a single participant with 4 dependent response values (MAE values). This approach ensured that, while participants were split as whole units, the within-subject structure of the data was still respected when comparing model performance across learning stages. For example, when assessing performance on trials 1–6 (first learning stage) versus trials 19–24 (fourth and final learning stage), the response values originated from the same two participants in the test set.

The test results, described in section 4.3.2.1 Individual neural markers, indicate that the overall shape of the neural measures remained consistent across learning conditions, with any learning effects manifesting solely as changes in the magnitude of the neural markers. Consequently, we expected no difference in error rates when predicting CSE based on ERD when the model was consistently updated to account for learning-induced amplitude changes. Since the model was adjusted to account for the significant variations in magnitude for either neural marker, and both training and test data originate from the same leaning stage, we anticipated that the error rates would remain stable—for instance, between the first six trials and the last six trials. A one-way rmANOVA across the different learning stages showed an unexpected significant difference between the MAE for the ‘within’ model, as shown in Figure 17, [$F(2.72,2932.49) = 291.46$, $p < .001$, $\eta^2 = .106$]. Follow up tests, in line with observations

from Figure 27, further showed that the error rate when predicting MEP values based on the relative progression of ERD strength was significantly lower in the early stages of learning compared to the later stages, where the error rate progressively increased [$t(1080) = -24$ to -11.5, all $ps < .001$], except between T16 and T1318 [$t(1080) = 1.21$, $p = 1$]. These results suggest that, despite updating the model to account for learning-induced changes in amplitude, predictions of CSE (in terms of MEP amplitude) end on average further from the true observed values as learning progressed. On the other hand, we did expect an increased error rate when the model was not adjusted to account for the learning induced amplitude changes. Specifically, when training had happened on data from the first learning stage, to then try to predict CSE values based on ERD levels from a later stage of learning. For example, predicting the CSE's MEP values in the last 6 trials when the model was trained on data from the first 6 trials. A one-way rmANOVA over the different learning stages showed, did show a significant difference between MAE resulting from model training and testing 'across' a level [$F(2.31,2491.58) = 12.84$, $p = < .001$, $\eta^2 = .005$], however as we can see in Figure 27 instead of predictions getting worse, the error rates are progressively going down. Follow up tests showed the error rate when predicting MEP values based on the relative progression of ERD strength was significantly higher in the early stages of learning compared to the later stages [$t(1080) = 1.24$ to 5.77, all $ps < .001$], except for T16-16 and T16-1318 [$t(1080) = 1.24$, $p = 1$], as well as T16-712 and T16-1318 [$t(1080) = -1.13$, $p = 1$]. These outcomes indicate that, despite the model being explicitly not updated to account for learning induced changes, predictions of CSE as MEP amplitude got (on average) better and closer to observed values.

Figure 27

Cross-Validated Model Comparison of Average Error Rates Across Learning Stages

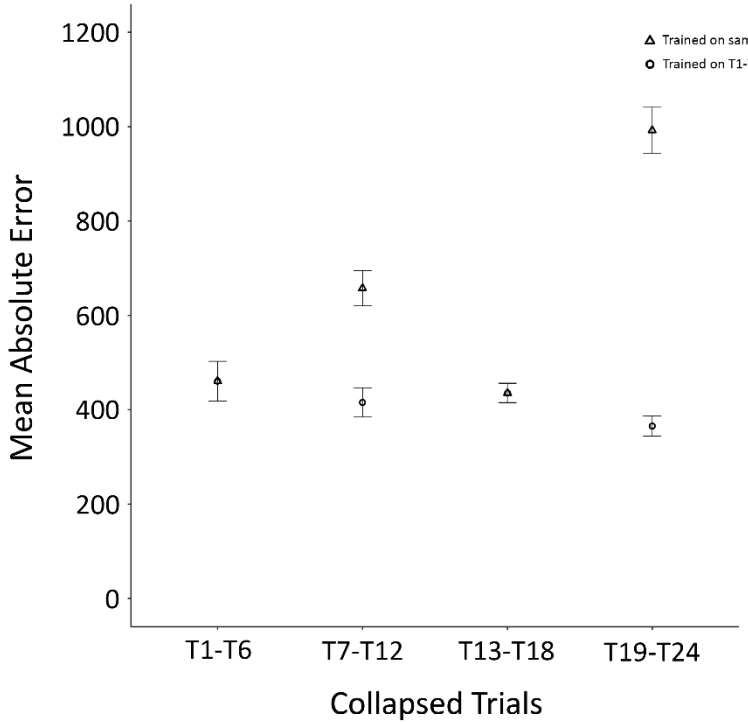

Note. The figure compares average error rates between a model updated at each learning stage to account for the learning induced changes in neural activity and resulting changes in variance ('within' model, triangles) and a static model trained only on the first six trials ('across' model, circles). In the across model, predictions for later trials were based on initial training without updates. The absence of separate markers for T1-T6 and T13-T18 indicates identical average performance between models in these stages.

4.4 Discussion

4.4.1 Behavioral findings

Results were once again in line with our expectations, and showed participants consistently improved at tapping out a specific sequence (i.e., learning over trials within a block) and became better at executing sequences in general (i.e., learning over blocks). Though this time (compared to the performance measures in the behavioral experiment) it seemed that the overall skill improvement affected the learning rate of the individual sequences. While participants became significantly better at tapping out sequences, there was no difference in the average maximum score obtained by the end of learning a sequence in the second half of the experiment compared to the first. This implies participants may have a ceiling effect of their maximum performance in the task (i.e., "the highest level they are able to perform to"). When they get better at performing the task overall, a new sequence will be performed better from the start. While they will still improve over several iterations of the same sequence, they will never go beyond their maximum performance score. Meaning, while participants still overall significantly improve over trials (learning an individual sequence) and the experiment in general (learning over blocks), the learning curve for an individual sequence becomes less steep as participants become better. If the task were another 5 or 10 blocks long, we might not see a further block effect either. However, we must note the effect sizes of the main effects compared to the interaction. While Block and Trial are small to medium effects, the interaction between them is so small we could argue it is negligible. Besides a ceiling effect being a new issue for the task, there are other reasons why we see the Block effect overshadowed by an interaction and, overall, less pronounced in the neuroimaging experiment than in the behavioral experiment. For example, this could be an unfortunate result of an accidental imbalance in the randomization of the sequence presentation and having more difficult sequences in later blocks. Having a bigger sample means a wider spread of participants, some participants are just low performers at the task. We can also not ignore how learning is potentially affected by the EEG+TMS set up. Maybe participants were more distracted or affected, or some unfortunate combinations of the points listed before resulted in some participants in this group performing worse. The interaction is statistically significant, yet we could argue and question the relevance and impact here. Taken together, the behavioral test results indicate we once again successfully improved participants their motor coordination using real-time feedback.

Having a background in some form of music training goes together with a higher perception of one's musical competence (even though participants still only perceive their skill as 'average'), compared to participants who have no music-based background. Our results showed such difference in perception did not carry over to the individuals self-perceived right-hand dexterity. Implying that having a musical background does not carry over to self-perceived higher hand coordination. These self-report scores

are in line with how learning rates were not affected by whether one had a musical background or not. Indicating that, while our motor task has a music-based element, musicians do not have an unfair advantage nor does it affect the tasks' ability to measure motor learning in the dominant right hand. The observation that those with musical training perceived their musical skill to be higher is not a surprising finding. Nor was it our objective for including these measures. The (improved from the behavioral experiment) musical competence and hand dexterity measures were included because our concern regarding musical training and performance in our task is twofold. One, an increased level of muscle skill due to the hand movements involved in playing the instrument and, two, if having higher musical competence leads to an advantage in our task because the task has a musical element (even though this is not our point of interest) (Pesek et al., 2020). The second part of our concern focuses on higher musical competence, which can exist without a person having ever received musical training. As such we wanted to make sure whether "participants with a musical background" is a valid differentiating factor. With our findings we can confidently move forward with the factor of 'having musical training or not' to further assess any confounding effects of musicality on our task performance and learning curves. We conclude that any differences in performance on the task between the groups is due to an advantage of musicality and not in muscle dexterity. Additionally, with no such difference in performance is found, our task is well made and suitable to allow us to conclude that learning effects are motor learning effects. Thus, musicians do not need to be excluded from the sample when using this task in a study.

Once again, we conclude that our theoretical assumption that our chosen sequences were of equivalent difficulty is not valid. Consistent with our observations in Chapter 3's behavioral experiment, sequence 3 is once again experienced as more difficult by participants than the other sequences. This time the difference is statistically much more pronounced than it was in the behavioral experiment. With an additional two other sequences (sequence 7 and 10) that came up as being experienced as more difficult. However**,** where sequence 7 appears to be perceived as more difficult to many, but not all other sequences**.** Sequences 3 and 10 appear to be equally difficult (no significant difference between them), and generally significantly more difficult than the other sequences; even more than sequence 7. All differences with sequence 4, on the other hand, seem to be driven by sequence 4 being easier than the other sequences. While this inequality in sequence difficulty is not ideal, it appeared to not have affected the tasks' ability to measure learning. Any issues more difficult sequences could have brought is most likely canceled out because of sequence randomization. Potentially, with better balanced stimuli (i.e., sequences) the task effects would be clearer. It is difficult to identify why some sequences were perceived as more difficult than others. This is unlikely to be due to the melodical aspects of the sequences, and has more to do with the kinematic aspect of the

associated fingers. Our reasoning first set forth in the discussion of Chapter 3 (that it is easier to move little finger to index than index to little finger) holds up for sequence 10 (see Appendix A2) . However, it is interesting to note that sequence 4, which holds similar patterns and finger involvement, is perceived to be easier. Sequence 7, however, consists entirely of movements following the consecutive order of our fingers. With a big part of sequence 7 made up of the 'easy' finger tap order (little finger to index). Potentially, what makes these sequences harder is the combination of these particular finger sequence orders and the finger being pressed down while keeping other fingers still. When you tap your fingers in order of little finger to index finger, the ease also comes from lifting all your fingers before bringing them down consecutively. Either way, the effort in balancing out the sequence randomization or their perceived difficulty might be beneficial for future use of the task. However, once again, despite the experienced differences in sequence difficulty. The task was not hindered in its' ability to allow training and observing of improvements in motor control over the course of practicing different sequences several times. As such, we have reason to believe that with more balanced stimuli the learning effects in this task may be more pronounced and cleaner.

We had two issues regarding RTs of the 1st button presses in the behavioral experiment. First, that participants sped up significantly over the course of the experiment. Second, the magnitude of the increased speed; how much participants sped up. Our results indicated that training did not prevent an increase in speed from occurring, but was successful in reducing the magnitude of this increase. When comparing the difference between both experiments their lowest and fastest points, participants in the neuroimaging experiment (who had the extra RT training during familiarization (stage 3)) sped up only half as much as participants of the behavioral experiment (who had no extra training). Some other interesting points in the context of RT training effects, but not enough to be meaningful on their own. First, looking at the fastest and slowest RTs among participant averages over the entire experiment. For the behavioral experiment we see -0.019s to 0.690s (a range of 709 ms) compared to the 0.079s to 0.781s (range of 702 ms) of the neuroimaging experiment. While the overall range across participants (meaning the difference between the slowest responder and fastest responder over the entire experiment) did not change. We do note a successful improvement in the response times for the neuroimaging experiment. Specifically, at no point did a participant (consistently) press their first button before (shows as a negative value for RTs) the first cue changed (i.e., go signal/start trial) or within the first 0.050s after the cue. A second point is that Table 8 has more consistent and smaller spread (IQR) of the RT among participants (between 90 and 110 ms) than in the behavioral experiment (see Table 4), where the IQR was between 120 and 195 ms. Though this may very well be due to difference in sample size between Chapter 3 and 4. We conclude that, while the 3rd familiarization stage did not prevent decrease in RT over experiment, it did seem to have aided

in making participant's response patterns more consistent and preventing too many early responses. An important caveat when talking about differences in RT between the two experiments (i.e., Chapter 3 and 4) is that it is tempting to attribute all observed differences to the addition of the 3rd familiarization stage (i.e., training of RT for 1st button press of the trial) as it is the only change made to the experimental paradigm. However, data was collected under very different circumstances. With the inclusion of EEG and TMS we changed the bodily experience of participants during the experiment. Participants in the behavior experiment did not have the sensory aspects of electrodes attached to their head or skin or the requirement to sit straight and still or a TMS device against their head. TMS is further known to affect RT in RT tasks (Ibáñez et al., 2020). While with training and the fixation cross count down we tried to emulate a predictive timing task (which was reported to be much more robust to this issue of TMS affecting RT; (Ibáñez et al., 2020) as much as possible (i.e., participants learn to internalize timing of the start of the trial). Ultimately, participants are still waiting for an external cue to indicate their first button press and thus could be affected by the TMS stimulation time points, especially those towards the end of the fixation cross or those during the 200ms delay at the start of the trial. Thus, any differences we observed, could be due to the extra training or the entire set up, or a combination of both.

4.4.2 Neuroimaging findings

While the specific mechanisms of neuroplasticity continue to be debated, it is well-established that learning is accompanied by the reorganization of synaptic connections**.** This study aimed to investigate how motor learning affects our three neural markers of motor control—ERD, MRCP, and CSE—specifically as motor function improves. A primary objective was to assess whether the relationships between these markers remain stable over time or require continuous recalibration, particularly in the context of predicting CSE for BCI applications.

4.4.2.1 Individual Neural Markers

Our results indicated that CSE continued to follow a cubic trajectory, remaining consistent and unaffected by learning. Overall were no substantial learning-related effects observed for CSE, except during the early stages of skill acquisition—specifically, in the first few trials when participants were initially learning to tap out a sequence. After this initial phase, CSE amplitude decreased significantly but then remained stable throughout the experiment.

The literature presents conflicting findings regarding how CSE is expected to change with learning. Our results do not align with the general assumption that CSE increases because of skill acquisition—at least not during the active learning phase. It is possible that an increase in MEP amplitude would have been observed had we analyzed block-by-block changes instead of collapsing across blocks. However,

the trend in Figure 26 suggests that if any change occurred over the course of the experiment, MEP amplitudes may have actually declined rather than increased.

Our findings do support the idea that increased CSE activity represents an optimal state for neural plasticity, particularly in facilitating the integration of feedback and feedforward commands. The observed increase in CSE was limited to the initial learning stage, where behavioral learning was steepest. Further research is needed to investigate this by comparing preparatory CSE activity during learning to a true resting baseline, where participants are not yet cognitively engaged in movement preparation.

Theoretical interpretations of our findings align with the broader view that reductions in neural activity over time reflect stronger synaptic connections and more efficient resource utilization. This suggests that rather than a sustained increase, CSE activity may be more dynamically linked to the demands of early motor learning before stabilizing as performance becomes more automatic.

Different from Chapter 2, MRCP did significantly decreased over time leading up to movement onset. However, its relationship with learning was ambiguous, showing both expected and unexpected patterns. At the block level, Figure 25 clearly demonstrates a nearly identical trend across blocks, which aligns with previous findings in sequential tapping tasks—where MRCP amplitude initially increases but later decreases once no further improvement occurs (Wright et al., 2011). At the trial level, although no significant learning effect was observed, the effect size was notably higher than that of alpha-band power, suggesting the possibility of high variance obscuring a true effect. Another notable observation is that while MRCP amplitude was slightly higher than in Chapter 2 (-5 µV compared to -2 µV), it remained relatively low. Previously, we suspected that the central reference used in Chapter 2 may have weakened the RP, but in the current study, we explicitly used mastoid references. One possible explanation is that our ICA procedure, which computed components from 1 Hz-filtered data but subtracted components from 0.1 Hz-filtered data, may not have been as effective in retaining low-frequency activity—potentially filtering out the slow amplitude decrease characteristic of the RP. Additionally, the classical MRCP shape was not observed, which could be attributed to the partially cued, partially self-initiated nature of the task. This aligns with our expectations, as such task structures often result in an MRCP that more closely resembles a contingent negative variation (CNV). However, despite this, we would still have expected a stronger decrease in amplitude. This raises the possibility that the absence of a significant learning effect in MRCP may not be due to the learning process itself but rather a limitation in our ability to reliably measure MRCP—potentially filtering out key components of the signal. Ultimately, the weak MRCP signal limits our ability to draw strong conclusions about its role in learning. Future studies aiming to examine MRCP alongside other neural markers—especially when combined with TMS—may require alternative preprocessing strategies to

ensure that necessary artifact removal for one measure does not compromise the integrity of another. Specifically, MRCP analysis may benefit from manual epoch rejection rather than full reliance on automated ICA-based cleaning procedures, as most MRCP studies do not even remove blinks.

ERD magnitude changed in accordance with motor learning, as participants significantly improved in sequential tapping—both within a single sequence and across sequences—though this effect was only significant for alpha-band ERD. The absence of a significant effect for beta-band ERD is likely due to high variance, as block-level effect sizes (η^2) were not substantially different between the two frequency bands. Overall, our findings align with the literature suggesting that ERD strength increases (i.e., relative power decreases) as movement execution improves. However, we once again observed an inverse pattern of ERD magnitude between alpha and beta, with beta showing greater magnitude than alpha—contrary to expectations. Despite this, both frequency bands exhibited lower ERD magnitudes than those observed in Chapter 2 and the broader literature (if we set aside the usual trend of higher magnitude in alpha). This discrepancy is likely due to the nature of our task, as we are comparing ERDs from a complex learning task to those elicited by simple or highly trained movements. While ERD in our task changed as a function of learning, performance improvement plateaued in later trials, both within a single sequence and towards the end of the experiment (Figures 12 and 20). When comparing ERD during skill acquisition to highly trained movements, it is important to consider the different learning timescales. What we observed here reflects fast learning within a single session, whereas the stronger ERD typically reported in the literature is often associated with slow learning over multiple sessions (including consolidation effects, such as those observed with sleep) (Dayan & Cohen, 2011; Hashemirad et al., 2016). Therefore, while ERD increased steadily with learning, it likely had not yet reached its full magnitude, as participants had only one session of practice. As discussed in 1.2 Motor Learning, when interpreting learning-related changes, we must avoid reasoning in absolutes—such as defining a fixed neural activity level for a "highly learned skill" versus a "just-started" movement. Most neural correlate studies covered in 1.1 Neural Activity of Motor Control likely reflect the average neural activity of well-practiced, highly automated movements, particularly simple tasks performed with the dominant right hand. These movements, repeated in various contexts over a lifetime, represent a kind of “final level” of learning. Our findings emphasize that motor learning is a continuum, where ERD strength may continue to increase with further training beyond a single session.

4.4.2.2 Inter-Dynamics of the Neural Markers

When we first discussed the importance of accounting for learning when using EEG measures to estimate CSE (1.4.2 Accounting for the Changing Neural Landscape during BCI), we posed several key questions: How does CSE evolve over time relative to ERD? Do ERD and CSE develop in parallel, or does

one adapt more rapidly than the other? If ERD shifts at a different pace than CSE, does this create a moving target for feedback timing, requiring continuous adaptation in BCI protocols? These questions remain central to understanding whether static assumptions about neural markers are sufficient or if learning-induced changes necessitate ongoing recalibration. The following discussion evaluates our findings in light of these questions, considering their implications for modeling CSE dynamics and optimizing BCI-driven rehabilitation strategies.

Statistical results indicated that learning primarily affected the magnitude of neural markers, while their overall temporal patterns remained consistent across learning stages. Given this, we expected no significant difference in error rates when the model was both trained and tested on data from the same learning stage—i.e., the updated 'within' model, which simulates a BCI system continuously adapting to neural marker changes during learning. If the relationship between ERD and CSE changed over time, updating the model should have accounted for these changes, maintaining prediction accuracy. Conversely, we expected a higher, and progressively increasing error rate when predicting CSE in a later learning stage using a model trained on early-stage data—the 'across' model—since it was not adjusted for learning-induced amplitude changes. However, this was not what we found. Instead, error rates progressively and significantly increased when the model was updated, while they decreased when the model remained static. Notably, the first and third learning stages (T1-6 and T13-18) showed no difference between models, while the changes in T7-12 and T19-24 drove the observed trend.

This outcome suggests that keeping the model fixed after early learning stages yields predictions that remain closer to the actual CSE point of interest. The underlying reason for this remains unclear, but one possibility lies in the relationship between behavioral learning patterns and CSE dynamics. As our results showed, CSE changes were mostly confined to the early trials, which corresponds to the steepest behavioral learning curve, and thus where performance variance is highest. Could early-stage variance in CSE be the best predictor of late-stage CSE changes? Or do patterns in early data better describe late-stage data than continuously updated models? Additionally, ERD exhibited more pronounced changes at later learning stages, whereas CSE remained more stable in amplitude. It is possible that these ERD shifts introduced greater variance that the updated model failed to account for, leading to higher error rates.

We are careful and reluctant to speculate on the true reason, meaning or factors driving the observed changes in predictive accuracy—both in relation to whether the model was updated or not and to the specific learning stages where changes occurred. While our validation methodology was theoretically sound, the high variance in our data, as indicated by elevated Mean Absolute Error (MAE) values, poses a challenge in interpreting these results with certainty. we note a clear improvement over Chapter 2,

likely driven by the absence of the delayed prediction effect, which substantially reduced MAE values (from ~10,000 to ~1,000). However, because our analysis was conducted across participants, inter-individual variability likely contributed significantly to the high overall error rates. A more effective approach would have been to train and test models on individual participant data, aligning better with how such models would be implemented in practice. Even if the overall error trends remained the same, participant-specific training would have likely yielded more stable error rates, making any interpretations more meaningful.

In hindsight, our estimation that within-participant cross-validation was infeasible due to insufficient data may have been overly conservative. Even for the smallest number of retained trials in a single learning stage (e.g., trials 1–6), each participant had at least 21 trials (see 4.3.2.2 Predictive Modeling). Using a leave-two-out cross-validation approach (training on 19, testing on 2) would have yielded a minimum of 210 iterations per training level per participant, which may have provided a more robust assessment.

Our findings challenge the initial proposal by Daly et al. (2018), which suggested using a fixed ERD percentage (e.g., 30%) to determine the timing of stimulation or feedback relative to MOn and the corresponding CSE level at that timepoint. Our results clearly show that learning affects the magnitude of neural markers, with ERD% changing as motor skill improves. This means that using a fixed ERD threshold to infer CSE timing would not ensure consistent responses, particularly as a person progresses in skill acquisition. Our predictive modelling further highlights this inconsistency issue. Even when models were updated with learning-induced changes in neural data (e.g., training on T7-12 data and predicting T7-12 data), fixed ERD thresholds did not reliably indicate CSE states. Interestingly, prediction accuracy improved when we ignored neural marker changes entirely (i.e., using T1-6 trained data to predict T7-12 or T13-18 data). However, this does not indicate a stable or reliable relationship but rather demonstrates that learning itself affects predictive modelling accuracy—making it difficult to ensure that the intended theoretical timing for stimulation or feedback is actually achieved. Another key consideration is the significance of CSE amplitude changes. It remains an open question what “optimal excitability” truly means in practical terms. Since the S-like trajectory of CSE over time was preserved despite learning effects, one could argue that absolute CSE amplitude may not be the most critical factor. If Daly et al.'s suggestion is based on targeting "peak CSE," the challenge shifts from relying on fixed ERD values to developing a method for reliably estimating the timing of this peak CSE state. This is particularly relevant in post-stroke motor rehabilitation, where the goal would be to predict and align with intended movement initiation during motor imagery-based training.

Ultimately, a cubic model does not do a good job to describe the relation between CSE and ERD, as indicated by our high error rates. While our methodology was conceptually valid, it may not have been

the most effective for deeper analysis. Our model struggled with the high variance in training data, most likely due to inter-individual differences. Although CSE values were standardized, ERD was not, meaning that while trends remained consistent, the actual percentage values varied considerably across participants. Future research should aim to retain enough trials to enable a participant-specific analysis, minimizing variance-related challenges.

Regarding the question of whether ERD and CSE are truly linked, our findings suggest that while there is some relationship, their dynamics appear to be largely independent, particularly in how they are influenced by learning. We observed that CSE shifts began roughly at the same time as ERD (~1.25s–1s before MOn), which is earlier than the previously assumed final 100 ms window. This temporal overlap suggests a shared preparatory process, but beyond this, their responses to learning diverged. Specifically, ERD was primarily affected by overall motor improvement, showing significant differences between early and late learning stages—both within a single sequence (first 12 vs. last 12 trials) and across the experiment (first half vs. second half). In contrast, CSE changes were largely confined to the earliest learning stage, with no significant difference between the start and end of the experiment. If more data were available, it would have been valuable to compare the average CSE response from the very first sequence to the last sequence, as averaging across the entire first half of the experiment may have obscured any progressive learning effects. These findings raise further questions about whether CSE adjustments are limited to early learning efforts, while ERD continues to evolve over extended practice.

Despite these limitations, our findings clearly demonstrate that learning affects the relationship between CSE and ERD, as evidenced by the differences in how the two models performed. However, this relationship appears inconsistent and unstable, and due to the high error rates, any further interpretation remains unreliable. While our results confirm that learning introduces changes, the precise nature of these changes cannot be meaningfully assessed given the variability in our data. Future research is needed to further investigate the instability in the CSE-ERD relationship, addressing the factors contributing to these inconsistencies with refined methodologies that allow for a more stable and individualized analysis.

4.4.2.3 Bridging Research and Application in BCI: General Reflection on Findings and Methods

One of the most striking inconsistencies in our results was the absence of pre-movement inhibition despite an otherwise cubic-like trend in CSE (Figure 26). While our data followed the expected S-like pattern—with an initial increase in excitability followed by a plateau—the anticipated decrease in amplitude before MOn did not occur. Instead, CSE continued to increase.

A possible explanation is that the temporal dynamics of CSE were affected by movement complexity. Unlike most studies that focus on simple single-button presses, our experiment involved multi-element sequences. While Hund-Georgiadis & Von Cramon (1999) suggested that movement complexity might engage different brain regions based on fMRI findings, it remains unclear whether this would translate to CSE differences, particularly in EEG-based studies where signal spread complicates localization. Furthermore, while Leung et al. reported that learning affects CSE amplitude, to our knowledge, no study has investigated whether movement complexity influences the pre-movement inhibition dip. If complexity does affect inhibition, this would imply that higher-order movement preparation can modulate excitability dynamics even at the level of basic movement initiation. Another possibility is that inhibition becomes more apparent only for highly trained actions, which would align with theories suggesting that pre-movement inhibition facilitates efficient motor execution for well-learned skills (Duque et al., 2017). However, this interpretation is inconsistent with theories proposing that CSE suppression plays a fundamental role in movement initiation, regardless of expertise level. It is also possible that methodological choices affected the detection of inhibition. Our data processing followed standard log transformation and within-subject z-scoring of MEP amplitudes, as recommended in Ibáñez et al. (2020) and Klein-Flügge & Bestmann (2012). However, pre-movement inhibition is often analyzed by comparing MEP amplitude changes relative to a baseline hand-at-rest condition (Duque et al., 2017). Since we did not use a resting baseline, this could have influenced the detectability of the suppression phase. Most studies using baselines rely on inter-trial intervals, which require strict guarantees that the participant's hand is truly at rest. Our data indicated that even during the fixation cross period, small pre-trial movements were common, making it difficult to ensure a true resting-state comparison.

Beyond methodological choices, inconsistencies in electrode placement for EMG recordings may have contributed to variability in MEP amplitude. We used the IFCN-recommended belly–tendon bipolar montage, but Garcia et al. (2017) argue that these standard electrode placements may not be optimal for assessing corticospinal excitability. However, since this montage remains the most widely used, we followed this standard to maintain comparability with previous research. Future work should consider testing alternative EMG electrode positions to assess whether findings remain consistent.

Additionally, gender differences may have introduced variability in MEP amplitudes, as over 50% of our sample consisted of female participants. Rivas-Grajales et al. (2023) reported that CSE and MEP amplitudes can be influenced by hormonal fluctuations, suggesting that future studies should control for menstrual cycle phase or, at minimum, ensure participants are in comparable hormonal states. Alternatively, limiting the sample to male participants could reduce this source of variability.

Another limitation concerns the accuracy of our movement onset estimation. To ensure consistency, we defined MOn as button press –90 ms, approximating the moment of muscle contraction. While this approach aligns with previous automated methods (Demandt et al., 2012; Klein-Flügge & Bestmann, 2012), it is less precise than manual visual detection (Ibáñez et al., 2020; Jankelowitz & Colebatch, 2002), which remains the gold standard. Although manual detection is time-consuming, it allows for trial-by-trial exclusion of early movements, which we were unable to do in this study. Future research should consider adopting a hybrid approach, such as using EMG power profiles to refine movement burst detection relative to resting-state power levels.

4.4.3 Future Considerations for BCI and Learning Research

To improve CSE and ERD estimation for BCI applications, future studies should:

1. Develop a more precise approach to predicting self-paced movement onset, ensuring consistent timing for TMS stimulation while maintaining an experimental design that balances predictive (PT) and reaction-based (RT) tasks.
2. Investigate CSE suppression with more robust baseline measures, comparing movement-related CSE changes to inter-trial resting states.
3. Improve EMG electrode placement and standardization to minimize variability in recorded MEP amplitudes.
4. Account for potential gender-based differences in CSE and MEP responses, either through hormonal cycle tracking or a more homogeneous participant sample.
5. Refine movement onset detection methods using EMG power profiling to better estimate the true moment of movement initiation.

By addressing these issues, future work can improve the stability, reliability, and interpretability of CSE and ERD measures, ultimately enhancing their applicability in motor learning research and BCI-driven rehabilitation strategies.

For our purposes of practical application—understanding how neural markers behave in a BCI rehabilitation setting—prioritizing within-session learning was the most relevant approach. However, it remains an open question how these effects evolve across multiple sessions. In a rehabilitation setting, learning within a single session is likely to be much slower than what we observed in healthy individuals, even with our best efforts to implement a challenging task. Moreover, rehabilitation typically extends over multiple sessions, meaning that both within- and across-session learning effects must be considered. Once these effects are well established in healthy participants, the next step

would be to examine how they translate to patient populations with slower learning rates. This is particularly relevant for understanding the relationship between CSE and ERD. Our results showed that ERD exhibited learning effects only after substantial practice, with improvements emerging after 12 trials for a single sequence and when comparing the first and second halves of the experiment. In contrast, CSE followed the opposite pattern, showing no general learning-related changes and, when considering sequence-specific learning, any observed effects were largely confined to the first six trials—where we also saw the steepest behavioral improvements (as noted in Chapter 3 before collapsing trials). These findings raise important questions about whether CSE remains stable across multiple sessions or if long-term changes emerge over extended learning periods. Christiansen et al. (2018) have previously discussed CSE adaptations both within and across sessions, but it remains unclear whether these dynamics would hold in the context of rehabilitation training. Relatedly, if patients learn at a slower rate and CSE is primarily involved in the initial stages of skill acquisition, would a patient population exhibit greater within-session fluctuations in CSE magnitude than we observed in healthy individuals? If so, what would this mean for the stability and reliability of the CSE-ERD relationship in a rehabilitation setting? These questions highlight the need for future research to investigate long-term changes in CSE and ERD and their implications for adaptive BCI protocols.

Chapter 5: Discussion

In this thesis, we investigated the neural activity associated with movement preparation and assessed how three of its neural correlates changed with motor skill improvement. We aimed to further our understanding of these neural markers to optimize rehabilitation aided by BCI. We built on the claim that CSE is a promising neural marker for determining optimal feedback timing and maximizing neuroplasticity (Daly et al., 2018). First, we aimed to improve understanding of the temporal evolution of CSE. Second, we further investigated the proposed link between CSE and ERD, offering deeper insight into their functional connectivity. This not only provides a foundation for future studies to expand on, but also highlights potential avenues to explore for practical applications of the CSE-ERD link in a BCI context. Lastly, we explored the changes of these neural markers' characteristics due to learning. In this chapter, we will place our findings into the context of the literature, discuss the limitations of our experiments, and propose future research based on our findings.

5.1 Developing a task to measure motor learning

For our studies, we chose a sequential tapping task, where participants learned several tapping sequences with each a differently ordered series of finger movements. Each finger movement would result in auditory feedback (i.e., a note), with a correct tapped sequence playing out a melody. As such our task mimicked the process of learning to play the piano. This task draws inspiration from previous research (Furuya et al., 2011; Hund-Georgiadis & Von Cramon, 1999), reworking the classical sequential tapping task by implementing auditory feedback to emulate explicit learning. The task was proven successful, as per our results reported in Chapter 3 and 4, we observed significant improvements in the task performance of the participants. Additionally, we presented a case for practice trials to reduce the number of times participants rushing their button presses (see methodological change of the inclusion of a third familiarization phase from Chapter 3 to 4). We found no significant difference between people with and without musical background. While those with musical background started with non-significantly higher accuracy scores, this did not prevent the learning effect from taking place. In conclusion, the experimental design presented in this thesis was adequate for the task based on the behavioral results. Participants learned a new set of movements, thus allowing us to investigate the neural correlates not only in relation to each other, but also in relation to learning new movements.

5.2 Decoding the CSE Timeline: Evidence for a Nonlinear Trajectory

As discussed in Chapter 1, CSE is a widely investigated neural correlate of motor control that represents the activity of the corticospinal pathway. CSE before MOn is suggested to represent preparatory neural activity involved in both the processing of sensory feedback and forwarding motor commands, thus

presenting itself as the optimal indicator to time sensory feedback to improve motor rehabilitation. Consequently, it is important to understand the full scope of the temporal dynamics of CSE, spanning a timeline broader than has been previously studied (van Wijk et al., 2012).

Our results indicate the temporal evolution of CSE, as measured by MEP amplitude in the 2 seconds leading up to MOn, is shaped as an S-like wave (3rd degree polynomial). Where an initial increase in amplitude is followed by a decline after which it once again changes direction to strongly move upward. This shape was identified in both Chapter 2 and 4. In the latter, we also showed that the 3rd degree polynomial shape is not affected by learning, implying that the s-like trajectory is a stable presentation of CSE activity. As per the findings of Chapter 4, CSE amplitudes decreased significantly following the early stages of learning and then remained consistent, keeping the S-like wave shape. Notably, while an exponential model was similarly able to explain a significant proportion of the data, albeit statistically significantly less than the 3rd degree polynomial model, conclusions from these results should be drawn within the analysis context. The tail-end (closest to MOn) of our 3rd degree polynomial model resembles an exponential function. This, together with the fact that in Chapter 2 over 80% of our retained data points fell into the last 500 ms leading to MOn, can unbalance the comparison in favor of the exponential function. In Chapter 4 we found further support that the CSE dynamics follow a cubic trajectory, showing that it is essential to consider the complete temporal evolution of CSE from early onset until MOn.

At this point, it is important to reiterate why we propose to investigate CSE tendencies from 2s before MOn, instead of just during the last 500 ms leading up to movement, as most CSE research focusing on the pre-movement inhibition (Chen et al., 1998; Ibáñez et al., 2020; Leocani et al., 2000, 2001; van Wijk et al., 2012). Early studies (Chen et al., 1998; Leocani et al., 2000, 2001) suggested that early onset ERD (~2 seconds pre-MOn) and MRCP were unlikely to be associated with CSE. However, they are all involved in the same motor system, with CSE's fellow neural markers (i.e. ERD and MRCP) of pre-movement activity starting as early as 2 seconds prior to MOn. As such we questioned why would we not observe meaningful fluctuations in early onset CSE? Those studies that say 'unlikely' are more than 20 years old, and later publications such as van Wijk et al. (2012) who make the same claim, also refer to those early studies. Even following our findings in Chapter 2 and 4 in support of the cubic trajectory, the exact shape of CSE is a debatable concept as in our study reported in Chapter 4, we did not find the period of inhibition, which has been widely reported as the most robust characteristics of CSE. Consequently, we also failed to find the supposed preparatory peak for CSE in Chapter 4, which was indicated by Daly et al. (2018). Our experimental design is unlikely to have caused the lack of finding, because it was recently shown that this CSE inhibition is preserved over RT, SP and PT. Our experiment

is a cross between RT and PT. Thus, we should reconsider calling this CSE inhibition a robust characteristic, or we should keep open the possibility that it is influenced by yet unknown factors.

In summary, we suggest that CSE should be investigated as a long neural marker, starting from ~2s before MOn, instead of just focusing on the last 500 ms leading up to movement. The shape of CSE is non-linear, it resembles an S-like wave that should be described by a 3rd degree polynomial function. While our tests leave room for the idea that an exponential model is also sufficient, it is important to consider that it is only the tail-end of CSE that shows an exponential trend. When we investigate a wider time window, the non-linear trajectory of CSE becomes evident.

5.3 Learning effect on individual neural markers

Throughout this thesis, we have been arguing for a better understanding of the temporal evolution of pre-movement neural markers as well as for the investigation on how these neural correlates change during motor learning. As we know, learning on the neural level includes the reorganization of synaptic connections and neural circuits. Understanding both trends, the temporal tendencies of neural correlates and how these tendencies are affected by learning, are vital for improving the current motor rehabilitation methods. In Chapter 4, we investigated the effects of learning on three neural markers of motor control (ERD, MRCP, and CSE).

In the previous section, we discussed the non-linear trajectory of CSE and we touched upon how learning affected CSE amplitudes. There was no overall effect of learning on the CSE's temporal evolution. The CSE amplitudes on the other hand were affected by learning. Specifically, during the first few trials when participants learned to tap a new sequence. After this early stage, CSE amplitude significantly decreased. This finding seemingly contradicts the belief that CSE increases due to skill acquisition (Kleim, 2009; Leung et al., 2017; McGregor et al., 2017). Rather, we assume that this early stage learning effect of CSE means that CSE activity may be more dynamically linked to early-stage learning. Suggesting that increased CSE activity represents an optimal state for neural plasticity (Daly et al., 2018; Gandolla et al., 2021; Ibáñez et al., 2020), a readiness to integrate feedback and feed forward signals. However, involvement may be limited to the most active and early stages of learning process.

We also investigated if learning affected alpha and beta ERDs. As discussed in Chapter 1, ERDs, in the frequency domain of 8-20 Hz (alpha and low beta band powers) are motor event induced potential shifts representing movement and movement preparation and intention (Daly et al., 2018; Fairhall et al., 2006).

One interesting finding of Chapter 4 was that learning significantly affected alpha ERD, but not beta. There can be multiple possible reasons behind this finding, such as the more variability for beta which comes from its wider spread over the scalp, and from the general interindividual differences (Toro et al., 1994). Pre-movement alpha is more focused spatially (Toro et al., 1994). Alpha ERD is commonly associated with inhibition release and top-down control (Klimesch, 2012), indicating activation of motor-related areas during movement execution and planning. Additionally, as there are alpha activities after movement, implying more involvement in refinement of movement could offer an explanation (Crone et al., 1998; Fogassi et al., 2005; Neuper & Pfurtscheller, 2001). Alpha has been observed in several regions related to attention and sensorimotor processing (Crone et al., 1998; Fogassi et al., 2005) implies alpha is most likely involved in "post-execution refinement of movement", a process involved in learning. Lastly, Van Der Cruijsen et al. (2021) recently suggested that the most important activities involved in motor learning are theta and alpha. Our findings support these arguments, further supporting the idea that alpha activity is heavily involved in movement preparation and post execution refinement.

MRCP has been said to reflect planning and preparation, with each of its two components (RP and NP respectively (Shibasaki & Hallett, 2006; Wright, Holmes, & Smith, 2011). We found an effect of time on MRCP in Chapter 4, where we identified a significant increase of MRCP amplitude leading up to MOn. There was no significant effect of learning on MRCP on the trial level, this was most likely due to high variability of the data. We theorize that this lack of solid finding could be due to side effects of filtering the neural data, running ICA decomposition, or differences between references (FCz used in Chapter 2, while mastoid used in Chapter 4). Moreover, we did not observe the classical shape or MRCP, most likely due to the nature of our learning task. The take home message of these findings is that both the preparation of neural data for identifying MRCP and the task used to study motor learning must be chosen carefully. Here, we suggest future studies to explore manual trial rejection instead of ICA component rejection.

5.4 Practical contributions

We presented results expanding our understanding of the interactive relationship between three neural markers, namely ERD, MRCP and CSE. In practical terms relevant for BCI, we provide further description of the temporal evolution of these three neural correlates, as well as we explored links between them. One of the main issues for BCI motor rehabilitation, that while CSE seems to be the best point for sensory feedback thus enhancing motor learning, we can only calculate CSE post hoc. By establishing the expected shape of CSE, the previously discussed 3rd degree polynomial shape, and the relationship between CSE and ERDs, we offer a potential avenue for real time CSE identification. While such improvements are far away from our current understanding, this thesis offers another step

towards unraveling the inner workings of pre-movement neural markers. If timing strategies are based on an inferred relationship between ERD and CSE, we must determine whether this relationship remains stable over time, or if changes in one marker leads to a misalignment in feedback delivery as learning progresses.

The rationale of our first hypothesis stems from our proposal to a different approach to define the relationship between CSE and ERD, considering both markers individually while analyzing their temporal alignment relative to MOn. Not only does this method offer a better overview of all the neural markers and dynamics in the same framework from the start, but there is also the practical aspect of inter/individual differences in ERD strength progressions. Although the average ERD strength reaches 50% following MOn, this value varies across individuals. For BCI applications, we propose identifying an optimal CSE time point relative to MOn (e.g., 500 ms before MOn) and then determining the corresponding ERD percentage for each individual at that specific time point. This value will most likely be different from person to person. This approach should be followed by the investigation on how ERD % changes during motor learning. Thus, we can develop a dynamic model assisting BCI rehabilitation techniques which are capable of accounting for individual differences (for example in ERD%) while working on universal tendencies (such as the shape of CSE). Therefore, the idea of a universal ERD % is unfeasible, as there is no assurance that by timing feedback to a static ERD % limit will affect the same part of the CSE activity. Furthermore, as BCI rehabilitation involves motor learning, we must take the changes in CSE and ERD into account during learning. In Chapter 4, we presented how the amplitude of CSE and ERD are affected by motor learning, and how this effect is unique for each neural marker. In conclusion, we should move our aim away from trying to identify constants and rather focus our efforts into developing dynamic models for neural activity leading up to MOn, where learning and individual differences are considered.

This dynamic understanding will enable research and rehabilitation efforts to develop more precise strategies for delivering sensory stimulation at optimal time points. Research that focuses on this route could start by comparing time points around preparatory peak, inhibition, or the steep increase closer to MOn. However significantly more research is required to explore the temporal evolution of multiple neural correlates and how the behave in relation to different types of feedback as well as movement (e.g., speed and complexity, different limbs, etc.).

To the best of our knowledge, if BCI studies are currently adjusting for the changes in the brain due to learning, they do it without specifically accounting for how these changes happen. These current studies simply update their model to the new variance in activity, much like how we simply retrained our “within model” in Chapter 4. Although our models are not perfect, initial findings suggest that

variance in early learning stages predicts later success. Consequently, updating models without accounting for this may reduce rather than enhance their effectiveness. However, our models should not be followed uncritically. The results of our studies should be taken as cautionary advice on how to take change into account in a concise manner. Further research is needed to either rule out the assumption that changes in neural signals do affect the efficacy of existing and new feedback strategies or find a way to adjust for these changes dynamically. Such research may involve real-time recalibration, feedback adjustments based on behavioral milestones, or staged interventions that adapt at key points in neural recovery. We propose developing a more refined, dynamic descriptive model of CSE and its relationship with ERD, even if purely observational. Additionally, a predictive model should be established to capture the precise changes in both neural markers during learning, particularly in its early stages.

5.5 Theoretical contributions

While the general aim of this thesis was to aid the practical application of BCI rehabilitation methods, our findings also offer theoretical contributions to the literature. Investigating the functional connectivity between pre-movement neural markers is crucial for mapping movement preparation at the neural level, yet the literature on this topic remains sparse.

Exploring functional connectivity of neural correlates not only has practical implications but also enhances our understanding of neural plasticity. Identifying connections between relevant neural markers can improve existing or create new BCI-based therapeutic approaches. Our goal should be to create a large-scale model of correlation and functional connectivity in pre-movement neural activity over the motor cortex. By mapping neural markers of upper limb movement and motor learning, this research contributes to a more dynamic way of viewing movement preparation and execution. Such a theoretical model would account for individual differences and learning, providing a more comprehensive representation of brain activity.

In this thesis, we aimed to create a predictive model for CSE based on ERD, further examining their correlative nature and the temporal evolution of CSE leading up to movement initiation, including MRCP as proposed by Daly et al. (2018). By focusing on functional connectivity and temporal dynamics, we advanced knowledge of the motor control neural circuit revisiting and testing previously held assumptions and proposing new ideas.

The functional connectivity of neural markers and the effects of learning on these connections remain mostly unexplored. Investigating functional connectivity provides insight into the mechanisms underlying motor system plasticity, helping to elucidate how the brain reorganizes to optimize motor performance. Understanding the neural circuit related to motor performance is the first step, followed

by analyzing changes in activity patterns and their relationships as motor skills improve. This thesis lays the groundwork for such investigations. Using EEG, we examined the motor network and its role in motor control, further exploring how these circuits are influenced by motor learning.

Our findings support the use of time-based EEG analyses to reveal the temporal dynamics of motor control. Tracking brain activity leading up to and during movement execution provides crucial insights into the timing of neural events involved in motor planning, execution, and feedback processing. Understanding neural synchronization over the motor cortex can enhance rehabilitation methods. Mapping the relationships between neural signatures of upper limb movement improves our understanding of motor activity and provides an indirect measure of CSE. When integrated with traditional BCI setups, this approach could increase efficacy.

Although previous studies found no correlation between ERD magnitude (in either frequency band) and MRCP amplitude (NS or peak MRCP 100ms after movement onset; Toro et al., 1994), Toro et al. noted that in the final 500ms before movement onset, ERD spread across the scalp coincides with MRCP NS lateralization. This suggests ERD and MRCP are related to similar motor cortex activation events. Furthermore, while ERD and MRCP likely originate from similar cortical areas, ERD responses vary by frequency band. Beta ERD is typically stronger than alpha ERD, but the largest alpha response overlaps with the region of peak MRCP amplitude, whereas beta ERD is more diffusely distributed. While MRCP and ERD overlap in areas of greatest response, there is no general correlation between larger MRCP amplitudes and greater ERD in either alpha or beta bands. The functional significance of these variations remains speculative (Toro et al., 1994). A key question is whether learning-induced changes in ERD and MRCP occur independently or coincide. Would reductions in alpha and beta power follow similar patterns, or would one remain more stable? Investigating these neural correlates and their functional connectivity during learning could provide more comprehensive insights into movement-related brain functions and movement intention detection—especially in motor rehabilitation contexts where the goal is to induce neural change.

We suggested in the introduction that ERD and CSE are likely linked, with ERD changes predicting CSE shifts. Our findings support this hypothesis, showing that CSE follows an S-like wave starting earlier than previously believed (1.25–1s before movement onset, rather than the assumed final 100ms). However, CSE and ERD respond differently to learning, evolving at distinct rates, suggesting they represent more than a single process. CSE appears to change initially and then stabilize in amplitude, whereas ERD continues to evolve as learning solidifies. This aligns with prior findings on ERD localization and function (Crone et al., 1998; Fogassi et al., 2005; Neuper & Pfurtscheller, 2001). High initial CSE may reflect increased neural excitability during early learning stages, when the brain is

actively reorganizing. In contrast, further reductions in ERD power likely reflect finer integration and motor representation updates as learning progresses.

ERD primarily differentiates general improvement levels, as shown by significant changes between the first 12 and last 12 trials (i.e., early vs. later learning stages) and across the experiment (first half vs. second half). In contrast, CSE is mainly influenced by initial learning efforts, showing differences between the first learning stage and later stages but no significant change from the beginning to the end of the experiment. This may suggest that CSE changes are less robust than ERD changes and require more data to detect learning effects reliably. Alternatively, inter-individual variability may be substantial, warranting longitudinal studies on motor learning's effects on CSE.

In summary, our study achieved its primary objectives, though certain aspects could be further optimized. We contributed to the scientific understanding of CSE by proposing that it takes an S-like shape; showed how CSE is mainly affected by early-stage learning, while ERDs are more generally affected; thus provided a deeper understanding of pre-movement neural activities. The following sections will discuss the limitations of our research and suggest directions for future studies.

5.6 Limitations

While we mention the concept of "optimal excitability" and its relation to CSE's temporal characteristics frequently, the aim of the studies in this thesis was to explore the unknown parameters pertaining this time point-the temporal evolution of CSE-and the related functional connectivity between neural markers. Thus, we cannot make a definitive statement on the actual point of CSE activity best for timing feedback to, beyond stressing the importance for future research to further explore CSE dynamics and mediators. Our hypotheses pertaining to CSE dynamics and relation to ERD were heavily based on the little amount of relevant research available and thus heavily limited by their experimental design. For example, the CSE measures of Daly et al. (2018) were dependent on ERD progressions, for which the analysis in Chapter 2 (Figure 7) showed the categorized ERD% did not fall in the expected ordered progression over time relative to MOn. The analysis in Chapter 4 addressed this specific design limitation by measuring CSE independent of ERD relative to MOn. However, interestingly we did not observe the robust CSE pre-movement inhibition (Ibáñez et al., 2020). A possible reason for the absence of inhibition in our results is the analysis presented in Chapter 4 might require a stricter thresholding of data, such as rejection of trials due to early movements and other artifacts, rather than only focusing on button press timings.

Accurately defining movement onset is also a challenge and limitation in our research. In Chapter 2, we presented data where MOn was defined by EMG data, while in Chapter 4 it was defined as the time when the participant pressed the buttons. Both methods have advantages and disadvantages. EMG

data can define MOn very specifically and account for early contractions prior to MOn; however, is very time labor intensive and subjected to research experience or algorithm flaws. Meanwhile, the button press provides a solid measurement of timing, however there is an unaddressed variability in time between MOn and the press of the button, as well as it is difficult to account for early movement or random twitches of the muscle. Meanwhile, the button press provides a solid measurement of timing, allows the exclusion of trials with early movement, however there is an unaddressed variability in time between MOn and the press of the button.

There are also general challenges around TMS+EEG methods, and even just TMS used in movement-based tasks. We tend to define baseline as "prior to MOn", however, for movement tasks, during that period the participant is already focused on the execution of movement. This muddies the waters when we aim to study the effects of learning. The issue surrounding the definition of a baseline is also complicated by the fact that during learning, the participant is most likely preparing for the movement continuously.

As with many EEG studies, ours also showed significant inter-individual variability. Thus, the previously suggested idea of using hard thresholds (i.e. 30% ERD means CSE peak) might not be a useful method. While our number of participants is not low, we acknowledge that our results would be stronger with a much higher number of participants, maybe even a longitudinal experimental design where the inter-individual differences could be better assessed.

5.7 Future research

It is essential that the functional connectivity of neural markers be further explored. Understanding their associations with different processes, part of processes or their regions of origin is crucial for the understanding of movement-related brain activity, and to support the development of better rehabilitation practices. This line of research should aim to uncover if the relations and dynamics stay constant across different contexts or if we can identify variables that only alter one (e.g., different types of movements, intent behind movement (RT, SP, PT..)). Such a theoretical interest for looking into functional connectivity should also exceed the practical application of it and aim for the general goal of mapping every brain function thus understanding our neural processes.

Despite being part of the same neural network, sharing a region of origin (Bai et al., 2006; Schultze-Kraft et al., 2016; Toro et al., 1994), start roughly 2 seconds prior to movement onset and are both discussed in relation, ERD and MRCP are rarely studied at the same time on either temporal characteristics or function. These neural markers are closely related to the same cognitive mechanism of motor control, but literature argues that physiologically they are independent from one another. As such, the exploration of MRCP at same time as ERD can hold the same practical role of estimating and

indicating CSE times points or changes, and advice on timing of stimulation (be it TMS pulses or sensory feedback by BCI set up). Furthermore, investigation of neural markers using the same time scale can expand our understanding of the neural functional connectivity of motor control (e.g. how do they behave relative to each other and CSE when learning, re-investigating if they are as independent processes as the literature claims, etc.). By mapping out the functional connectivity and correlations of the brain, we can further practical applications and understandings of neural processes on a greater network level. Since MRCPs and ERD might have different topographical patterns and time course evolution over the movement stages (Shibasaki & Hallett, 2006) combining these EEG measurements might provide more comprehensive features for understanding movement-related brain functions and detecting movement intentions.

Importantly, future research should uncover more information about CSE. For example, it remains unclear whether the optimal timing for intervention is the maximal CSE or its suppression phase. A critical consideration is the interpretation of the term “point of optimal excitability” in relation to CSE activity. Different research objectives may require distinct definitions of this concept. For instance, if the goal is to time stimulation for an intended physiological effect (similar to how PAS work), the optimal point refers to when stimulation arrives along the corticospinal tracks to induce plasticity-enhancing effects. This point may be fixed in time relative to MOn. However, if the goal is to engage external stimulation or trigger internally generated activity (e.g., a participant performing a specific exercise or MI), the optimal point may vary depending on the protocol used.

Avoiding confusion between these interpretations is crucial, as the optimal point for stimulation delivery is not necessarily the same as the optimal point for initiating externally or internally driven neural activity. Future research should distinguish between these concepts and define context-specific criteria for determining optimal excitability.

Additionally, while not explored in these studies, future research should place the findings about CSE in the context of feedback type (visual, electrical, etc.), as it is possible that the “optimal timing” depends on these factors as well.

Lastly, in the context of stroke rehabilitation, it is crucial to mention that CSE is affected by the injury (Veldema et al., 2021). As such, when this research is implemented in the practical phase, a new factor must be considered. Thus, future research will have to investigate how CSE changes due to injury, and how this can interact with the changes of CSE during learning.

As such, we propose that future research should aim for analyzing multiple neural correlates and investigate their relationship while controlling for goal and feedback types. This way, we can take a

significant step from researching single components of the pre-MOn neural activity towards describing the whole process including how one neural correlate leads to another, thus describing the process as a dynamic flow instead of a static line of blocks.

5.8 Conclusion

We aimed to map relationships between neural signatures of upper limb movement and motor learning, and use the gained understanding to improve BCI, more optimal aid for motor rehab and advance our understanding of motor learning on a neural level. However, the neural markers' functional connectivity and dynamic when we learn (i.e., perform better in motor skill-based tasks) is poorly understood.

We demonstrated the importance of functional connectivity analysis to create a dynamic model for neural activity during learning, showed how neural markers such as ERD, MRCP and CSE changes when new skills are learned, and presented a potential method for predicting the timing of "optimal excitability". These steps in mapping out the inner workings of our brain are vital for both theoretical and practical reasons. Firstly, the scientific conquest of understanding how the human brain functions; secondly, the practical applications of these results can improve our current motor rehabilitation methods using BCI.

While our research had limitations and posed further questions to be answered in future studies, the findings presented in this thesis will act as another building block for mapping out our neural activity.

Bibliography

Abbasi, O., & Gross, J. (2020). Beta-band oscillations play an essential role in motor–auditory interactions. *Human Brain Mapping*, *41*(3), 656–665. https://doi.org/10.1002/HBM.24830

Ackerley, S. J., Stinear, C. M., & Byblow, W. D. (2011). Promoting use-dependent plasticity with externally-paced training. *Clinical Neurophysiology*, *122*(12), 2462–2468. https://doi.org/10.1016/J.CLINPH.2011.05.011

Adank, I. P., Kennedy-Higgins, D., Maegherman, G., Hannah, R., Nuttall, H., & Adank, P. (2018). *Effects of coil orientation on Motor Evoked Potentials from Orbicularis Oris and First Dorsal*. https://doi.org/10.1101/262261

Ang, K. K., & Guan, C. (2013). Brain-Computer Interface in Stroke Rehabilitation. *Journal of Computing Science and Engineering*, *7*(2), 139–146. https://doi.org/10.5626/JCSE.2013.7.2.139

Ang, K. K., Guan, C., Chua, K. S. G., Ang, B. T., Kuah, C. W. K., Wang, C., Phua, K. S., Chin, Z. Y., & Zhang, H. (2011). A large clinical study on the ability of stroke patients to use an EEG-based motor imagery brain-computer interface. *Clinical EEG and Neuroscience*, *42*(4), 253–258. https://doi.org/10.1177/155005941104200411

Aono, K., Miyashita, S., Fujiwara, Y., Kodama, M., Hanayama, K., Masakado, Y., & Ushiba, J. (2013). Relationship between event-related desynchronization and cortical excitability in healthy subjects and stroke patients. *Tokai Journal of Experimental and Clinical Medicine*, *38*(4), 123–128.

Avila, A., & Chang, J. Y. (2014). EMG onset detection and upper limb movements identification algorithm. *Microsystem Technologies*, *20*(8–9), 1635–1640. https://doi.org/10.1007/s00542-014-2194-8

Bagozzi, R. P., & Dholakia, U. M. (2014). Three Roles of Past Experience in Goal Setting and Goal Striving. In T. Betsch & S. Haberstroh (Eds.), *The Routines of Decision Making* (pp. 21–38). Psychology press.

Bai, O., Vorbach, S., Hallett, M., & Floeter, M. K. (2006). Movement-related cortical potentials in primary lateral sclerosis. *Annals of Neurology*, *59*(4), 682–690. https://doi.org/10.1002/ana.20803

Bardi, L., Bundt, C., Notebaert, W., & Brass, M. (2015). Eliminating mirror responses by instructions. *Cortex*, *70*, 128–136. https://doi.org/10.1016/J.CORTEX.2015.04.018

Barker-Collo, S., Feigin, V., Lawes, C., Senior, H., & Parag, V. (2010). Natural history of attention deficits and their influence on functional recovery from acute stages to 6 months after stroke. *Neuroepidemiology*, *35*(4), 255–262. https://doi.org/10.1159/000319894

Berghuis, K. M. M., De Rond, V., Zijdewind, I., Koch, G., Veldman, M. P., & Hortobágyi, T. (2016). Neuronal mechanisms of motor learning are age dependent. *Neurobiology of Aging*, *46*, 149–159. https://doi.org/10.1016/j.neurobiolaging.2016.06.013

Berridge, M. J. (1998). Neuronal Calcium Signaling. *Neuron*, *21*(1), 13–26. https://doi.org/10.1016/S0896-6273(00)80510-3

Billingham, L., Malottki, K., Investigation, N. S.-C., & 2012, undefined. (2012). Small sample sizes in clinical trials: a statistician's perspective. *Ctsicn.OrgL Billingham, K Malottki, N StevenClinical Investigation, 2012•ctsicn.Org*, *2*(7), 655–657. https://doi.org/10.4155/CLI.12.62

Bolognini, N., Russo, C., & Edwards, D. J. (2016). The sensory side of post-stroke motor rehabilitation. *Restorative Neurology and Neuroscience*, *34*(4), 571–586. https://doi.org/10.3233/RNN-150606

Bonita, R. (1992). Epidemiology of stroke. *The Lancet*, *339*(8789), 342–344. https://doi.org/10.1016/0140-6736(92)91658-U

Brainard, D. H. (1997). The Psychophysics Toolbox. *Spatial Vision*, *10*(4), 433–436. https://doi.org/10.1163/156856897X00357

Brass, M., & Heyes, C. (2005). Imitation: is cognitive neuroscience solving the correspondence problem? *Trends in Cognitive Sciences*, *9*(10), 489–495. https://doi.org/10.1016/J.TICS.2005.08.007

Brunia, C. H. M., van Boxtel, G. J. M., & Böcker, K. B. E. (2012). Negative Slow Waves as Indices of Anticipation: The Bereitschaftspotential, the Contingent Negative Variation, and the Stimulus-Preceding Negativity. . In S. J. Luck & E. S. Kappenman (Eds.), *The Oxford Handbook of Event-Related Potential Components.* (pp. 189–207). Oxford University Press.

Bussler, F. (2020, September 30). *This Animal Eats Its Brain, Becomes a Plant, Came to Europe via Warship, and Reproduces By Shooting Off Sex Organs*. DataDrivenInvestor. https://medium.datadriveninvestor.com/this-animal-eats-its-brain-becomes-a-plant-came-to-europe-via-warship-and-reproduces-by-58ab261cc6ee

Butterfill, S. A., & Sinigaglia, C. (2014). Intention and Motor Representation in Purposive Action. *Philosophy and Phenomenological Research*, *88*(1), 119–145. https://doi.org/10.1111/j.1933-1592.2012.00604.x

Button, K. S., Ioannidis, J. P. A., Mokrysz, C., Nosek, B. A., Flint, J., Robinson, E. S. J., & Munafò, M. R. (2013). Power failure: why small sample size undermines the reliability of neuroscience. *Nature Reviews Neuroscience 2013 14:5*, *14*(5), 365–376. https://doi.org/10.1038/nrn3475

Buzsáki, G. (2011). *Rhythms of the brain*. Oxford University Press Inc.

Cannon, E. N., Yoo, K. H., Vanderwert, R. E., Ferrari, P. F., Woodward, A. L., & Fox, N. A. (2014). Action experience, more than observation, influences mu rhythm desynchronization. *PLoS ONE*, *9*(3), 1–8. https://doi.org/10.1371/journal.pone.0092002

Carey, L. M., Matyas, T. A., & Oke, L. E. (1993). Sensory loss in stroke patients: Effective training of tactile and proprioceptive discrimination. *Archives of Physical Medicine and Rehabilitation*, *74*(6), 602–611. https://doi.org/10.1016/0003-9993(93)90158-7

Carson, R. G., & Kennedy, N. C. (2013). Modulation of human corticospinal excitability by paired associative stimulation. *Frontiers in Human Neuroscience*, *7*(DEC), 1–28. https://doi.org/10.3389/fnhum.2013.00823

Cassim, F., Szurhaj, W., Sediri, H., Devos, D., Bourriez, J. L., Poirot, I., Derambure, P., Defebvre, L., & Guieu, J. D. (2000). Brief and sustained movements: Differences in event-related (de)synchronization (ERD/ERS) patterns. *Clinical Neurophysiology*, *111*(11), 2032–2039. https://doi.org/10.1016/S1388-2457(00)00455-7

Chen, J. C., & Shaw, F. Z. (2014). Progress in sensorimotor rehabilitative physical therapy programs for stroke patients. *World Journal of Clinical Cases : WJCC*, *2*(8), 316. https://doi.org/10.12998/WJCC.V2.I8.316

Chen, L. W., Glinsky, J. V., Islam, M. S., Hossain, M., Boswell-Ruys, C. L., Kataria, C., Redhead, J., Xiong, Y., Gollan, E., Costa, P. D., Denis, S., Ben, M., Chaudhary, L., Wang, J., Hasnat, M. A. K., Yeomans, J., Gandevia, S. C., & Harvey, L. A. (2020). The effects of 10,000 voluntary contractions over 8 weeks on the strength of very weak muscles in people with spinal cord injury: a randomised controlled trial. *Spinal Cord 2020 58:8*, *58*(8), 857–864. https://doi.org/10.1038/s41393-020-0439-1

Chen, R., Yaseen, Z., Cohen, L. G., & Hallett, M. (1998). Time course of corticospinal excitability in reaction time and self- paced movements. *Annals of Neurology*, *44*(3), 317–325. https://doi.org/10.1002/ana.410440306

Christiansen, L., Madsen, M. J., Bojsen-Møller, E., Thomas, R., Nielsen, J. B., & Lundbye-Jensen, J. (2018). Progressive practice promotes motor learning and repeated transient increases in corticospinal excitability across multiple days. *Brain Stimulation*, *11*(2), 346–357. https://doi.org/10.1016/j.brs.2017.11.005

Cicinelli, P., Marconi, B., Zaccagnini, M., Pasqualetti, P., Filippi, M. M., & Rossini, P. M. (2006). Imagery-induced Cortical Excitability Changes in Stroke: A Transcranial Magnetic Stimulation Study. *Cerebral Cortex*, *16*(2), 247–253. https://doi.org/10.1093/CERCOR/BHI103

Clarkson, A. N., & Carmichael, S. T. (2009). Cortical excitability and post-stroke recovery. *Biochemical Society Transactions*, *37*(6), 1412–1414. https://doi.org/10.1042/BST0371412

Cohen, M. X. (2019). A better way to define and describe Morlet wavelets for time-frequency analysis. *NeuroImage*, *199*, 81–86. https://doi.org/10.1016/J.NEUROIMAGE.2019.05.048

Crasta, J. E., Thaut, M. H., Anderson, C. W., Davies, P. L., & Gavin, W. J. (2018). Auditory priming improves neural synchronization in auditory-motor entrainment. *Neuropsychologia*, *117*, 102–112. https://doi.org/10.1016/J.NEUROPSYCHOLOGIA.2018.05.017

Crone, N. E., Miglioretti, D. L., Gordon, B., Sieracki, J. M., Wilson, M. T., Uematsu, S., & Lesser, R. P. (1998). Functional mapping of human sensorimotor cortex with electrocorticographic spectral analysis. I. Alpha and beta event-related desynchronization. *Brain*, *121*(12), 2271–2299. https://doi.org/10.1093/BRAIN/121.12.2271

Daly, I., Blanchard, C., & Holmes, N. P. (2018). Cortical excitability correlates with the event-related desynchronization during brain-computer interface control. *Journal of Neural Engineering*, *15*(2). https://doi.org/10.1088/1741-2552/aa9c8c

Dayan, E., & Cohen, L. G. (2011). Neuroplasticity subserving motor skill learning. *Neuron*, *72*(3), 443–454. https://doi.org/10.1016/j.neuron.2011.10.008

de Sousa, D. G., Harvey, L. A., Dorsch, S., & Glinsky, J. V. (2018). Interventions involving repetitive practice improve strength after stroke: a systematic review. *Journal of Physiotherapy*, *64*(4), 210–221. https://doi.org/10.1016/J.JPHYS.2018.08.004

Delorme, A., & Makeig, S. (2004). EEGLAB: an open source toolbox for analysis of single-trial EEG dynamics including independent component analysis. *Journal of Neuroscience Methods*, *134*, 9–21. http://www.sccn.ucsd.edu/eeglab/

Demandt, E., Mehring, C., Vogt, K., Schulze-Bonhage, A., Aertsen, A., & Ball, T. (2012). Reaching movement onset- and end-related characteristics of EEG spectral power modulations. *Frontiers in Neuroscience*, *MAY*. https://doi.org/10.3389/fnins.2012.00065

Dhana, K. (2016, April 30). *Identify, describe, plot, and remove the outliers from the dataset*. https://datascienceplus.com/identify-describe-plot-and-removing-the-outliers-from-the-dataset/

Dobkin, B. H. (2009). Motor rehabilitation after stroke, traumatic brain, and spinal cord injury: common denominators within recent clinical trials. *Current Opinion in Neurology*, *22*(6), 563–569. https://doi.org/10.1097/WCO.0B013E3283314B11

Du Prel, J. B., Hommel, G., Röhrig, B., & Blettner, M. (2009). Confidence Interval or P-Value?: Part 4 of a Series on Evaluation of Scientific Publications. *Deutsches Ärzteblatt International*, *106*(19), 335. https://doi.org/10.3238/ARZTEBL.2009.0335

Duque, J., Greenhouse, I., Labruna, L., & Ivry, R. B. (2017). Physiological Markers of Motor Inhibition during Human Behavior. *Trends in Neurosciences*, *40*(4), 219–236. https://doi.org/10.1016/J.TINS.2017.02.006

Efron, B. (1982). The Jackknife, the Bootstrap and Other Resampling Plans. *CBMS-NSF Regional Conference Series in Applied Mathematics*, *Monograph 38*. https://doi.org/10.1137/1.9781611970319

Erichsen, T. (2019). *LoopMIDI [Computer Software]* (1.0.16.27). https://www.tobias-erichsen.de/software/loopmidi.html

Fairhall, S. L., Kirk, I. J., & Hamm, J. P. (2006). *Volition and the idle cortex: Beta oscillatory activity preceding planned and spontaneous movement*. https://doi.org/10.1016/j.concog.2006.05.005

Feldman, D. E. (2012). The Spike-Timing Dependence of Plasticity. *Neuron*, *75*(4), 556–571. https://doi.org/10.1016/j.neuron.2012.08.001

Fogassi, L., Ferrari, P. F., Gesierich, B., Rozzi, S., Chersi, F., & Rizzolatti, G. (2005). Parietal Lobe: From Action Organization to Intention Understanding. *Science*, *308*(5722), 662–667. https://doi.org/10.1126/science.1106138

Franz, M., Richner, L., Wirz, M., Von Reumont, A., Bergner, U., Herzog, T., Popp, W., Bach, K., Weidner, N., & Curt, A. (2017). Physical therapy is targeted and adjusted over time for the rehabilitation of locomotor function in acute spinal cord injury interventions in physical and sports therapy. *Spinal Cord 2017 56:2*, *56*(2), 158–167. https://doi.org/10.1038/s41393-017-0007-5

Fritsch, F. N., & Butland, J. (1984). A Method for Constructing Local Monotone Piecewise Cubic Interpolants. *SIAM Journal on Scientific and Statistical Computing*, *5*(2), 300–304. https://doi.org/10.1137/0905021

Fritsch, F. N., & Carlson, R. E. (1980). Monotone Piecewise Cubic Interpolation. *SIAM Journal on Numerical Analysis*, *17*(2), 238–246. https://doi.org/10.1137/0717021

Furuya, S., Flanders, M., & Soechting, J. F. (2011). Hand kinematics of piano playing. *Journal of Neurophysiology*, *106*(6), 2849–2864. https://doi.org/10.1152/jn.00378.2011

Gandolla, M., Ferrante, S., Ferrigno, G., Baldassini, D., Molteni, F., Guanziroli, E., Cotti Cottini, M., Seneci, C., & Pedrocchi, A. (2017). Artificial neural network EMG classifier for functional hand

grasp movements prediction. *Journal of International Medical Research*, *45*(6), 1831–1847. https://doi.org/10.1177/0300060516656689

Gandolla, M., Niero, L., Molteni, F., Guanziroli, E., Ward, N. S., & Pedrocchi, A. (2021). Brain Plasticity Mechanisms Underlying Motor Control Reorganization: Pilot Longitudinal Study on Post-Stroke Subjects. *Brain Sciences 2021, Vol. 11, Page 329*, *11*(3), 329. https://doi.org/10.3390/BRAINSCI11030329

Ganguly, K., & Poo, M. ming. (2013). Activity-dependent neural plasticity from bench to bedside. *Neuron*, *80*(3), 729–741. https://doi.org/10.1016/J.NEURON.2013.10.028/ASSET/92B3E1A3-E4F0-4B54-A746-8EE3EB89EF9C/MAIN.ASSETS/GR2.JPG

Garcia, M. A. C., Souza, V. H., & Vargas, C. D. (2017). Can the Recording of Motor Potentials Evoked by Transcranial Magnetic Stimulation Be Optimized? *Frontiers in Human Neuroscience*, *11*, 413. https://doi.org/10.3389/FNHUM.2017.00413

Ginhoux, R., Renaud, P., Zorn, L., Goffin, L., Bayle, B., Foucher, J., Lamy, J., Armspach, J. P., & De Mathelin, M. (2013). A custom robot for Transcranial Magnetic Stimulation: First assessment on healthy subjects. *Proceedings of the Annual International Conference of the IEEE Engineering in Medicine and Biology Society, EMBS*, 5352–5355. https://doi.org/10.1109/EMBC.2013.6610758

Giuffre, A., Kahl, C. K., Zewdie, E., Wrightson, J. G., Bourgeois, A., Condliffe, E. G., & Kirton, A. (2021). Reliability of robotic transcranial magnetic stimulation motor mapping. *Journal of Neurophysiology*, *125*(1), 74–85. https://doi.org/10.1152/JN.00527.2020

Gomez-Tames, J., Hamasaka, A., Laakso, I., Hirata, A., & Ugawa, Y. (2018). Atlas of optimal coil orientation and position for TMS: A computational study. *Brain Stimulation*, *11*(4), 839–848. https://doi.org/10.1016/j.brs.2018.04.011

Guerrero, F. N., & Spinelli, E. M. (2018). *Biopotential acquisition for brain–wheelchair interfaces*. https://doi.org/10.1016/B978-0-12-812892-3.00004-2

Guger, C., Millán, J. del R., Mattia, D., Ushiba, J., Soekadar, S. R., Prabhakaran, V., Mrachacz-Kersting, N., Kamada, K., & Allison, B. Z. (2018). Brain-computer interfaces for stroke rehabilitation: summary of the 2016 BCI Meeting in Asilomar. *Brain-Computer Interfaces*, *5*(2–3), 41–57. https://doi.org/10.1080/2326263X.2018.1493073

Habibollahi Saatlou, F., Rogasch, N. C., McNair, N. A., Biabani, M., Pillen, S. D., Marshall, T. R., & Bergmann, T. O. (2018). MAGIC: An open-source MATLAB toolbox for external control of transcranial magnetic stimulation devices. In *Brain Stimulation* (Vol. 11, Issue 5, pp. 1189–1191). Elsevier Inc. https://doi.org/10.1016/j.brs.2018.05.015

Haggard, P., & Eimer, M. (1999). On the relation between brain potentials and the awareness of voluntary movements. *Experimental Brain Research*, *126*(1), 128–133. https://doi.org/10.1007/S002210050722/METRICS

Hamano, T., Lüders, H. O., Ikeda, A., Collura, T. F., Comair, Y. G., & Shibasaki, H. (1997). The cortical generators of the contingent negative variation in humans: a study with subdural electrodes. *Electroencephalography and Clinical Neurophysiology*, *104*(3), 257–268. https://doi.org/10.1016/S0168-5597(97)96107-4

Hannah, R., Cavanagh, S. E., Tremblay, S., Simeoni, S., & Rothwell, J. C. (2018). Selective Suppression of Local Interneuron Circuits in Human Motor Cortex Contributes to Movement Preparation. *Journal of Neuroscience*, *38*(5), 1264–1276. https://doi.org/10.1523/JNEUROSCI.2869-17.2017

Hashemirad, F., Zoghi, M., Fitzgerald, P. B., & Jaberzadeh, S. (2016). The effect of anodal transcranial direct current stimulation on motor sequence learning in healthy individuals: A systematic review and meta-analysis. *Brain and Cognition*, *102*, 1–12. https://doi.org/10.1016/j.bandc.2015.11.005

Hatem, S. M., Saussez, G., della Faille, M., Prist, V., Zhang, X., Dispa, D., & Bleyenheuft, Y. (2016). Rehabilitation of motor function after stroke: A multiple systematic review focused on techniques to stimulate upper extremity recovery. *Frontiers in Human Neuroscience*, *10*(SEP2016), 1–22. https://doi.org/10.3389/fnhum.2016.00442

Hebb, D. O. (1949). *The Organization of Behavior; A Neuropsychological Theory* (Vol. 65). New York: Wiley. https://doi.org/10.2307/1418888

Hernandez-Pavon, J. C., Kugiumtzis, D., Zrenner, C., Kimiskidis, V. K., & Metsomaa, J. (2022). Removing artifacts from TMS-evoked EEG: A methods review and a unifying theoretical framework. *Journal of Neuroscience Methods*, *376*, 109591. https://doi.org/10.1016/J.JNEUMETH.2022.109591

Hodges, P. W., & Bui, B. H. (1996). A comparison of computer-based methods for the determination of onset of muscle contraction using electromyography. *Electroencephalography and Clinical Neurophysiology - Electromyography and Motor Control*, *101*(6), 511–519. https://doi.org/10.1016/S0921-884X(96)95190-5

Holsheimer, J., & Feenstra, B. W. A. (1977). Volume conduction and EEG measurements within the brain: a quantitative approach to the influence of electrical spread on the linear relationship of activity measured at different locations. *Electroencephalography and Clinical Neurophysiology*, *43*(1), 52–58. https://doi.org/10.1016/0013-4694(77)90194-8

Hossmann, K. A. (2006). Pathophysiology and therapy of experimental stroke. In *Cellular and Molecular Neurobiology* (Vol. 26, Issues 7–8, pp. 1057–1083). https://doi.org/10.1007/s10571-006-9008-1

Hund-Georgiadis, M., & Yves Von Cramon, D. (1999). Motor-learning-related changes in piano players and non-musicians revealed by functional magnetic-resonance signals. *Experimental Brain Research*, *125*(4), 417–425. https://doi.org/10.1007/s002210050698

Hurtier, J., Van Dokkum, L., Dalhoumi, S., Coffey, A., Perrey, S., Jourdan, C., Dray, G., Ward, T., Froger, J., & Laffont, I. (2016). A closed-loop BCI system for rehabilitation of the hemiplegic upper-limb: A performance study of the systems ability to detect intention of movement. *Annals of Physical and Rehabilitation Medicine*, *59*, e88. https://doi.org/10.1016/j.rehab.2016.07.201

Ibáñez, J., Hannah, R., Rocchi, L., & Rothwell, J. C. (2020). Premovement Suppression of Corticospinal Excitability may be a Necessary Part of Movement Preparation. *Cerebral Cortex*, *30*(5), 2910–2923. https://doi.org/10.1093/CERCOR/BHZ283

Ilmoniemi, R. J., & Kičić, D. (2010). Methodology for Combined TMS and EEG. *Brain Topography*, *22*(4), 233. https://doi.org/10.1007/S10548-009-0123-4

Ivaldi, M., Cugliari, G., Peracchione, S., & Rainoldi, A. (2017). Familiarity affects electrocortical power spectra during dance imagery, listening to different music genres: independent component analysis of Alpha and Beta rhythms. *Sport Sciences for Health*, *13*(3), 535–548. https://doi.org/10.1007/S11332-017-0379-0/METRICS

Ives, J. C., & Wigglesworth, J. K. (2003). Sampling rate effects on surface EMG timing and amplitude measures. *Clinical Biomechanics*, *18*(6), 543–552. https://doi.org/10.1016/S0268-0033(03)00089-5

Jackson, A., & Zimmermann, J. B. (2012). Neural interfaces for the brain and spinal cord—restoring motor function. *Nature Reviews Neurology 2012 8:12*, *8*(12), 690–699. https://doi.org/10.1038/nrneurol.2012.219

Jankelowitz, S. K., & Colebatch, J. G. (2002). Movement-related potentials associated with self-paced, cued and imagined arm movements. *Experimental Brain Research*, *147*(1), 98–107. https://doi.org/10.1007/s00221-002-1220-8

Jeannerod, M. (1995). Mental imagery in the motor context. Special Issue: The neuropsychology of mental imagery. *Neuropsychologia*, *33*(11), 1419–1432. http://wexler.free.fr/library/files/jeannerod (1995) mental imagery in the motor context.pdf

Jongbloed-Pereboom, M., Nijhuis-Van der Sanden, M. W. G., & Steenbergen, B. (2015). Implicit and explicit motor learning in typically developing children: effects of task, age and working memory. *Physiotherapy*, *101*, e693–e694. https://doi.org/10.1016/j.physio.2015.03.3541

Kal, E., Prosée, R., Winters, M., & Van Der Kamp, J. (2018). Does implicit motor learning lead to greater automatization of motor skills compared to explicit motor learning? A systematic review. *PLOS ONE*, *13*(9), e0203591. https://doi.org/10.1371/JOURNAL.PONE.0203591

Kal, E., Winters, M., Van Kamp, J. Der, Houdijk, H., Groet, E., Bennekom, C., & Scherder, E. (2016). Is Implicit Motor Learning Preserved after Stroke? A Systematic Review with Meta-Analysis. *PLOS ONE*, *11*(12), e0166376. https://doi.org/10.1371/JOURNAL.PONE.0166376

Kamen, G., & Gabriel, D. A. (2010). *Essentials of Electromyography* (Canada: Human Kinetics., Ed.). Human Kinetics Publishers.

Kassambara, A. (2023). *rstatix: Pipe-Friendly Framework for Basic Statistical Tests* (R package version 0.7.2). https://CRAN.R-project.org/package=rstatix

Khalighinejad, N., Brann, E., Dorgham, A., & Haggard, P. (2019). Dissociating Cognitive and Motoric Precursors of Human Self-Initiated Action. *Journal of Cognitive Neuroscience*, *31*(5), 754–767. https://doi.org/10.1162/JOCN_A_01380

Khalighinejad, N., Schurger, A., Desantis, A., Zmigrod, L., & Haggard, P. (2018). Precursor processes of human self-initiated action. *NeuroImage*, *165*(August 2017), 35–47. https://doi.org/10.1016/j.neuroimage.2017.09.057

Kitago, T., & Krakauer, J. W. (2013). Motor learning principles for neurorehabilitation. *Handbook of Clinical Neurology*, *110*, 93–103. https://doi.org/10.1016/B978-0-444-52901-5.00008-3

Kleim, J. A. (2009). Synaptic Mechanisms of Learning. *Encyclopedia of Neuroscience*, 731–734. https://doi.org/10.1016/B978-008045046-9.01316-4

Kleim, J. A., Kleim, E. D., & Cramer, S. C. (2007). Systematic assessment of training-induced changes in corticospinal output to hand using frameless stereotaxic transcranial magnetic stimulation. *Nature Protocols*, *2*(7), 1675–1684. https://doi.org/10.1038/nprot.2007.206

Kleiner, M., Brainard, D., Pelli, D., Ingling, A., Murray, R., & Broussard, C. (2007). What's new in psychtoolbox-3. *Perception*, *36*(ECVP Abstract Supplement). https://nyuscholars.nyu.edu/en/publications/whats-new-in-psychtoolbox-3

Klein-Flügge, M. C., & Bestmann, S. (2012). Time-dependent changes in human corticospinal excitability reveal value-based competition for action during decision processing. *Journal of Neuroscience*, *32*(24), 8373–8382. https://doi.org/10.1523/JNEUROSCI.0270-12.2012

Klimesch, W. (2012). Alpha-band oscillations, attention, and controlled access to stored information. *Trends in Cognitive Sciences*, *16*(12), 606–617. https://doi.org/10.1016/j.tics.2012.10.007

Kübler, A., Kleih, S., & Mattia, D. (2017). Brain Computer Interfaces for Cognitive Rehabilitation After Stroke. In *Biosystems and Biorobotics* (Vol. 15, pp. 847–852). Springer International Publishing. https://doi.org/10.1007/978-3-319-46669-9_138

Lakany, H., & Conway, B. A. (2007). Understanding intention of movement from electroencephalograms. *Expert Systems*, *24*(5), 295–304. https://doi.org/10.1111/j.1468-0394.2007.00435.x

Lattari, E., Arias-Carrión, O., Monteiro-Junior, R. S., Mello Portugal, E. M., Paes, F., Menéndez-González, M., Silva, A. C., Nardi, A. E., & Machado, S. (2014). Implications of movement-related cortical potential for understanding neural adaptations in muscle strength tasks. *International Archives of Medicine*, *7*(1), 9. https://doi.org/10.1186/1755-7682-7-9

Lavazza, A. (2016). Free will and neuroscience: From explaining freedom away to new ways of operationalizing and measuring it. *Frontiers in Human Neuroscience*, *10*, 197548. https://doi.org/10.3389/FNHUM.2016.00262/BIBTEX

Leocani, L., Cohen, L. G., Wassermann, E. M., Ikoma, K., & Hallett, M. (2000). Human corticospinal excitability evaluated with transcranial magnetic stimulation during different reaction time paradigms. *Brain*, *123*(6), 1161–1173. https://doi.org/10.1093/BRAIN/123.6.1161

Leocani, L., Toro, C., Manganotti, P., Zhuang, P., & Hallett, M. (1997). Event-related coherence and event-related desynchronization/synchronization in the 10 Hz and 20 Hz EEG during self-paced movements. *Electroencephalography and Clinical Neurophysiology/Evoked Potentials Section*, *104*(3), 199–206. https://doi.org/10.1016/S0168-5597(96)96051-7

Leocani, L., Toro, C., Zhuang, P., Gerloff, C., & Hallett, M. (2001). Event-related desynchronization in reaction time paradigms: a comparison with event-related potentials and corticospinal excitability. *Clinical Neurophysiology*, *112*(5), 923–930. www.elsevier.com/locate/clinph

Lepage, J. F., Saint-Amour, D., & Théoret, H. (2008). EEG and neuronavigated single-pulse TMS in the study of the observation/execution matching system: Are both techniques measuring the same process? *Journal of Neuroscience Methods*, *175*(1), 17–24. https://doi.org/10.1016/J.JNEUMETH.2008.07.021

Leung, M., Rantalainen, T., Teo, W. P., & Kidgell, D. (2017). The corticospinal responses of metronome-paced, but not self-paced strength training are similar to motor skill training.

European Journal of Applied Physiology, *117*(12), 2479–2492. https://doi.org/10.1007/s00421-017-3736-4

Leuthold, H., & Jentzsch, I. (2002). Distinguishing neural sources of movement preparation and execution: An electrophysiological analysis. *Biological Psychology*, *60*(2–3), 173–198. https://doi.org/10.1016/S0301-0511(02)00032-7

Leuthold, H., Sommer, W., & Ulrich, R. (2004). Preparing for Action: Inferences from CNV and LRP. *Https://Doi.Org/10.1027/0269-8803.18.23.77*, *18*(2–3), 77–88. https://doi.org/10.1027/0269-8803.18.23.77

Li, J. (2016). Assessing spatial predictive models in the environmental sciences: Accuracy measures, data variation and variance explained. *Environmental Modelling & Software*, *80*, 1–8. https://doi.org/10.1016/J.ENVSOFT.2016.02.004

Li, J. (2017). *Assessing the accuracy of predictive models for numerical data: Not r nor r 2 , why not? Then what?* https://doi.org/10.1371/journal.pone.0183250

Libet, B., Gleason, C. A., Wright, E. W., & Pearl, D. K. (1983). Time of conscious intention to act in relation to onset of cerebral activity (readiness-potential). The unconscious initiation of a freely voluntary act. *Brain : A Journal of Neurology*, *106 (Pt 3)*(3), 623–642. https://doi.org/10.1093/BRAIN/106.3.623

Lisman, J., & Spruston, N. (2005). Postsynaptic depolarization requirements for LTP and LTD: A critique of spike timing-dependent plasticity. *Nature Neuroscience*, *8*(7), 839–841. https://doi.org/10.1038/nn0705-839

Lissek, S., Vallana, G. S., Güntürkün, O., Dinse, H., & Tegenthoff, M. (2013). Brain Activation in Motor Sequence Learning Is Related to the Level of Native Cortical Excitability. *PLOS ONE*, *8*(4), e61863. https://doi.org/10.1371/JOURNAL.PONE.0061863

Litvak, V., Komssi, S., Scherg, M., Hoechstetter, K., Classen, J., Zaaroor, M., Pratt, H., & Kahkonen, S. (2007). Artifact correction and source analysis of early electroencephalographic responses evoked by transcranial magnetic stimulation over primary motor cortex. *NeuroImage*, *37*(1), 56–70. https://doi.org/10.1016/J.NEUROIMAGE.2007.05.015

Lo, A. C., Guarino, P. D., Richards, L. G., Haselkorn, J. K., Wittenberg, G. F., Federman, D. G., Ringer, R. J., Wagner, T. H., Krebs, H. I., Volpe, B. T., Bever, C. T., Bravata, D. M., Duncan, P. W., Corn, B. H., Maffucci, A. D., Nadeau, S. E., Conroy, S. S., Powell, J. M., Huang, G. D., & Peduzzi, P. (2010). Robot-Assisted Therapy for Long-Term Upper-Limb Impairment after Stroke. *New England Journal of Medicine*, *362*(19), 1772–1783. https://doi.org/10.1056/NEJMoa0911341

Maier, M., Ballester, B. R., & Verschure, P. F. M. J. (2019). Principles of Neurorehabilitation After Stroke Based on Motor Learning and Brain Plasticity Mechanisms. *Frontiers in Systems Neuroscience*, *13*, 463323. https://doi.org/10.3389/FNSYS.2019.00074/BIBTEX

Makoto's preprocessing pipeline. (n.d.). (2022, May 20). https://sccn.ucsd.edu/wiki/Makoto's_preprocessing_pipeline

Maresch, J., Mudrik, L., & Donchin, O. (2021). Measures of explicit and implicit in motor learning: what we know and what we don't. *Neuroscience & Biobehavioral Reviews*, *128*, 558–568. https://doi.org/10.1016/J.NEUBIOREV.2021.06.037

Maslovat, D., Chua, R., Klapp, S. T., & Franks, I. M. (2018). Preparation of timing structure involves two independent sub-processes. *Psychological Research*, *82*(5), 981–996. https://doi.org/10.1007/s00426-017-0877-3

McGregor, H., Vesia, M., Rinchon, C., Chen, R., & Gribble, P. (2017). Changes in corticospinal excitability associated with motor learning by observing. *Changes in Corticospinal Excitability Associated with Motor Learning by Observing*, 205385. https://doi.org/10.1101/205385

Micera, S., Vannozzi, G., Sabatini, A. M., & Dario, P. (2001). Improving detection of muscle activation intervals. *IEEE Eng Med Biol Mag.*, *20*(6), 38–46. http://ieeexplore.ieee.org/xpls/abs_all.jsp?arnumber=982274

Monniot, C., Monniot, F., & Laboute, P. (1991). *Coral Reef Ascidians of New Caledonia* (Vol. 30). ORSTOM. https://books.google.co.il/books?hl=iw&lr=&id=S3FtLQVpagsC&oi=fnd&pg=PA5&dq=Monniot+%26+Monniot,+1991&ots=HKWztGgeH2&sig=W4U5W4GNR4s8Nma_rHI2DtnuCA0&redir_esc=y#v=onepage&q=Monniot %26 Monniot%2C 1991&f=false

Mrachacz-Kersting, N., Jiang, N., Thomas Stevenson, A. J., Niazi, I. K., Kostic, V., Pavlovic, A., Radovanovic, S., Djuric-Jovicic, M., Agosta, F., Dremstrup, K., & Farina, D. (2016). Efficient neuroplasticity induction in chronic stroke patients by an associative brain-computer interface. *Journal of Neurophysiology*, *115*(3), 1410–1421. https://doi.org/10.1152/jn.00918.2015

Mrachacz-Kersting, N., Kristensen, S. R., Niazi, I. K., & Farina, D. (2012). Precise temporal association between cortical potentials evoked by motor imagination and afference induces cortical plasticity. *Journal of Physiology*, *590*(7), 1669–1682. https://doi.org/10.1113/jphysiol.2011.222851

Müller-Putz, G. R., Daly, I., & Kaiser, V. (2014). Motor imagery-induced EEG patterns in individuals with spinal cord injury and their impact on brain–computer interface accuracy. *Journal of Neural Engineering*, *11*(3), 035011. https://doi.org/10.1088/1741-2560/11/3/035011

Murphy, T. H., & Corbett, D. (2009). *Plasticity during stroke recovery: from synapse to behaviour*. https://doi.org/10.1038/nrn2735

Native Instruments GmbH. (2019). *KONTAKT 6 PLAYER [Computer Software]* (6.2.2). https://www.native-instruments.com/ni-tech-manuals/kontakt-player-manual/en/welcome-to-kontakt-player

Nepveu, J.-F., Thiel, A., Tang, A., Fung, J., Lundbye-Jensen, J., Boyd, L. A., & Roig, M. (2017). A Single Bout of High-Intensity Interval Training Improves Motor Skill Retention in Individuals With Stroke. *Neurorehabilitation and Neural Repair*, *31*(8), 726–735. https://doi.org/10.1177/1545968317718269

Neuper, C., & Pfurtscheller, G. (2001). Event-related dynamics of cortical rhythms: Frequency-specific features and functional correlates. *International Journal of Psychophysiology*, *43*(1), 41–58. https://doi.org/10.1016/S0167-8760(01)00178-7

Nikolov, P., Hassan, S. S., Schnitzler, A., & Groiss, S. J. (2021). Influence of High Pass Filter Settings on Motor Evoked Potentials. *Frontiers in Neuroscience*, *15*(April), 1–5. https://doi.org/10.3389/fnins.2021.665258

Nys, G. M. S. (2005). *The Neuropsychology of Acute Stroke : Characterisation and Prognostic Implications* [Utrecht University Repository]. dspace.library.uu.nl/handle/1874/3284

O'Malley, M. K., Ro, T., & Levin, H. S. (2006). Assessing and Inducing Neuroplasticity With Transcranial Magnetic Stimulation and Robotics for Motor Function. *Archives of Physical Medicine and Rehabilitation*, *87*(12 SUPPL.), 59–66. https://doi.org/10.1016/j.apmr.2006.08.332

Park, H., Kim, J. S., & Chung, C. K. (2013). Differential Beta-Band Event-Related Desynchronization during Categorical Action Sequence Planning. *PLoS ONE*, *8*(3). https://doi.org/10.1371/journal.pone.0059544

Pelli, D. G. (1997). The VideoToolbox software for visual psychophysics: transforming numbers into movies. *Spatial Vision*, *10*(4), 437–442. https://doi.org/10.1163/156856897X00366

Pesek, M., Medvešek, Š., Podlesek, A., Tkalčič, M., & Marolt, M. (2020). A Comparison of Human and Computational Melody Prediction Through Familiarity and Expertise. *Frontiers in Psychology*, *11*, 557398. https://doi.org/10.3389/FPSYG.2020.557398/BIBTEX

Pfurtscheller, G., & Lopes Da Silva, F. H. (1999). Event-related EEG/MEG synchronization and desynchronization: Basic principles. *Clinical Neurophysiology*, *110*(11), 1842–1857. https://doi.org/10.1016/S1388-2457(99)00141-8

Pfurtscheller, G., Müller, G. R., Pfurtscheller, J., Gerner, H. J., & Rupp, R. (2003). 'Thought' – control of functional electrical stimulation to restore hand grasp in a patient with tetraplegia. *Neuroscience Letters*, *351*(1), 33–36. https://doi.org/10.1016/S0304-3940(03)00947-9

Pfurtscheller, G., & Neuper, C. (1997). Motor imagery activates primary sensorimotor area in humans. *Neuroscience Letters*, *239*(2–3), 65–68. https://doi.org/10.1016/S0304-3940(97)00889-6

Pichiorri, F., Morone, G., Petti, M., Toppi, J., Pisotta, I., Molinari, M., Paolucci, S., Inghilleri, M., Astolfi, L., Cincotti, F., & Mattia, D. (2015). Brain–computer interface boosts motor imagery practice during stroke recovery. *Annals of Neurology*, *77*(5), 851–865. https://doi.org/10.1002/ANA.24390

Pichiorri, F., Morone, G., Pisotta, I., Secci, M., Cincotti, F., Paolucci, S., Molinari, M., & Mattia, D. (2013). Randomized Controlled Trial to Evaluate a BCI-Supported Task-Specific Training for Hand Motor Recovery after Stroke. *Biosystems and Biorobotics*, *1*, 501–505. https://doi.org/10.1007/978-3-642-34546-3_80

Piña-Ramírez, O., Valdés-Cristerna, R., Medina-Bañuelos, V., & Yañez-Suárez, O. (2018). P300-based brain-computer interfaces. *Smart Wheelchairs and Brain-Computer Interfaces: Mobile Assistive Technologies*, 131–170. https://doi.org/10.1016/B978-0-12-812892-3.00007-8

Pino, G. Di, Pellegrino, G., Assenza, G., Capone, F., Ferreri, F., Formica, D., Ranieri, F., Tombini, M., Ziemann, U., Rothwell, J. C., & Lazzaro, V. Di. (2014). *NATURE REVIEWS | NEUROLOGY Modulation of brain plasticity in stroke: a novel model for neurorehabilitation*. https://doi.org/10.1038/nrneurol.2014.162

Por, E., van Kooten, M., & Sarkovic, V. (2019). Nyquist–Shannon sampling theorem. *Leiden University*, *1*(1), 5.

R Core Team. (2023). *R: A Language and Environment for Statistical Computing* (R 4.3.1). Art. R 4.3.1. https://www.R-project.org/

Raffin, E., Harquel, S., Passera, B., Chauvin, A., Bougerol, T., & David, O. (2020). Probing regional cortical excitability via input–output properties using transcranial magnetic stimulation and electroencephalography coupling. *Human Brain Mapping*, *41*(10), 2741–2761. https://doi.org/10.1002/hbm.24975

Remsik, A., Young, B., Vermilyea, R., Kiekoefer, L., Abrams, J., Elmore, S. E., Schultz, P., Nair, V., Edwards, D., & Williams, J. (2017). *Extremity Motor Function After Stroke*. *13*(12), 445–454. https://doi.org/10.1080/17434440.2016.1174572.A

Rivas-Grajales, A. M., Barbour, T., Camprodon, J. A., & Kritzer, M. D. (2023). The Impact of Sex Hormones on Transcranial Magnetic Stimulation Measures of Cortical Excitability: A Systematic Review and Considerations for Clinical Practice. *Harvard Review of Psychiatry*, *31*(3), 114–123. https://doi.org/10.1097/HRP.0000000000000366

Robertson, E. M. (2007). The serial reaction time task: Implicit motor skill learning? *Journal of Neuroscience*, *27*(38), 10073–10075. https://doi.org/10.1523/JNEUROSCI.2747-07.2007

Rohrbaugh, J. W., & Gaillard, A. W. K. (1983). Sensory and Motor Aspects of the Contingent Negative Variation. In A. W. K. Gaillard & W. Ritter (Eds.), *Tutorials in Event Related Potential Research: Endogenous Components* (Vol. 10, Issue C, pp. 269–310). North Holland Publishing. https://doi.org/10.1016/S0166-4115(08)62044-0

Ross, J. M., Comstock, D. C., Iversen, J. R., Makeig, S., & Balasubramaniam, R. (2022). Cortical mu rhythms during action and passive music listening. *Journal of Neurophysiology*, *127*(1), 213–224. https://doi.org/10.1152/JN.00346.2021/ASSET/IMAGES/LARGE/JN.00346.2021_F004.JPEG

Rossi, S., Hallett, M., Rossini, P. M., & Pascual-Leone, A. (2011). Screening questionnaire before TMS: An update. *Clinical Neurophysiology*, *122*(8), 1686. https://doi.org/10.1016/j.clinph.2010.12.037

Rossi, S., Hallett, M., Rossini, P. M., Pascual-Leone, A., Bestmann, S., Berardelli, A., Brewer, C., Cantello, R., Chen, R., Classen, J., Di Lazzaro, V., Epstein, C. M., Fregni, F., Karp, B., Lefaucheur, J.-P., Physiologie, S., Fonctionnelles, E., Henri Mondor, H., Sarah Lisanby, F., … Zangen, A. (2009). Safety, ethical considerations, and application guidelines for the use of transcranial magnetic stimulation in clinical practice and research q. *Clinical Neurophysiology*, *120*, 2008–2039. https://doi.org/10.1016/j.clinph.2009.08.016

Rossini, P. M., Burke, D., Chen, R., Cohen, L. G., Daskalakis, Z., Di Iorio, R., Di Lazzaro, V., Ferreri, F., Fitzgerald, P. B., George, M. S., Hallett, M., Lefaucheur, J. P., Langguth, B., Matsumoto, H., Miniussi, C., Nitsche, M. A., Pascual-Leone, A., Paulus, W., Rossi, S., … Ziemann, U. (2015). Non-invasive electrical and magnetic stimulation of the brain, spinal cord, roots and peripheral nerves: Basic principles and procedures for routine clinical and research application. An updated report from an I.F.C.N. Committee. *Clinical Neurophysiology : Official Journal of the International Federation of Clinical Neurophysiology*, *126*(6), 1071. https://doi.org/10.1016/J.CLINPH.2015.02.001

Rousselet, G. A. (2012). Does filtering preclude us from studying ERP time-courses? In *Frontiers in Psychology* (Vol. 3, Issue MAY, p. 131). Frontiers. https://doi.org/10.3389/fpsyg.2012.00131

Sakamaki, I., Tavakoli, M., & Adams, K. (2018). Generating forbidden region virtual fixtures by classification of movement intention based on event-related desynchronization. *2017 IEEE*

Global Conference on Signal and Information Processing, GlobalSIP 2017 - Proceedings, *2018-January*, 418–422. https://doi.org/10.1109/GLOBALSIP.2017.8308676

Schaefer, R. S., Morcom, A. M., Roberts, N., & Overy, K. (2014). Moving to music: Effects of heard and imagined musical cues on movement-related brain activity. *Frontiers in Human Neuroscience*, *8*(SEP), 109217. https://doi.org/10.3389/FNHUM.2014.00774/ABSTRACT

Scherer, R., Müller-Putz, G., Friedrich, E. V. C., Pammer-Schindler, V., Wilding, K., Keller, S., & Pirker, J. (2017). Games for BCI Skill Learning. In *Handbook of Digital Games and Entertainment Technologies*. Springer, Singapore. https://doi.org/10.1007/978-981-4560-50-4_6

Scherer, R., & Vidaurre, C. (2018). Motor imagery based brain–computer interfaces. *Smart Wheelchairs and Brain-Computer Interfaces: Mobile Assistive Technologies*, 171–195. https://doi.org/10.1016/B978-0-12-812892-3.00008-X

Schultze-Kraft, M., Birman, D., Rusconi, M., Allefeld, C., Görgen, K., Dähne, S., Blankertz, B., & Haynes, J. D. (2016). The point of no return in vetoing self-initiated movements. *Proceedings of the National Academy of Sciences of the United States of America*, *113*(4), 1080–1085. https://doi.org/10.1073/pnas.1513569112

Schurger, A., Sitt, J. D., & Dehaene, S. (2012). An accumulator model for spontaneous neural activity prior to self-initiated movement. *Proceedings of the National Academy of Sciences of the United States of America*, *109*(42). https://doi.org/10.1073/pnas.1210467109

Seo, N. J., Lakshminarayanan, K., Lauer, A. W., Ramakrishnan, V., Schmit, B. D., Hanlon, C. A., George, M. S., Bonilha, L., Downey, R. J., DeVries, W., & Nagy, T. (2019). Use of imperceptible wrist vibration to modulate sensorimotor cortical activity. *Experimental Brain Research*, *237*(3), 805–816. https://doi.org/10.1007/s00221-018-05465-z

Seo, S. (2006). *A Review and Comparison of Methods for Detecting Outliers in Univariate Data Sets* [Master Thesis, University of Pittsburgh.]. https://d-scholarship.pitt.edu/7948/

Shakeel, A., Navid, M. S., Anwar, M. N., Mazhar, S., Jochumsen, M., & Niazi, I. K. (2015). A Review of Techniques for Detection of Movement Intention Using Movement-Related Cortical Potentials. *Computational and Mathematical Methods in Medicine*, *2015*. https://doi.org/10.1155/2015/346217

Shibasaki, H., & Hallett, M. (2006). What is the Bereitschaftspotential? *Clinical Neurophysiology*, *117*(11), 2341–2356. https://doi.org/10.1016/J.CLINPH.2006.04.025

Siemionow, V., Yue, G. H., Ranganathan, V. K., Liu, J. Z., & Sahgal, V. (1998). Relationship between Movement-related Cortical Potential and Voluntary Muscle Activation. *NeuroImage*, *7*(4 PART II), 303–311. https://doi.org/10.1016/s1053-8119(18)31767-1

Singh, B., & Natsume, K. (2022). Readiness potential reflects the intention of sit-to-stand movement. *Cognitive Neurodynamics*, *17*(3), 605. https://doi.org/10.1007/S11571-022-09864-5

Soon, C. S., Brass, M., Heinze, H. J., & Haynes, J. D. (2008). Unconscious determinants of free decisions in the human brain. *Nature Neuroscience 2008 11:5*, *11*(5), 543–545. https://doi.org/10.1038/nn.2112

Stancák, A., & Pfurtscheller, G. (1996). The effects of handedness and type of movement on the contralateral preponderance of μ-rhythm desynchronisation. *Electroencephalography and Clinical Neurophysiology*, *99*(2), 174–182. https://doi.org/10.1016/0013-4694(96)95701-6

Stefan, K. (2000). Induction of plasticity in the human motor cortex by paired associative stimulation. *Brain*, *123*(3), 572–584. https://doi.org/10.1093/brain/123.3.572

Stefan, K., Kunesch, E., Benecke, R., Cohen, L. G., & Classen, J. (2002). Mechanisms of enhancement of human motor cortex excitability induced by interventional paired associative stimulation. *Journal of Physiology*, *543*(2), 699–708. https://doi.org/10.1113/jphysiol.2002.023317

Stinear, C. M., Byblow, W. D., Steyvers, M., Levin, O., & Swinnen, S. P. (2006). Kinesthetic, but not visual, motor imagery modulates corticomotor excitability. *Experimental Brain Research*, *168*(1–2), 157–164. https://doi.org/10.1007/S00221-005-0078-Y/METRICS

Tabie, M., & Kirchner, E. A. (2013). EMG onset detection: Comparison of different methods for a movement prediction task based on EMG. *BIOSIGNALS 2013 - Proceedings of the International Conference on Bio-Inspired Systems and Signal Processing*, 242–247. https://doi.org/10.5220/0004250102420247

Tan, S. H., & Tan, S. B. (2010). The correct interpretation of confidence intervals. *Proceedings of Singapore Healthcare*, *19*(3), 276–278. https://doi.org/10.1177/201010581001900316

Tarkka I. M., & Hallett M. (1991). topography of scalp-recorded motor potentials in human finger movement. In *Journal of Clinical Neurophysiology* (pp. 331–341).

Thaut, M. H., & Abiru, M. (2010). Rhythmic Auditory Stimulation in Rehabilitation of Movement Disorders: A Review Of Current Research. *Music Perception*, *27*(4), 263–269. https://doi.org/10.1525/MP.2010.27.4.263

Toro, C., Deuschl, G., Thatcher, R., Sato, S., Kufta, C., & Hallett, M. (1994). Event-related desynchronization and movement-related cortical potentials on the ECoG and EEG. *Electroencephalography and Clinical Neurophysiology/ Evoked Potentials*, *93*(5), 380–389. https://doi.org/10.1016/0168-5597(94)90126-0

Travers, E., Khalighinejad, N., Schurger, A., & Haggard, P. (2020). Do readiness potentials happen all the time? *NeuroImage*, *206*(116286). https://doi.org/10.1016/j.neuroimage.2019.116286

Trigili, E., Grazi, L., Crea, S., Accogli, A., Carpaneto, J., Micera, S., N., V., & A., P. (2019). Detection of movement onset using EMG signals for upper-limb exoskeletons in reaching tasks. *Journal of NeuroEngineering and Rehabilitation*, *16*(1). http://www.embase.com/search/results?subaction=viewrecord&from=export&id=L626989339%0Ahttp://dx.doi.org/10.1186/s12984-019-0512-1

Van Boxtel, G. J. M., Geraats, L. H. D., Van den Berg-Lenssen, M. M. C., & Brunia, C. H. M. (1993). Detection of EMG onset in ERP research. *Psychophysiology*, *30*(4), 405–412. https://doi.org/10.1111/j.1469-8986.1993.tb02062.x

Van Der Cruijsen, J., Manoochehri, M., Jonker, Z. D., Andrinopoulou, E.-R., Frens, M. A., Ribbers, G. M., Schouten, A. C., & Selles, R. W. (2021). Theta but not beta power is positively associated with better explicit motor task learning. *NeuroImage*, *240*, 118373. https://doi.org/10.1016/j.neuroimage.2021.118373

Van Peppen, R. P. S., Kwakkel, G., Wood-Dauphinee, S., Hendriks, H. J. M., Van der Wees, P. J., & Dekker, J. (2004). The impact of physical therapy on functional outcomes after stroke: what's the evidence? *Http://Dx.Doi.Org/10.1191/0269215504cr843oa*, *18*(8), 833–862. https://doi.org/10.1191/0269215504CR843OA

van Wijk, B. C. M., Beek, P. J., & Daffertshofer, A. (2012). Neural synchrony within the motor system: What have we learned so far? *Frontiers in Human Neuroscience*, *6*(SEPTEMBER), 31431. https://doi.org/10.3389/FNHUM.2012.00252/BIBTEX

Varone, G., Hussain, Z., Sheikh, Z., Howard, A., Boulila, W., Mahmud, M., Howard, N., Morabito, F. C., & Hussain, A. (2021). Real-Time Artifacts Reduction during TMS-EEG Co-Registration: A Comprehensive Review on Technologies and Procedures. *Sensors 2021, Vol. 21, Page 637*, *21*(2), 637. https://doi.org/10.3390/S21020637

Veldema, J., Nowak, D. A., & Gharabaghi, A. (2021). Resting motor threshold in the course of hand motor recovery after stroke: a systematic review. *Journal of NeuroEngineering and Rehabilitation*, *18*(1), 158. https://doi.org/10.1186/s12984-021-00947-8

Vernet, M., Bashir, S., Robertson, E., & Pascual-Leone, A. (2011). Motor cortical and distributed network modulation during visuo-motor learning: A TMS-EEG study. *Journal of Vision*, *11*(11), 936–936. https://doi.org/10.1167/11.11.936

Vidaurre, C., Sander, T. H., & Schölgl, A. (2011). BioSig: The Free and Open Source Software Library for Biomedical Signal Processing. *Computational Intelligence and Neuroscience*, *2011*, 12. https://doi.org/10.1155/2011/935364

Wagner, T. H., Lo, A. C., Peduzzi, P., Bravata, D. M., Huang, G. D., Krebs, H. I., Ringer, R. J., Federman, D. G., Richards, L. G., Haselkorn, J. K., Wittenberg, G. F., Volpe, B. T., Bever, C. T., Duncan, P. W., Siroka, A., & Guarino, P. D. (2011). An economic analysis of robot-assisted therapy for long-term upper-limb impairment after stroke. *Stroke*, *42*(9), 2630–2632. https://doi.org/10.1161/STROKEAHA.110.606442

Walker, M. P., Brakefield, T., Morgan, A., Hobson, J. A., & Stickgold, R. (2002). Practice with sleep makes perfect: Sleep-dependent motor skill learning. *Neuron*, *35*(1), 205–211. https://doi.org/10.1016/S0896-6273(02)00746-8

Ward, N. S. (2015). Does neuroimaging help to deliver better recovery of movement after stroke? *Current Opinion in Neurology*, *28*(4), 323–329. https://doi.org/10.1097/WCO.0000000000000223

Wassermann, E. M. (1998). Risk and safety of repetitive transcranial magnetic stimulation: Report and suggested guidelines from the International Workshop on the Safety of Repetitive Transcranial Magnetic Stimulation, June 5-7, 1996. *Electroencephalography and Clinical Neurophysiology - Evoked Potentials*, *108*(1), 1–16. https://doi.org/10.1016/S0168-5597(97)00096-8

Weavil, J. C., & Amann, M. (2018). Corticospinal excitability during fatiguing whole body exercise. *Progress in Brain Research*, *240*, 219–246. https://doi.org/10.1016/bs.pbr.2018.07.011

Williams, J., Pearce, A. J., Loporto, M., Morris, T., & Holmes, P. S. (2012). The relationship between corticospinal excitability during motor imagery and motor imagery ability. *Behavioural Brain Research*, *226*(2), 369–375. https://doi.org/10.1016/J.BBR.2011.09.014

Winkler, I., Debener, S., Muller, K. R., & Tangermann, M. (2015). On the influence of high-pass filtering on ICA-based artifact reduction in EEG-ERP. *Proceedings of the Annual International Conference of the IEEE Engineering in Medicine and Biology Society, EMBS*, *2015-Novem*, 4101–4105. https://doi.org/10.1109/EMBC.2015.7319296

Winstein, C., & Requejo, P. (2015). Innovative Technologies for Rehabilitation and Health Promotion: What Is the Evidence? *Physical Therapy*, *95*(3), 294–298. https://doi.org/10.2522/ptj.2015.95.2.294

Winstein, C., Wing, A. M., & Whitall, J. (2003). Motor control and learning principles for rehabilitation of upper limb movements after brain injury. In *Handbook of Neuropsychology* (Vol. 9, pp. 79–138). http://www.bham.ac.uk/symon

Woldag, H., & Hummelsheim, H. (2002). Evidence-based physiotherapeutic concepts for improving arm and hand function in stroke patients: A review. *Journal of Neurology*, *249*(5), 518–528. https://doi.org/10.1007/S004150200058/METRICS

Wolpert, D. M., Ghahramani, Z., & Flanagan, J. R. (2001). Perspectives and problems in motor learning. *Trends in Cognitive Sciences*, *5*(11), 487–494. https://doi.org/10.1016/S1364-6613(00)01773-3

Wolpert, D. M., & Miall, R. C. (1996). Forward models for physiological motor control. *Neural Networks*, *9*(8), 1265–1279. https://doi.org/10.1016/S0893-6080(96)00035-4

Wright, D. J., Holmes, P. S., & Smith, D. (2011). Using the movement-related cortical potential to study motor skill learning. *Journal of Motor Behavior*, *43*(3), 193–201. https://doi.org/10.1080/00222895.2011.557751

Yang, L., Shen, L., Nan, W., Tang, Q., Wan, F., Zhu, F., & Hu, Y. (2017). Time course of EEG activities in continuous tracking task: a pilot study. *Computer Assisted Surgery*, *22*(0), 1–8. https://doi.org/10.1080/24699322.2017.1378604

Yekutiel, M., & Guttman, E. (1993). A controlled trial of the retraining of the sensory function of the hand in stroke patients. *Journal of Neurology Neurosurgery and Psychiatry*, *56*(3), 241–244. https://doi.org/10.1136/jnnp.56.3.241

Yousry, T. A., Schmid, U. D., Alkadhi, H., Schmidt, D., Peraud, A., Buettner, A., & Winkler, P. (1997). *Localization of the motor hand area to a knob on the precentral gyrus A new landmark*. *120*, 141–157.

Zack, J. (2006, November 14). *Introduced Species Summary Project - Sea Squirt (Didemnum sp.)*. Introduced Species Summary Project - Columbia University. https://www.columbia.edu/itc/cerc/danoff-burg/invasion_bio/inv_spp_summ/Didemnum_sp.html

Zhuang, P., Toro, C., Grafman, J., Manganotti, P., Leocani, L., & Hallett, M. (1997). Event-related desynchronization (ERD) in the alpha frequency during development of implicit and explicit learning. *Electroencephalography and Clinical Neurophysiology*, *102*(4), 374–381. https://doi.org/10.1016/S0013-4694(96)96030-7

Zorowitz, R., & Brainin, M. (2011). Advances in brain recovery and rehabilitation 2010. *Stroke*, *42*(2), 294–297. https://doi.org/10.1161/STROKEAHA.110.605063/SUPPL_FILE/ZOROWITZ_294.PDF

Appendix

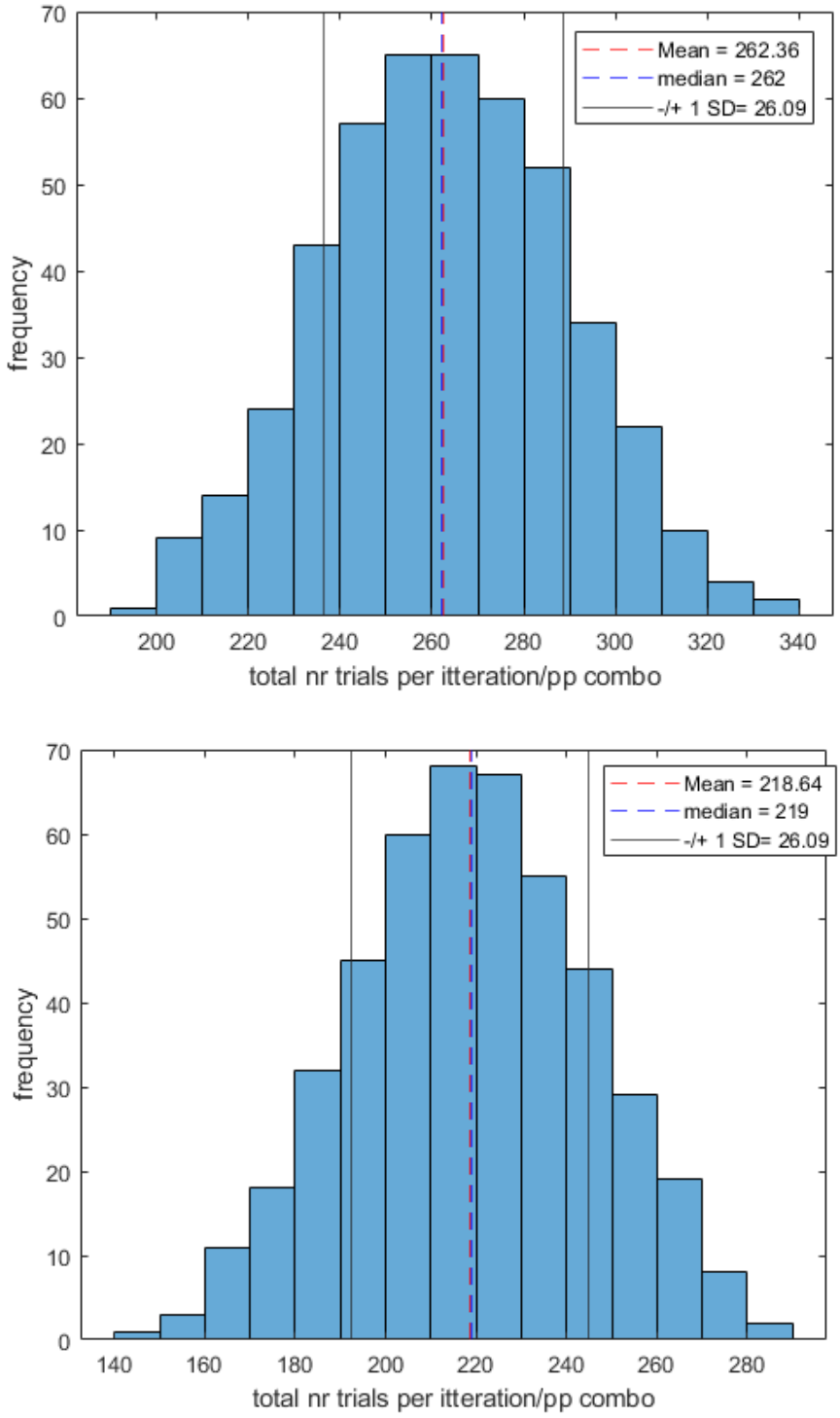

Appendix A1. Distribution Retained Trials split across Training (top) and Test (bottom) sets. At the extremes we have a training set of all 6 participants with the lowest number of trials (counts trials 193), which stands across a test set of 5 participants with the highest number of trials (counts 288) with a difference of 95 trials. On the other extreme we have difference of 185 trials when all 6 participants make up the training set (counts total of 333 trials) compared to the 5 lowest in the test set (counts 148 trials).

questions on motor dexterity.
→ musicians and gamers affect learning outcomes? → because pre-existing extensive training in sequential hand muscle skill

- Musical skill
    - Type of instrument(s):

      _____

    - Total number of years practiced:

      _____

    - How long ago: (e.g., from age 5-15, or started at age 6 – present)

      _____

    - Currently playing? :

      _____

    - Other (e.g., used to play in orchestra, now only play occasionally at home) :

      _____

- Game skills
    - Do you play any games (video or physical) involving high amounts of dexterity

      Yes / No

      (specify type) _____

    - If digital circle type of controls

      hand held controller / mouse and keyboard

    - How often (average amount of hours / week) do you game

      _____

Appendix A2. First version of motor dexterity questions. As presented to participants.

Preliminary study questions on motor dexterity.
Do musicians affect learning outcomes, because pre-existing extensive training in sequential hand muscle skill and sense of rhythm?

- Motor skill
  - How would you rate your **right hand dexterity / muscle control**?

Far worse than most		Worse than most		Average		Better than most		Far better than most
1	2	3	4	5	6	7	8	9

- Musical skill
  - What would you rate **your general musical competence**?

Very poor				average				excellent
1	2	3	4	5	6	7	8	9

  - Type of musical practice: instrument(s), singing, conducting… :

    _____

  - Total number of years practiced music and/or instruments:

    _____

  - How long ago: (e.g., from age 5-15, or started at age 6 – present)

    _____

  - Currently playing? :

    _____

    Other (e.g., used to play in orchestra, now only play occasionally at home) :

    _____

Appendix A3. second version of motor dexterity questions. As presented to participants.

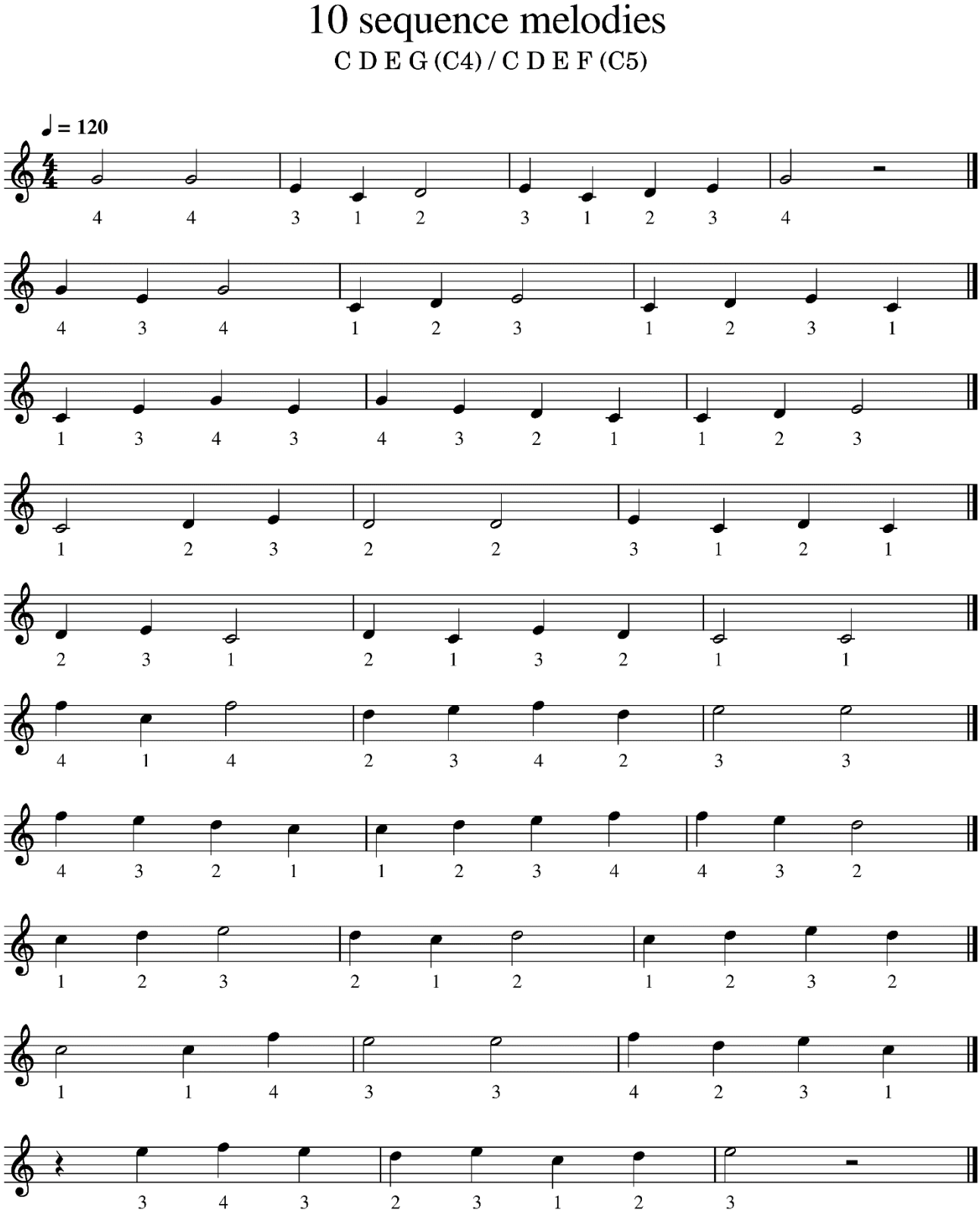

Appendix A4. Melodic passages used as baselines for the motor sequences.

Appendix A5

t-values of Pairwise Post-Hoc tests for a One-Way rmANOVA on Equivalence of Sequence Difficulty

Sequences	Seq 1	Seq 2	Seq 3	Seq 4	Seq 5	Seq 6	Seq 7	Seq 8	Seq 9	Seq 10
Seq 1		1.83	3.96*	-0.7	1.81	0.37	2.06	1.02	0.36	2.2
Seq 2			3	-2.36	0.4	-1.31	0.25	-0.37	-1.42	1.32
Seq 3				-5.51**	-3.27	-3.69	-3.14	-5.11**	-4.11*	-1.27
Seq 4					3.37	1.09	2.51	2.18	1.09	3.28
Seq 5						-1.69	-0.12	-1.22	-1.75	1.18
Seq 6							1	0.65	-0.08	1.99
Seq 7								-0.54	-2.04	1.34
Seq 8									-0.7	1.5
Seq 9										2.99
Seq 10										

Note: pairwise t-test test statistics, complimentary to the p-values in Table 3. df = 17

Appendix A6

t-values of Pairwise Post-Hoc tests for a One-Way rmANOVA on Equivalence of Sequence Difficulty

Sequences	Seq 1	Seq 2	Seq 3	Seq 4	Seq 5	Seq 6	Seq 7	Seq 8	Seq 9	Seq 10
Seq 1		1.63	8.44 ***	-2.84	2.25	1.476	5.04 ***	3.07	1.61	8.09 ***
Seq 2			8.88 ***	-3.62*	0.63	-0.19	4.31 ***	1.15	-0.15	7.95 ***
Seq 3				-10.61 ***	-6.95 ***	-7.76 ***	-3.62*	-6.69 ***	-8.48 ***	-0.63
Seq 4					4.54**	3.68*	5.99 ***	4.75 ***	3.68*	10.72 ***
Seq 5						-0.89	3.27	0.47	-0.75	7.41 ***
Seq 6							3.69*	1.40	0.11	7.45 ***
Seq 7								-2.69	-3.41	3.57*
Seq 8									-1.29	5.71 ***
Seq 9										7.09 ***

Note: pairwise t-test test statistics, complimentary to the p-values in Table *6.* df = 57

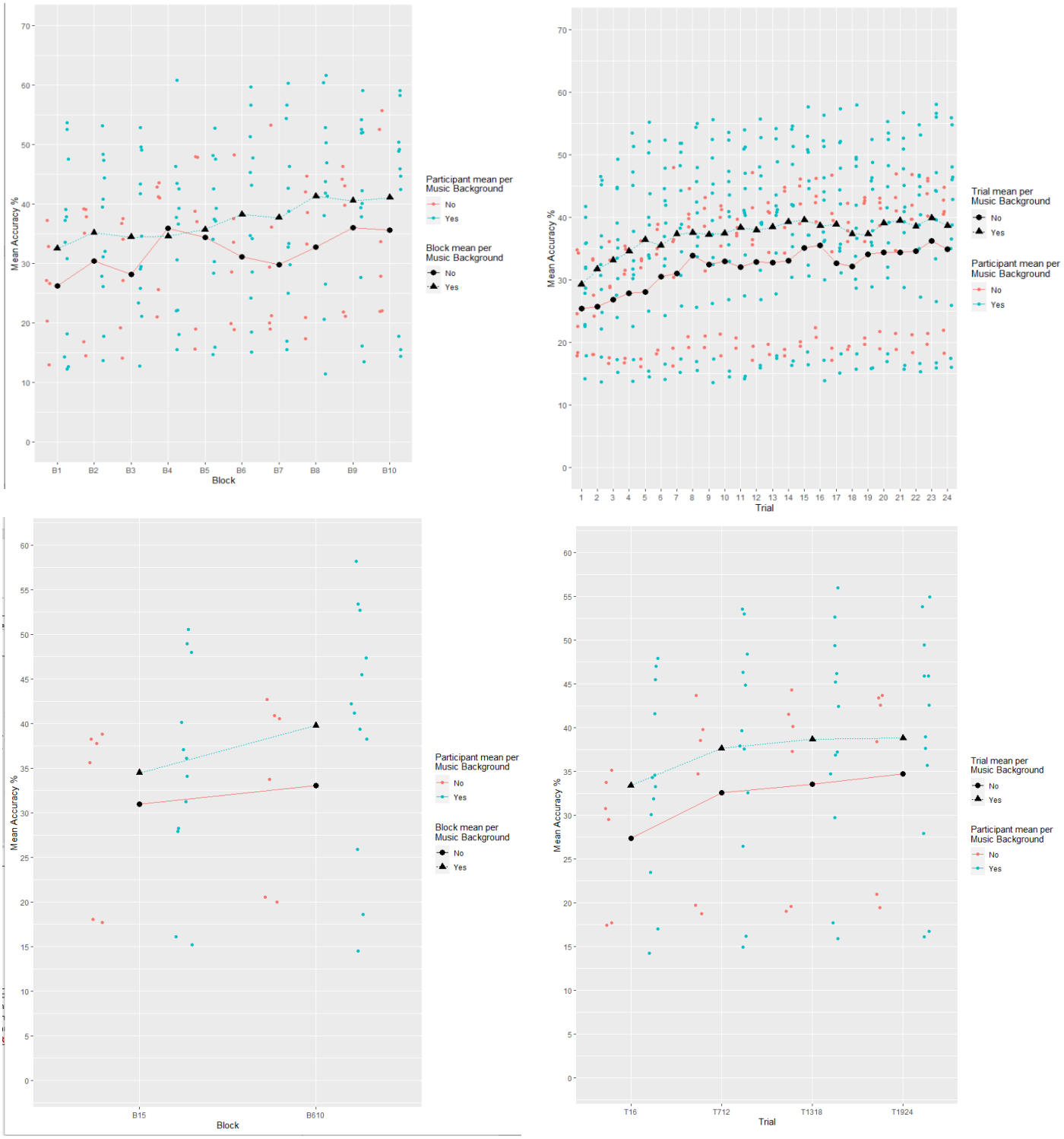

Appendix A7. Complimentary to Figure 12. Figures show the average performance scores over blocks and trials between participants with and without a musical background. Showing a general difference in ACC score, where those without musical background score on average a little lower than those with musical background. However, this difference was not considered significant and did not affect the learning trend (our main interest).